Assays to Forensically Assess Exposure of Plasma and Serum to Thawed Conditions

by

Nilojan Jehanathan

A Dissertation Presented in Partial Fulfillment
of the Requirements for the Degree
Doctor of Philosophy

Approved October 2022 by the
Graduate Supervisory Committee:

Chad R. Borges, Chair
Jia Guo
Wade Van Horn

ARIZONA STATE UNIVERSITY

December 2022

ABSTRACT

Plasma and serum are the most commonly used liquid biospecimens in biomarker research. These samples may be subjected to several pre-analytical variables (PAVs) during collection, processing and storage. Exposure to thawed conditions (temperatures above -30 °C) is a PAV that is hard to control, and track and could provide misleading information, that fail to accurately reveal the in vivo biological reality, when unaccounted for. Hence, assays that can empirically check the integrity of plasma and serum samples are crucial.

As a solution to this issue, an assay titled ΔS-Cys-Albumin was developed and validated. The reference range of ΔS-Cys-Albumin in cardio vascular patients was determined and the change in ΔS-Cys-Albumin values in different samples over time course incubations at room temperature, 4 °C and -20 °C were evaluated. In blind challenges, this assay proved to be successful in identifying improperly stored samples individually and as groups. Then, the correlation between the instability of several clinically important proteins in plasma from healthy and cancer patients at room temperature, 4 °C and -20 °C was assessed. Results showed a linear inverse relationship between the percentage of proteins destabilized and ΔS-Cys-Albumin regardless of the specific time or temperature of exposure, proving ΔS-Cys-Albumin as an effective surrogate marker to track the stability of clinically relevant analytes in plasma. The stability of oxidized LDL in serum at different temperatures was assessed in serum samples and it stayed stable at all temperatures evaluated.

The ΔS-Cys-Albumin requires the use of an LC-ESI-MS instrument which limits its availability to most clinical research laboratories. To overcome this hurdle, an absorbance-based assay that can be measured using a plate reader was developed as an alternative to the ΔS-Cys-Albumin assay. Assay development and analytical validation procedures are reported herein. After that, the range of absorbance in plasma and serum from control and cancer patients were determined and the change in absorbance over a time course incubation at room temperature, 4 °C and -20 °C was assessed. The results showed that the absorbance assay would act as a good alternative to the ΔS-Cys-Albumin assay.

DEDICATION

Dedicated to my beloved parents Mr Pakkiyarasa Jehanathan and Mrs. Arudselvarani Jehanathan and my sweet little sisters Nithiyananthana Imasalan and Narmatha Jehanathan for being a great source of motivation, inspiration and support throughout my journey

ACKNOWLEDGMENTS

I would like to offer my first and foremost thanks and gratitude to my pillar of support, advisor and mentor, Prof. Chad R. Borges for his extraordinary guidance, understanding, patience and most importantly his immense knowledge and professional experience he showed during my graduate studies at the School of Molecular Sciences at Arizona State University. Without his mentorship and counsel I would not be the person who I am today. His mentorship was paramount in providing a well-rounded experience consistent my long-term career goals. He encouraged me not only to grow as an experimentalist but also to finish this dissertation academically while guiding me through the rough road as an independent thinker. He not only cared about my academic growth, but also genuinely cared about my physical and mental wellbeing. During my study period at ASU, I have adored him as a great advisor and a good leader with goal-oriented personality. I am really grateful to have him in my life as my mentor and I could not have asked for a better advisor than him.

Secondly, I would like to express my appreciation to Prof. Jia Guo and Prof. Wade Van Horn, who served as my dissertation committee members. Their thoughtful questions and comments were valued greatly. They were very supportive, responded to my queries in a timely manner, and always tried their best to accommodate my requests for meetings even during their busiest times. Also, I would like to convey my sincere thanks to all the other professors and staff at ASU that have helped me along the way. I gratefully remind the training, support and contribution, which polished me in several ways as a scientist, provided by Dr. Stephen Rogers who retired recently from our lab.

I remember the generosity and encouragement of past and present colleagues of our laboratory and I am thankful to Dr. Erandi Kapuruge, Dr. Jesus Aguilar, Dr. Joshua Jeffs, Dr. Jorvani Cruz Villarreal, Dr. Stephanie Thibert, Dr. Yueming Hu, Ms. Kazi Waheeda, Mr Aaron Gabriel, Mr. Agbor Tanyi, Mr. Emil Ljungberg, Mr. Jaren Cantorna and Mr. Schuyler Kremer for their valuable help in research work.

I would like to thank Dr. Dhenugen Logeswaran and Dr. Nirupa Nagaratnam without whom I would not have landed at ASU. I would also like to thank Mr. Renokanthan Gopalan, Mr. Tharshan Gopalan. Mrs. Komaladevi Gopalan, Mr. Juderishan Eswararasha, Mrs. Jeyatharshika Antonyrajah, Mr. Rupalavan Pathmanathan, Mrs Gayathri Ganesan, Mr. Jeyakaran Thavathurairaja, Mrs. Sukanniya Jeyakaran, Mr & Mrs Kulanathan, Mr. Senal Liyanage, Mr. Kohilan Jeyasothy, Mr. Abhik Manna, Mr. Ankush Tyagi, Mr. Saurabh Sharma, Mr. Adhitya Shyamala Pandiyan and Mr. Charitha Rajapakse who have given me their unequivocal support throughout, as always, for which my mere expression of thanks likewise does not suffice. I praise the enormous amount of help and teachings to all those whom I have missed to mention above but helped me in numerous ways to my success.

Last but not the least, my warmest gratitude goes to my father, mother, periyappa, periyamma, my little sisters, family members and my ever-loving friends Mr. Dominic Alexander, Mr. Sageenthan Mohanpremkumar and Mr. Hinthujan Muthulingam for their love, care, moral support and advice throughout my life.

TABLE OF CONTENTS

Page

CHAPTER Page

CHAPTER Page

CHAPTER Page

LIST OF TABLES

Table Page

LIST OF FIGURES

Figure Page

Figure Page

Figure Page

LIST OF ABBREVIATIONS

AFP	Alpha-Fetoprotein
ANOVA	Analysis of Variance
AlbSH	Native (Reduced) Albumin
ApoE	Apolipoprotein E
CD40L	Cluster of differentiation 40 Ligand
CHTN	Cooperative Human Tissue Network
CI	Confidence Interval
CVD	Cardiovascular diseases
Cys	Cysteine
Cys-Cys	Cystine
DMSO	Dimethyl Sulfoxide
EDTA	Ethylenediaminetetraacetic Acid
EGF	Epidermal Growth Factor
EGFR	Epidermal Growth Factor Receptor
ELISA	Enzyme-Linked Immunosorbent Assay
ES	External Standard
ESI	Electrospray Ionization
GC	Gas Chromatography
GI	Gastrointestinal
HBS	HEPES Buffered Saline
HPLC	High Pressure Liquid Chromatography
HSA	Human Serum Albumin

IRB	Institutional Review Board
TCEP	Immobilized Tris(2-carboxyethyl)phosphine
K2EDTA	Dipotassium ethylenediaminetetraacetic acid
LC	Liquid Chromatography
LDL	Low-Density Lipoprotein
LiHep	Lithium Heparin
LOD	Limit of detection
LOQ	Limit of quantification
Met	Methionine
MIHS	Maricopa Integrated Health System
MMP	Matrix Metalloproteinase
MoSA	Method of Standard addition
mRNA	Messenger RNA
MS	Mass Spectrometry
MWCO	Molecular Weight Cut-Off
NCI	National Cancer Institute
NIH	National Institutes of Health
NSE	Neuron Specific Enolase
PAI-1	Plasminogen Activator Inhibitor 1
PAV	Preanalytical variables
PBS	Phosphate Buffered Saline
P/S	Plasma and Serum

PTMs	Post Translational Modifications
QA	Quality Assurance
QC	Quality Control
Q-TOF	Quadrupole Time of Flight
RMSD	Root Mean Squared Deviation
sCD40L	Soluble Cluster of differentiation 40 Ligand
S-Cys-Albumin	S-Cysteinylated (Oxidized) Albumin
SD	Standard Deviation
SOPs	Standard Operating Procedures
SPE	Solid Phase Extraction
TCEP	Tris(2-carboxyethyl)phosphine
TIMP-1	Tissue Inhibitor of Metalloproteinases 1
TFA	Trifluoracetic Acid
VCAM-1	Vascular Cell Adhesion Molecule-1
VEGF	Vascular Endothelial Growth Factor
VWH	ValleyWise Health
XIC	Extracted Ion Chromatograph

CHAPTER 1

INTRODUCTION

1.1. Biomarker research

The Biomarkers Definitions Working Group, a subgroup of the National Institutes of Health (NIH), has defined the term biomarker as “a characteristic that is objectively measured and evaluated as an indicator of normal biological processes, pathogenic processes, or pharmacological responses to a therapeutic intervention” (1). Biomarkers have been used in several valuable clinical applications such as a diagnostic tool in identifying patients with a disease or abnormal condition, staging or classification of the disease, a prognostic indicator that is used to measure the progress of a disease in a patient, a way to predict and examine the clinical response of treatment, predicting and monitoring drug toxicity (2). They are also used for several drug discovery and drug development applications. These include usage as indicators in screening for potential drug candidates, endpoint targets in pharmacodynamic experiments, determining the drug dosage for the expected effect, evaluating the efficacy of drugs in clinical trials, and understanding the side effects of drug candidates (2).

There are numerous biomarkers currently in use. For example, gene variations in apolipoprotein E (APOE) are used to assess the risk of developing Alzheimer´s disease throughout live (3). Breast Cancer genes 1 and 2 (BRCA1/2) mutations are used as prognostic biomarkers to predict the likelihood of recurrence of breast cancer (4). Low density lipoprotein (LDL) cholesterol levels are used as surrogate markers to check the efficacy of lipid-lowering drugs (5). The presence of HLA-B*1502 allele is used as a safety biomarker to predict serious skin reactions to drugs such as carbamazepine (6).

When developing a biomarker, it is compulsory to understand the pathophysiological correlation between the clinical outcome and the biomarker to make sure that the biomarker accurately represents the clinical condition or the effect of the treatment. Biomarker development process involves two distinct validation approaches i.e. analytical validation and clinical validation (7). During analytical validation several technical performance characteristics of a biomarker assay such as accuracy (how accurately can the assay measure the analyte of interest), analytical sensitivity (smallest quantity of the analyte that can be accurately measured in a sample), analytical specificity (ability of the assay to measure a particular analyte apart from the other molecules present in a sample) and reproducibility (intra and inter assay precision) are tested whether they are acceptable for the proposed context of use (7, 8). However, this does not guarantee the biomarker's effectiveness in clinical context. Clinical validation examines whether the correlation between the biomarker and the outcome interest are acceptable for the proposed context of use and this process varies depending on the purpose of the biomarker (7, 9). For an example, during this procedure in a diagnostic biomarker assay development, the biomarker is checked for its clinical sensitivity (percentage of people with a conditions who are identified by the assay as positive for the condition), clinical specificity (percentage of people without the condition who are identified by the assay as negative for the condition) and clinical accuracy (percentage of correctly identified people either as negative or positive in the population) (8, 10, 11).

1.2. Samples employed in biomarker research

Different human tissues or biofluids, which are commonly referred to as biospecimens, can be used in biomarker research depending on the nature and purpose of the

application. Human tissue specimens are obtained from a patient from a biopsy for diagnostic or prognostic purposes or by a surgical procedure for treatment, in different sizes and states (12). Collected tissue samples are commonly stored either as frozen tissue samples or formalin fixed and paraffin embedded (FFPE) samples. Biofluids used for research purposes include blood, plasma, serum, saliva, urine, and cerebrospinal fluid. Most biomarker research employs biofluids since they can be quickly obtained in an inexpensive and less invasive manner. Hence, they are very useful and easier to be translated into a diagnostic test that requires routine sample collection for disease monitoring, where frequent collection of tissue specimens from a patient is cumbersome (13). The most commonly used biofluids are blood-related plasma and serum. Plasma is the liquid portion of blood, which is procured by removing blood cells by centrifugation from blood that was collected in specialized tubes containing anticoagulants such as EDTA, heparin or citrate to prevent blood from clotting. Serum is the liquid that is obtained after letting the blood sample to clot for 30 to 60 minutes at room temperature (14). During the clotting process more than 300 metabolites and proteins are released into the serum from platelets (15). Several studies have proposed that secreted small proteins and peptides in plasma and serum are corresponded with pathophysiological conditions and would be potential targets for diagnostic and prognostic biomarkers (16). Since plasma and serum are abundant in water-soluble proteins, they have become the most favored and widely used biospecimens in proteomic research.

1.3. Reproducibility issues in biomarker research

There are several successful biofluid based biomarkers that help in disease diagnosis and patient management (17). However, replication efforts in many promising biomarker

findings in biological fluids have shown poor reproducibility, and the poor reproducibility not only affects biomarker research but also drug discovery efforts (17–20). An article published in 2015 mentioned that every year approximately 12025 early-stage breast cancer patients are affected by false positive and false negative human epidermal growth factor receptor 2 (HER2) test results which result in an economic societal loss of around 1 billion USD (21). Transforming growth factor-beta (TGF-β1) is a radiation-inducible cytokine and the increase of its level in plasma could be utilized as a predictive marker for radiation-induced liver damage, but it has been demonstrated that when plasma samples were improperly handled which leads to platelet damage, the level of TGF-β1 in plasma significantly increased leading to false conclusions (22). In 2012 U.S. Preventive Services Task Force (USPSTF) recommended against Prostate-specific antigen (PSA)-based screening for prostate cancer making it not really as useful as previously thought (23). C-reactive protein was introduced to clinics as a prognostic marker for coronary artery disease and later shown to be unsuccessful (24). Some genetic tests promoted by for-profit companies that recommend personalized nutrition and other lifestyle health recommendations have shown limited validity and questionable or no clinical use (25).

Many factors could compromise the reproducibility and reliability of biomarkers including pre-analytical variables, analytical variables, assay-related variables, and cohort-related factors. Most of these variables could be controlled or minimized by careful experimental designs. However, many pre-analytical variables can still affect the results even before the analytical phase starts even in a carefully validated assay, where

thorough experimental design and efforts have been put to eliminate analytical, assay-related, and cohort-related variables.

1.4. Pre-analytical variables (PAV) that affect biomarker research

Ex vivo biospecimen handling and storage conditions have the potential to impact measurements of certain clinical biomarkers as much or more than in vivo conditions of interest and utilization of compromised biospecimens in biomedical research can lead directly to false conclusions (12, 26–35). Experts in biomarker development agree that this is a major problem in biomedical research. This fact has been increasingly recognized by top-tier clinical chemistry journals, which have begun to require documentation of biospecimen handling conditions in manuscript submissions (36–43). The danger of false conclusions is particularly strong for untargeted biomarker discovery studies or in cases of targeted analysis where the stability of the target analytes have not yet been validated. There are numerous PAVs that can compromise the integrity of tissues and biofluids collected for biomedical research.

For blood plasma and serum (P/S) samples, several PAVs such as degree of hemolysis, time exposed to thawed conditions, type of collection tube, collection volume, number of tube inversions, centrifugation time, chemical additives, number of freeze thaw cycle etc. could be introduced during sample collection, transport, processing, and storage (44). According to previously published data, approximately 60-70% of errors that occur in testing of blood related biospecimens in the pathology laboratory are due to mishandling of biospecimens in the pre-analytical phase (28, 44, 45). For tissue specimens, several factors affect the integrity of the tissue specimens before they are is stored in a biobank.

These factors include size of specimen, temperature of room, cold ischemia time, total time in fixative, type of fixation, rate and method of freezing (12).

These PAVs affect samples in different ways hindering the ability of assays in explaining what the biological reality of the samples is. Hemolysis, which is generally defined as rupture of erythrocytes resulting in increased concentration of cellular components including cell free hemoglobin creates many analytical issues. The released chemicals create chemical interference in some analytical techniques. For example, in hemolysed samples, creatine kinase activity is falsely elevated due to the release of adenylate kinase from erythrocytes (46). Hemolysis also cause spectral overlap at some wavelengths (415, 540 and 570 nm), and dilutes analytes that are more abundant in blood than in blood cells (45). For different clinical tests, blood is drawn in specialized tubes that contain different additives (EDTA, Lithium/Sodium heparin, Sodium citrate). For example, hematological assays can only be carried out in EDTA samples which are irreversibly anticoagulated, sodium citrate added reversibly anticoagulated samples are required for hemostasis assays, and immunochemistry tests need serum or lithium-heparin samples(45). Blood collected in a wrong container will not be suitable for performing the assay and if used would produce misleading results. Since these tubes have additives, drawing correct volume of blood into these tubes is very important. For example, under filing of plasma tubes affect the results of clotting factors assay and activated partial thromboplastin time (45). Serum samples that were not let to properly clot would retain cellular components and the samples let to clot for prolonged period would lead to cell lysis in the clot and release of cellular elements which was observed to affect the protein and metabolite profile of serum (47). Proteins introduced by prolonged clotting include hemoglobin (α

and β), inter-alpha-trypsin inhibitor H4, C3a anaphylatoxin, platelet factor 4, fibrinogen α, and neutrophil defensins (15, 48). Even a 2 hour delay between blood collection and processing was shown to increase the levels of lactate dehydrogenase, aspartate aminotransferase, and γ-glutamyl transferase in serum samples (49).

Some of these variabilities could be identified and the problematic samples could be eliminated by experienced staff. For example, degree of hemolysis, type of collection tube or collection volume in a specialized tube would be so obvious to notice in visual inspection or could be detected by an analyzer and any samples that exhibited unacceptable error could be eliminated. However, most pre analytical variables that affect P/S samples are not so obvious to notice and not even visible. Some of these factors could be controlled by establishing and following standardized protocols, but not all. Among these PAVs, exposure to thawed conditions (temperatures higher than -30 °C) is the most difficult to control and track over the life of most P/S samples especially at the individual aliquot level and, when unaccounted for, could produce misleading results in clinical research that do not correctly represent the biological reality in vivo (50)(51).

1.5. Effect of exposure to thawed conditions on biospecimen integrity

According to European Pharmacopoeia, freezing point of P/S samples is -30 °C (50). P/S samples stored at -20 °C may visually look frozen, but they are not completely frozen at that point and biochemical reactions will continue to occur in those samples stored at any temperatures above -30 °C. Different studies have documented instability of several biomolecules upon storage of P/S samples at sub optimal storage conditions.

Protein concentrations have been observed to decrease by 50% in serum samples stored at -20 °C (Tissue Inhibitor of Metalloproteinases-1 (TIMP-1) after 8 months, Vascular Endothelial Growth Factor (VEGF) after 5 months, and VEGF receptor 2 (VEGF-R2) within 3 months) (15). The level of C-terminally cleaved fragment of cystatin C in cerebrospinal fluid was recommended as a diagnostic marker for multiple sclerosis or clinically isolated syndromes, yet another group was unsuccessful in reproducing the finding due to improper storage of samples. When the samples were stored at -20 °C instead of -80 °C, cystatin C underwent a N-terminal cleavage which resulted in artifactually lowered levels of C-terminally cleaved fragment (52, 53). Another study showed increased oxidation of proteins in plasma stored at -20 °C. Human Serum Albumin reached complete oxidation state after about 6 weeks at -20 °C and Apolipoprotein A-I showed evidence of oxidation after 4 months at -20 °C and steadily continued to increase thereafter (34). A study on the stability of vitamins in EDTA plasma at -20 °C showed a significant decrease in vitamin E concentration after 6 months of storage and levels of vitamin A, total carotenoids, ß-carotene and folic acid dramatically declined after 1 year (54) and another study on stability of vitamin E in long term storage of serum samples at -20 °C exhibited highly reduced levels in 7-13 months (55). Storage at -20 °C was shown to increase the levels of F2-isoprostanes in plasma samples (56). Concentrations of norepinephrine, dopamine, and epinephrine in plasma were noticed to decrease after 1 month of storage at -20 °C (57). Circulating miRNA levels in plasma were observed to have decreased after storage at -20 °C for 4 months (58). Hence, it is evident that integrity of all types of biomolecules in P/S samples is affected by improper storage at -20 °C. In most of the above mentioned cases no

significant changes were observed when samples are stored at -70 °C or below. As expected, storage at 4 °C was observed to worsen the stability issue. However, storing P/S samples at -20 °C for either shorter or longer periods is a common practice, especially when -80 °C freezers are unavailable in collection sites. Exposure to thawed conditions could also commonly occur during other unexpected situations like -80 °C freezer failure, power outages, delays in shipment and loss of dry ice, or the need to re-aliquot samples etc.

1.6. Archived samples increase the risk of samples exposure to thawed conditions

Clinical research heavily relies on archived human P/S samples for developing biomarkers for numerous disease conditions. P/S samples are stored in repositories for a long period time for several reasons. These samples are both scientifically and financially precious. When a set of samples collected for a particular study is stored after the first study is over and used for a secondary study after a certain period of time, that saves a lot of money and time spent on sample collection for the second study. Accruing patient samples for a clinical research study, especially from patients with certain conditions or with regular use of a particular drug, could take months to years. Sometimes even after spending several months, the number of samples collected might be inadequate in size for certain analysis. Utilization of archived samples helps the investigators by saving time and increasing the number of samples included in the study thus strengthening the confidence of the findings of biomarker research. This not only helps the researcher but also the entire scientific community.

Biobanks collect, process, store and distribute different types of biospecimens according to the established standard operating protocols and provide with systematically organized data related to each sample such as genetic, health and other personal information (59). Hence, researchers have easy access to samples required for their study that enables rapid analysis of samples by cutting down the time spent on sample collection. Also, biobanks reduce the need of ethical clearance from agencies like Institutional Ethics Committees or Institutional Review Board since this was already acquired during samples collection. In the last decade, there has been a significant proliferation in the establishment and expansion of biobanks as a key feature of the research landscape globally and in the USA (59). Biobanks in the USA are affiliated to medical and academic research institutions, public health systems, or private entities(60). P/S samples are the most commonly stored samples in the USA i.e. 77% of the biobanks. They receive samples from several sources including specimens directly collected from individuals (75%), residual collections from either hospital and other clinical settings (57%), and research studies (13%) (60).

Although the use of archived samples help researchers in many ways, this escalates the risk of subjection of samples to PAVs, especially to exposure to thawed conditions and raises a question about the integrity and quality of the samples stored at biobanks given that there is immense diversity in origin and organizational features among different biobanks (61–63).

1.7. Assuring the quality of samples used in biomedical research

As explained earlier, ex vivo biospecimen handling and storage conditions have the potential to impact measurements of certain clinical biomarkers as much or more than in

vivo (clinical) conditions of interest. As such, utilization of compromised biospecimens in biomedical research can lead directly to false conclusions. Though this problem is sometimes ignored or given low priority, more and more biomedical researchers are becoming aware of the potential disasters that can be caused by employing biospecimens in their research that have an undocumented or questionable history. A common solution to this problem is to seek out biospecimens collected by reputable investigators using a well-established or well accepted protocol or standard operating procedure (SOP) and for which there is at least an oral history of storage conditions. While this approach generally passes as acceptable, it lacks rigor.

There are strictly established SOPs in place to minimize the errors during sample collection, processing and storage but, sometimes paper trails do not disclose the exact story of how the samples were handled and stored throughout its lifetime. There are at least two occasions we are aware of where this happened as discussed later in this report (64, 65). The best practice is to store P/S samples at -80 °C immediately after collection and processing. However, -80 °C freezers are not available at all collection sites which leads to temporary storage at -20 °C or 4 °C for a short period of time. The longer the samples stay at the temporary storage the more damage occurs to the samples i.e. the first sample in a temporary storage situation may not be as fresh as the last sample collected and this raises a question about how comparable these samples are of their biological nature. Clinical P/S samples are commonly transported within a country and across the globe for research purposes. Transporting them on dry ice to keep the samples frozen is the routine practice, but delays due to transportation issues may cause the samples to run out of dry ice which would lead to partial or complete thawing of the samples.

Unforeseen power outages might increase the temperature in the freezers. These are some situations where there is a possibility of the loss of integrity of the P/S samples due to exposure to thawed conditions that are not controlled by SOPs and not documented most of the times (e.g., aliquoting for unanticipated analyses). Hence relying completely on SOPs lacks rigor because it does not include empirical verification of biospecimen quality. Evidence-based verification of biospecimen quality is important because, while seldom discussed, investigators in charge of procuring and archiving specimens for biomedical research have an inherent professional (and sometimes monetary) conflict of interest with disclosing incidents that may result in some or all of their collection being deemed less than pristine. The best solution to confirm the integrity of P/S is to empirically assess the quality of the specimen using a molecular marker or a quality control assay that will help ensure the quality of the specimens thus the quality of the research conducted using those samples.

An ideal sample integrity biomarker assay that could be applied to each sample in a clinical study, should focus on the analysis of an endogenous analyte which would empirically and quantitatively reveal the integrity of the sample, representing the inevitable molecular modifications generated through biochemical reactions that take place when P/S samples are exposed to thawed conditions, throughout the entire life span of the sample (66). These modifications include enzyme-mediated biomolecular degradation, reaching an equilibrium state which is never reached in vivo, macromolecular denaturation, artifactual ex vivo oxidation etc. Molecular alterations that are used in the assay to track the integrity should not be prone to intentional modifications by any stabilization processes. Also, alterations considered in the assay in

the employed QA marker should take place in the similar time interval in which the most sensitive biomolecules used as biomarkers present in the P/S sample are changed beyond their original in vivo status.

Multiple efforts have been exerted to identify and develop potential markers that serve as an indicator for exposure to thawed conditions, yet none of these efforts turned out as completely developed quality control tools (67, 68). Soluble CD40 ligand (sCD40L) has been developed as a biomarker to test the integrity of serum samples (69). When serum samples are exposed to higher temperatures the level of sCD40L decreases and this assay can identify the exposure by measuring the sCD40L level by a commercially available ELISA. The shortcoming of this assay is that it has been studied only to detect sample exposure to temperatures above 20 °C and it is not suitable for plasma sample since the sCD40L is continuously secreted by platelets and increases the level of sCD40L in plasma samples. In a similar effort by Borges et al in 2014, the authors studied the possibility of utilizing two protein markers for oxidative stress as markers for biospecimen integrity of P/S samples(34). The two protein modifications they targeted were S-cysteinylation of human serum albumin (HSA) and methionine sulfoxidation of Human apolipoprotein A-I (apoA-I). They discovered increased level of these modifications were exhibited in P/S samples intentionally incubated at thawed conditions suggesting that these oxidative modifications are elevated by artificial ex vivo oxidation in improperly stored P/S samples (Figure1.1). S-cysteinlyation of HSA started within hours at room temperature and reached its peak within a week. Methionine sulfoxidation of apoA-I started to increase within a week at room temperature and continued to increase through 36 days. At -20 °C storage both reactions were slower than at room

temperature as expected, where HSA oxidation reached its plateau in 6 weeks and ApoA-I oxidation did not start until 3 months and continued to increase after 3 months. None of these modifications were observed to occur in P/S samples stored at -80 °C up to 300 days (34). These results suggest that s-cysteinylation of HSA has the potential to be developed as a marker to assess the P/S samples integrity.

1.8. Delta S-Cysteinylated Albumin (ΔS-Cys-Albumin) as a marker for biospecimen integrity

HSA is a highly water soluble multifunctional multi-domain monomeric globular protein with a molecular weight of 66.4 kDa. It is mainly synthesized by hepatocytes in liver and continuously secreted into the blood stream (70). It is the most abundant protein in human P/S that controls the colloid osmotic pressure of plasma and modulates fluid distribution between body compartments (71). HSA in blood or P/S samples is composed of 585 amino acids including 35 cysteine (Cys) residues, among which 34 are involved in forming 17 stabilizing structural disulfide bonds (70). The remaining Cys34 bears a free terminal sulfhydryl functional group representing the largest fraction of free thiol in human plasma providing antioxidant activity in blood. Cys34 is situated at the surface of HSA and is susceptible for oxidation that results in mixed disulfide bond formation. In healthy adult population majority of Cys34 remains in its free thiol form (70-80%) and the rest form mixed disulfides with cysteine, homocysteine or glutathione resulting in S-Cys-Albumin (70). Borges et al. showed that the percentage of S-Cys-Albumin increases when P/S are exposed to thawed conditions. High abundance of HSA in P/S samples enables relative quantification of the S-Cys-Albumin in these samples by a simple dilute and shoot liquid chromatography- mass spectrometry method (LC-MS) (34). Chapter 2 of

this dissertation discusses the efforts taken to develop and validate the relative quantification of S-Cys-Albumin as a marker for the detection of P/S exposure to thawed conditions. However, during the analysis of population range of the relative abundance of S-Cys-Albumin, it was noticed that some fresh samples displayed higher percentage of S-Cys-Albumin closer to the maximum percentage of S-Cys-Albumin that can be reached by some samples after a complete oxidation by intentional incubation at 37 °C. This restricted the utilization of the relative abundance of S-Cys-Albumin as a marker. Thus the ΔS-Cys-Albumin assay was developed and validated as an alternative approach. ΔS-Cys-Albumin is the difference in the relative abundance of S-Cys-Albumin before and after an incubation that drives the samples to reach complete oxidation. This assay has been used in a recent study and proven to be successful in identifying exposure to thawed conditions (65). For this study, plasma samples from lung cancer patients were collected from 12 different sites. ΔS-Cys-Albumin assay showed that 2 sites among the 12 showed abnormally low ΔS-Cys-Albumin values suggesting compromised sample integrity. This observation was well aligned with the fact that these samples were temporarily stored at -20 °C (43-271 days) where none of the other sites stored samples at -20 °C (65). One another occasion, this assay forced the investigators to disclose a major thaw incident during a natural disaster that occurred to the control samples (but not the cases) in sets of serum samples from stage I lung cancer patients as well as age/gender/smoking matched controls (64).

Several recent scientific publications have documented the timeframe that several clinical analytes lose their stability and these intervals are within the range that can be detected by ΔS-Cys-Albumin (Table1.1). Chapter 3 reports concurrent analysis of the stability of

proteins of clinical interest at 23 °C, 4 °C and -20 °C in along with ΔS-Cys-Albumin measurements with the aim of constructing an empirical linkage between the stability of proteins of clinical interest at all major storage temperatures and ΔS-Cys-Albumin.

1.9. An alternative approach to the delta ΔS-Cys-Albumin assay

Although the ΔS-Cys-Albumin assay possesses most of the qualities to be employed as a standard quality control marker for biospecimen integrity, it requires the use of LC/MS. Not all clinical laboratories are equipped with an LC-MS instrument and this limits the availability of this assay to most clinical laboratories. Converting this assay to a common plate reader-based format would bring access to this assay to almost all clinical and preclinical laboratories. Chapter 4 of this report discusses the development and validation of an absorbance-based alternative to the ΔS-Cys-Albumin assay.

Figures

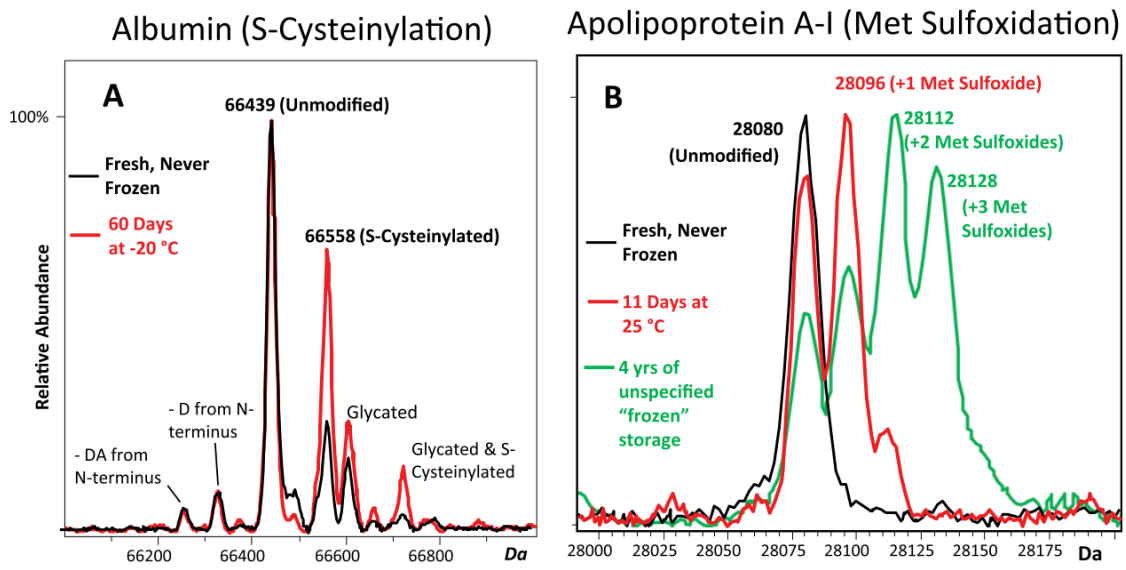

Figure1.1: Charge deconvoluted electrospray ionization mass spectra of (A) albumin and (B) ApoA-I from plasma samples from healthy donors. The figure shows increased abundance of oxidized proteoforms under sub-optimal storage conditions. The ΔS-Cys-Albumin value is the difference in the fractional abundance of S-Cys-Albumin between fresh and exposed samples. Obtained from Borges et al (2014)

Tables

Table 1.1: Targeted, multi-analyte stability studies conducted in plasma/serum showing the percent of clinical analytes that exhibited instability at various times and temperatures.

Plasma (P) or Serum (S)	Type of Biomolecule	Assay or Platform	Number of Analytes	Thawed condition	% of Unstable Biomolecules	Ref
P	**Proteins**	SOMAscan	1305	4 °C for 24 hrs	**2.1%**	(72)
P	**Proteins**	SOMAscan	1305	25 °C for 24 hrs	**5.7%**	(72)
P	**Proteins**	Luminex	22	4 °C for 24 hrs	**3.4%**	(73)
P	**Proteins**	Luminex	22	25 °C for 24 hrs	**11.0%**	(74)
P	**Proteins**	Luminex	25	-20 °C for 9 days	**8.0%**	(75)
P	**Peptides**	LC-MS/MS	43	4 °C for 24 hrs	**23.2%**	(74)
P	**Peptides**	LC-MS/MS	43	25 °C for 24 hrs	**39.5%**	(74)
P or S	**Hormones**	Cobas® or Liaison®	23	4 °C for 24 hrs	**8.7%**	(76)
P or S	**Hormones**	Cobas® or Liaison®	23	25 °C for 24 hrs	**17.4%**	(76)
P or S	**Hematology Markers**	Advia 120® or STAR®	19	4 °C for 24 hrs	**5.3%**	(76)
P or S	**Hematology Markers**	Advia 120® or STAR®	19	25 °C for 24 hrs	**5.3%**	(76)
P or S	**Ions/ Metabolites**	Modular® PP	39	4 °C for 24 hrs	**2.6%**	(76)
P or S	**Ions/ Metabolites**	Modular® PP	39	25 °C for 24 hrs	**7.7%**	(76)
P	**Metabolites**	LC-MS/MS or GC/MS	237	4 °C for 24 hrs	**3.5%**	(74)
P	**Metabolites**	LC-MS/MS or GC/MS	237	25 °C for 24 hrs	**11.0%**	(74)
P	**Metabolites**	LC-MS/MS or GC/MS	262	4 °C for 16 hrs	**11.5%**	(77)
P	**Metabolites**	LC-MS/MS or GC/MS	262	25 °C for 16 hrs	**23.2%**	(77)
S	**Metabolites**	LC-MS/MS	127	25 °C for 12 hrs	**17.3%**	(78)
S	**Metabolites**	LC-MS/MS or GC/MS	225	25 °C for 24 hrs	**21.0%**	(79)

CHAPTER 2

DELTA-S-CYS-ALBUMIN: A LAB TEST THAT QUANTIFIES CUMULATIVE EXPOSURE OF ARCHIVED HUMAN BLOOD PLASMA AND SERUM SAMPLES TO THAWED CONDITIONS

2.1. Preamble

In this chapter, linearity assessment, population range survey, and time course incubation analysis at different temperatures were conducted by me and everything else was conducted by Dr. Joshua Jeffs. To give a complete context to the reader, this chapter includes all the experiments conducted to completely validate the assay. This chapter is a reformatted version of a paper that was published in 2019 (64).

2.2. Introduction

Collection, processing, storage, and handling expose clinical biospecimens to pre-analytical variables that, when unaccounted for, have the potential to produce misleading results in downstream clinical research (26, 33, 80–82). For blood plasma and serum (P/S) samples, numerous pre-analytical variables such as the type of collection tube, degree of tube filling, number of tube inversions, degree of hemolysis, and pre-centrifugation delay can quantitatively impact clinical measurements (28, 31, 83, 84). Arguably, however, exposure to the thawed state (i.e. temperatures >30 °C (50)) is the most difficult pre-analytical variable to track and control over the lifetime of a P/S biospecimen particularly at the individual aliquot level.

There is widespread agreement regarding the need for robust biospecimen quality control (QC)/quality assurance (QA) checks in biomarker discovery and validation work. Yet

relatively little research effort focuses on this arena. P/S specimens are among the most commonly employed biospecimens in biomarker-related research but, to date, no gold standard marker of P/S integrity has been identified and put into widespread, routine use. This is evidenced by the fact that despite the recent emphasis on robustness and reproducibility, the U.S. National Cancer Institute (NCI, part of the National Institutes of Health) does not currently require any empirical evidence based QA thresholds be met before preexisting P/S specimens are employed in NCI-sponsored research. This QC/QA problem is widespread: In 2014, for example, out of 455 NCI-sponsored extramural grants that involved biospecimens, 287 (63%) relied on pre-existing samples; over 100 of these sponsored projects employed pre- existing P/S (85).

Written documentation that includes the types of specimens analyzed and the specimen storage conditions is now required for manuscript submissions to leading clinical research journals (36, 38, 39), but as we have experienced and describe herein, paper trails are insufficient to guarantee disclosure of incidents that may compromise specimen integrity. The possible reasons for this are rarely discussed but may range from poor note taking to conflicts of interest with disclosing incidents that may have resulted in biospecimen damage. Moreover, paper trails lack the ability to rigorously quantify the molecular integrity of specimens that may have experienced minor “exposure” incidents that are either not captured in the documentation or, if they were, cannot be precisely assigned to individual samples or aliquots. Yet if temperature unstable or even potentially temperature unstable markers are to be analyzed in a set of P/S samples, it is critically important to know the biomolecular integrity of every sample.

This line of reasoning implies that a gold standard metric of P/S integrity should involve some form of empirical, quantitative biomolecular analysis that, if necessary, could be applied to every sample in a clinical study (whether the sample was collected prospectively or is to be analyzed retrospectively) even if the study employed thousands of P/S samples. As such, the ideal assay would focus on endogenous analyte(s), require a very low sample volume, require minimal sample preparation, be automatable from the point of fully frozen P/S to the point of generating the final report, and be both inexpensive and rapid. Moreover, the majority, if not all, of the representative molecular alterations caused by unavoidable (bio)chemical processes that occur on P/S exposure to the thawed state should be captured by the integrity marker. Such processes include (1) drifting toward an equilibrium state that is never actually reached in vivo, (2) ex vivo oxidation (because of P/S samples taking on a dissolved oxygen concentration of up to 0.25 mM (86, 87) a concentration that is orders of magnitude higher than that observed in the P/S compartment in vivo where oxygen is primarily carried on hemoglobin inside red blood cells), (3) enzyme-mediated biomolecular degradation, and (4) macromolecular denaturation. Additionally, changes in the QA marker(s) should occur in the same time frame in which some of the most "fragile" time-sensitive biomolecules within the P/S sample are altered beyond their original in vivo status. And finally, if intended as generally representative, thawed-state sensitive changes in QA marker(s) should neither be inhibited nor accelerated by stabilization practices that focus on a single mechanism of ex vivo alteration such as protease inhibitors or heat-based "inactivation."

Together, these characteristics are quite stringent and are unlikely to be met by a single QA analyte or assay. As such, it should at least be possible to link changes in the QA

marker to changes in specific analytes of interest by analyzing both concurrently. When linked empirically, this is possible for most imaginable QA markers. However, the best QA markers will be those for which a (bio)chemical rate law can be determined. This will make it possible for the marker(s) to serve as a molecular stopwatch for the timespan of thawed-state exposure and effectively place an exposure time stamp on each sample. With the rate law for the QA marker established, it would be possible for any investigator to link their assay(s) of interest to the QA marker by simply following good assay development guidelines and conducting a stability time course with their clinical analyte(s) of interest.

In 2014 we reported that two of the most abundant P/S proteins, albumin and apolipoprotein A-I, were susceptible to ex vivo oxidation events that occur over two non-overlapping time segments in P/S specimens exposed to temperatures >-30 °C yet the proteins were stable when P/S was kept at -80 °C (34). These proteins were measured in a single dilute-and- shoot LC-MS assay of the intact proteins that required less than 1 µl of P/S (34). It was clear that albumin oxidation (S-cysteinylation of its single free cysteine residue) would meet most of the ideal QA marker specifications described above, but the in vivo reference range for the percentage of albumin in this oxidized state and the multireaction rate law for the formation of S-cysteinylated albumin were not known. Subsequently (and as reported herein), we made measurements that provided an estimate of the population reference range for the fraction of albumin in its S-cysteinylated form (S-Cys-Albumin), but found that it was close to the maximum degree of S-cysteinylation obtained by some samples ex vivo i.e. once albumin had consumed all of the free cysteine (Cys) and cystine (Cys-Cys) equivalents present. This limited, in theory, the

useable dynamic range of S-Cys-Albumin as a P/S QA marker. Nevertheless, the population reference range for albumin in P/S is known (88) and those for Cys and Cys-Cys in plasma are well estimated (89, 90). Thus assuming that albumin is the only significant oxidative consumer of Cys equivalents, it is possible to calculate that if S-Cys-Albumin is measured in a fresh plasma sample then intentionally driven to its maximum possible value ex vivo (34), 99% of the human population under age 60 should experience a change in S-Cys-Albumin between these two measurements (ΔS-Cys-Albumin) of 11–30%. (This range increases in persons over age 60 to 17–38% because albumin concentrations decrease (91) and Cys-Cys concentrations increase (89) with age.) Charge deconvoluted ESI-mass spectra of albumin that illustrate the ΔS-Cys-Albumin phenomenon are provided in **Figure 2.1**. Given that the inter-assay precision for measurement of S-Cys-Albumin is 1.6% (34) and thus for ΔS-Cys-Albumin is 2.2% (92), we intentionally pursued ΔS-Cys-Albumin as a QA marker for exposure of P/S samples to the thawed state.

Here we report development of an assay for S-Cys-Albumin, estimates for the population reference ranges for S-Cys-Albumin and ΔS-Cys-Albumin, and the multireaction rate law for formation of S-Cys-Albumin at room temperature (which facilitates back calculation of P/S sample exposure times). We also provide insights into the role of dissolved oxygen in driving S-Cys-Alb formation, the results of a blind challenge of the ability of ΔS-Cys-Alb to detect exposures of both groups of P/S samples and individual P/S samples to the thawed state, and an unplanned case study in which ΔS-Cys-Alb detected and subsequently prompted disclosure of a biospecimen integrity discrepancy in a set of nominally pristine serum samples collected under NIH sponsorship.

2.3. Materials and Methods

2.3.1. Materials and Reagents

Highly purified human serum albumin (Cat. No. A3782), L-cysteine (C7352), trifluoroacetic acid (TFA, 299537), L-Cystine dihydrochloride (C6727), Amicon Ultra-4 centrifugal filter, MWCO = 50 kDa (Z740191), Maleimide (129585), Sodium hydroxide (367176), HEPES (H3375) and Sodium chloride (S7653) for preparation of HEPES-buffered saline solution (HBS buffer) were purchased from Sigma-Aldrich (St. Louis, MO). LC-MS grade Acetonitrile (TS- 51101), LC-MS grade water (TS-51140), Hydrochloric acid (50-878-166), Pierce BCA protein assay kit (23227), and Methanol (A456) were purchased from ThermoFisher Scientific (Waltham, MA). Chelex 100 resin (1421253) was purchased from Bio-Rad Laboratories (Hercules, CA). SPE cartridges (SPE-P0005-03BB) purchased from Silicycle (Quebec, Canada). L-Cystine-3,3,3',3'-D4 (DLM-9812-PK) was purchased from Cambridge Isotope Laboratories, Inc. (Andover, MA). N- Methyl-N-Trimethylsilyl Trifluoroacetamide (MSTFA) (24589-78-4) was purchased from Regis Technologies (Morten Grove, IL). All non-LC-MS solvents were of HPLC grade.

2.3.2. Collection of plasma and serum samples

Matched K_2EDTA plasma and serum samples were collected under informed consent and IRB approval from non-acute cardiac patients presenting with chest pain suggestive of coronary artery disease and undergoing coronary angiogram, cardiac stress test and/or coronary computed tomography angiography at Maricopa Integrated Health System. Patients were a 40/60 mixture of females/males, ranging in age from 34–85 years (mean ± S.D. was 60 ± 9.6 years). None of the patients had severe or end-stage renal disease

(i.e. estimated glomerular filtration rate, eGFR < 30 ml/min*1.73 m^2) and none were on hemodialysis; only 11 had eGFR values < 60 ml/min*1.73 m^2. Samples were collected and processed as described above for the healthy volunteer. Times of draw, centrifugation and placement at -80 °C were recorded for every individual sample. Sample hemolysis was noted by visual comparison to a color chart, resulting in placement of samples into categories of minimal, mild, moderate, and high hemolysis corresponding to < 20 mg hemoglobin/dL, 20–50 mg/dL and 50–250 mg mg/dL and > 250 mg/dL, respectively. Samples with > 250 mg/dL hemolysis were excluded; results from such samples are not reported herein.

2.3.3. Measurement of S-Cys-Albumin and ΔS-Cys-Albumin in cardiac patients

P/S samples were 1000x diluted with 0.1% TFA, by mixing 0.5 µL P/S sample with 500 µL of 0.1% TFA in a 1500 µL Eppendorf snap-cap polypropylene test tube. Ten microliters of the diluted sample was immediately injected into LC-MS and analyzed. Then 9.5 µL of the same original P/S (undiluted) sample was placed into a 600 µL Eppendorf snap-cap polypropylene test tube and incubated in a 37 °C oven for 18 hours to drive the sample to reach its maximum level of S-Cys-Albumin to measure the ΔS-Cys-Albumin. After the incubation, the sample was diluted 1000x with 0.1% TFA in a similar manner and then shot onto the LC-MS. The difference between relative abundance of S-Cys-Albumin before and after this 18-hours incubation at 37 °C represents constitutes ΔS-Cys-Albumin. Notably, for all measurements of S-Cys-Albumin, matched plasma and serum samples were prepared by the same analyst and analyzed one right after another (interspersed) on the LC/MS instrument.

2.3.4. LC-ESI-MS analysis

The data reported here were collected on different instruments using a modified HPLC step- gradient that provided nearly complete chromatographic separation of albumin and apolipoprotein A-I. Relative quantification of intact albumin proteoforms was done by liquid chromatography-electrospray ionization-mass spectrometry (LC-ESI-MS) on either a Dionex Ultimate 3000 HPLC equipped with a 1:100 flow splitter connected to a Bruker maXis 4G quadrupole-time-of-flight (Q-TOF) mass spectrometer or an Agilent 1260 Infinity II HPLC connected to an Agilent 6530 ESI-Q-TOF instrument. Both instruments have an ion source design in which the spray needle is held at ground and the inlet of the instrument is brought to a high negative potential in positive ion mode. The Agilent instrument was employed for time course measurements at different temperatures, linearity evaluation, and for ~ 2/3 of the ΔS-Cys-Alb population measurements; the Bruker instrument was used ~ 1/3 of the population measurements. In the following instrument and data processing descriptions, Agilent instrument parameters are listed in brackets next to the Bruker instrument parameters: A trap-and-elute form of LC-MS was carried out in which 5 µL [10 µL] of sample was loaded via a loading pump at 10 µl/min [200 µl/min] in 80% water containing 0.1% formic acid (Solvent A) / 20% acetonitrile [containing 0.1% formic acid] (Solvent B) onto an Optimize Technologies protein captrap configured for uni-directional [bi- directional] flow on a 10-port diverter valve. The trap was then rinsed at this solvent composition with the HPLC loading pump at 10 µl/min [200 µl/min] for 3 minutes [1 minute]. The flow over the captrap was then switched to the micro pump, which was set at a flow rate of 3 µL/min [200 µl/min] and composition of 65/35 A/B. This composition was held until 4.5 min [2.5 min.]. From 4.5-

4.6 min. [2.5-2.6 min.] the composition was ramped to 55/45 A/B then held. From 7.5-7.6 min. [5.5-5.6 min.] the composition was ramped to 20/80 A/B then held. Then from 9.4-9.5 min.[6.6-6.7 min.] the composition was ramped back to 80/20 A/B in preparation for the next injection. Following the valve switch at 3 minutes [1 minute], the captrap eluate was directed to the mass spectrometer operating in positive ion, TOF-only mode, acquiring spectra in the m/z range of 300 to 3000 [100 – 3,200]. ESI settings for the Agilent G1385A [dual AJS ESI] capillary microflow nebulizer ion source were as follows: End Plate Offset -500 V, Capillary -4500 V [VCap 5,700 V; nozzle voltage (expt) 2,000 V], Nebulizer nitrogen 3 Bar [45 psig], Dry Gas nitrogen 3.0 L/min at 225 °C [7 L/min at 325 °C; sheath gas 11 L/min at 250 °C]. Data were acquired in profile mode at a digitizer sampling rate of 4 GHz. Spectra rate control was by summation at 1 Hz.

Data Analysis: As previously described (34), approximately 1 minute of recorded spectra were averaged across the chromatographic peak apex of albumin. The electrospray ionization charge- state envelope was deconvoluted with Bruker DataAnalysis v4.2 software [MaxEnt software] to a mass range of 1000 Da on either side of any identified peak. Charge deconvolution settings were established to ensure that the relative peak widths and signal-to-noise ratios of the raw spectra were reproduced in the deconvoluted spectra. Deconvoluted spectra were baseline subtracted to the same degree on both instruments, and all peak heights were calculated, tabulated and exported to a spreadsheet for further analysis. Peak heights were used for quantification as opposed to peak areas, because of the lack of baseline resolution for some of the peaks.

2.3.5. Linearity Assay

To check the linearity of S-Cys-Alb measurements, known ratios of the native form (completely reduced) and S-cysteinylated (completely oxidized) albumin were mixed in 10% increments from 0 to 100% of S-Cys-Alb resulting in a final HSA concentration of 0.78 mM. This required creating and isolating fully reduced form of albumin (AlbSH) where no S-Cys-Albumin present and fully S-Cys-Albumin where no AlbSH form is present. Pure AlbSH was prepared starting with a 1 mM concentration of commercially prepared albumin in HBS buffer (pH 7.4). The sample was aliquoted into 500 µL volumes and mixed with 300 µL of 10 mM Cys, followed by incubation for 1 hour at room temperature. After the incubation period, 1 µL of sample was diluted in 600 µL of 0.1% TFA and analyzed to verify complete reduction of albumin. The aliquots were then split into 200 µL aliquots in Amicon Ultra- 4 centrifugal spin filters (MWCO 50K). Each sample had 4 mL of HBS buffer added and then was centrifuged for 10 minutes at 4,000 x g to a final volume of approximately 200 µL, this process was repeated 7 times, facilitating Cys removal and protein concentration. All aliquots were then combined and albumin concentration was determined with a BCA protein assay, following the manufacturer's protocol. In order to verify that no structural disulfide bonds were reduced and only the free Cys residue (Cys34) was reduced in the reduced sample, 5 µL of AlbSH was incubated with 5 µL of 50 mM maleimide in ammonium acetate buffer (pH 5). This was incubated at 50 °C for 15 minutes and then 1 µL of sample was mixed with 500 µL of 0.1% TFA and analyzed by LC-MS (**Figure 2.2**). Pure S-Cys-Alb was obtained by following the same protocol but instead incubating 0.5 mM commercially prepared albumin with 1 mM Cys-Cys. All samples were stored at -80 °C until further

analysis. To eliminate copper catalyzed reoxidation of AlbSH, trace quantities of copper and other transition metals were minimized by pre-treating all buffers with Chelex 100 resin per the manufacturer's batch wise instructions. The S-Cys-Albumin and AlbSH forms of HSA were mixed in different ratios resulting in 0.78 mM final concentration of HSA and 40 µL total volume as mentioned above. These samples were diluted 500x by mixing 1 µL of the prepared sample with 500 µL of 0.1% TFA and analyzed in technical replicates at each ratio.

2.3.6. Time course incubations

P/S samples from three patients each with high, medium and low values for ΔS-Cys-Albumin were selected from the population. Several 50 µL aliquots of matched plasma and serum from these three patients were incubated at 23 °C, 4 °C, and -20 °C for 4, 28, and 65 days, respectively. There were separate aliquots (50 µL) dedicated for each time point. After each incubation, the level of S-Cys-Albumin was measured. Then, 9 µL of these samples were intentionally oxidized to the maximum level by incubation at 37 °C for 18 hours, the level of S-Cys-Albumin was recorded and ΔS-Cys-Albumin values were calculated.

2.3.7. Rate Law Determination

The rate law for formation of S-Cys-Albumin in the P/S environment is governed by the chemical reactions listed in **Figure 2.3**. The rate law for Equation 2 was previously determined by Kachur et al. (93). Thus, to obtain a complete combined rate law for formation of S-Cys-Albumin, the rate laws for the forward and reverse reactions described in Equation1 were determined using the method of initial rates. The approach

to rate law determination entailed measuring the initial rate of the forward (and, separately, reverse) reaction by plotting S-Cys-Alb (or AlbSH) concentration in molar units (M) vs. time (s). The initial phase of these plots was linear. From this initial linear phase, the slope was obtained and recorded as the initial rate (vo). This process was repeated for multiple starting concentrations of reactants in which none of the products were initially present. This latter requirement made it necessary to create and isolate AlbSH in which no S-Cys-Alb was present and, for the reverse reaction, S-Cys-Alb in which essentially no AlbSH was present. Pure AlbSH and S-Cys-Albumin were prepared using the same protocols mentioned in the linearity assay experiments. To eliminate interference from equation 2 of **Figure 2.3** during the rate law determinations, trace quantities of copper and other transition metals were minimized by pre-treating all buffers with Chelex 100 resin per the manufacturer's batch-wise instructions. Desferrioxamine (0.2 mM) was also added to the buffers employed in rate law determinations. To determine initial rates, pure AlbSH at concentrations ranging from 30-60 μM or pure S-Cys-Alb (30-90 μM) were incubated with free Cys-Cys or Cys (300-900 μM) at 23 °C, respectively (**Table 2.1** & **2.2**). A control sample with no added Cys-Cys or Cys was also prepared to ensure that no artefactual oxidation or reduction occurred. Time courses for albumin oxidation and reduction were acquired by diluting 0.5 μL of a sample into 0.1% TFA to a final concentration of 1 μM albumin at various time points, which was then analyzed by LC-MS to provide time point concentrations of S-Cys- Alb and AlbSH. Time points were taken more frequently during the initial linear portion which yielded a slope that was used to determine the initial rate of reaction for each of the varying concentrations. The method of initial rates was then used to determine the

reaction orders and rate constants for the disulfide-exchange oxidation and reduction of albumin (94). Slopes of log vo vs. log reactant concentration (at several concentrations of the second reactant) were used to determine reaction orders and non-linear regression of the entire forward-reaction dataset and reverse reaction dataset was employed to determine the forward and reverse rate constants, respectively.

2.3.8. Rate Law-Based Model Verification in Actual Serum and Plasma

Immediately following collection, matched serum and K_2EDTA plasma from a healthy donor were each split into two 95-µL portions: One portion was spiked with Cys and Cys-Cys (in 5 µL of HBS buffer, pH 7.4) to increase the concentration of Cys by 12 µM and the concentration of Cys-Cys by 62 µM; the second portion was diluted by the same amount but without added Cys or Cys-Cys. These specimens were then incubated at 23 °C for 4 days, with numerous measurements of S-Cys-Alb collected initially and then at least once a day after Day 1. The data were then fit with the predictive model (using Wolfram Mathematica 10.2 or MatLab 2016), using the empirically determined initial concentrations of all species, determined as follows:

Fresh aliquots of matched P/S samples were sent to ARUP Laboratories to determine concentrations of albumin (total), free copper and total copper. Initial fractions of S-Cys-Alb and AlbSH were determined using the S-Cys-Alb assay described above. These fractions were then converted to actual concentrations by multiplying by the total albumin concentration.

Cys-Cys concentration was determined from quadruplicate aliquots of serum and, separately, plasma using solid phase extraction (SPE) and gas chromatography-mass

spectrometry (GC-MS) with procedures adapted from previously published reports (95–97). Calibration curve samples were prepared in 40 mg/ml albumin in HBS buffer (pH 7.4) with the addition of 0, 15, 30, 45, 60, or 90 μM of Cys-Cys. Three microliters of 2 mM Cys-Cys-d_4 internal standard in 1 M ammonium hydroxide and 1 M ammonium bicarbonate (pH 9.4) was combined with 96.5 μL of P/S and calibration curve samples, followed by 0.5 μL of 1 mM Cys-d_3 internal standard in 1 M ammonium hydroxide and 1 M ammonium bicarbonate (pH 9.4). Proteins were then immediately precipitated by first adding 200 μL of acetonitrile and then 300 μL of 0.2 M HCl which lowered the sample pH, minimizing disulfide exchange reactions. Samples were incubated on ice for 30 minutes and then centrifuged for 2 minutes at 13,000xg to remove protein precipitate. Sample supernatant was then stored on ice until ready for cation exchange SPE. The SPE cartridges were conditioned with 2 mL acetonitrile and then equilibrated with 2 mL of 0.1 M HCl. The entire sample was then loaded onto the cartridge and washed with 2 mL methanol. Samples were then eluted with 2 mL of 5% ammonium hydroxide in methanol into silanized glass test tubes and then dried down using a Savant SC250EXP SpeedVac Concentrator. After samples were dry, 50 μL of acetonitrile and 50 μL of N-methyl-N-(trimethylsilyl)trifluoroacetamide (MSTFA) were added and then incubated for 30 minutes at 85 °C. Samples were then loaded into GC-MS autosampler vials and injected onto the GC-MS.

GC-MS analysis was carried out on an Agilent Model A7890 gas chromatograph (equipped with a CTC PAL autosampler) coupled to a Waters GCT (time-of-flight) mass spectrometer. One microliter of the sample was injected in split mode onto an Agilent split-mode liner that contained a small plug of silanized glass wool. The injector

temperature was set at 280 °C and the split ratio was 5:1. The carrier gas was regulated in constant flow mode at 0.8 mL/min. The capillary column was a 30-m fused silica DB-5MS with a 0.25 μM film thickness and 0.250 mm inner diameter. The temperature program was started at 100 °C with initial holding for 1 minute and was increased at the rate of 10 °C/min to 300 °C and held for 3 minutes. The temperature was then increased 30 °C/min to 325 °C, with final holding of 3 minutes. The temperature of the transfer line to the MS was 280 °C. Mass spectra were obtained by standard (70 eV) electron ionization scanning from m/z 40 to 800 at a spectral accumulation rate of 0.09 seconds/spectrum.

Quantification was done by integrating summed extracted ion chromatogram (XIC) peak areas, using QuanLynx software. The peaks were integrated automatically and verified manually. The extracted ions (± 0.15 m/z units) used for quantification were: Cys-Cys (m/z 411.1 and 232.1), Cys-Cys-d_4 (m/z 415.1 and 234.1), Cys (m/z 220.1, 232.1, and 322.1), Cys-d_2 (which results from reduction of Cys-Cys-d_4 during derivatization as described below; m/z 222.1, 234.1, and 324.1) and Cys-d_3 (m/z 223.1, 235.1, and 325.1). All summed XIC peak integrals were exported to a spreadsheet for further analysis.

Cys-Cys is partially reduced to Cys during the derivatization step that is necessary to facilitate analysis by GC-MS. As such, Cys ions were used in the quantification of Cys-Cys. However, in order to use Cys in this quantification scheme it was necessary to subtract out any signal that was due to the endogenous Cys. This was done by spiking in 5 μM Cys-d_3 into each sample, which is equivalent to the concentration of endogenous Cys in P/S samples (as explained in the next paragraph and illustrated in **Figure 2.4**). The

magnitude of the summed XIC areas from Cys-d_3 was then assumed to represent the magnitude of the summed XIC areas from endogenous Cys. Thus, the total area of the summed XICs from Cys-d_3 was subtracted from the summed XIC areas of endogenous Cys. All residual summed XIC peak area from Cys ions was then considered to be derived from Cys-Cys. Prior to making this calculation, however, isotopic overlap between natural forms of Cys ions and their d_2-labeled internal standard counterparts was corrected for based on the known isotopic distribution of each fragment ion employed for quantification. This isotope correction procedure was analogous to that which has previously been employed and widely used elsewhere (98, 99).

Given the initial concentrations of AlbSH, S-Cys-Alb, free and total copper, and Cys-Cys determined above, all rate law models with initial Cys concentrations anywhere within the physiologically observed range (89, 90) revealed that by the time plasma and serum were separated from whole blood, the concentration of Cys in P/S had equilibrated to a steady state concentration of ~ 5 μM (**Figure 2.4**). Given this information and the fact that, relative to Cys-Cys, Cys contributes ≤ 5% of the total Cys equivalents in P/S, an initial Cys concentration of 5 μM was assumed in all kinetic models.

2.3.9. Statistical analysis

Statistical analyses and nonlinear regression were carried out with Graphad Prism 8.1.0. Statistical power calcu- lations were made using Piface version 1.76.

2.4. Results

2.4.1. Time and temperature for the ex vivo incubation

The highest temperature to which human P/S is exposed in its normal in vivo environment is 37 °C; as such, this temperature was chosen as the intentional ex vivo incubation temperature for the ΔS-Cys-Albumin assay. To determine the time required to maximize S-Cys-Albumin, as well as the impact of blood collection type and the effect of varying Cys and Cys-Cys concentrations on the time required to reach a maximum value of S-Cys-Albumin, a matched collection of K_2EDTA plasma, sodium heparin plasma, and serum from a healthy donor was ob tained and S-Cys-Albumin was measured in the freshly processed samples. Portions of each specimen were then fortified with an additional 1 µM Cys and 10 µM Cys-Cys or 2 µM Cys and 20 µM Cys-Cys. These added concentrations represent ~ 1 and 2 standard deviations (SDs) of the mean values of ~ 10 µM Cys and ~ 62 µM Cys-Cys seen in the plasma of typical donors (89, 90). Nine microliter aliquots of each unique P/S sample were then incubated in sealed 0.6-ml tubes at 37 °C and S-Cys- Alb was measured at 4, 18, 24 and 30-h time points. (Three separate 9-µl aliquots were made for each time point.) Differences between matched serum and plasma were negligible, with all specimens reaching their maximum value of S-Cys-Albumin by 18 h. Addition of Cys and Cys-Cys to the samples resulted in a higher maximum value of S-Cys-Albumin but did not alter the time required to reach it (**Figure 2.5**).

2.4.2. ΔS-Cys-Albumin Assay Precision, Linearity, Accuracy, Sensitivity, and Limits of Detection

As stated in the introduction, we previously determined the inter-assay precision for measurements of S-Cys-Albumin to be 1.6% (34). Because ΔS-Cys-Albumin is the difference between two S-Cys-Albumin measurements, the precision of ΔS-Cys-Albumin can be calculated by propagating the error for this subtractive operation (92); when done so it is found to be 2.2%. Thus, for a ΔS-Cys-Albumin value of 20%, this corresponds to an inter-assay %CV of 11%.

To check the linearity completely reduced and oxidized forms of HSA were created. Complete reduction and oxidation of the HSA was confirmed by LC-MS analysis (**Figure 2.2A-B**). To ensure that no structural disulfide bonds were reduced during the reduction process, reduced HSA was alkylated with maleimide. The results showed that there was a mass shift of exactly +97 Da that is caused by alkylation at the free Cys34 residue in HSA (**Figure 2.2C**). The mass shift of exactly +97 Da, with no peaks at +2*97 Da (66,633 Da, corresponding to two alkylation events) or +3*97 Da etc. indicate that the reduced albumin possessed only a single free Cys residue as expected. This confirmed no structural disulfide bonds were reduced. The linearity of S-Cys-Albumin measurements was determined by mixing known ratios of fully reduced and fully oxidized (S-cysteinylated) albumin in 10% increments from 0 to 100% S-Cys-Albumin at a final concentration of 0.78 mM. Samples were then diluted 500-fold in 0.1% TFA and analyzed in technical replicates at each ratio (**Figure 2.6**). The slope ± S.E., y-intercept ± S.E., and R^2 value of the least-squares linear regression line were 1.0 ± 0.011, 0.76 ± 0.66, and 0.998, respectively. The slope of 1.0 indicates that the assay has unit sensitivity

(i.e. change in instrument read-out per unit change in known relative concentration). Limits of detection were not determined as this figure of merit is not important to this assay given that > 99% of the U.S population has P/S albumin concentrations in the range of 490–810 μM (88). Likewise, there is no need for measurements of S-Cys-Albumin in actual P/S that are < 5% or > 95% (see next section).

Overall accuracy was determined based on each data point from the aforementioned linearity experiment (**Figure 2.6**). The average deviation from the known percent abundance of S-Cys-Albumin was 0.78; the average absolute deviation was 1.2.

2.4.3. Population estimates

Nonacute cardiac patients presenting with chest pain suggestive of coronary artery disease undergoing coronary angiogram, cardiac stress test and/or coronary computed tomography angiography at the recom- mendation of a cardiologist are likely to be individuals under continual low to moderate levels of systemic oxidative stress, a situation that could potentially raise their endogenous levels of S-Cys-Albumin above that of nominally healthy individuals. As such, these cardiac patients represented a clinical population that could potentially pose a challenge to the theoretically usable dynamic range of the ΔS-Cys-Albumin assay. To estimate the typical values of S-Cys-Albumin and ΔS- Cys-Alb observed in fresh samples from these patients, matched K_2EDTA plasma and serum samples were collected from 106 of them. P/S specimens were collected under rig- orous guidelines to ensure the highest possible sample quality. Accordingly, samples from 9 patients were excluded because of hemolysis > 250 mg/dL (n = 7) or patient history of hemodialysis/kidney failure (n = 2; eGFR < 30 ml/min*1.73

m^2). Fresh K_2 EDTA plasma and serum were found to have similar but significantly different values of S-Cys-Albumin (paired t test, $p < 0.001$; **Figure 2.7**). Following incubation of 9 µL aliquots at 37 °C for 18 h, S-Cys-Albumin was measured again and the difference between the two meas urements was recorded as ΔS-Cys-Albumin. Both the maximum value of S-Cys-Albumin and ΔS-Cys-Albumin were found to be significantly higher in plasma than serum (paired t test, $p < 0.001$; **Figure 2.7**). All distributions were Gaussian (D'Agostino and Pearson normality test; $p > 0.05$). The mean value of ΔS-Cys-Albumin in cardiac patient plasma ± 95% CI of mean was 20.9% ± 0.75% and in serum was 15.5% ± 0.64%. Standard deviations were 3.7% and 3.2%, respectively. Empirically, these values suggest that ΔS-Cys-Albumin values in 95% of fresh cardiac patient plasma and serum samples will fall in the ranges of 14–28% and 9.1–22%, respectively.

2.4.4. Time Courses

Fifty microliter aliquots of matched serum and plasma from three patients selected from each of the three tertiles of the population distributions for ΔS-Cys-Albumin were incubated at 23 °C, 4 °C, and -20 °C for 4, 28, and 65 days, respectively (**Figure 2.8**). Separate 50 µL aliquots were employed for each time point. Inter-individual variability in the (nonlinear) rates of decay of ΔS-Cys-Albumin in both serum and plasma was evident at all temperatures.

2.4.5. Quantitative Model for Ex vivo Formation of S-Cys-Albumin Determination

2.4.5.1. Determination of Rate Laws

The major reactions that govern the ex vivo formation of S-Cys-Albumin in P/S include Eq. 1 and Eq. 2 in **Figure 2.3**. The average initial starting concentrations of each reactant and product in P/S are known. As such, knowledge of the rate law governing the formation of S-Cys-Albumin coupled with measurement of ΔS-Cys-Albumin could, in theory, provide an estimate of the time spent by P/S samples at the temperature at which the rate law was determined. The rate law (including k_3) for Eq. 2 was previously determined by Kachur et al. (93); the rate laws for the forward and reverse reactions in Eq. 1 of **Figure 2.3** were determined here at 23 °C. Eq. 1 (**Figure 2.3**) is initially linear in both the forward and reverse directions (**Figure 2.9**). Thus, to be able to model a simultaneous system of chemical reactions comprised of Eqs. 1 and 2, the forward and reverse rate laws for Eq. 1 were determined using the method of initial rates (94). To obtain albumin in fully reduced or fully oxidized form, high purity human se- rum albumin was fully reduced with Cys or fully oxidized with Cys-Cys, then spin-filtered to purify and concentrate the protein. Verification of complete reduction and oxidation was carried out by LC-MS analysis of the intact protein following alkylation with maleimide to verify that no structural disulfide bonds were reduced (**Figure 2.2**). Starting conditions for all incubations employed to determine the forward and reverse rate laws for Eq. 1 of **Figure 2.3** are provided in supplemental **Table 2.1** and **2.2**., respectively. The slopes of plots of log v_o (initial rate) versus log [reactant concentration] (for several different co-reactant concentrations) revealed that the reaction order for all species in Eq. 1 (**Figure 2.3**) was 1 (**Figure 2.10**). Subsequently, the data in **Table 2.1** were fit to Eq.3 (**Figure**

2.3) and nonlinear regression was employed to determine that $k_1 = 0.095 \pm 0.017\ M^{-1}s^{-1}$. Likewise, the data in **Table 2.2** were fit to Eq. 4 **(Figure 2.3**) and nonlinear regression was employed to determine that $k_2 = 3.37 \pm 0.44\ M^{-1}s^{-1}$. Given that k_1 and k_2 were determined at 23 °C, their values are consistent with the values of $0.6 \pm 0.1\ M^{-1}s^{-1}$ and $6.6 \pm 0.4\ M^{-1}s^{-1}$, respectively, that were recently determined by Bocedi et al. at 37 °C (100).

Once the forward and reverse rate laws for Eq. 1 had been determined, a series of differential equations that simultaneously consider the chemical reactions in Eqs. 1 and 2, and their respective rate laws, were assembled (**Figure 2.3 Eqs.5-8**). In Equations 5–8, [Cu(II)] is the total concentration of copper (which stays constant), and K_y and K_z represent the first and second equilibrium dissociation constants pertaining to Cys complexation of Cu(II) that are involved in the copper- catalyzed oxidation of Cys to Cys-Cys at pH 7.4 as described by Kachur et al. (93). Eqs. 5–8 cannot be solved explicitly, but numerical solutions at any point in time are obtainable once all constants and starting concentrations are supplied.

2.4.5.2. Assessment of Quantitative Model in Serum and Plasma

To evaluate the ability of the combined rate law model (**Figure 2.3 Eqs. 5–8**) to predict formation of S-Cys-Albumin in actual serum and plasma, matched serum and plasma were collected from a healthy donor. Serum was collected into and handled in trace metal-free tubes to facilitate quantification of copper. Initial concentrations of S-Cys-Albumin, AlbSH, Cys-Cys and free and total copper for use in the predictive model were made as described in Materials and Methods. Measurement of Cys was deemed unnecessary because according to the model, by the time serum or plasma are processed

from whole blood the concentration of Cys drops to a steady state at about 5 µM—regardless of whether or not the initial concentration starts at the low or high end of physiological Cys concentrations observed in human plasma (**Figure 2.4**), and which, in terms of Cys equivalents, is within the error of Cys-Cys quantification. Immediately following collection, aliquots for measurement of initial reactant and product concentrations were created and sent out for analysis or kept in-house at -80 °C until they were analyzed. A 100 µL aliquot of each specimen in a closed 1.5-ml snap-cap tube was then incubated at 23 °C for 4 days on a rotating vortex mixer (200 RPM), with numerous measurements of S-Cys-Albumin collected initially and then at least once a day after Day 1. The data were then fit with the predictive model, using the empirically determined initial concentrations of all species along with rate and equilibrium constants pertinent to the model, determined as described above (k_1 and k_2; Eq. 1 at 23 °C) or as previously determined (k_3, K_y and K_z; Eq. 2 at 37 °C (93)) (**Figure 2.11**). To best approximate the latter three parameters at the actual temperature of the experiment (23 °C), a value of -50 kJ/mol was estimated as the enthalpy of reaction per Cys ligand binding to Cu(II) based on the known enthalpy of Cys binding to other divalent cations (101) (the value for binding to Cu(II) is unknown). Integration of the van't Hoff equation provides the following formula to estimate the change in an equilibrium association constant (K) with temperature (T) given the estimated change in enthalpy (ΔH°) (94):

$$\ln K_2 = \ln K_1 - \frac{\Delta H^\circ}{R}\left(\frac{1}{T_2} - \frac{1}{T_1}\right) \qquad \text{(Eq. 9)}$$

where R is the ideal gas constant. Application of this formula to K_y and K_z resulted in a 2.5-fold decrease in each value (to 2.0×10^{-6} M and 3.5×10^{-4} M, respectively). The same

factor was applied to estimate k_3 as 0.13 s^{-1} as well—a factor in the middle of the range of the fold-change expected for a 14 °C decrease in temperature. All plasma copper was assumed to be catalytically available and half of serum copper, 95% of which is bound to ceruloplasmin (102), was assumed to be catalytically available because only about 40% of ceruloplasmin-bound copper resides in the Cu(II) oxidation state (103). The RMSD fit (expressed as %CV) of the model to serum was 6.1% and that for K_2EDTA plasma was 6.3% (**Figure 2.11**). Models in which only free copper, only the ~ 5% of copper not bound to ceruloplasmin, or all copper in serum were assumed to be catalytically available reveal that, as modeled, a major portion of bound copper must indeed be catalytically available (**Figure 2.12**). Additional models in which K_y, K_z , and k_3 were run at their 37 °C-values and 10-fold below these values are also provided to illustrate how shifts in these parameters impact the kinetic model (**Figure 2.13**).

Before initial freezing, separate aliquots of the matched serum and plasma samples were spiked with Cys and Cys- Cys (in a minimal volume of HBS buffer, pH 7.4) to increase the concentration of Cys by 12 µM and the concentration of Cys-Cys by 62 µM—putting these concentrations into a su per-physiological range at twice the normal concentrations observed in normal human plasma (89, 90). Such concentrations of Cys and Cys-Cys have only been observed in patients with kidney failure (104). This experiment was conducted in order to test the hypothesis that oxygen could become rate limiting under the extreme concentrations of Cys and Cys-Cys that can sometimes be observed in samples from patients with kidney failure. The observed albumin S-cysteinylation trajectory in the matched serum and plasma samples that were fortified with 62 µM Cys-Cys and 12 µM Cys did not match the model predictions in which oxygen is assumed to

never become rate-limiting (**Figure 2.14**). Taken together, the observed versus modeled results (**Figure 2.11 – 2.14**) reveal that a kinetics model in which oxygen is assumed to never become rate-limiting may be applicable to P/S samples with physiologically normal concentrations of Cys and Cys-Cys, but that a new model that includes (depends on) [O_2(aq)] as a reactant must be developed to accurately predict S-Cys-Albumin formation kinetics in P/S samples from patients with kidney failure. Simulation results from a currently speculative model in which parameters for 1) the rate constant for re-oxidation of Cu(I) to Cu(II) by O_2 (aq) and 2) a constant that defines continual seepage of O_2 into the reaction vessel are estimated (**Figures 2.15 & 2.16**). This model suggests that by accounting for [O_2(aq)], it will likely be possible to use a single model to predict the kinetics of S-Cys-Albumin formation in P/S from both physiologically normal patients and from renal failure patients that contain high concentrations of Cys and Cys-Cys.

To evaluate the practical effect on S-Cys-Albumin of processing plasma normally then storing samples under an inert atmosphere in sealed vials, parallel incubations of freshly collected plasma in air and under a nitrogen atmosphere (using a Spilfyter "Hands-in-a-Bag" artificial atmospheric chamber) were conducted. Initial rates of S-Cys-Albumin formation under the two atmospheres were nearly identical, but eventually diverged and resulted in a modestly lower maximum concentration of S-Cys-Albumin in the sample incubated under nitrogen (**Figures 2.17**). These experimental results compare favorably with the [O_2(aq)]-dependent model in which a modest concentration of O_2(aq) (70 µM) is assumed at the outset but no further O_2 is allowed to enter the unfortified sample over time (**Figure 2.16**), panel n, predicted versus observed unfortified samples).

2.4.6. Blind Challenges of ΔS-Cys-Albumin as a Marker of P/S Exposure to the Thawed State

Two separate challenges were conducted for ΔS-Cys-Albumin as a marker of P/S exposure to thawed conditions in which the analyst was blinded to sample identities. The first study was a group-wise challenge wherein discrete groups of samples were either exposed to thawed conditions or properly stored at -80 °C as groups. The second blind challenge involved proper storage or mistreatment of discrete, individual samples. Before unblinding, the analyst was only aware that there would be a group-wise challenge and an individual sample challenge; he was unaware of any other aspect of the experimental design described below.

2.4.6.1. Group-wise Blind Challenge

Matched plasma and serum were collected from the same individual on three separate days, all spaced at least 6 days apart. This produced six unique but not highly disparate samples. Ten 50 µL aliquots were created from each sample, creating ten groups, each of which contained one aliquot each of the original six specimens. These groups were then randomly assigned: two groups were kept continually at -80 °C, and one group was subjected to each of the following eight conditions: 23 °C for 2h, 23 °C for 4h, 23 °C for 6h, 23 °C for 8h, 4 °C for 8h, 4 °C for 16 h, -20 °C for 24 h, and -20 °C for 48 h. The samples were then given to the analyst with only a coded identifier on each sample that corresponded to its unique group. ΔS-Cys- Alb was then measured in each sample (**Figure 2.18A**). The distributions of all data sets overlapped to some degree, indicating that it would likely be difficult to distinguish control group(s) from mistreated group(s). As such, data were analyzed using a statistical approach designed to limit type II errors

(i.e one-way ANOVA followed by uncorrected Fisher's LSD with $p < 0.1$ serving as the cutoff for statistical significance). Based on this analysis, it was clear that Groups 1 and 3 had higher mean values of ΔS-Cys-Albumin than all other groups, except for Group 7, whose status was unclear. Moreover, the ΔS-Cys-Albumin values in Groups 1 and 3 were consistent with fresh samples or those kept at -80 °C (**Figure 2.7**). Thus Groups 1 and 3 were named by the analyst as control groups. Group 7 could not be definitively categorized but was guessed/presumed to also be a properly handled control group. All other groups were assigned as having been exposed to thawed conditions of some sort. On unblinding it was revealed that all assignments except for Group 7 had been made correctly (**Figure 2.18A**).

2.4.6.2. Individual Blind Challenge

Ten additional 50 µL aliquots were made from the six samples described in the preceding paragraph, producing a total of 60 specimens. These aliquots were made at the same time as the others to avoid an additional freeze-thaw cycle. Twelve of these specimens (n = 2 aliquots of each of the original six P/S samples) were kept at -80 °C. One aliquot each of the original six P/S samples was then subjected to each of the following eight conditions: 23 °C for 24 h, 23 °C for 48 h, 23 °C for 72 h, 23 °C for 7 days, 4 °C for 7 days, 4 °C for 14 days, -20 °C for 60 days, -20 °C for 90 days. The samples were then given to the analyst. Each individual test tube had only a single, completely unique coded identifier on it. ΔS-Cys-Albumin was then measured in each sample. Because statistical analysis cannot be conducted on single samples, a ΔS-Cys-Albumin integrity cutoff had to be assigned. Based on the Gaussian distribution of ΔS-Cys-Albumin in plasma and serum from nominally unhealthy patients (**Figure 2.7**), it can be predicted that 99% of fresh

plasma samples from patients without renal failure have ΔS-Cys-Albumin values in the range of 11–30%; and 99% of fresh serum samples have ΔS-Cys-Albumin values in the range of 7.2–24%. These ranges were determined based on the means ± 2.58 SDs of the plasma and serum samples represented in **Figure 2.7B**. Thus, ΔS-Cys-Albumin values of 11% for plasma and 7.2% for serum were set as the cutoffs for this individual sample-level blind challenge. Using these cutoffs, all 60 individual specimens were categorized correctly (**Figure 2.18B**).

2.4.7. Case Study: Application of ΔS-Cys-Albumin to Nominally Pristine Archived Serum Samples

Following development of the ΔS-Cys-Albumin assay, an unplanned event occurred in our laboratory in which it was needed. In short, a set of serum samples from stage I lung cancer patients and corresponding age, gender and smoking status matched controls were undergoing glycan "node" analysis (105–109) as part of an unrelated project. The samples were collected under NIH-sponsorship by seasoned investigators with well-defined standard operating procedures and, on paper, there should not have been any specimen integrity problems. As part of the glycan "node" assay, relative blood glucose concentrations were (unintentionally) determined. The relative blood glucose concentrations in these samples indicated unexpectedly elevated levels of blood glucose in the cases. We have previously observed that albumin glycation increases significantly over time in P/S samples exposed to thawed conditions (110); as such, despite the fact that there was a pristine paper trail associated with these samples, we decided to measure ΔS-Cys-Albumin in them. The mean values of ΔS-Cys-Albumin were significantly different between the cases and controls ($p < 1 \times 10^{-20}$, student's t test) and there was

nearly no overlap in their ΔS-Cys-Albumin distributions (**Figure 2.19**). Because ΔS-Cys-Albumin is not a marker of stage I lung cancer, these data indicated an integrity discrepancy between the two sets of serum samples. On showing these data to the clinical investigators who had provided the samples, it was ultimately disclosed that the -80 °C freezers in which the control samples had been stored had experienced a power outage for about 3–4 days during a natural disaster. Using the combined rate law model described above (**Figure 2.3 Eqs. 5–8**) in combination with the average population values for ΔS-Cys-Albumin determined here (**Figure 2.7**), the trajectories of ΔS-Cys-Albumin in fresh plasma and serum samples with low, average and high ΔS- Cys-Alb values running at low and high rates of reaction (where rates are largely dependent on P/S copper concentration) were calculated (**Figure 2.20**). From the average ΔS-Cys-Albumin with average decay rate curve for serum (red line in **Figure 2.20B**) and the mean ± 95% CI of 5.2 ± 1.4 from the control set of samples from this lung cancer study (**Figure 2.19**), it was estimated that the average control serum samples had been exposed to the equivalent of room temperature (~ 23 °C) for 23 h with lower and upper 95% CI-based bounds of 17 and 32 h—an estimate that aligns with the fact that despite losing power for 3–4 days, the freezers had not been opened.

2.5. Discussion

2.5.1. Utility of ΔS-Cys-Albumin

ΔS-Cys-Albumin serves as an effective indicator of P/S exposure to thawed conditions (temperatures > -30 °C (50)) over time frames at 23 °C, 4 °C, and -20 °C (**Figure 2.8**) that are well aligned with the stability of many important clinical analytes (68, 76, 111). As an endogenous marker that serves as a P/S QA tool, it is unique in that not only is its

mechanism of formation known, but the chemical rate law governing its change in P/S over time has also been established. This level of characterization of an endogenous P/S QA marker is without precedent.

As illustrated in the blind challenge set of experiments, ΔS-Cys-Albumin, in practice, may be measured and interpreted within questionable group(s) of samples or in individual samples that have no connection to any other samples whatsoever. In doing so, a single group may be statistically compared with the population mean of ΔS-Cys-Albumin in fresh plasma or serum as established here. Multiple groups may be compared with one another (e.g. as in **Figure 2.18A**) or to the aforementioned population means. The number of samples required from a group of plasma or serum samples to achieve at least 80% power to detect a particular exposure time at the equivalent of room temperature are provided in **Table 2.3**. This table should serve as a useful guide with regard to planning QA/QC inquiries into existing plasma or serum sample sets. Individual samples, on the other hand, must be compared with a population distribution-based ΔS-Cys-Albumin cutoff value such as those 2.58 SDs below the population means established for plasma and serum in the individual-level blind challenge here

2.5.2. Alignment with Theoretical Predictions

In most fresh samples, ΔS-Cys-Albumin in plasma and serum is above 10% and 12%, respectively, (**Figure 2.7B**). The observed range of ΔS-Cys- Alb in plasma and serum (**Figure 2.7B**) lies in-line within the theoretical range of 11–38% for ΔS-Cys-Albumin that can be predicted based on the average plasma concentrations of albumin, Cys-Cys and Cys observed in the human population (88–90). This predicted range of ΔS-Cys-

Albumin does not consider the possibility that other P/S proteins, such as alpha-1-antitrypsin may consume Cys-Cys/Cys equivalents in thawed P/S potentially accounting for slightly lower mean values of ΔS- Cys-Alb than predicted in both plasma and serum (112). Notably, the overall degree of inter-individual variability observed would be expected for any endogenous marker of P/S integrity.

Besides inter-individual differences in ΔS-Cys-Albumin, there are inter-individual differences in the kinetics of ΔS-Cys-Albumin decay over time at temperatures above the freezing point of P/S (**Figure 2.8**). Predictions for the inter-individual variability in time course trajectories at 23 °C were provided (**Figure 2.20**). These are in line with the variability in person-to-person trajectories observed in **Figure 2.8**. Notably, the time course trajectory for serum sample #008 tends to float above the other two samples at 23 °C and 4 °C but is aligned with the other two samples at -20 °C (**Figure 2.8**). This did not occur for the plasma samples. As we have not yet determined the rate law at -20 °C this observation opens up a new question about the behavior of ΔS-Cys-Albumin in serum as it approaches its freezing point. At this point we do not yet have an evidence- backed explanation for this phenomenon. Most likely it is related to the facts that (1) plasma and serum do not exhibit simple eutectic behavior near their freezing point of -30 °C (51, 113) and (2) the seemingly unique properties of plasma and serum from this particular patient are mitigated by this non- eutectic behavior in serum but not plasma. This was an unexpected observation, but it does not contradict other data presented herein or diminish the functional utility of the ΔS- Cys-Alb assay with regard to its ability to detect minor exposures to thawed conditions within small groups of samples (**Figure 2.18A**) or longer exposures in individual samples (**Figure 2.18B**); moreover, the potential variability

within the time course trajectory predictions (kinetics) is well-estimated (**Figure 2.20**).As such, given the potentially open-ended nature of an inquiry to explain this phenomenon, it will be investigated in a future study.

2.5.3. ΔS-Cys-Albumin Differences Between Plasma and Serum

Matched plasma and serum samples were prepared (diluted) and run interspersed with one another on the LC-MS instrument with the same analyst preparing both the plasma and serum samples. As such, systematic error is not likely to account for the observed difference between plasma and serum. The major source of the discrepancy in ΔS-Cys-Albumin between matched plasma and serum samples was not the initial value of S-Cys-Albumin but was rather the maximum value reached following incubation for 18 h at 37 °C (**Figure 2.7A**). This discrepancy is not observed in all samples; yet the source of the discrepancy is unclear as it is not related to the difference in pre-centrifugation delay between the matched serum and plasma samples, nor is it related to serum clotting time (**Figure 2.21**). Neither is it related to the visually documented degree of hemolysis or the difference in degree of hemolysis between plasma and serum (hemolysis data not shown). Clotting factors such as Factor XIII contain free Cys residues and may consume some free Cys and/or Cys-Cys equivalents during the clotting process—which in some, but not necessarily all cases (**Figure 2.21**), may consume a significant portion of available free Cys and/or Cys- Cys equivalents. This would make these equivalents unavailable for reaction with albumin during serum storage.

Matrix effects cannot yet be ruled out as a contributing explanation to the differences in ΔS-Cys-Albumin between matched plasma and serum. These are unlikely to play a

substantial role, however, because they would depend on there being some compositional difference between plasma and serum that varies in magnitude between individuals (reaching zero in some cases—see **Figure 2.21**) and preferentially suppresses either the native or S-cysteinylated proteoform of albumin to a greater extent than the other form whereas both forms are present in P/S at relatively similar absolute concentrations. Moreover, nearly all of the difference is carried by the second measurement of S-Cys-Albumin (**Figure 2.7A**) which would not be expected if matrix effects alone were responsible for the difference.

Given that the existence of a difference between plasma and serum does not impact the functional utility of the ΔS-Cys-Alb assay toward detection of samples that have been exposed to thawed conditions (**Figures 2.18 & 2.19**) and that identification of the source(s) of the difference is currently an open- ended problem, identification of the source(s) will be addressed in a future study.

2.5.4. Importance and Limitations of the Rate Law

The chemical reactions that contribute to S-Cys-Albumin formation in P/S ex vivo are known (**Figure 2.3 Eqs. 1–2**). This made it possible to move beyond empirical cataloguing of instability trends and actually deter- mine rate laws and develop a mathematical model to facilitate (1) prediction of how the QA marker will behave across a wide range of reactant and product starting concentrations and (2) back-calculation of the approximate time at which a P/S specimen has been exposed to the temperature at which the rate law was determined (**Figure 2.20**).

The initial rate law model developed here assumes that the concentration of dissolved oxygen, $[O_2(aq)]$, in P/S is not rate-limiting. This appeared to hold true in samples that possessed a physiologically normal concentration of Cys and Cys-Cys (**Figure 2.11**). Two observations, however, suggested that the $[O_2(aq)]$ in P/S was very close to becoming rate-limiting: First, storage of unfortified plasma under nitrogen after initial processing was found to limit the overall formation of S-Cys- Alb (**Figure 2.17**). And second, the rate at which S-Cys-Albumin forms in unfortified P/S samples was accurately predicted by the model that does not take $[O_2(aq)]$ into account whereas the rate at which S-Cys-Albumin forms in P/S samples fortified with extra Cys and Cys-Cys is significantly overestimated by this model (**Figure 2.14**). Yet the rate at which S-Cys-Albumin forms in both unfortified and fortified P/S can be predicted using a model that takes $[O_2(aq)]$ into account (**Figures 2.15 & 2.16**). Thus, the present model based on **Figure 2.3 Eqs. 5–8** alone, should be employed only under two conditions: First, when P/S samples are known to have been stored under air, and second, in patient populations without kidney disease requiring hemodialysis.

The rate and equilibrium constants associated with Figure **2.3 Eq. 2** were determined for Cu(II) in a 40 mM sodium phosphate buffer (93), a solution wherein the copper ions would be complexed to the various protonated forms of phosphate ions present. In serum, however, 95% of copper is bound to ceruloplasmin (102) and in K_2EDTA plasma essentially all of the copper is bound to the ~ 5mM EDTA present. As such, the values of k_3, K_y and K_z employed here—although shown to be reasonably accurate empirically (**Figures 2.11 & 2.13**) are not necessarily accurate representations of these values as they exist in P/S. This may explain why the predicted rates of S-Cys-Albumin formation in

serum and plasma are, for the first several hours, faster and slower, respectively, than observed (**Figure 2.11**). Transition metals besides copper—most prominently iron—may also play some role in catalyzing **Figure 2.3 Eq. 2** in P/S. "Free" or nontransferrin bound iron is typically in the nM range in serum (114). Moreover, we have previously observed that Cu(II) ions are a far more efficient catalyst of intramolecular disulfide bond formation than are Fe(III) ions (115). As such, "free" iron in serum likely contributes negligibly to **Figure 2.3 Eq. 2**. In plasma, however, Fe(III)-EDTA may play a significant role in this reaction potentially accounting, at least in part, for the higher-than-predicted initial rate of S-Cys-Albumin formation (**Figure 2.11**). Efforts are underway to develop a comprehensive rate law that takes [O_2(aq)] and all relevant metals, complexed as they are within P/S, into account across the range of temperatures likely to be encountered by P/S samples.

2.5.5. Practical Impact of Storing P/S Under an Inert Atmosphere

We have previously shown that the degree of air headspace above P/S samples stored at -20 °C does not significantly impact the overall rate of S-Cys-Albumin formation (34). However, dissolved oxygen is involved in the oxidation of Cys to Cys-Cys (**Figure2.3 Eq. 2**) and its potential range in an aqueous solution such as P/S (0–250 µM (86, 87)) lies in the range of the total concentration of Cys equivalents in P/S—which includes the Cys equivalents in Cys-Cys and can exceed 150 µM. As such, we evaluated the impact of nitrogen as a headspace gas (relative to air) on the formation profile of S-Cys-Albumin in plasma. The results (**Figure 2.17**) suggest that once P/S samples are exposed to air, storing them under an inert atmosphere may provide a modest but significant ability to mitigate oxidative biomolecular damage.

2.5.6. Implications of Study Results for Single Measurements of S-Cys-Albumin

Several studies have suggested that S-Cys-Albumin may be useful as a marker of systemic oxidative stress in various disease conditions (116–118). As shown here, S-Cys-Alb's susceptibility to change ex vivo undermines the utilization of S-Cys-Albumin as a biomarker of oxidative stress unless extreme care is taken to rigorously document specimen exposure to thawed conditions before measurement. At the same time, the fact that the range of S-Cys-Albumin observed in fresh samples overlaps with the range of maximum values of S-Cys-Albumin observed after samples have been intentionally incubated in the thawed state (**Figure 2.7**) precludes the use of a single measurement of S-Cys-Albumin as a marker of P/S integrity.

2.5.7. Limitations of ΔS-Cys-Albumin

Two known confounders place minor limits on the use of ΔS-Cys-Albumin as a P/S QA tool: First, patients with poor kidney function who require hemodialysis are susceptible to abnormally elevated levels of circulating Cys and Cys-Cys (104); they may also have elevated levels of S-Cys-Albumin (118–121) though these studies did not explicitly consider the possible ex vivo formation of S-Cys-Albumin. Elevated S-Cys-Albumin in vivo does not impact ΔS-Cys-Albumin, but elevated circulating Cys and Cys-Cys may account for ΔS- Cys-Alb levels above 40%. Such samples would take slightly longer periods of time to reach the lower values of ΔS-Cys- Alb considered to represent samples exposed to thawed conditions. However, if the samples are known to come from kidney failure patients, this fact can potentially be considered vis-a`-vis the rate law established above. Second, human albumin mutations represent the only qualitative ΔS-Cys-Albumin assay confounder. These are rare in most populations (with average rates of 0.001–0.03%

(122))—but even if such samples were measured, the highly accurate mass spectrometric measurements of the intact protein on which the ΔS-Cys-Albumin assay is based would detect all but the inconsequential isobaric protein variants.

2.5.8. Linking ΔS-Cys-Albumin to the Stability of Clinically Important Biomolecules

The degree to which the measurable quantities of other biomolecules, including unrelated proteins/proteoforms, lipids, and nucleic acids are impacted during the time it takes ΔS-Cys-Albumin to reach zero will be described in separate publications. A few articles in the past several years have tabulated the stabilities of common clinical analytes in P/S, many of which are unstable within time frames that would readily be detected by ΔS-Cys-Albumin (68, 76, 111). Such co-instability with ΔS-Cys-Albumin illustrates that ΔS-Cys-Albumin does not change too rapidly or too slowly to possess substantial QA/QC utility. Conceptually, we view the development of a low-volume, inexpensive P/S QA marker that is based on known chemical reactions and their established rate laws (i.e. mathematical model) that can be used to approximate the amount of time a specimen has spent at the equivalent of room temperature to represent a critical waypoint in biobanking quality assurance. Ultimately, however, setting a ΔS-Cys- Alb cutoff that defines samples as "bad" depends on the intended use(s) of the samples. Moreover, prioritizing the tradeoff between keeping/using "bad" samples and throwing away "good" samples will always involve economic as well as scientific considerations. This means that functionally clarifying the meaning of QA marker measurements will always be context-dependent. Yet because the kinetic behavior of ΔS- Cys-Alb has been well defined here (at least at 23 °C), the only "added ingredient" necessary to link clinically important bio-

markers of interest to ΔS-Cys-Albumin is to independently characterize their empirical stability in P/S at room temperature, which is often done as part of careful analytical method development. Once this has been done, the time point at which initial instability occurred can be mapped to a clinical marker- specific ΔS-Cys-Albumin cutoff vis-a`-vis the kinetics model established here (see, for example, **Figure 2.20**). This will allow the rapid, inexpensive, low-volume measurement of ΔS-Cys-Albumin in unknown samples to provide direct insights into the validity of clinical biomarker measurements in any archived P/S specimen, regardless of their presumed storage and handling history.

2.5.9. Conclusions

ΔS-Cys-Albumin, measured via a low-volume (≤10 μL), dilute-and-shoot, LC/MS assay, is an effective protein oxidation-based QC/QA marker for plasma and serum exposure to thawed conditions (i.e. >-30 °C). Both the mechanism of ex vivo change for ΔS-Cys-Albumin and its rate law have been established. Though in need of fine tuning vis-a`-vis determination of the rate law for oxidation of cysteine to cystine under conditions highly specific to ex vivo plasma and serum, the multireaction rate law governing the formation of S-Cys-Albumin has been determined and empirically shown to be capable of accurately predicting S-Cys-Albumin formation in plasma and serum. Thus, when population averages of the relevant reactants are assumed, the combined rate law facilitates estimation of the time frame over which plasma and serum samples with unknown storage and handling histories have been exposed to the equivalent of room temperature conditions. As such, the stability of any clinical biomarker of interest can readily be linked to ΔS-Cys-Albumin by conducting a room temperature stability study of the marker regardless of the mechanism by which it exhibits instability. When plasma

and serum samples are grouped, we have shown that ΔS-Cys-Albumin can detect room temperature exposures of as little as 2 h—yet several days at room temperature are required for plasma and serum samples to reach the ΔS-Cys-Albumin minimum value of zero. By modeling the rate law using the population survey of fresh, matched plasma and serum from cardiac patients as input data, it can be seen that as few as 12 serum or 8 plasma samples from an unknown group are required to provide ≥ 80% power to detect 3 h of exposure to the equivalent of room temperature conditions. Mistreatment of individual samples can also be detected when their ΔS-Cys-Albumin values are 3 SDs below the population means (i.e. < 11% for plasma or 7.2% for serum). In summary, ΔS-Cys-Albumin readily identifies poorly stored or handled plasma and serum specimens and provides investigators a robust tool by which to prevent their inclusion in clinical research studies.

Figures

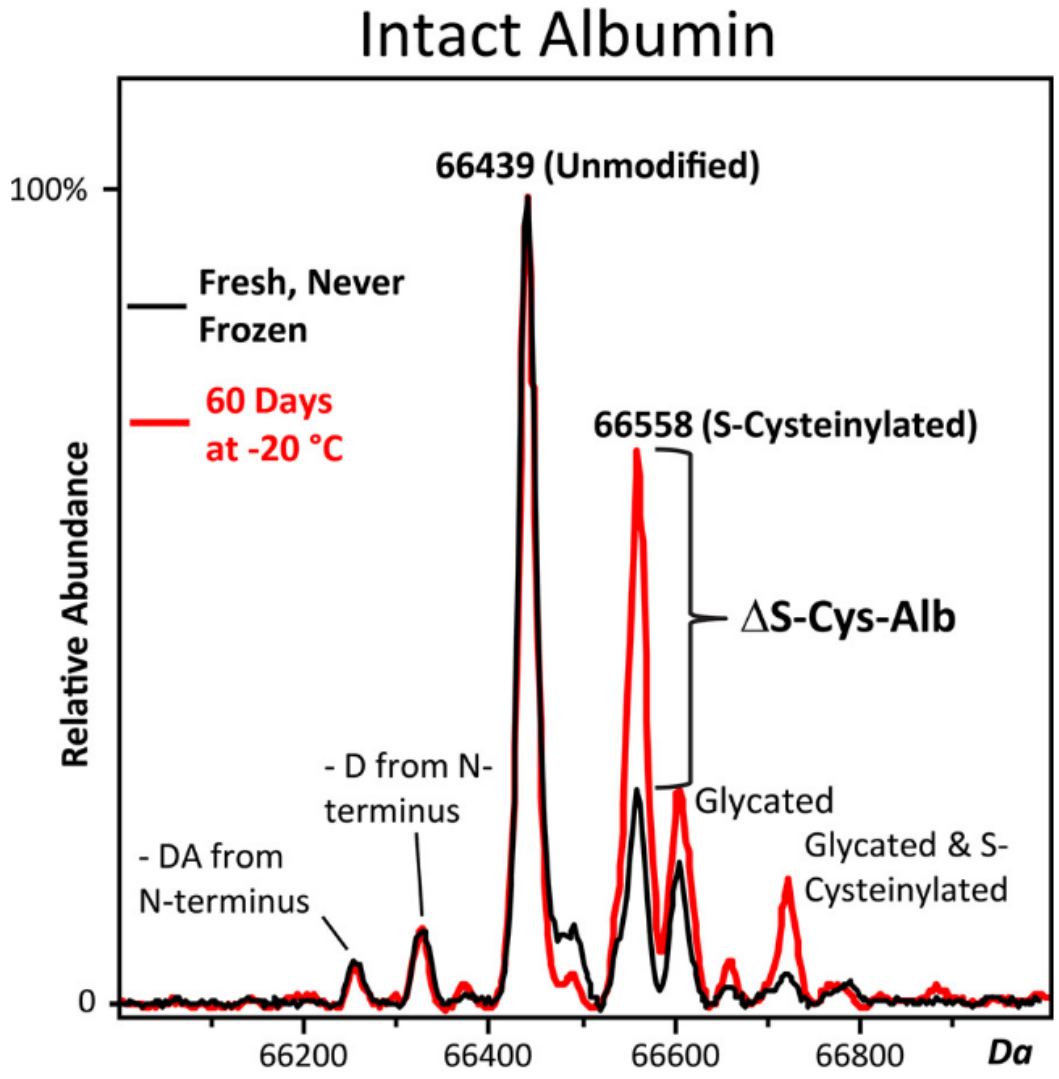

Figure 2.1: Charge deconvoluted ESI-mass spectra of albumin that illustrate ΔS-Cys-Albumin. The black spectrum is from a fresh sample obtained immediately after centrifugation. The red spectrum is from the same sample stored for 60 days at -20 °C. The same shift occurs when P/S samples are intentionally incubated at 37 °C for 18 h. As indicated, small fractions of albumin are N-terminally truncated, and both the native and S-cysteinylated forms may be glycated.

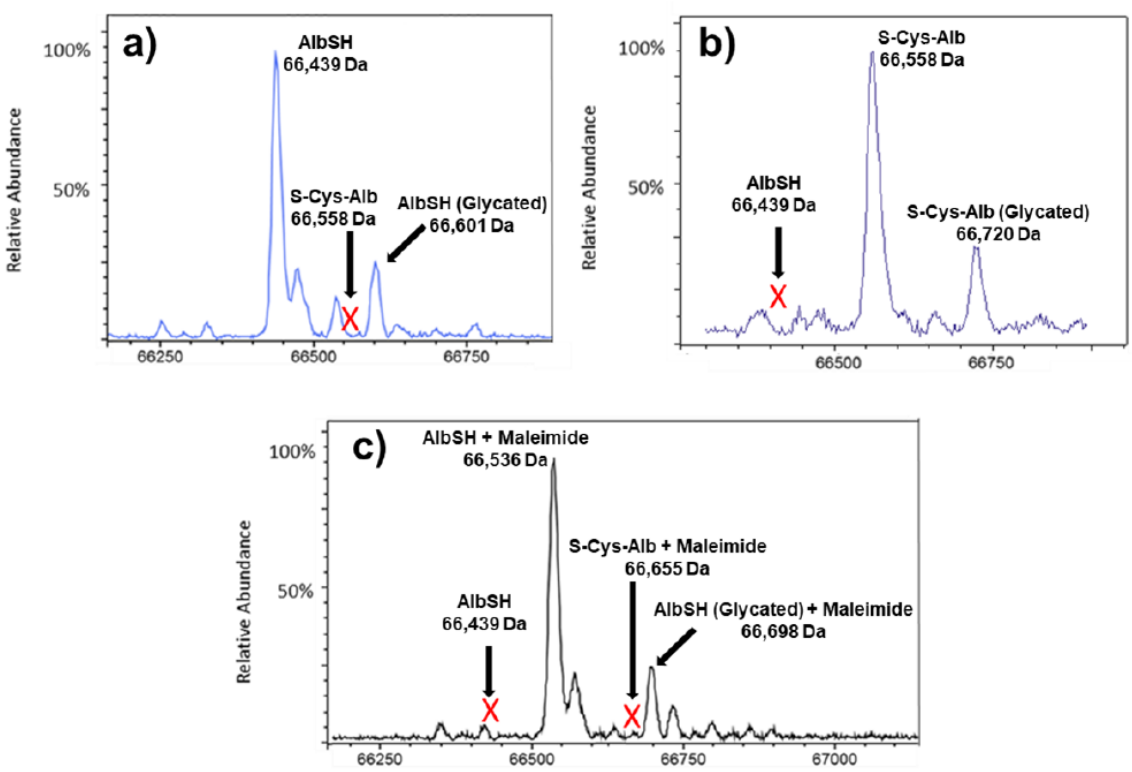

Figure 2.2: Charge deconvoluted ESI-mass spectra of the a) completely reduced and b) completely oxidized albumin. C) To verify that no structural disulfide bonds were reduced during reduction the sample was alkylated with maleimide. The mass shift of exactly +97 Da, with no peaks at +2*97 Da (66,633 Da, corresponding to two alkylation events) or +3*97 Da etc. indicate that the reduced albumin possessed only a single free Cys residue as expected.

$$AlbSH + Cys\text{-}Cys \underset{k_2}{\overset{k_1}{\rightleftharpoons}} SCysAlb + Cys \qquad \text{(Eq. 1)}$$

$$2Cys + O_2 \xrightarrow[k_3]{Cu(II)} Cys\text{-}Cys + H_2O_2 \qquad \text{(Eq. 2)}$$

$$v_o = k_1[AlbSH][Cys\text{-}Cys] \qquad \text{(Eq. 3)}$$

$$v_o = k_2[SCysAlb][Cys] \qquad \text{(Eq. 4)}$$

$$\frac{d[AlbSH]}{dt} = -k_1[AlbSH][Cys\text{-}Cys] + k_2[SCysAlb][Cys] \qquad \text{(Eq. 5)}$$

$$\frac{d[Cys\text{-}Cys]}{dt} = -k_1[AlbSH][Cys\text{-}Cys] + k_2[SCysAlb][Cys] + \frac{k_3[Cu(II)][Cys]}{K_z\left(1 + \frac{K_y}{[Cys]}\right) + [Cys]} \qquad \text{(Eq. 6)}$$

$$\frac{d[SCysAlb]}{dt} = k_1[AlbSH][Cys\text{-}Cys] - k_2[SCysAlb][Cys] \qquad \text{(Eq. 7)}$$

$$\frac{d[Cys]}{dt} = k_1[AlbSH][Cys\text{-}Cys] - k_2[SCysAlb][Cys] - 2\left(\frac{k_3[Cu(II)][Cys]}{K_z\left(1 + \frac{K_y}{[Cys]}\right) + [Cys]}\right) \qquad \text{(Eq. 8)}$$

Figure 2.3: The chemical reactions governing the ex vivo formation of S-cysteinylated albumin (Equation 1 and 2) and associated rate law equations. AlbSH is the native reduced form of albumin, Cys-Cys is cystine, SCysAlb is S-cysteinylated albumin, and Cys is cysteine.

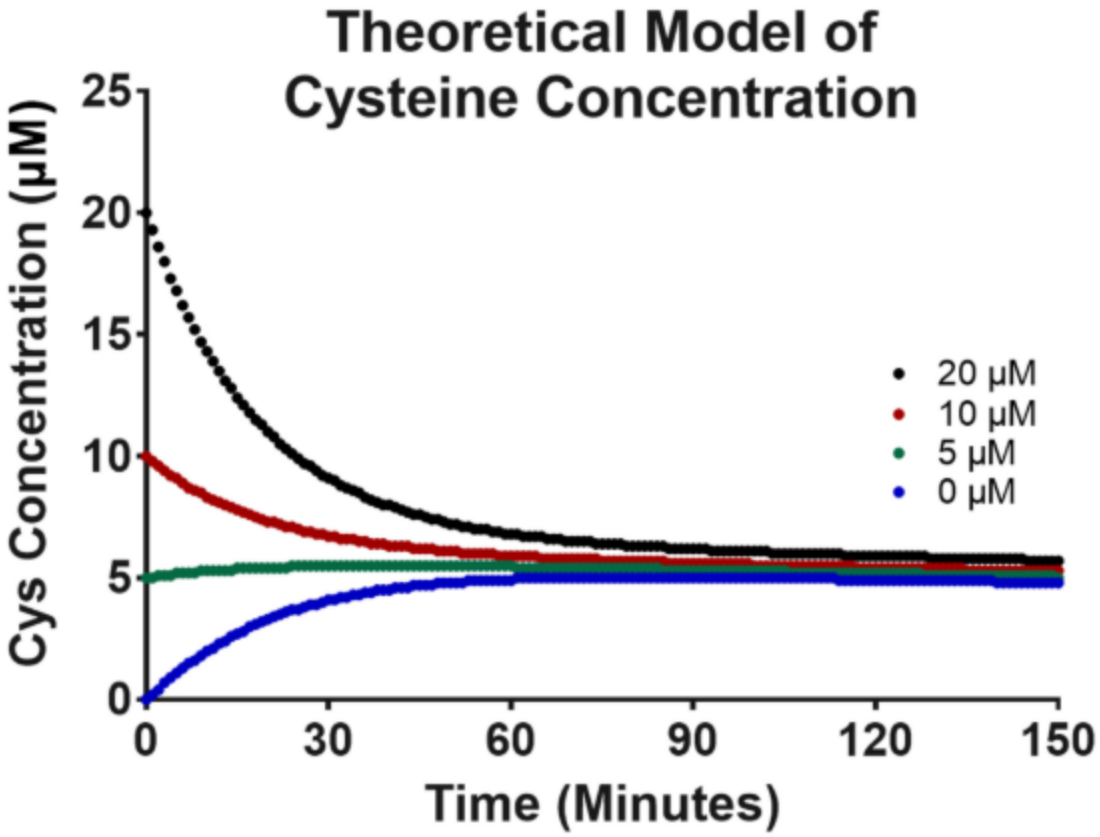

Figure 2.4: Reaction kinetics models based on the empirically determined rate law (Equations 5-8 of **Figure 2.3**) illustrating that by the time serum or plasma are processed from whole blood (~ 60 min), the concentration of Cys approaches a near steady-state concentration of about 5 µM—regardless of whether or not the initial concentration started at the low or high end of physiological Cys concentrations observed in human plasma (89, 90).

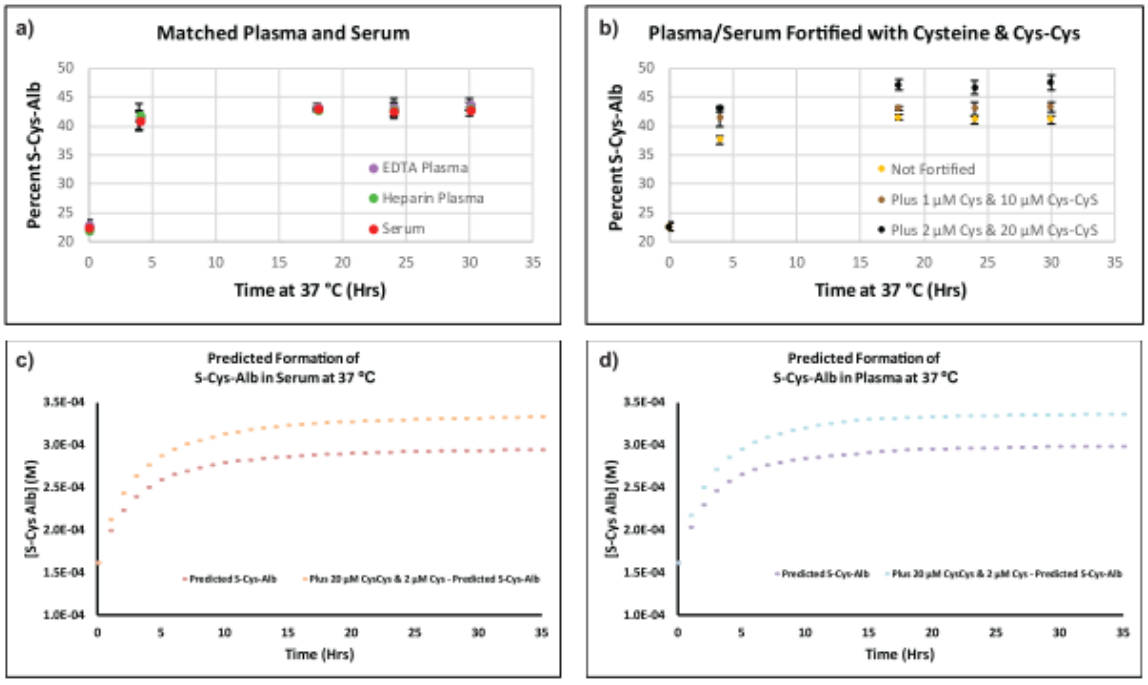

Figure 2.5: Determination of the time required at 37 °C to maximize S-Cys-Albumin in P/S samples. Empirical evaluation (panels a-b): a) Nine-microliter aliquots of matched K_2EDTA plasma, sodium heparin plasma, and serum from a healthy donor were incubated in closed 0.6-mL test tube at 37 °C for up to 30 hrs. No significant differences were found between plasma and serum or between the two types of plasma. No changes were observed after 18 hrs at 37 °C. n = 3 per data point; error bars represent SD. b) Each P/S sample was divided into 3 portions; one was left unmodified, to the second was added 1 µM Cys and 10 µM Cys-Cys, and to the third was added 2 µM Cys and 20 µM Cys-Cys. The addition of Cys and Cys-Cys results in an increase in the maximum value of S-Cys-Albumin observed, but does not increase the time frame required to reach the maximum obtainable value of S-Cys-Albumin at 37 °C. Data from both types of plasma and serum were pooled and are displayed together as mean ± SD (n = 9 per data point). Panels c-d provide theoretical trajectories for S-Cys-Albumin formation in P/S based on the rate law model described for **Figure 2.20**. These also reach a plateau by 18 hrs. Input parameters include age-weighted population averages for AlbSH (484 µM) and S-Cys-Albumin (484 µM) (88, 91), Cys-Cys (65 µM) (89, 90), Cys (5 µM—see **Figure 2.4**); the population average for total Cu(II) (18.7 µM) (88)—all of which is assumed catalytically available in plasma and 50% of which is assumed to be catalytically available in serum; k_3 (0.32 $M^{-1}s^{-1}$), K_y (5.1 x 10^{-6} M) and K_z (8.8 x 10^{-4} M) as determined by Kachur et al. at 37 °C (93); and k_1 (0.6 $M^{-1}s^{-1}$) and k_2 (6.6 M^{-1} s^{-1}) as recently determined by Bocedi et al. at 37 °C (100).

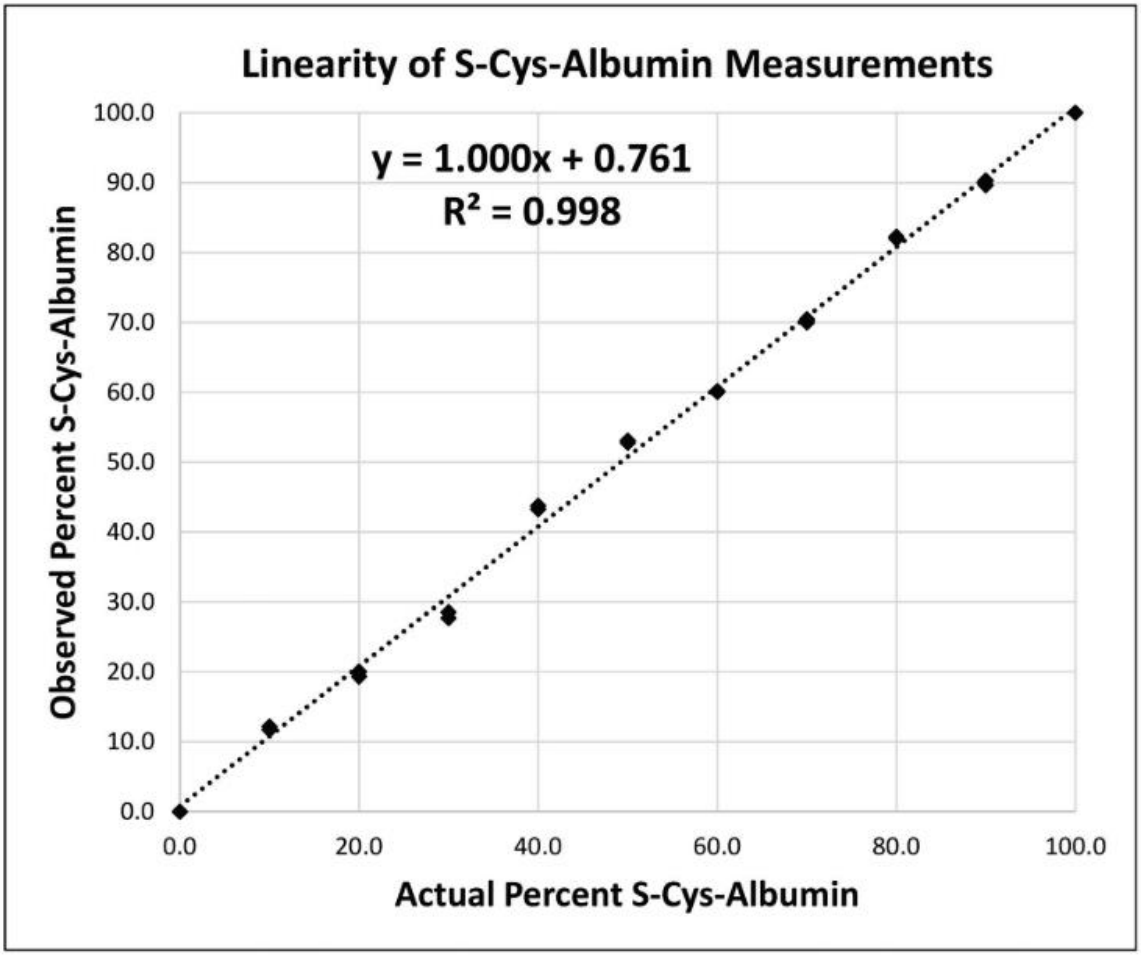

Figure 2.6: Linearity of S-Cys-Albumin measurements

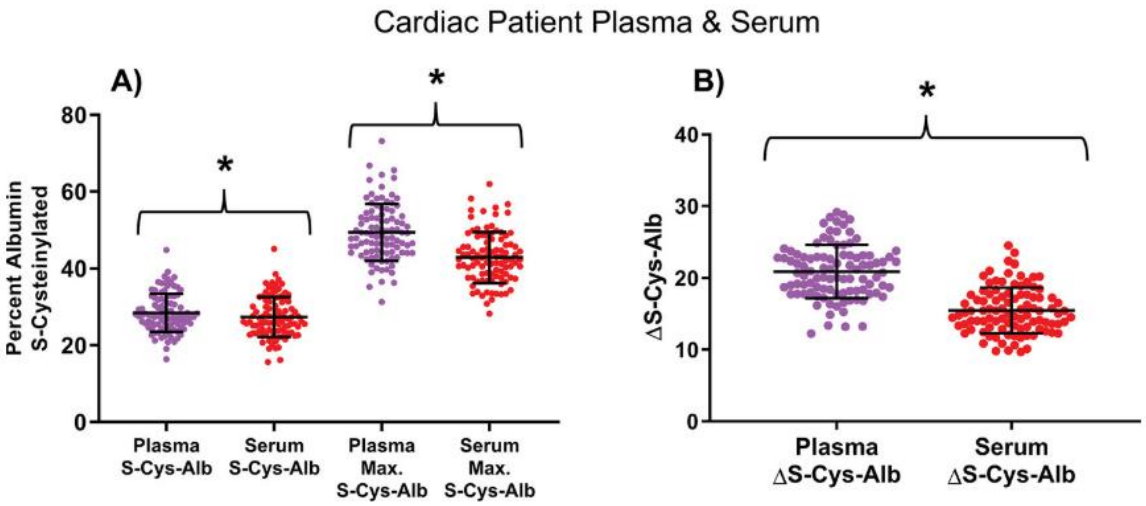

Figure 2.7: S-Cys-Albumin and ΔS-Cys-Albumin in fresh, rapidly processed samples from cardiac patients. A) S-Cys-Albumin and maxed-out S-Cys-Albumin observed in fresh samples from matched K_2EDTA plasma and serum samples from cardiac patients undergoing coronary angiogram, cardiac stress test and/or coronary computed tomography angiography. B) ΔS-Cys-Albumin, calculated from panel A by taking individual sample differences between maxed-out S-Cys-Albumin and S-Cys-Albumin. Error bars represent mean ± S.D.; n = 97 per group; * indicates a significant difference between means of indicated groups with $p < 0.0001$, paired t-tests.

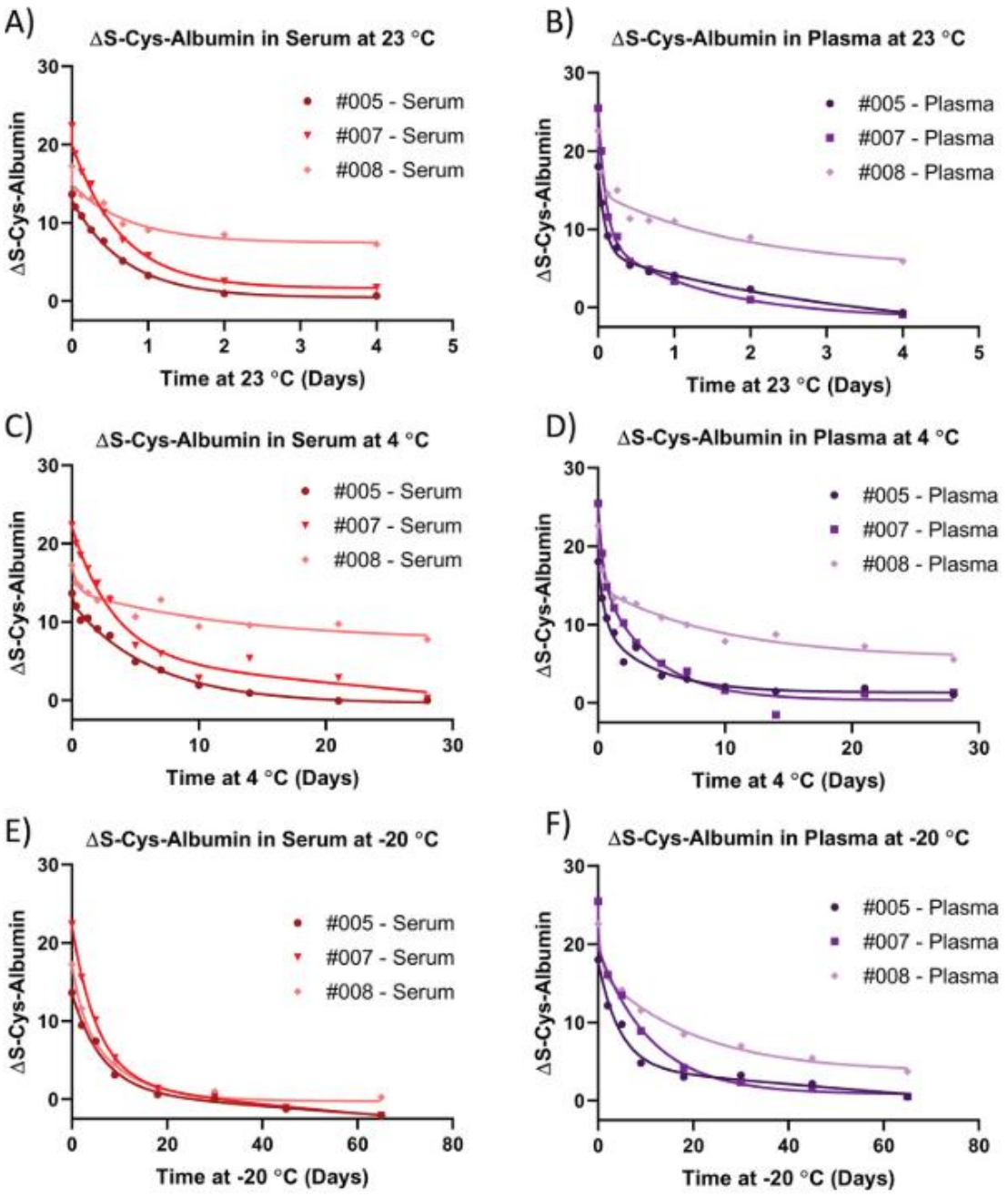

Figure 2.8: Time courses for ΔS-Cys-Albumin decay in matched serum and plasma from three separate patients (as indicated by patient numbers in the figure legends) at A–B, 23 °C, C–D, 4 °C, and E–F, -20 °C. Lines drawn are meant to serves as visual guides.

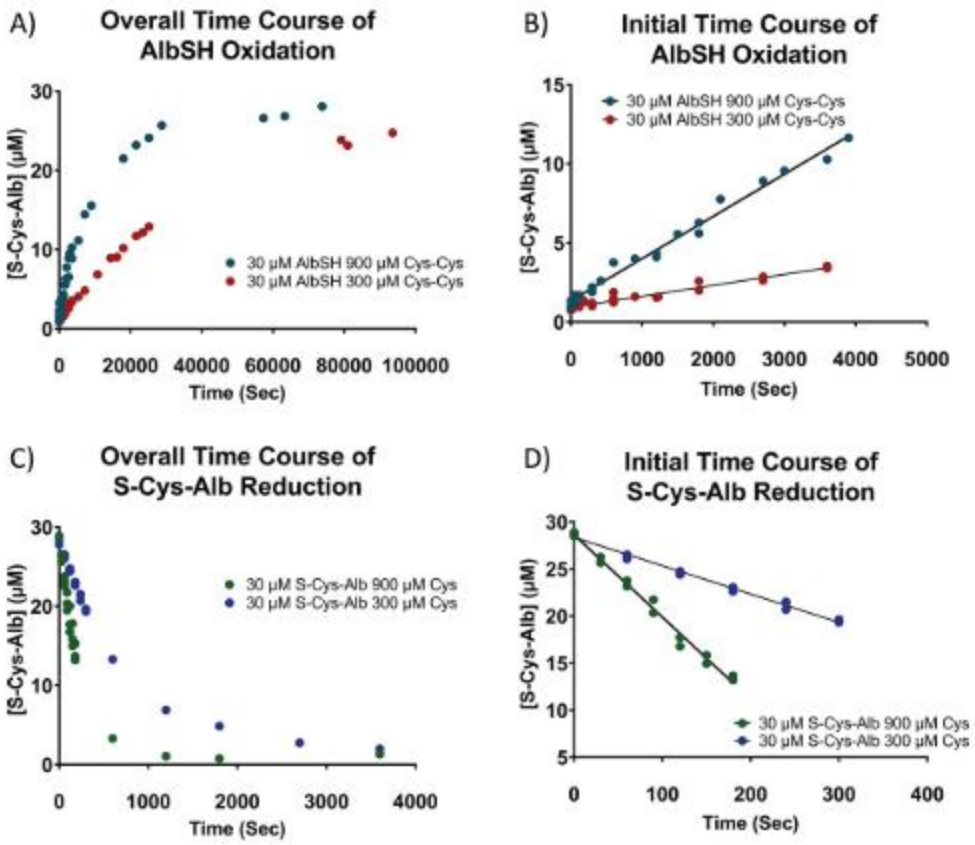

Figure 2.9: Rates of albumin oxidation (S-cysteinylation) and reduction at 23 °C. A) Overall time course for albumin S-cysteinylation (oxidation) and B) initial rate for albumin S-cysteinylation starting with 30 μM AlbSH and 300 or 900 μM Cys-Cys. C) Overall time course for re- duction of S-Cys-Albumin and D) initial rate for reduction of S-Cys-Albumin starting with 30 μM S-Cys-Albumin and 300 or 900 μM Cys.

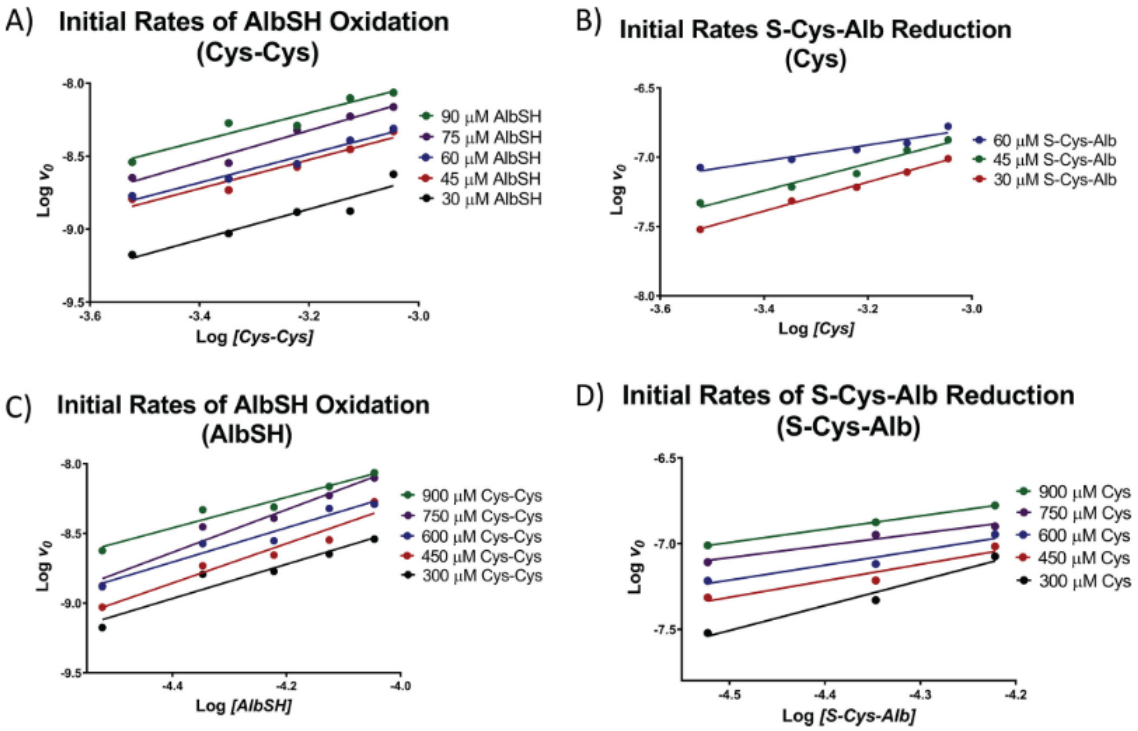

Figure 2.10: Log-log plots employed to determine the reaction order for all species in the reversible oxidation (S-cysteinylation) of AlbSH by Cys-Cys Eq. 1. The average slopes for A, B, C, and D were 1.01 ± 0.05, 0.87 ± 0.25, 1.30 ± 0.17 and 0.96 ± 0.30, respectively. Thus, both the forward and reverse reactions were determined to be first order with respect to each reactant.

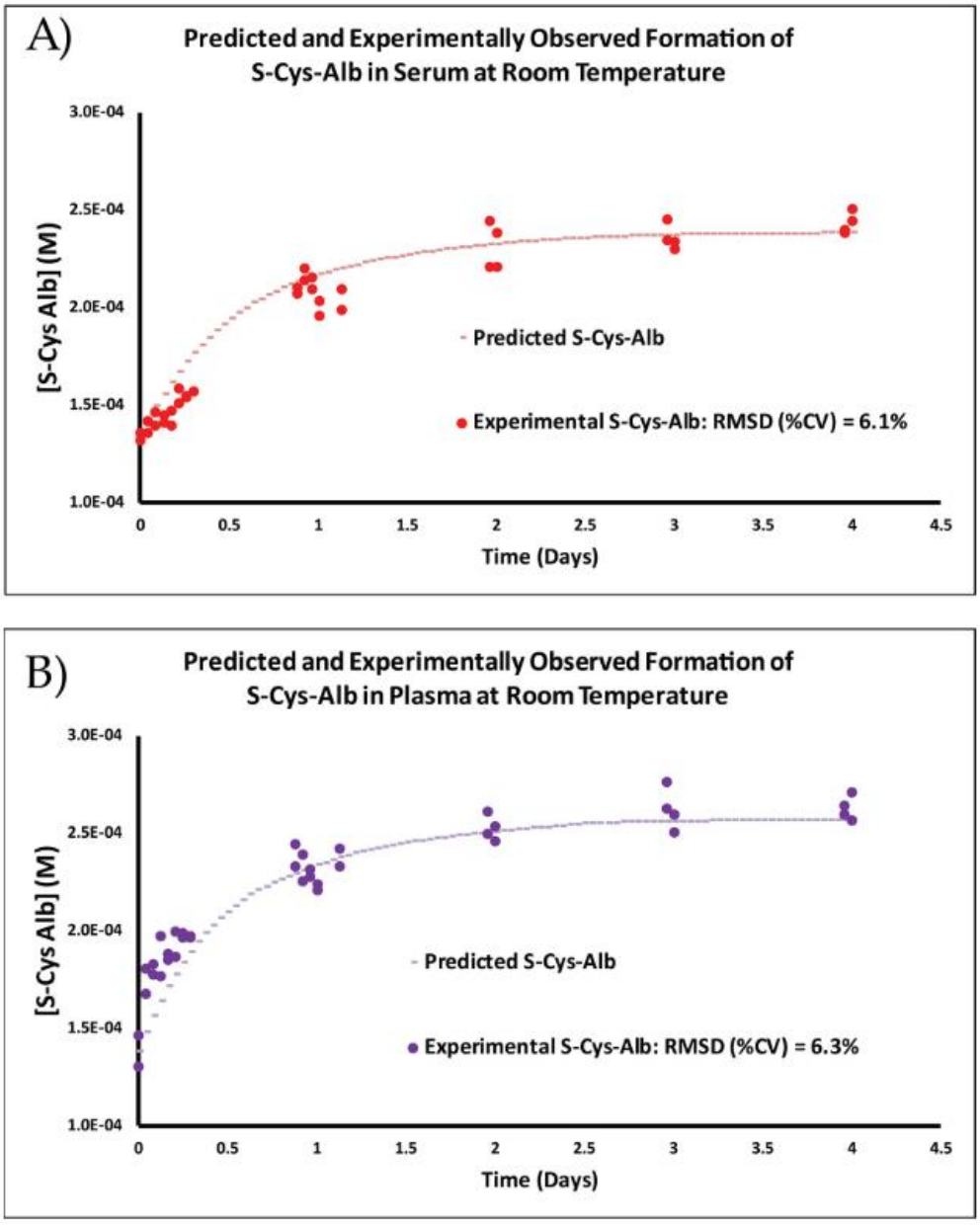

Figure 2.11: Observed and rate law model-predicted formation of S-Cys-Albumin in matched A, serum and B, K_2EDTA plasma from a healthy donor Observed and rate law model-predicted formation of S-Cys-Albumin in matched A, serum and B, K_2EDTA plasma from a healthy donor. Circles represent natural, unfortified serum or plasma containing initially measured concentrations of AlbSH = 609 µM (serum) or 605 µM (plasma); S-Cys-Albumin = 134 µM (serum) or 138 µM (plasma); Cys-Cys = 52 µM (serum) or 58 µM (plasma); Cys = 5 µM (inferred, not measured, see "Results" text and supplemental Figure 2.4); and Cu(II) = 12.6 µM. Dashed lines represent rate model-predicted trajectories for S-Cys-Albumin formation based on numerical solutions to Eqs. 5–8 (Figure 2.3) employing the rate and equilibrium constant parameters described in the main text.

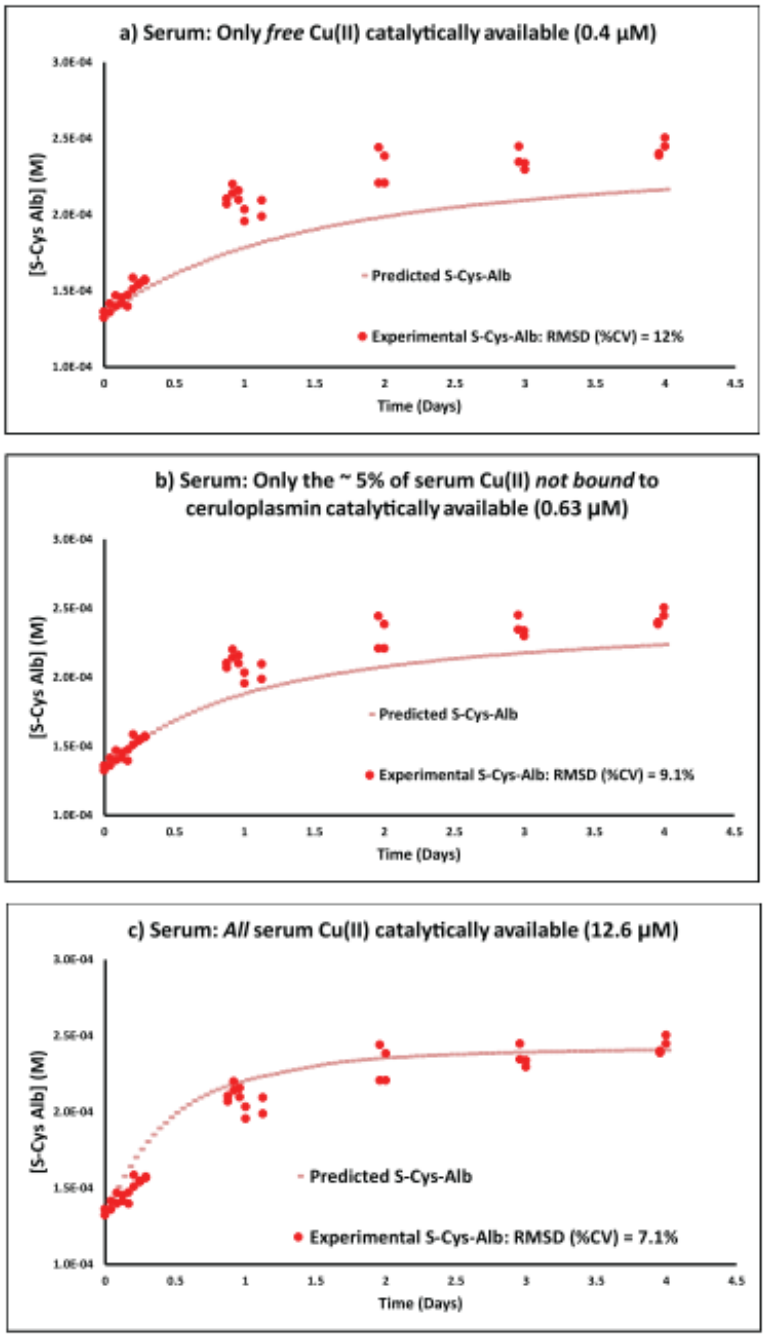

Figure 2.12: Kinetics simulations in which a) only free serum Cu(II) (0.4 µM), b) the ~5% of serum Cu(II) not bound to ceruloplasmin (0.63 µM), and c) all Cu(II) in serum (12.6 µM) is assumed to be catalytically available.

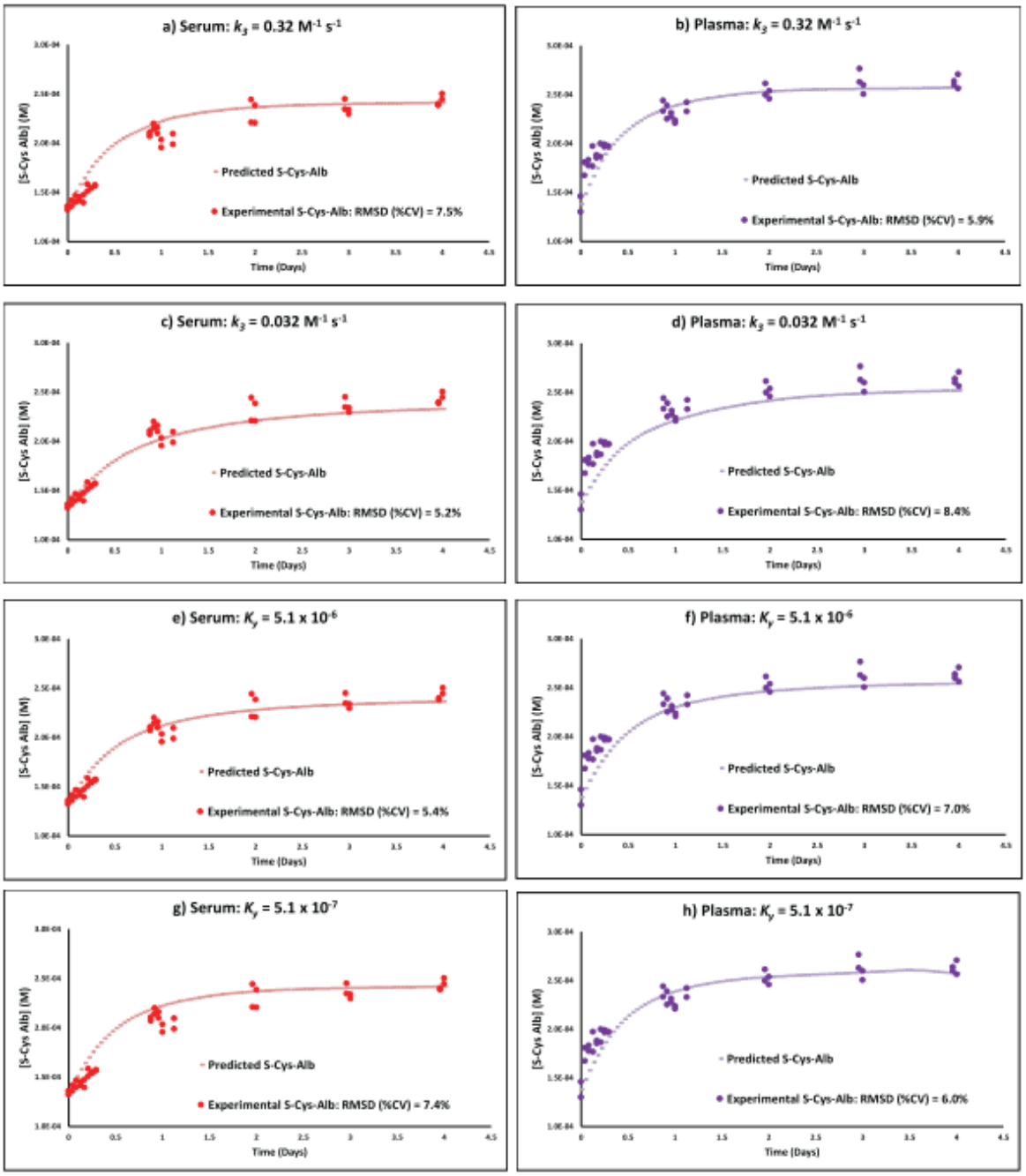

Figure 2.13: (continued on next page)

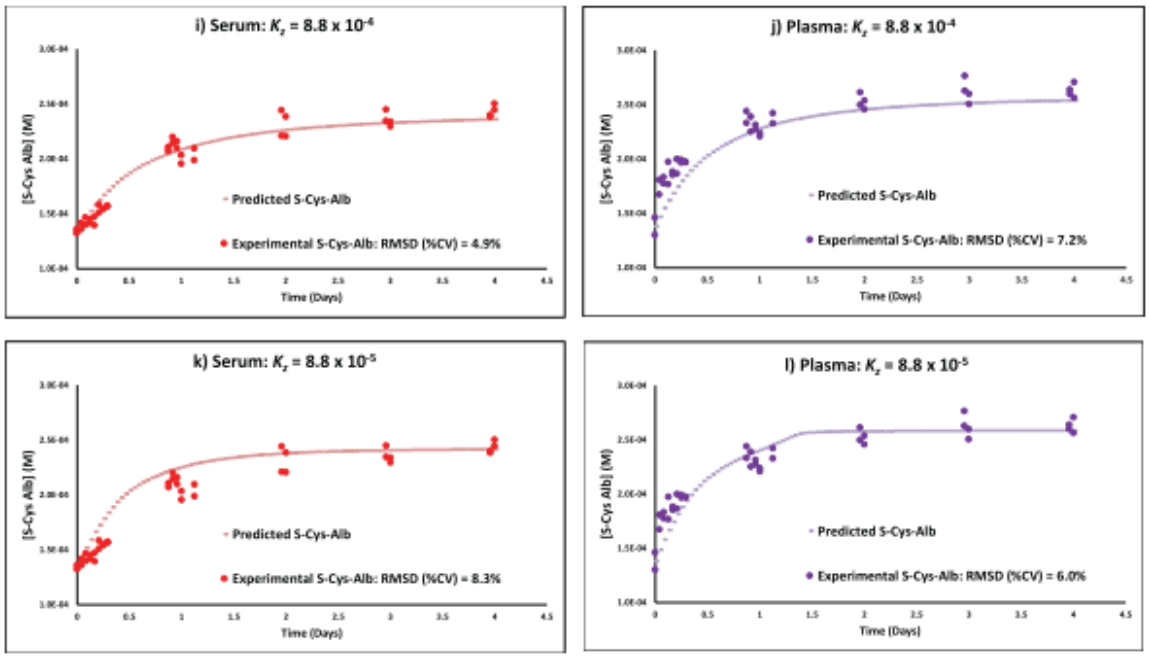

Figure 2.13: Kinetics simulations in which the Rxn 2 rate law constants k_3, K_y and K_z are individually changed to their 37 °C values or 10x below these values. a-b) Serum and plasma, respectively, where k_3 = 0.32 $M^{-1}s^{-1}$, the value established by Kachur et al. (93) at 37 °C; c-d) k_3 = 0.032 $M^{-1}s^{-1}$; e-f) K_y = 5.1 x 10^{-6}M, the value established by Kachur et al. (93) at 37 °C; g-h) K_y = 5.1 x 10^{-7} M; i-j) K_z = 8.8 x 10^{-4} M, the value established by Kachur et al. (93) at 37 °C; k-l) Kz= 8.8 x 10^{-5} M.

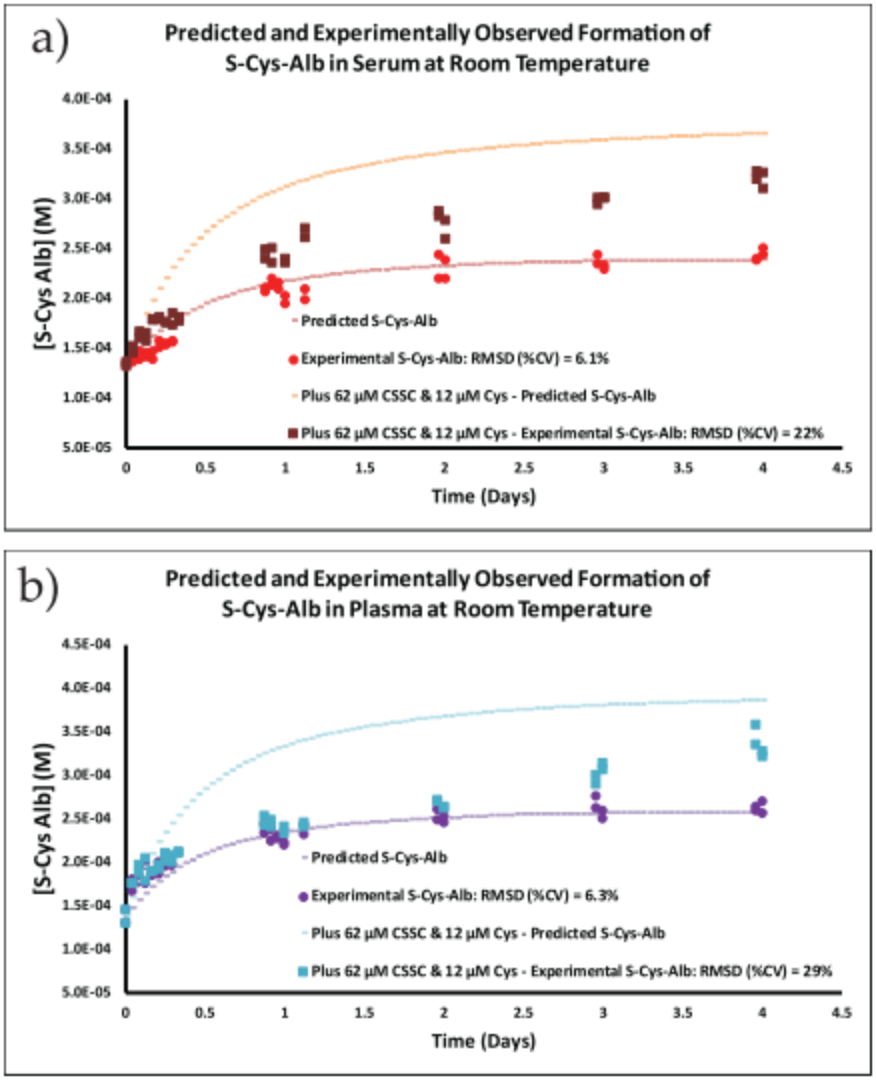

Figure 2.14: Observed and rate law model-predicted formation of S-Cys-Albumin in matched a) serum and b) K_2EDTA plasma from a healthy donor. Circles represent natural, unfortified serum or plasma containing initially measured concentrations of AlbSH = 609 µM (serum) or 605 µM (plasma); S-Cys-Albumin = 134 µM (serum) or 138 µM (plasma); Cys-Cys = 52 µM (serum) or 58 µM (plasma); Cys = 5 µM (inferred, not measured, see Results text and supplemental Figure 2.4); and Cu(II) = 12.6 µM. Squares represent aliquots of the same samples into which extra Cys-Cys and Cys were fortified, bringing the final concentration of Cys-Cys to 114 µM (serum) or 120 µM (plasma) and Cys to 17 µM (serum & plasma). Dashed lines represent rate model-predicted trajectories for S-Cys-Albumin formation based on numerical solutions to Eqns. 5-8 employing the rate and equilibrium constant parameters described in the main text. The poor model fit for samples fortified with extra Cys-Cys and Cys appears to be due to the concentration of dissolved oxygen, [O2(aq)], becoming rate limiting under these fortified conditions (**Figure 2.16**). Cys-Cys is abbreviated as CSSC in the legends.

a) ***Chemical Reactions***

$$AlbSH + Cys\text{-}Cys \underset{k_2}{\overset{k_1}{\rightleftharpoons}} SCysAlb + Cys \quad (1)$$

$$2Cys + O_2 \xrightarrow[k_3]{Cu(II)} Cys\text{-}Cys + H_2O_2 \quad (2)$$

$$\left\{ \begin{array}{l} Cys + Cu(II) \xrightarrow{k_x} 1/2\,Cys\text{-}Cys + Cu(I) \quad (10) \\ Cu(I) + O_2 \xrightarrow{k_4} Cu(II) + O_2^{\cdot-} \quad (11) \end{array} \right\}$$

Rate Equations

$$\frac{d[AlbSH]}{dt} = -k_1[AlbSH][Cys\text{-}Cys] + k_2[SCysAlb][Cys] \quad (5)$$

$$\frac{d[Cys\text{-}Cys]}{dt} = -k_1[AlbSH][Cys\text{-}Cys] + k_2[SCysAlb][Cys] + \frac{k_3[Cu(II)][Cys]}{K_x\left(1 + \frac{K_y}{[Cys]}\right) + [Cys]} \quad (6)$$

$$\frac{d[SCysAlb]}{dt} = k_1[AlbSH][Cys\text{-}Cys] - k_2[SCysAlb][Cys] \quad (7)$$

$$\frac{d[Cys]}{dt} = k_1[AlbSH][Cys\text{-}Cys] - k_2[SCysAlb][Cys] - 2\left(\frac{k_3[Cu(II)][Cys]}{K_x\left(1 + \frac{K_y}{[Cys]}\right) + [Cys]}\right) \quad (8)$$

$$\frac{d[Cu(II)]}{dt} = -2\left(\frac{k_3[Cu(II)][Cys]}{K_x\left(1 + \frac{K_y}{[Cys]}\right) + [Cys]}\right) + k_4[Cu(I)][O_2] \quad (12)$$

$$\frac{d[Cu(I)]}{dt} = 2\left(\frac{k_3[Cu(II)][Cys]}{K_x\left(1 + \frac{K_y}{[Cys]}\right) + [Cys]}\right) - k_4[Cu(I)][O_2] \quad (13)$$

$$\frac{d[O_2]}{dt} = k_{O_2} - k_4[Cu(I)][O_2] \quad (14)$$

Figure 2.15: Kinetics model that take O_2(aq) into account. Chemical and mathematical rate equations. Reactions. 10-11 break apart Reaction. 2 to show how O_2(aq) recycles Cu(I) into Cu(II) and allows Cu(II) to serve as the reaction catalyst. The rate law described by Kachur et al. (93) for Reaction 2 omits O_2 (i.e., assumes it is not rate limiting) and takes into account the equilibrium binding affinities for the first and second Cys liganding to Cu(II). Thus, strictly speaking, it is actually the rate law for Reaction 10—but one in which the Cu(I) produced is assumed to be immediately recycled back to Cu(II). When O_2(aq) is in short supply, Reaction 11 can become rate limiting and must be taken into account in the model.

Taking O_2(aq) into account requires three additional differential equations (Eqns. 12-14), two additional reaction components (O_2(aq) and Cu(I)) and two additional rate constants (k_4 and k_{O2}). Simulations based on this model (**Figure 2.16**) should be considered speculative because not all of these parameters are known: O_2(aq) was estimated at 30% saturation (70 µM) and Cu(I) was assumed to initially exist only in trace quantities (i.e., < 1% of total Cu or 0.1 µM). k_4 will vary depending on how Cu(II) is bound in P/S. A value of 200 M^{-1} s^{-1} was employed based on the known rate constant for the reaction of O_2(aq) with the Fe(II)-EDTA complex (123) (that for the Cu(I)-EDTA complex is unknown). k_{O2} is a constant that describes the rate at which O_2(g) from the headspace above the P/S sample dissolves, becoming how O_2(aq). It was estimated at 1 x 10^{-10} M/s.

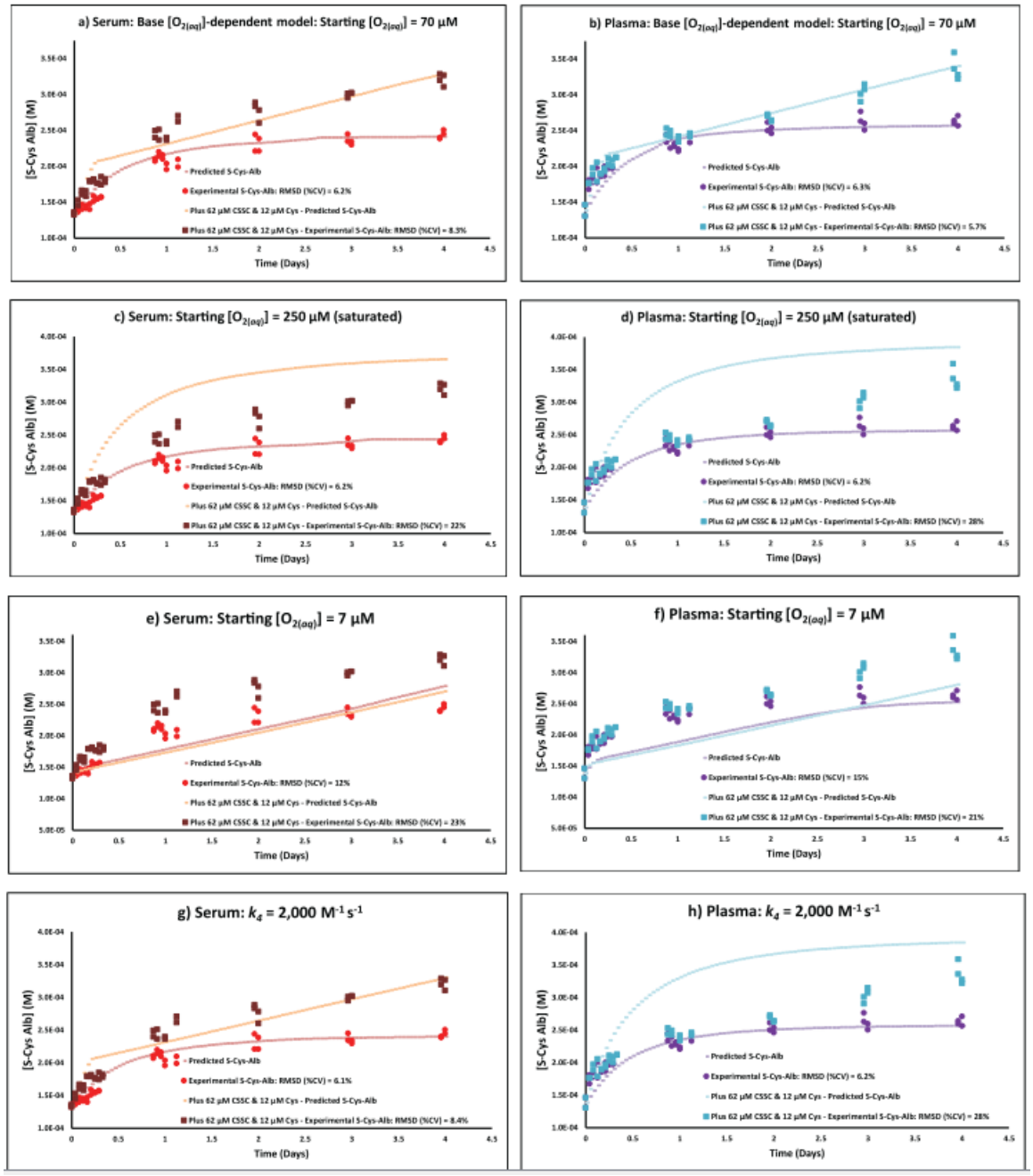

Figure 2.16: Continued on next page

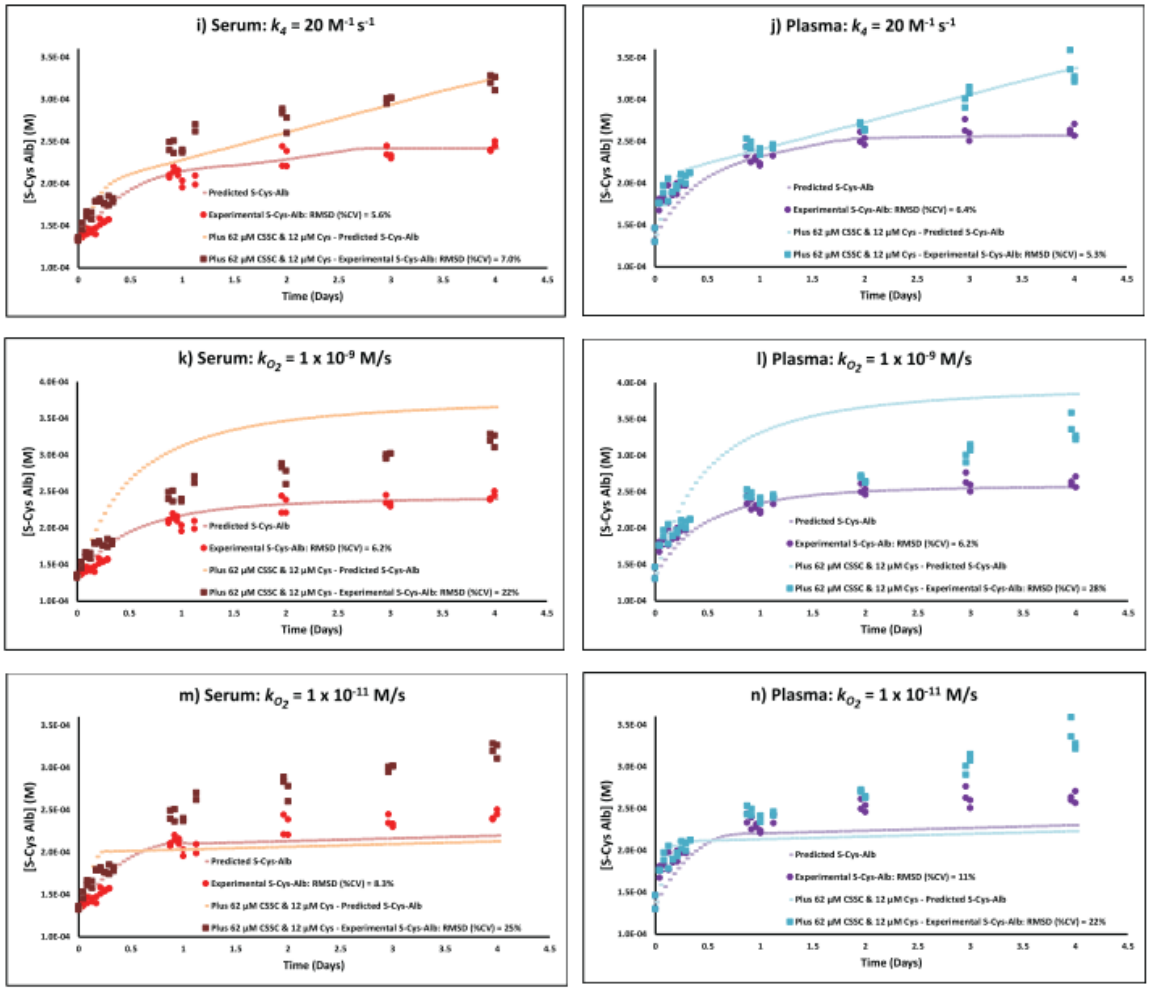

Figure 2.16: Simulations that take O_2(aq) into account. Model predictions (lines), overlaid on actual results (symbols), that take into account best estimates for the additional parameters (reaction components and rate constants) required for an O_2(aq)–dependent model as described in **Figure 2.15**. Here, panels a-b, correspond to serum and K_2EDTA plasma with starting O_2(aq) = 70 µM, respectively. All other parameters in the model exist as described in **Figure 2.11**. Additional panels vary the starting concentration of one reaction component or one rate constant at a time (generally -10x or +10x unless physically unreasonable) to evaluate its effect on the model. c-d) Starting O_2(aq) = 250 µM (saturation); e-f) Starting O_2(aq) = 7 µM; g-h) k_4 = 2,000 $M^{-1}s^{-1}$; i-j) k_4 = 20 M^{-1} s^{-1} ; k-l) k_{O2} = 1 x 10^{-9} M/s; m-n) k_{O2} = 1 x 10^{-11} M/s. (This simulates placing P/S into a nitrogen (low O_2(g)) atmosphere following initial processing (which permits a modest initial concentration of O_2(aq) to develop in the sample—i.e., ~ 70 µM). The trajectory difference between the predicted and observed formation of S-Cys-Albumin matches, approximately, the difference between the unfortified plasma sample incubated under nitrogen and the one incubated under air in **Figure 2.17**). Cys-Cys is abbreviated as CSSC in the legends.

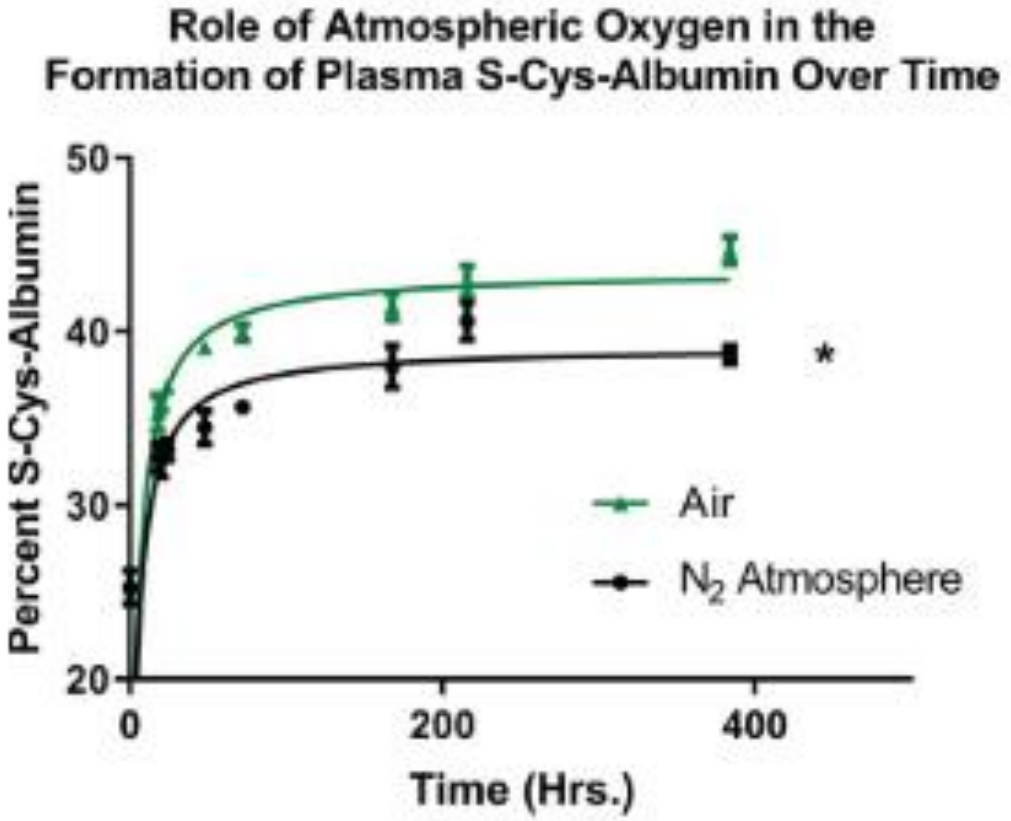

Figure 2.17: Formation of S-Cys-Albumin over time in aliquots of the same plasma incubated at 23 °C in air (green triangles) or under a nitrogen atmosphere (black circles). The nitrogen atmosphere modestly but significantly lowered the total fraction of S-Cys-Albumin formed (* $p < 0.01$; Wilcoxon matched pairs signed-rank test. $n = 4$ per time point; error bars represent S.D.)

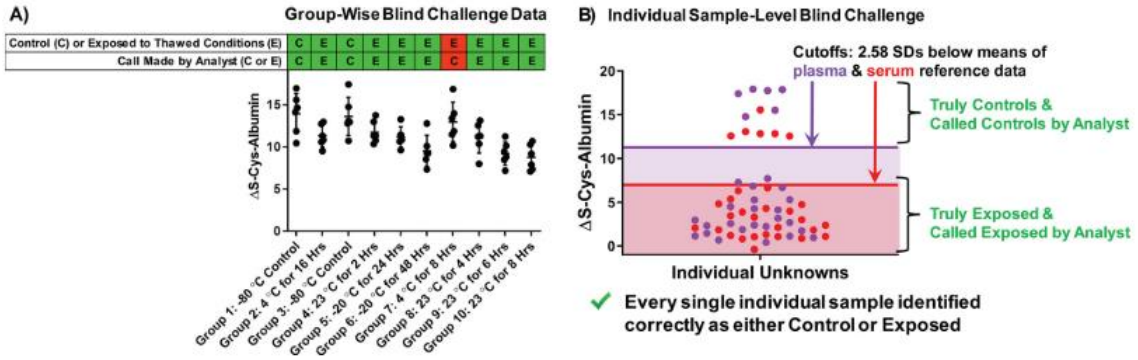

Figure 2.18: Results from blinded challenges of the ability of ΔS-Cys-Albumin to distinguish A, groups of samples exposed to various thawed conditions (listed below each group), and B, individual samples exposed to various thawed conditions including 23 °C for 24 h, 23 °C for 48 h, 23 °C for 72 h, 23 °C for 7 days, 4 °C for 7 days, 4 °C for 14 days, -20 °C for 60 days, -20 °C for 90 days (n = 6 per condition); controls kept at -80 °C (n = 12). Out of a total of 70 calls of "control" versus "exposed" that had to be made between these two studies, only one was made incorrectly (see panel a).

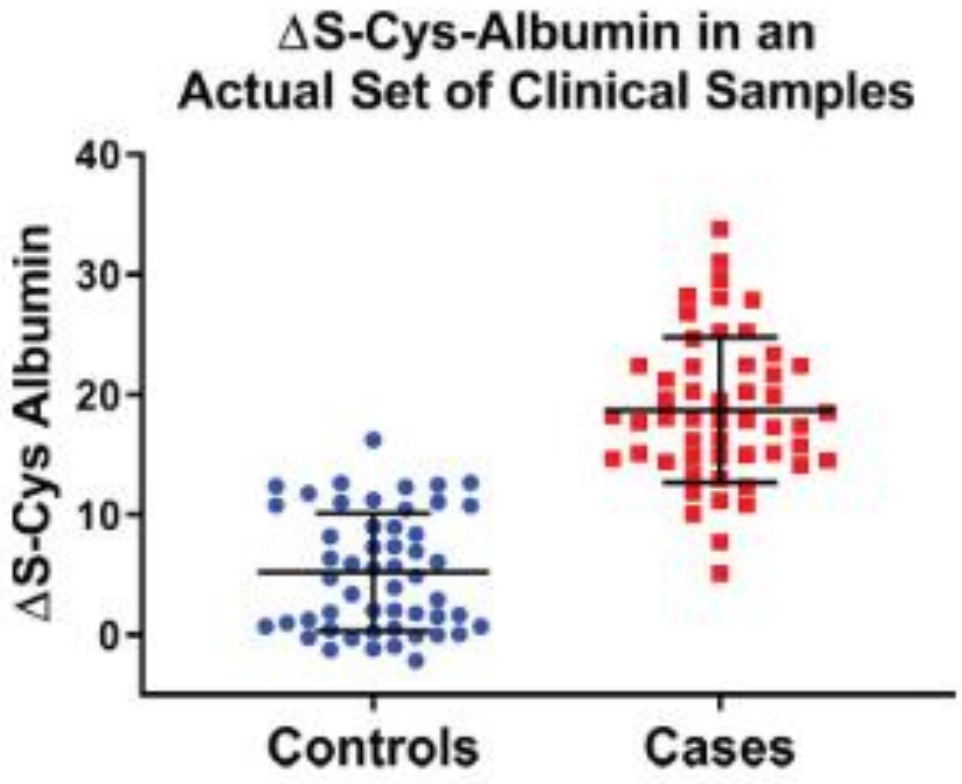

Figure 2.19: Δ-Cys-Alb results from a case study of serum samples with an excellent pedigree but in which an integrity discrepancy was suspected (see main text for details). The values of ΔS-Cys- Alb in the controls barely overlapped with those of the cases (receiver operating characteristic curve c-statistic = 0.96) and the mean value of ΔS-Cys-Albumin was strongly significantly lower in the controls than it was in the cases ($p < 1 \times 10^{-20}$; two-tailed student's t test). ΔS- Cys-Alb in the stage I lung cancer cases was essentially the same as it was in fresh samples from cancer free patients (**Figure 2.7 and 2.18**), meaning that the difference in ΔS-Cys-Albumin between the cases and controls in this set cannot be because of the presence of cancer— leaving variable exposure to the thawed state as the only reasonable explanation for the difference observed. This was subsequently confirmed by the sample providers.

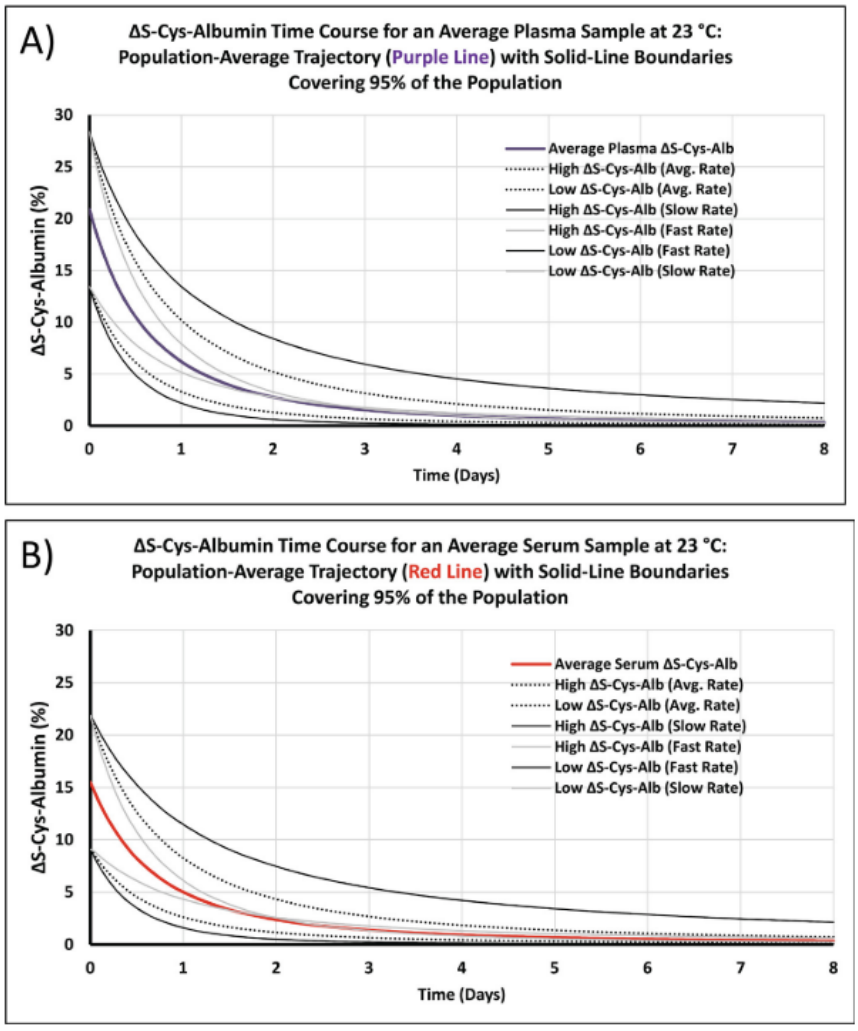

Figure 2.20: Modeled time course trajectories for ΔS-Cys-Albumin in A) plasma and B) serum. Colored curves indicate average trajectories based on known population average starting concentrations for all relevant reactants, products and the copper catalyst. For details and rate model constants refer to the publication (64). Curves with average rates (including the colored traces) are based on the population average values for P/S copper (88) and the ratio of AlbSH/S-Cys-Albumin determined here (**Figure 2.7**). Curves with fast rates or slow rates are based on P/S copper concentrations and AlbSH/S-Cys-Albumin ratios that are 2 SDs above or below the population averages. All starting reactant, product and catalyst concentrations are provided in **Table 2.4**. These curves are useful for relating ΔS-Cys-Albumin measurements in unknown samples to the amount of time the sample(s) have spent at the equivalent of 23 °C: For groups of unknown samples, the measured ΔS-Cys-Albumin mean ± 95% CI can be overlaid on the colored traces to estimate the mean ± least and greatest amounts of exposure time. For individual unknown samples, the measured ΔS-Cys-Albumin value can be related to exposure time via the colored trace and the least and greatest likely exposure times can be estimated from the solid black lines.

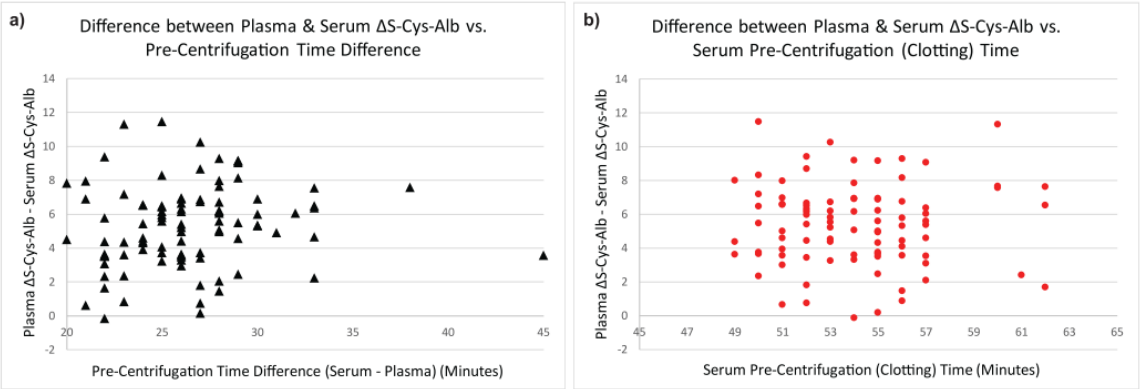

Figure 2.21: The difference between matched plasma and serum sample ΔS-Cys-Albumin values was not correlated to a) the pre-centrifugation time difference between plasma and serum or b) serum pre-centrifugation (clotting) time. ($p > 0.05$ in both cases; Spearman correlation).

Tables

Table 2.1: Initial concentrations employed for determining the rate law for S-cysteinylation (oxidation) of albumin (AlbSH) by cystine (Cys-Cys). Values listed inside the pivot table are initial rates in units of M/s.

	$[Cys\text{-}Cys]_0$ (M)				
$[AlbSH]_0$ (M)	0.0003	0.00045	0.0006	0.00075	0.0009
0.00003	6.68E-10	9.35E-10	1.31E-09	1.33E-09	2.38E-09
0.000045	1.61E-09	1.85E-09	2.67E-09	3.52E-09	4.67E-09
0.00006	1.69E-09	2.21E-09	2.8E-09	4.06E-09	4.88E-09
0.000075	2.25E-09	2.84E-09	4.77E-09	5.92E-09	6.87E-09
0.00009	2.88E-09	5.33E-09	5.12E-09	7.9E-09	8.61E-09

Table 2.2: Initial concentrations employed for determining the rate law for reduction of S-cysteinylated albumin (S-Cys-Albumin) by cysteine (Cys). Values listed inside the pivot table are initial rates in units of M/s.

	$[Cys]_0$ (M)				
$[S\text{-}Cys\text{-}Alb]_0$ (M)	0.0003	0.00045	0.0006	0.00075	0.0009
0.00003	3.008E-08	4.84E-08	6.0667E-08	7.79E-08	9.75E-08
0.000045	4.679E-08	6.091E-08	7.608E-08	1.12E-07	1.33E-07
0.00006	8.413E-08	9.616E-08	1.1294E-07	1.26E-07	1.67E-07

Table 2.3: ΔS-Cys-Albumin kinetics for average plasma and serum samples at 23 °C, with the corresponding number of samples required (n-values; based on statistical power calculations) to detect the indicated time of exposure.

Time at 23 °C (Hrs)	Plasma		Serum	
	ΔS-Cys-Albumin	One-Group Comparison to Population Mean at Time 0: n for ≥ 80% Power to Detect Exposure Time[b]	ΔS-Cys-Albumin	One-Group Comparison to Population Mean at Time 0: *n* for ≥ 80% Power to Detect Exposure Time[b]
0	20.9	–	15.5	–
1	19.6	52	14.6	79
2	18.4	15	13.8	23
3	17.3	8	13.0	12
4	16.3	6	12.3	8
5	15.4	5	11.7	6
6	14.5	4	11.1	5
7	13.7	4	10.5	5
8	13.0	4	10.0	4
9	12.3	3	9.5	4
10	11.7	≤ 3	9.0	4
11	11.1	≤ 3	8.6	4
12	10.6	≤ 3	8.2	3
13	10.1	≤ 3	7.9	≤ 3
14	9.6	≤ 3	7.5	≤ 3
15	9.1	≤ 3	7.2	≤ 3
16	8.7	≤ 3	6.9	≤ 3
17	8.3	≤ 3	6.6	≤ 3
18	8.0	≤ 3	6.3	≤ 3
19	7.7	≤ 3	6.1	≤ 3
20	7.3	≤ 3	5.8	≤ 3
21	7.0	≤ 3	5.6	≤ 3
22	6.7	≤ 3	5.4	≤ 3
23	6.5	≤ 3	5.2	≤ 3
24	6.2	≤ 3	5.0	≤ 3

Table 2.4: Starting reactant and product concentrations for **Figure 2.20**

	Alb_{tot}		AlbSH		S-Cys-Alb		Cys-Cys		Cys		Cu		Fraction S-Cys-Alb		ΔS-Cys-Alb (as fraction)	
	Plasma	Serum	Plasma	Serum	Plasma	Serum	Plasma	Serum	Plasma	Serum	Plasma	Serum	Plasma	Serum	Plasma	Serum
Average P/S ΔS-Cys-Albumin	646	646	462	469	184	177	65.0	47.5	5	5	18.7	9.35	0.285	0.274	0.209	0.155
High P/S ΔS-Cys-Albumin (Avg. Rate) [a]	540	540	386	392	154	148	73.9	56.5	5	5	18.7	9.35	0.285	0.274	0.283	0.218
Low P/S ΔS-Cys-Albumin (Avg. Rate)	752	752	538	546	214	206	48.3	31.7	5	5	18.7	9.35	0.285	0.274	0.135	0.091
High P/S ΔS-Cys-Albumin (Slow Rate)	540	540	333	336	207	204	73.9	56.5	5	5	9.5	4.75	0.384	0.378	0.283	0.218
High P/S ΔS-Cys-Albumin (Fast Rate)	540	540	440	448	100	92	73.9	56.5	5	5	27.9	13.95	0.185	0.170	0.283	0.218
Low P/S ΔS-Cys-Albumin (Fast Rate)	752	752	611	624	139	128	48.3	31.7	5	5	27.9	13.95	0.185	0.170	0.135	0.091
Low P/S ΔS-Cys-Albumin (Slow Rate)	752	752	463	468	289	284	48.3	31.7	5	5	9.5	4.75	0.384	0.378	0.135	0.091

[a] All concentrations are in units of micromolar

[b] Fraction S-Cys-Alb and ΔS-Cys-Alb are based on the population values determined here. Total albumin (Alb_{tot}) is based on the U.S. age distribution weighted population average for serum albumin (10,11). Cu(II) is based on the U.S. population average concentration of copper in serum (12); values for the kinetics model are halved in serum due to the sequestration of copper in ceruloplasmin as explained in the main text. Cys is fixed at 5 micromolar as explained in the main text. Cys-Cys was set based on Alb_{tot} and the targeted ΔS-Cys-Alb (as fraction) value. AlbSH and S-Cys-Alb were set based on the targeted Fraction S-Cys-Alb value.

[c] High/Low ΔS-Cys-Albumin values are based on 2 SDs above/below the population mean. Fast/slow rates are based on copper concentrations that are 2 SDs above/below the population mean and Fraction S-Cys-Alb that is 2 SDs bellow/above the population mean.

CHAPTER 3

TRACKING THE STABILITY OF CLINICALLY RELEVANT BLOOD PLASMA PROTEINS WITH DELTA-S-CYS-ALBUMIN—A DILUTE-AND-SHOOT LC/MS-BASED MARKER OF SPECIMEN EXPOSURE TO THAWED CONDITIONS

3.1. Introduction

As the acellular component of blood, plasma/serum (P/S) exchanges biological information in the form of biomolecules with every organ system in the body. Because it carries this wealth of information and can be non-invasively collected, P/S is one of the most common biospecimens employed in biomedical research. Moreover, P/S samples collected during clinical studies frequently carry potential research value well beyond that intended by the original research design and are therefore archived for future research purposes. Millions of P/S samples are currently stored in biobanks around the world awaiting withdrawal and subsequent queries on the molecular information they contain. The answers to these queries, however, reflect both in vivo and ex vivo biochemistry—meaning that if the latter has impacted the former, incorrect and potentially misleading information will be obtained. This can readily occur when pre-analytical variables (PAVs) are inadequately controlled (12, 26, 28, 33, 80, 81, 83, 124).

During sample collection, processing, transport and storage, every biospecimen is exposed to PAVs. While the number of PAVs can be quite large (30, 31, 80, 83, 125–127), proper sample handling techniques can keep them tightly controlled, protecting in vivo biochemistry from ex vivo modulation. Many, if not most PAVs present themselves during collection and initial processing, providing a single window of opportunity to

either handle them correctly or not. For example, P/S PAVs such as the type of blood collection tube, proper collection tube filling, number of collection tube inversions, pre-centrifugation delay, and post-centrifugation delay are all completed in a single pass and the record of these PAVs will not ever have an opportunity to change during the life of the P/S specimen. Other PAVs, however, are constantly subject to change.

Of these, the PAV that is arguably the most difficult to control and track over the life of an archived specimen is exposure to thawed conditions. P/S does not fully freeze until the temperature is -30 °C or colder (50). When thawed, a wide range of ex vivo biochemical reactions can take place, distorting the portrait of in vivo biochemistry that the samples are supposed to reflect. While many if not most researchers who handle P/S know that it should be stored at -80 °C or colder, the facts that not all labs possess a -80 °C freezer, that -20 °C freezers are common, that P/S appears (visually) to be frozen at -20 °C, and that many clinical research protocols allow at least temporary storage of newly collected specimens to be stored at -20 °C for days to weeks before transfer to a -80 °C freezer means that many P/S samples become compromised by temporary storage at -20 °C. Moreover, even after placement in a -80 °C freezer, an ever-present risk of exposure to thawed conditions remains in place for the life of every aliquot of P/S. For example, -80 °C freezer failures occur, delays during sample shipments may result in the loss of dry ice and induce thawing, and there may be need(s) to re-aliquot samples. Thus, thawing remains a constant threat to the integrity all P/S samples until they have been analyzed.

For any given collection of samples, the scale of the problem depends on the degree to which specimen biomolecules no longer reflect in vivo reality. But it is not immediately

obvious that for common biomarker discovery and related investigations *even a very low percentage of molecules deviating from in vivo reality* presents a major *false discovery trap*: Several studies over the past decade have estimated the percentages of different types of biomolecules that are quantitatively altered upon P/S exposures to common thawed conditions (72, 73, 76–79). They have found that generally low percentages (i.e., 2-20%) of biomolecules are unstable when the specimens in which they reside are exposed to common thawed conditions. On its surface, this gives the appearance that the problem is insignificant. A quick thought experiment, however, demonstrates the opposite: Imagine a set of serum samples from stage I lung cancer patients that has been paired with age/gender/smoking-matched samples from at-risk but cancer-free donors to comprise a case/control study. If each sample contains 50,000 different measurable biomolecules (i.e., 50,000 qualitatively different metabolites, proteins, miRNAs, etc.) we might optimistically estimate that 5 of these might serve as effective markers of stage I lung cancer. If, however, a portion of the case specimens were exposed to a > -30 °C thaw event while the control samples were not (or vice versa—a rather common scenario as we have shown (64, 68), resulting in statistically significant shifts in the concentration of *only 2%* of exposed-sample biomolecules, this would introduce a *200-fold excess* ((50,000 * 0.02) / 5 = 200) of falsely altered biomolecules relative to the number of bona fide biomarkers waiting to be discovered. Hence the *false discovery trap*: The seemingly minor thaw event has introduced a clinical reality-hiding minefield of false / irreproducible “discoveries” waiting to mislead investigators and waste time and money in the process (**Figure. 3.1**).

Of course, P/S thawing results in multiple different types of ex vivo biomolecular change. Proteins are susceptible to artifactual ex vivo post translational modifications such as glycation (110, 128, 129), oxidation (both S-cysteinylation (34, 64) and methionine sulfoxidation (34)), and proteolytic degradation (130–133). Modifications such as these can potentially impact protein quantification without any indication that they have occurred—particularly when quantification is dependent on specific molecular interactions that may be silently disrupted by these modifications (e.g., immunoassays). Numerous examples of apparent changes in protein concentrations occurring due to P/S exposure to thawed conditions are summarized elsewhere (65, 68, 76, 111). Unfortunately, enzymatic, oxidative and/or other ex vivo chemical processes do not solely impact proteins; they impact every major class of biomolecule, including small molecules/metabolites (57, 134, 135) lipids (56, 136), cholesterol (136), peptides (80), nucleic acids such as miRNAs (58), and, to a modest degree, glycans (137–139). This problem should be of substantial concern to biomedical researchers who employ archived blood P/S in their research, as such evidence suggests that without comprehensive documentation on how these archived P/S samples have been handled and stored, it may be impossible to properly determine their suitability for specific projects.

Unfortunately, documentation alone does not always suffice as sufficient evidence of P/S integrity. We have recently shown via two independent incidents that empirical molecular evidence—above and beyond paper trails—may be required to accurately document the integrity of archived P/S samples (64, 65). These discoveries were enabled by our recent development of a biomarker of P/S exposure to thawed conditions known as ΔS-Cys-Albumin (64), which quantifies cumulative exposure of P/S to thawed conditions (i.e.,

temperatures > -30 °C (50)). In summary, it is a 10-µL, dilute-and-shoot, intact-protein liquid chromatography-mass spectrometry (LC/MS)-based assay of the relative abundances of albumin proteoforms. The assay is based on the fact that the relative abundance of S-cysteinylated (oxidized) albumin in P/S increases inexorably but to a maximum value under 100% when samples are exposed to temperatures above -30 °C. The difference in the relative abundance of S-cysteinylated albumin (S-Cys-Albumin) before and after an intentional incubation that drives this proteoform to its maximum level is denoted as ΔS-Cys-Albumin. ΔS-Cys-Albumin in fully expired samples is zero. The range (with mean ± 95% CI) observed for ΔS Cys Albumin in freshly collected plasma is 12-29% (20.9 ± 0.75%; n = 97), and in matched serum it is 10-24% (15.5 ± 0.64%; n = 97) (64). Cumulative exposure is calculated via a multi-reaction biochemical rate law that we and others have established (64, 93) and that we have shown is applicable to actual plasma & serum samples, enabling back-calculation of the time at which unknown P/S specimens have been exposed to the equivalent of room temperature (64).

Rate law-based linkage of ΔS-Cys-Albumin to the equivalence of exposure time at room temperature provides an intrinsic connection between ΔS-Cys-Albumin and any clinical biomarker with a known stability profile at room temperature. But for candidate clinical biomarkers without known stability profiles or P/S samples that may be known to have only been exposed to refrigeration or -20 °C storage, a definitive connection between ΔS-Cys-Albumin and marker stability remains poorly established. Thus, the purpose of this study was to concurrently evaluate the stability of proteins of interest to pre-clinical research at -20 °C, 4 °C and 23 °C in conjunction with ΔS-Cys-Albumin measurements

in order to begin to forge an empirical linkage between protein stability at all major storage temperatures and ΔS-Cys-Albumin.

3.2. Materials and Methods

3.2.1. Plasma and serum sample collection

Matched serum, lithium heparin plasma, and K_2EDTA plasma were collected (in that order) from gastrointestinal (GI) cancer patients and cancer-free donors under informed consent and local IRB approval by the Cooperative Human Tissue Network (CHTN; Nashville, TN) or Valleywise Health (Phoenix, AZ). Specimens were collected in compliance with the Declaration of Helsinki principles. Analysis of the specimens as described in this article was approved by the Arizona State University IRB. Basic donor demographics and disease status information is provided in **Table 3.1**. Patients with compromised kidney function (i.e., eGFR < 60 mL/min per 1.73m^2) were excluded due to the possibility that poor kidney function can, in theory, result in abnormally high ΔS-Cys-Albumin measurements (64).

In total, 84 patients were enrolled in this study. Thirty seven were GI cancer patients and 47 were cancer-free control donors. ΔS-Cys-Albumin in their matched K_2EDTA plasma, lithium heparin plasma, and serum was measured at baseline. Of these patients, matched K_2EDTA plasma and serum from 24 of them were employed for the ΔS-Cys-Albumin time courses. K_2EDTA plasma from these 24 patients was employed for measurements of the clinically relevant proteins. The data shown in **Figure 3.2** from 97 non-acute cardiac patients were originally described elsewhere (64) and were simply included in **Figure 3.2** for the sake of comparison.

A strict blood collection and processing protocol was followed that included the following: Plasma tubes were pre-chilled to 0-4 °C. Collection tubes were properly filled (any partially filled tubes were rejected). Immediately after collection serum tubes were inverted (never shaken) five times and plasma tubes were inverted eight times. Serum was allowed to clot at room temperature for 45 minutes. Matched plasma was placed on ice while serum clotted, then all tubes were centrifuged at 4 °C. Plasma and serum were then immediately aliquoted on ice. Aliquots were placed in a -80 °C freezer within 2 hours from the time of initial draw. To verify the timing of all processing steps, time stamps were recorded at 1) the time of initial draw, 2) time of centrifugation completion, and 3) the time at which aliquots were placed at -80 °C. Plasma or serum with a visually estimated degree of hemolysis > 250 mg/dL were excluded.

Plasma and serum samples were shipped to Arizona State University (Tempe, AZ) overnight on dry ice. Upon receipt, specimens were verified as frozen and then unpacked into a -80 °C freezer equipped with continuous temperature monitoring. All specimens were allowed to sit in the -80 °C for at least 7 days prior to thawing to ensure that any residual CO_2 in the headspace had been exchanged for air in order to avoid any CO_2-induced sample acidification effects (140).

3.2.2. Initial Analysis and Thawed-State Stability Studies

All samples were randomized prior to analysis using a random number generator for run order assignment. ΔS-Cys-Albumin in pristine, never-thawed aliquots was measured within a time range of 12-20 months after initial specimen collection, during which time specimens were kept continually at -80 °C.

Following collection of baseline ΔS-Cys-Albumin values, K_2EDTA plasma and matched serum from 12 GI cancer patients and 12 cancer-free control donors were selected for inclusion in thawed-state stability studies based on their initial ΔS-Cys-Albumin values being equally distributed across the entire range of initial ΔS-Cys-Albumin values measured. Thawed-state stability studies involved incubation of separate aliquots of these plasma and serum samples for up to 65 days at -20 °C, 28 days at 4 °C, or 96 hours at 23 °C. ΔS-Cys-Albumin was measured in both plasma and serum; proteins of clinical interest were only measured in K_2EDTA plasma.

A separate aliquot for each individual non-baseline thawed-state time point *and* protein assay (either 20 μL for ΔS-Cys-Albumin or 100 μL for protein measurements), was created from a parent aliquot that had never previously been thawed. To create these aliquots, the parent sample was thawed and kept on ice with strict time tracking for a period of 3.4 ± 1.1 (SD) min for the 23 °C-exposed samples, 8.5 ± 2.0 min for the 4 °C-exposed samples, and 14.2 ± 3.0 min for the -20 °C-exposed samples—by which times all temperature exposure time courses were started. Time course aliquots were immediately placed at -80 °C upon completion of their time/temperature exposure period. Once all time courses were completed, time course aliquots were randomized and ΔS-Cys-Albumin or the clinically relevant proteins were measured in them. Clinically relevant proteins at all stability time points (including baseline) were measured as a randomized set of 240 K_2EDTA plasma samples by multiplexed immunoassay on the either the Luminex 100 or 200 platform by MyriadRBM (Austin, TX). Each protein was measured once in each sample. Given that patient specimens were collected over a period of about one year, clinically relevant proteins were analyzed within a time range of 18-30

months after initial specimen collection. With the exception of intentional thawed-state incubation periods, all specimens were kept continually at -80 °C prior to analysis. After all ΔS-Cys-Albumin and clinically relevant protein time course specimens were analyzed, ΔS-Cys-Albumin was once again measured in a residual never-thawed aliquot of each sample in order to verify the long term stability of ΔS-Cys-Albumin at -80 °C. This occurred one year after the initial ΔS-Cys-Albumin measurements in never-thawed samples were made.

3.2.3. Statistical Analysis

To evaluate the stability of clinically established protein biomarkers in K_2EDTA plasma, the concentration measured for each analyte at each condition was compared with its respective control aliquot kept continuously at -80 ℃. Data consisted of n = 24 subject samples measured longitudinally over time at temperatures of 23 °C, 4 °C, and -20 °C, respectively. First, we performed descriptive statistics and analyzed ΔS-Cys-Albumin at the baseline data (at time = 0), comparing the effect of health status (cancer vs. normal), gender (male vs. female), and race (white vs. black) using a two-sample t-test. The age effect was tested using simple linear regression. Second, we analyzed longitudinal ΔS-Cys-Albumin data using linear mixed effects models to account for the repeated measures within subjects. Specifically, we consider the full model as follow:

$$y_{ij} = \beta_0 + \beta_1 age_i + \beta_2 status_i + \sum_{j=1}^{q} \beta_{3j} t_{ij} + \sum_{j=1}^{q} \beta_{4j} age_i t_{ij} + \sum_{j=1}^{q} \beta_{5j} status_i t_{ij} + \epsilon_{ij}$$

where y_{ij} is the concentration of ΔS-Cys-Albumin for the i^{th} subject at j^{th} time point, age_i is the age for the i^{th} subject, $status_i$ is 1 if i^{th} subject's status is cancer and 0 otherwise, t_{ij}=1 if y_{ij} is observed at the j^{th} time point, and t_{ij}=0 otherwise, ϵ_{ij} is an error term, and q is

the number of time points observed excluding the baseline. We employed a step-down approach that dropped the interaction term of status and time if they were non-significant and used reduced models with the main effects only.

The same approach was used to analyze the 21 clinically relevant proteins, with natural logarithm transformed y values to improve normality. Using the reduced model, the least square means of the y values at each time point were computed and compared between the baseline and any of the other time points using Wald tests. Bonferroni corrections were applied to adjust the calculated *p*-values of the 21 proteins for pairwise comparisons between time points. Bonferroni-adjusted *p*-values less than 0.05 were regarded as statistically significant. All the analyses were conducted at each temperature separately. Serum and K_2EDTA plasma samples were additionally separated when analyzing ΔS-Cys-Albumin.

Finally, we conducted repeated measures correlation (141) to quantify the association between ΔS-Cys-Albumin and each unstable protein. Pearson correlation coefficients were calculated to quantify the association between ΔS-Cys-Albumin and the percentage of destabilized proteins. We used GraphPad Prism® software (version 9.3.1) for descriptive statistics, t-tests and repeated measures (RM)-ANOVA; MIXED procedure in SAS 9.4 (SAS Inst. Inc., Cary, NC) for linear mixed effects models and R 4.1.0 (R foundation, Vienna, Austria) and R rmcorr package for correlation analyses.

3.2.4. Laboratory Procedures

3.2.4.1. Measurement of ΔS-Cys-Albumin

P/S samples were prepared and the percentage of albumin in the S-cysteinylated form (S-Cys-Albumin) was measured as previously described (34, 64). Briefly, one microliter of plasma or serum was diluted 1000-fold in 0.1% (v/v) trifluoroacetic acid (TFA) and injected onto an LC-MS instrument where albumin was concentrated and desalted on a protein cap-trap then eluted directly into the mass spectrometer for measurement of the intact protein and relative quantification of its proteoforms. Nine microliters of the same plasma or serum sample was then placed in a 0.6-mL polypropylene Eppendorf snap-cap tube and incubated in a dry oven at 37 °C for 24 hours. One microliter of this sample was then diluted 500-fold in 0.1% TFA and injected onto the LC-MS for analysis. ΔS-Cys-Albumin is defined as the *difference* between the percentage of albumin in the S-cysteinylated form before and after the overnight incubation at 37 °C that drives the percentage of S-Cys-Albumin to its maximum value (64).

3.2.4.2. Measurement of Clinically Relevant Proteins

Twenty-five clinically relevant proteins were measured via three multi-analyte profile assays (MAPs) in each 100-µL K_2EDTA plasma aliquot from the thawed-state stability studies. MAPs were preconfigured and validated by MyriadRBM and included "HCANCER2", "HMP8" and "HMPC38".

The HCANCER2 MAP included Amphiregulin, Epidermal Growth Factor (EGF), Epidermal Growth Factor Receptor (EGF-R), Epiregulin, Heparin-Binding EGF-Like

Growth Factor (HB-EGF), Placenta Growth Factor (PGF), Platelet-Derived Growth Factor BB (PDGF-BB), and Tenascin-C.

The HMP8 MAP included Adiponectin, Alpha-2-Macroglobulin (A2M), Ferritin, Myoglobin, Plasminogen Activator Inhibitor 1 (PAI-I), T-Cell-Specific Protein RANTES, Tissue Inhibitor of Metalloproteinases-1 (TIMP-1), Tumor necrosis factor receptor-2 (TNF-R2), Vascular Cell Adhesion Molecule-1 (VCAM-1), EN-RAGE and Pulmonary and Activation-Regulated Chemokine (PARC).

The HMPC38 MAP included Alpha-Fetoprotein (AFP), Cancer Antigen 125 (CA-125), Cancer Antigen 19-9 (CA-19-9), Carcinoembryonic Antigen (CEA), Human Chorionic Gonadotropin beta (hCG-b) and Neuron-Specific Enolase (NSE).

Samples were measured in random order by trained MyriadRBM personnel who thawed samples for the minimal required time and kept them on ice when thawed prior to analysis. Comprehensive assay validation data are available from MyriadRBM or the corresponding author upon request.

Four of the above proteins were measured but were below the LOQ in the vast majority of samples and were therefore not reported here. These included amphiregulin, epiregulin, PGF, and hCG-b. For a few of the 21 proteins reported on here, one or more patients had concentrations that were at or below the LOQ for all stability time points. These included Alpha-Fetoprotein (14 patients always below LOQ), CA-19-9 (6 such patients), CEA (1 such patient). Data on these proteins from such patients were excluded from statistical analysis. There were also instances in which at least one but not all protein concentrations from a given patient were reported as being at or below the LOQ.

This occurred at least once for AFP, CA-125, CA19-9, CEA, EGF, HB-EGF, and PDGF-BB. (**Figure 3.3** provides a graphical view of the overall minor extent of these occurrences.) These data points were included in the statistical analysis as being at the LOQ because they were known to not be higher than the LOQ and, for baseline measurements (time = 0), this information alone was potentially helpful in facilitating the detection of a protein instability when protein concentrations apparently increased over time—which constituted the vast majority of instabilities detected (such as that of EGF). In all such cases, had the LOQ been lower, it would have enhanced rather than diminished the magnitude of an instability finding. Consistency in this practice, however, meant that including non-baseline measurements at the LOQ tended to otherwise blunt the ability to statistically detect unstable proteins.

3.3. Results

3.3.1. ΔS-Cys-Albumin Baseline Values in Fresh Plasma and Serum Samples

In 2019 we published baseline values for fresh, rapidly processed, matched K_2EDTA plasma and serum samples from 97 non-acute patients with cardiovascular disease (CVD) (64). The clinical characteristics of these donors with CVD are described elsewhere (64) but their baseline ΔS-Cys-Albumin data are provided here for comparison alongside new data from 37 GI cancer patients, and 47 cancer-free control donors. (Illustrative raw and charge deconvoluted mass spectral data are provided elsewhere (34).) Matched LiHep plasma was also collected from the GI cancer patients and cancer-free control donors (**Figure 3.2**). An elevation of ΔS-Cys-Albumin in the serum of GI cancer patients compared to the other two patient cohorts was observed. Similarly, ΔS-Cys-Albumin in K_2EDTA plasma was higher in CVD patients than in the cancer-free control donors. The

difference in ΔS-Cys-Albumin between LiHep plasma groups did not quite reach statistical significance (**Figure 3.2A**). Within CVD patients and cancer-free controls, ΔS-Cys-Albumin in K_2EDTA plasma was higher than that of serum in matched collections; and in the cancer-free controls it was also higher than LiHep plasma (**Figure 3.2B-D**). No differences in matched collections were observed, however, between the three matrices in GI cancer patients. Baseline ΔS-Cys-Albumin values in chemotherapy patients (not annotated in **Figure 3.2**) did not differ from cancer patients who were not on chemotherapy at the time of blood draw (t-test; $p > 0.5$). The range (with mean ± 95% CI) observed for ΔS-Cys-Albumin in fresh (baseline) GI cancer patient serum was 12-32% (19.0% ± 1.5%). In their K_2EDTA plasma it was 13-31% (19.6% ± 1.3%). And in their lithium heparin plasma it was 12-32% (18.6% ± 1.5%). For the cancer-free controls, these values were for serum were 10-24% (16.3% ± 1.0%), for K_2EDTA plasma were 13-27% (18.6% ± 1.0%), and for lithium heparin plasma were 10-24% (16.4% ± 0.92%). For comparison and as described elsewhere (22), non-acute CVD patient serum was 10-24% (15.5% ± 0.64%) and their K_2EDTA plasma was 12-29% (20.9% ± 0.75%).

Effects of age, gender and race on baseline ΔS-Cys-Albumin values in the GI cancer patients and cancer-free control donors were also assessed. No significant differences were observed between genders or races for any matrix (t-tests; $p > 0.05$; see **Table 3.1** for n-values). ΔS-Cys-Albumin was slightly but consistently linearly correlated with age in all three matrices (**Figure 3.4**). In serum slope = 0.079 ΔS-Cys-Albumin units/yr, $p = 0.015$, Pearson correlation coefficient (r) = 0.26; in K_2EDTA plasma slope = 0.074 ΔS-Cys-Albumin units/yr, $p = 0.013$, r = 0.27; in LiHep plasma slope = 0.064 ΔS-Cys-Albumin units/yr, $p = 0.039$, r = 0.23. After adjusting for age, the differences between GI

cancer patients and cancer-free controls for serum and LiHep plasma (**Figure 3.2A**) were diminished, but not eliminated (t-test; serum $p = 0.020$, K_2EDTA plasma $p = 0.63$, LiHep plasma $p = 0.029$). And as expected, adjustment for age did not alter the fact that ΔS-Cys-Albumin was significantly higher in K_2EDTA plasma relative to serum and LiHep plasma in matched collections from the cancer-free control patients.

3.3.2. ΔS-Cys-Albumin Time Courses at 23 °C, 4 °C, and -20 °C

A separate aliquot for each individual time point was created from parent samples that had never previously been thawed. To create these aliquots, the parent sample was thawed and kept on ice for strictly limited and documented time periods as described in the *Experimental* section. ΔS-Cys-Albumin was measured at 9-11 different time points per exposure temperature (23 °C, 4 °C, or -20 °C) in K_2EDTA plasma and serum aliquots from 12 GI cancer patients and 12 cancer-free donors.

K_2EDTA plasma and serum results are shown separately (**Figure 3.5**) because, as mentioned above and as we have previously described, K_2EDTA plasma and serum tend to have both different initial ΔS-Cys-Albumin values in matched samples and different rates of change when the samples are exposed to thawed conditions (64). Control measurements of ΔS-Cys-Albumin in never-thawed aliquots of these K_2EDTA plasma and serum samples that were kept continuously at -80 °C for approximately one year after the initial baseline ΔS-Cys-Albumin measurements were made showed no significant change from their original measurements (**Figure 3.6**)). An initial mixed effects model confirmed a strong interaction between matrix type and time ($p < 0.001$ at all temperatures). As such, K_2EDTA plasma and serum time courses were subsequently

analyzed separately by mixed effect models that included patient age, health status, and time at the indicated temperature as main effects and patient age x time and health status x time as interactions.

Neither interaction was found to be statistically significant in either K_2EDTA plasma or serum—meaning that there was no statistical evidence that patient age or health status impacted the manner in which ΔS-Cys-Albumin decayed over time. Data were re-analyzed after eliminating these interactions from the model in order to robustly identify significant main effects: As expected, exposure time at all three temperatures resulted in strongly significant changes in ΔS-Cys-Albumin values (Bonferroni adjusted $p < 1 \times 10^{-8}$). Patient health status did not significantly impact overall K_2EDTA plasma time course results at any temperature (**Figure 3.5A-C**), but it did significantly impact overall serum time course results at all three temperatures (Bonferroni adjusted $p < 0.05$; **Figure 3.5D-F**). This indicated that GI cancer patient serum samples tended to have slight to modestly higher ΔS-Cys-Albumin values than the cancer-free control donors regardless of any thawed-state exposure that may have occurred. Overall, these results are consistent with the fact that ΔS-Cys-Albumin in the serum of cancer patients started (at baseline) at significantly higher values than in the serum of cancer-free donors. (**Figure 3.5A**). The mixed effects model also revealed that patient age had a slight but statistically significantly impact on overall K_2EDTA plasma time course results at 4 °C and -20 °C and significantly impacted overall serum time course results at 23 °C (Bonferroni adjusted $p < 0.05$; time courses stratified by age are not shown). These observations were consistent with the weak correlations of ΔS-Cys-Albumin with patient age observed in fresh K_2EDTA plasma and serum samples. As noted below, however, the vast majority of

clinically relevant proteins in fresh K_2EDTA plasma samples had much stronger correlations with patient age than did ΔS-Cys-Albumin.

3.3.3. Clinically Relevant Protein Time Courses at 23 °C, 4 °C and -20 °C

Twenty-one clinically relevant proteins (**Table 3.2**) were measured by Luminex assay in the K_2EDTA plasma samples from both the GI cancer patients and cancer-free controls at baseline plus three additional time points per temperature (**Figure 3.3**). At baseline, there were no significant differences in any clinically relevant protein based on gender, race, or health status after correcting for multiple comparisons. Notably, however, all of these proteins except α-fetoprotein (AFP) and carcinoembryonic antigen (CEA) were strongly significantly correlated with patient/donor age (**Table 3.3**).

Several proteins exhibited instability in K_2EDTA plasma over time at 23 °C, 4 °C and -20 °C (**Figure 3.7 and Figure 3.3**). Repeated measures-based mixed effects models were used to determine which proteins changed in a statistically significant manner over time at each temperature. Interactions of patient age × exposure time and patient health status × exposure time at each temperature were considered (along with patient age, health status and exposure time as main effects) but no interactions were found to be statistically significant. As such, the mixed effects model was simplified to include only patient age, health status and exposure time at each temperature as main effects. Following the identification of significantly altered proteins, Wald tests were applied to identify which time point(s) were significantly different from baseline. Here, criteria of raw *p*-value less than 0.05/63 (due there being 21 proteins compared at 3 time points per temperature) or 7.9×10^{-4} *and* fold change > 10% were both required to consider a protein as significantly

altered by a given time-temperature exposure (**Figure 3.7**). The proteins most strongly and consistently impacted by exposure of K_2EDTA plasma to 23 °C, 4 °C or -20 °C were neuron specific enolase (NSE), epidermal growth factor (EGF), plasminogen activator inhibitor-1 (PAI-1), and RANTES (a.k.a. CCL5).

3.3.4. Relationships Between ΔS-Cys-Albumin and Unstable Clinically Relevant Proteins

Concurrent quantitative changes in ΔS-Cys-Albumin and each of these four unstable proteins were analyzed for consistency by repeated measures correlation (141). Strong correlations were found at most temperatures ($p < 0.001$, with $p < 0.05/12$ or 0.0042 considered significant due to multiple comparisons) (**Figure 3.8**). EGF, PAI-1, and RANTES all exhibited apparent increases in concentration as ΔS-Cys-Albumin decreased (i.e., with increased exposure time) at all three temperatures. NSE was unique in that at 23 °C and 4 °C it initially increased, but then decreased at longer exposure times (**Figure 3.8** and **Figure 3.3**). At -20 °C, however, it only exhibited an apparent increase over the time span monitored.

Finally, the relationship between ΔS-Cys-Albumin and the total percentage of destabilized proteins in K_2EDTA plasma was evaluated, considering the data from all three temperatures together (**Figure 3.9**). Proteins were considered significantly changed based on the *p*-value and fold-change criteria described above for the data in **Figure 3.8**. In addition, to account for the increase-then-decrease behavior of NSE (or similarly behaving proteins), once a protein reached the threshold for significant change (destabilization), all future time points for the protein at that temperature were also

considered points at which the protein was destabilized. A clear inverse linear relationship was found ($r = -0.61$ and $p < 0.0001$).

For the 23 °C time course the once-changed-then-always-subsequently-changed policy noted above pertaining to **Figure 3.9** had no effect. For the 4 °C time course, the policy kept only NSE significant when it might not otherwise have been. But this is appropriate because based on the 23 °C time course (**Figure 3.8 and Figure 3.3**) as NSE had an excursion in the positive direction then proceeded downward, transitioning through a false negative range. No other proteins in the 4 °C time course were affected by this policy. For the -20 °C time course the policy kept only EGF at 65 days positive. Without the policy, EGF at 65 days would not have been considered statistically significant within **Figure 3.9** because it had an elevated p-value (though its fold-change was actually increased to 1.9-fold at this time point). If the EGF point at 65 days was not considered significant, this would shift the mean data point in **Figure 3.9** that is lowest and furthest to the right on its x-axis to about 20.6%, which would actually bring it closer to the regression line—a result that shows that as it relates to proteins other than NSE, this policy actually caused a slight departure from the linear correlation shown in **Figure 3.9**.

3.3.5. Discussion

ΔS-Cys-Albumin was reported by our group as an endogenous marker of blood plasma and serum exposure to thawed conditions (> -30 °C) in 2019 (64). It is unique amongst candidate markers for this purpose because it has been extensively characterized and validated: Its mechanism of formation is understood; the multi-reaction rate law that governs albumin S-cysteinylation at 23 °C was established and can be used to

approximate exposure times of unknown samples; the population reference range for fresh samples from CVD patients was determined in 2019 (and has now been estimated here for GI cancer patients and cancer-free controls); it has passed both group-wise and individual sample-level blind challenges; and it has been employed with "real life" samples to detect previously undisclosed thawed-state exposures of nominally pristine samples being employed for biomarker discovery and validation purposes (64, 65). The 2019 paper (64) provides the information needed for laboratories to set guidelines on how ΔS-Cys-Albumin values in unknown samples can be used to evaluate the quality of P/S samples prior to starting a proteomic analysis. Here we have extended the potential utility of ΔS-Cys-Albumin by generating empirical stability time course profiles from two dozen individual patients for both serum and K_2EDTA plasma at -20 °C, 4 °C and 23 °C. Moreover, we have empirically linked ΔS-Cys-Albumin to the stability of 21 clinically relevant proteins (as measured by Luminex assay) and have shown how drops in plasma ΔS-Cys-Albumin below the range observed in pristine samples can serve as a surrogate indicator to estimate the percentage of immunoassay-measured proteins that have been destabilized in mishandled specimens (**Figure 3.9**).

Such empirical linkage of ΔS-Cys-Albumin to protein stability is useful for situations in which the stability of (pre)clinically important protein(s) of interest at room temperature is not known and therefore cannot be linked to a ΔS-Cys-Albumin cutoff threshold via its established rate law. This linkage, combined with the established mechanism of instability, known rate law, and other validation criteria described above make ΔS-Cys-Albumin the most thoroughly characterized and validated marker of blood plasma/serum exposure to thawed conditions to date—by a substantial margin.

In this study we extended measurements of ΔS-Cys-Albumin in freshly collected and processed (baseline) samples from matched serum and K_2EDTA plasma to include matched LiHep plasma as well. ΔS-Cys-Albumin in LiHep samples was the same as in serum samples, but ΔS-Cys-Albumin in K_2EDTA plasma of healthy and CVD patients tended to run a bit higher than matched serum (and LiHep) plasma. ΔS-Cys-Albumin in freshly collected and processed samples from cancer patients, however, was the same across all three matched matrices. The mechanism behind this discrepancy is not clear, but seems to be driven by modestly elevated levels of ΔS-Cys-Albumin in cancer patient serum vs. serum from the other two patient cohorts (**Figure 3.2A**). In fact, though it may not have quite reached statistical significance, ΔS-Cys-Albumin was modestly elevated in every matrix from cancer patients relative to the cancer-free control donors.

Elevated ΔS-Cys-Albumin could be caused by high cysteine/cystine concentration and/or low albumin concentrations. The most likely cause of elevated cysteine/cystine is poor renal function (64, 104), but patients with compromised renal function (eGFR < 60 mL/min per 1.73m^2) were excluded from this study. Hypoalbuminemia, however, is common in cancer patients (142) and can be associated with chemotherapy (143) as well as diminished patient survival rates (144). Most cancer patients were not undergoing chemotherapy at the time of blood collection, and those that were did not have different ΔS-Cys-Albumin values. Absolute concentrations of albumin were not determined, leaving modest hypoalbuminemia as the most likely explanation for slightly elevated ΔS-Cys-Albumin in the cancer patients relative to controls. (Notably, even after correction for age, the significant difference in baseline serum ΔS-Cys-Albumin between cancer patients and cancer-free donors remained.) The source of the difference in ΔS-

Cys-Albumin between serum and plasma was investigated in 2019 (64). No definitive explanation was identified, but the pre-centrifugation time difference between plasma and serum as well as serum clotting time were ruled out as contributors to this phenomenon.

The slight increase in baseline ΔS-Cys-Albumin observed with patient age was consistent with known decreases in P/S albumin concentration and modest increases in cysteine/cystine with age (89, 91). Notably, most of the clinically relevant proteins in baseline specimens were more strongly correlated with patient/donor age than was ΔS-Cys-Albumin (**Table 3.3**).

Variability amongst individual patient time course profiles is expected (64). The results observed here (**Figure 3.5**) are in line with the theoretical ΔS-Cys-Albumin decay curves at 23 °C based on the previously established rate law and known population reference ranges for starting concentrations of reactants and products (64). Serum tends to run at the upper limit predicted, but this probably has to do with the difficulty in estimating the concentration of catalytically available copper in the original model (64). This estimation is difficult because approximately 95% of copper is bound to ceruloplasmin in serum (102) where it is much less catalytically available relative to K_2EDTA plasma (64) where it has been extracted from ceruloplasmin and is mostly bound to EDTA.

The observation that ΔS-Cys-Albumin in serum decreases at least at fast, if not faster, at -20 °C compared to its rate of decrease at 4 °C was unexpected. Plasma and serum are partially (non-eutectically) frozen at -20 °C (50, 113). This creates a non-native system of reactants and products that are likely differently concentrated compared to when all components of plasma or serum are in the liquid state. The rate laws for the relevant

reactions have not been determined at 4 °C or -20 °C, but regardless of whether or not the reactions exhibit Arrhenius behavior, it remains possible that this differently concentrated state may lead to a situation in which the reactions run faster despite the colder temperature. Of course, this may also be reflected in the rates of other biochemical reactions—hence the need for an *empirical* linkage between ΔS-Cys-Albumin and proteins of clinical interest.

Additionally, as we have previously observed, copper is less catalytically available in serum than it is in EDTA plasma—which is likely due to the fact that it is mostly bound to ceruloplasmin in serum (64). This may account for the fact that this effect is only observed in serum—that is, in a partially frozen state at -20 °C, ceruloplasmin's structure may be altered, allowing copper to become abnormally catalytically available. At this point, however, this conjecture is strictly speculative.

The mechanisms behind the documented protein instabilities are only partially understood at this point. PAI-I is known to be released from platelets during freeze-thaw cycles (145) and in the presence of residual thrombin activity (146). For the other proteins that exhibited instability, it is logical to conclude that biomolecular changes that took place upon exposure to thawed conditions resulted in disruption of protein epitope(s) that were involved in mediating the protein interaction-based quantification. The mechanisms behind these disruptions may include artifactual oxidation (especially of free cysteine and/or methionine residues (147, 148), cf. **Table 3.2**), proteolysis, or other forms of ex vivo post-translational modification (110)—even, theoretically, disturbances to tertiary or quaternary protein structure that disrupt epitopes involved the quantification

process. Interestingly, NSE has a particularly large number of free cysteine residues (**Table 3.2**) that may be susceptible to ex vivo oxidation by mechanisms akin to those that drive albumin S-cysteinylation (34, 64, 115). A list of proteins measured in this study alongside details of the clonality (i.e., polyclonal or monoclonal) of capture and detection antibodies that were employed is provided in **Table 3.2**. While one might expect assays that rely monoclonal antibodies to be more susceptible to disruption in target protein epitopes, no clear pattern emerged from this information that would suggest that the clonality of antibody reagents employed had a major impact on the observed stability of plasma proteins.

Conclusions: The work presented here reinforces the fact that the exposure of human plasma to thawed-state conditions (i.e., > -30 °C) can lead to apparent quantitative changes in non-trivial percentages of clinically important proteins as measured by molecular interaction-based assays (e.g., antibody-based protein assays) (73, 149–152). Concurrent measurements of ΔS-Cys-Albumin and the concentrations of 21 proteins of interest to (pre)clinical research provided a direct empirical linkage between these clinically important proteins and ΔS-Cys-Albumin—allowing ΔS-Cys-Albumin to be used as a surrogate indicator of the suitability of plasma samples for analysis of the clinically relevant protein(s). Additionally, the data presented here show how ΔS-Cys-Albumin measurements can approximate the overall extent to which the proteome of plasma sample(s) has been altered (as detected by molecular interaction-based assays) due to exposure to thawed-state conditions. Therefore, ΔS-Cys-Albumin can now be used as *both* a marker of cumulative exposure to thawed state conditions as well as an estimator of cumulative damage to clinically important proteins present in plasma. This

latter feature, facilitated by the data in **Figure 3.9**, may serve as an effective means of using ΔS-Cys-Albumin measurements to empirically gauge the risk of false discovery when employing archived specimens for research purposes.

Figures

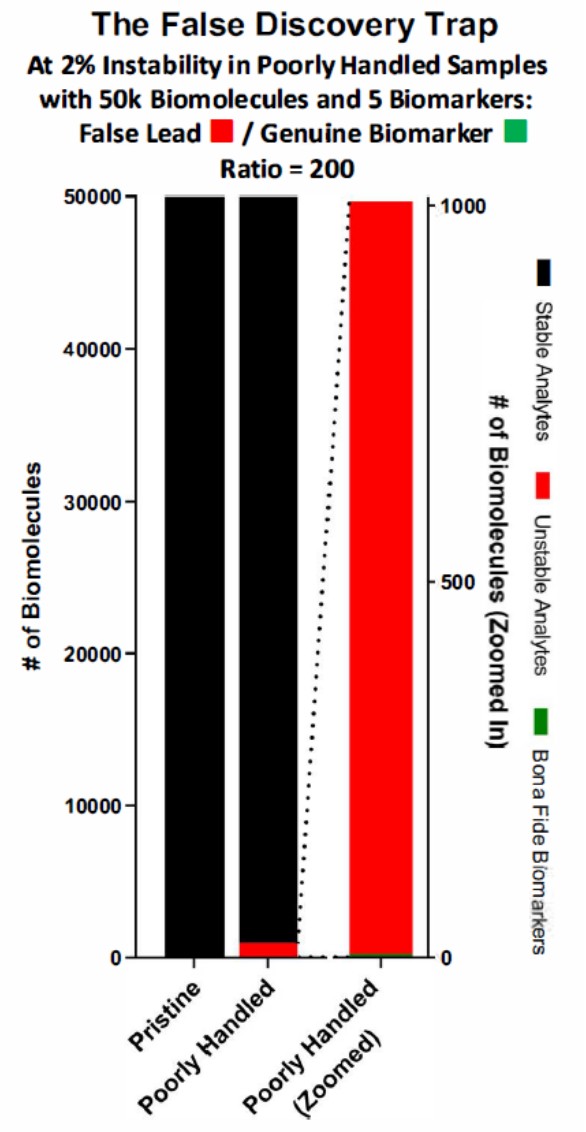

Figure 3.1: The False Discovery Trap. Unstable biomolecules within a poorly handled cohort will change relative to any other cohort with which they are compared, giving them the appearance of biomarkers. Under modest cohort mishandling that introduces quantitative instability into just 2% of analytes, a severe false lead-to-genuine biomarker ratio is introduced, creating a minefield of false discoveries that can be difficult if not impossible to avoid.

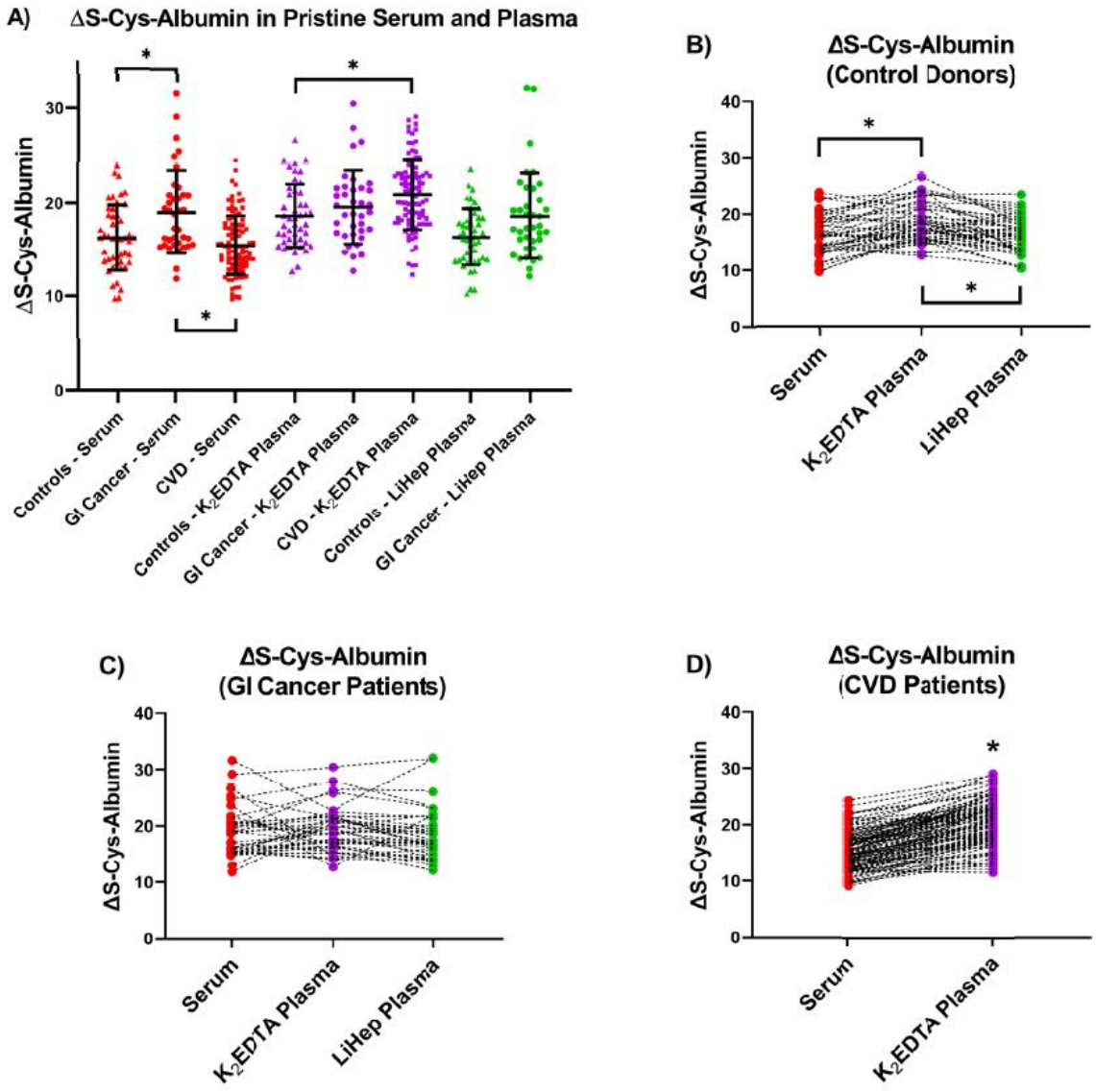

Figure 3.2: ΔS-Cys-Albumin in fresh, rapidly processed human serum and matched plasma samples. A) Comparisons between cancer-free control donors (n = 47), GI cancer patients (n = 37), and non-acute cardiac (CVD) patients (n = 97) for each matrix. Error bars represent mean ± SD; from left to right these values are: 16.3 ± 3.5, 19.0 ± 4.4, 15.5 ± 3.2, 18.6 ± 3.4, 19.6 ± 3.9, 20.9 ± 3.7, 16.4 ± 3.1, and 18.6 ± 4.6. * Indicates a significant difference between means of indicated groups based on a one-way ANOVA with Tukey's posthoc test or a t-test. Results were compared to a Bonferroni-corrected p-value threshold to account for multiple comparisons (i.e., $p < 0.05/7$ or 0.0071). B-D) Matched collections within each patient group, including B) cancer-free control donors, C) GI cancer patients, and D) CVD patients. * Indicates a significant difference between matched sets with $p < 0.00625$; repeated measures (RM) ANOVA with Tukey's posthoc test or paired t-test.

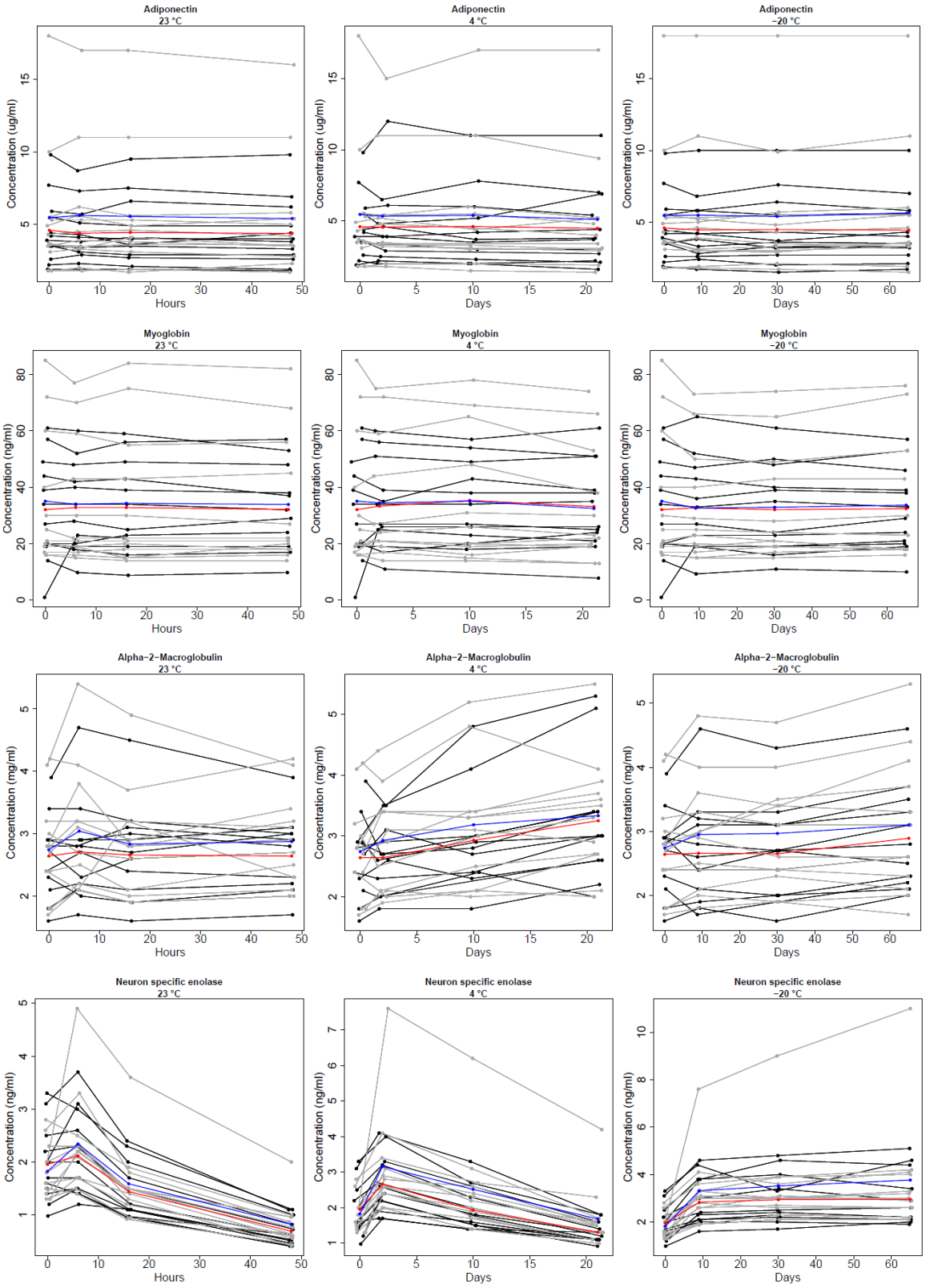

Figure 3.3: Continued on next page

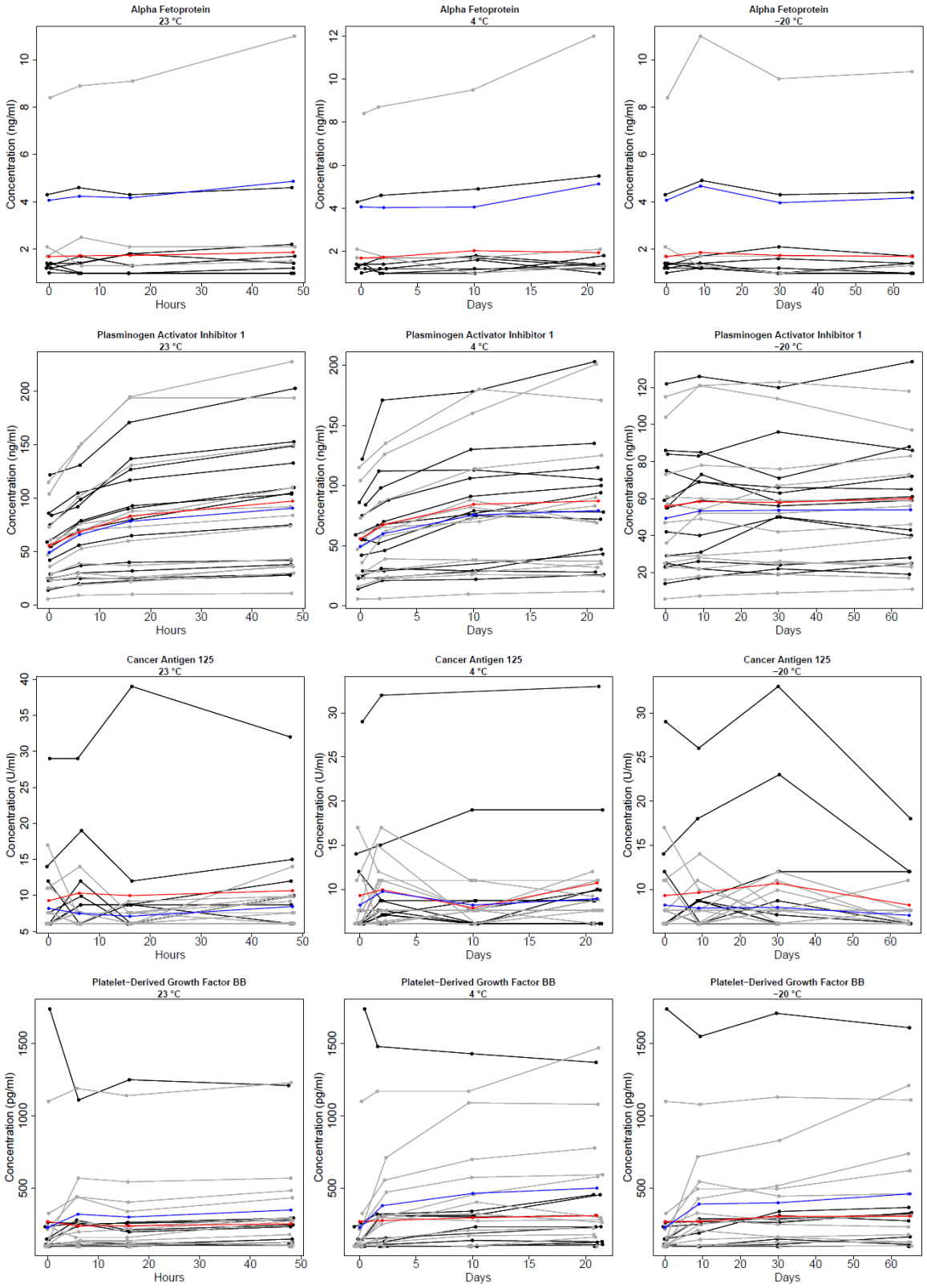

Figure 3.3: Continued on next page

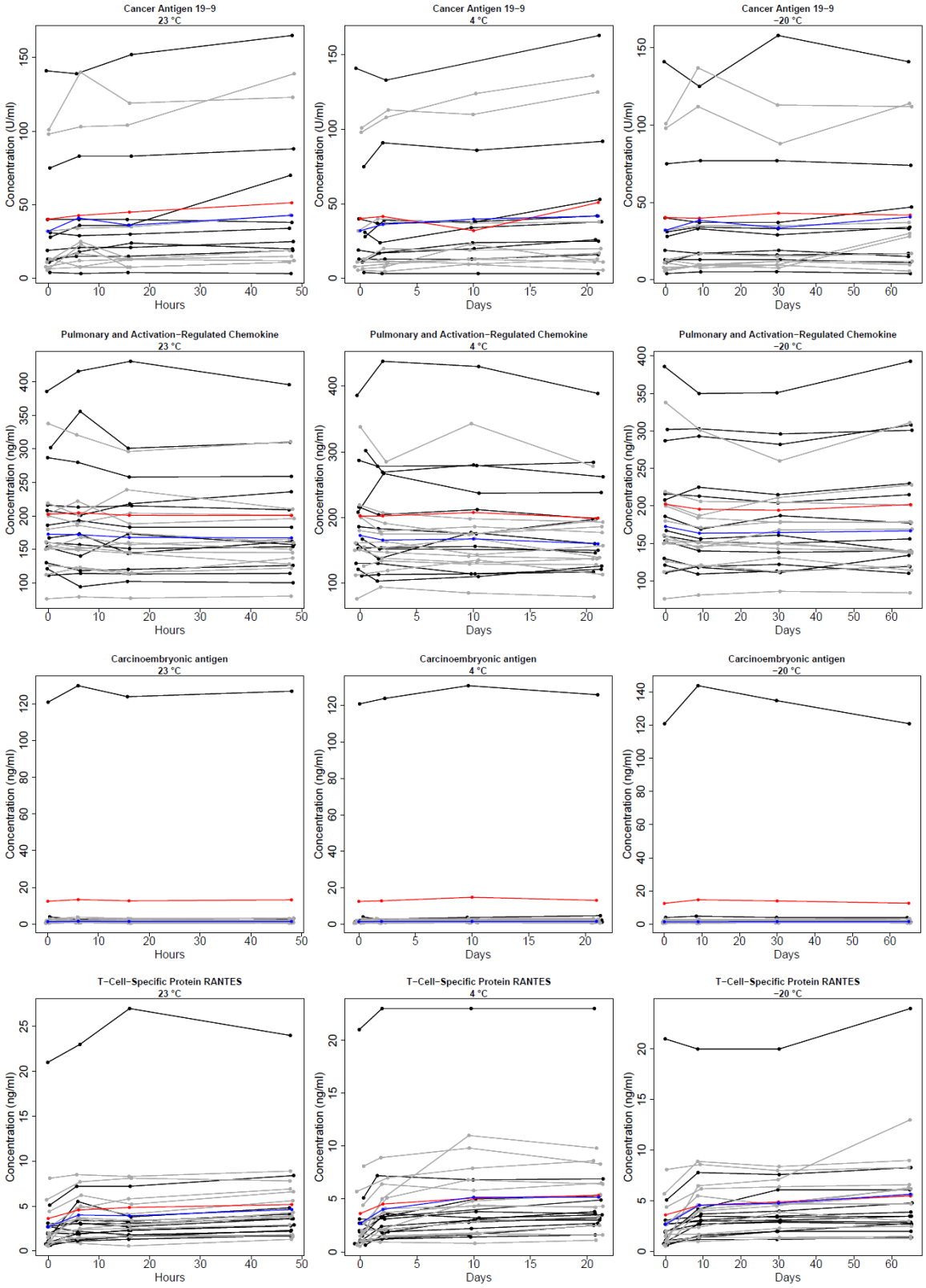

Figure 3.3: Continued on next page

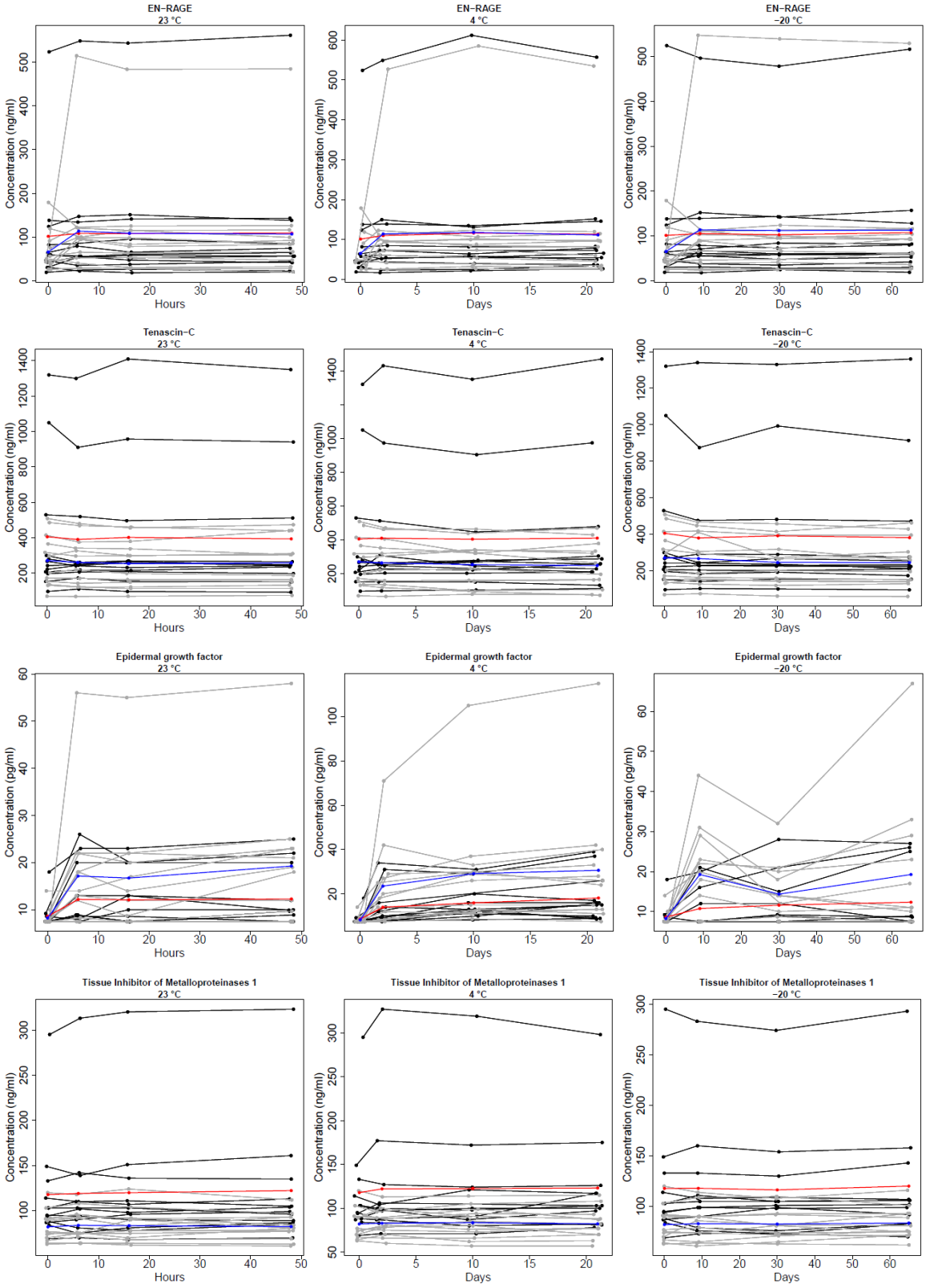

Figure 3.3: Continued on next page

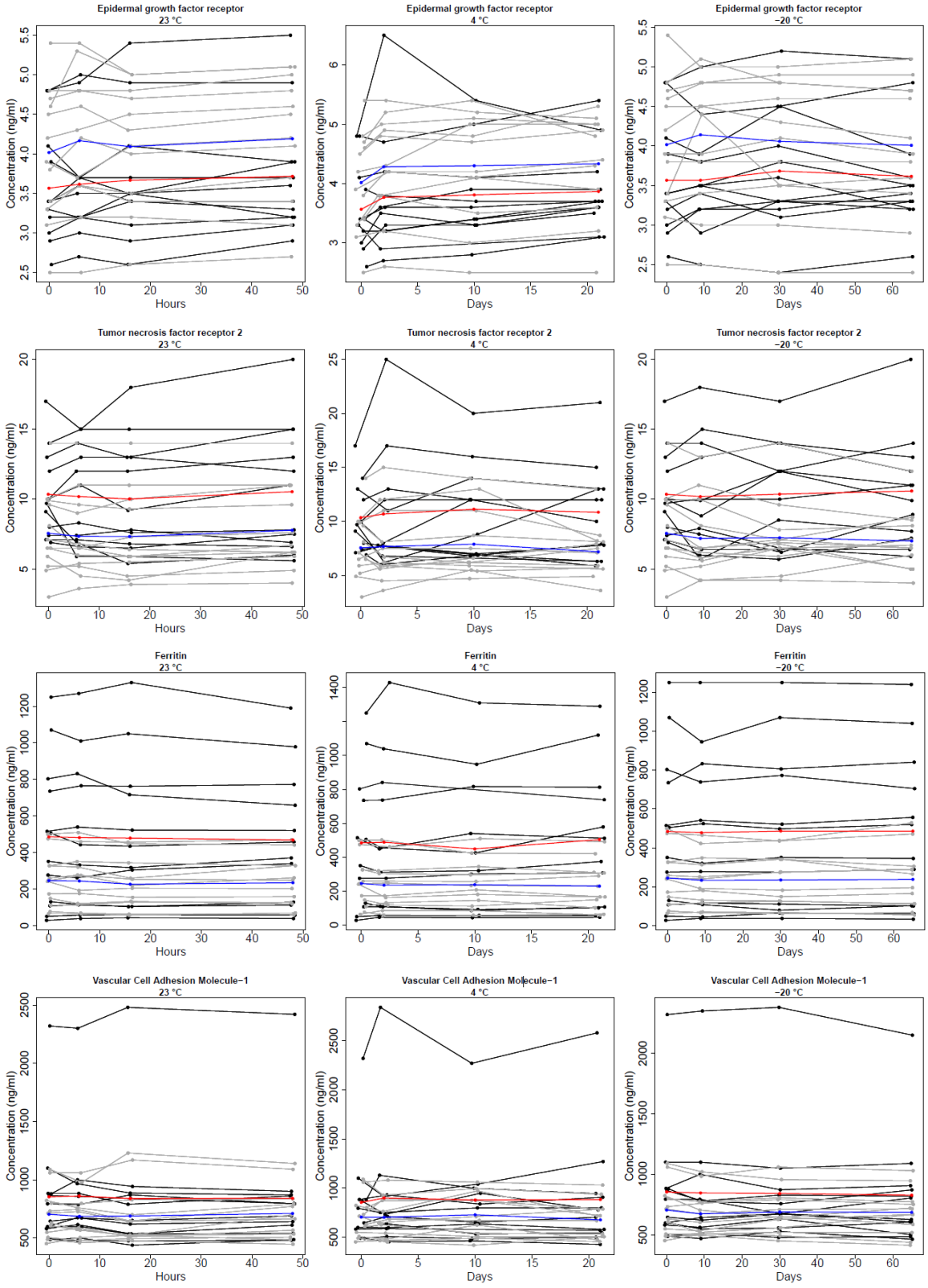

Figure 3.3: Continued on next page

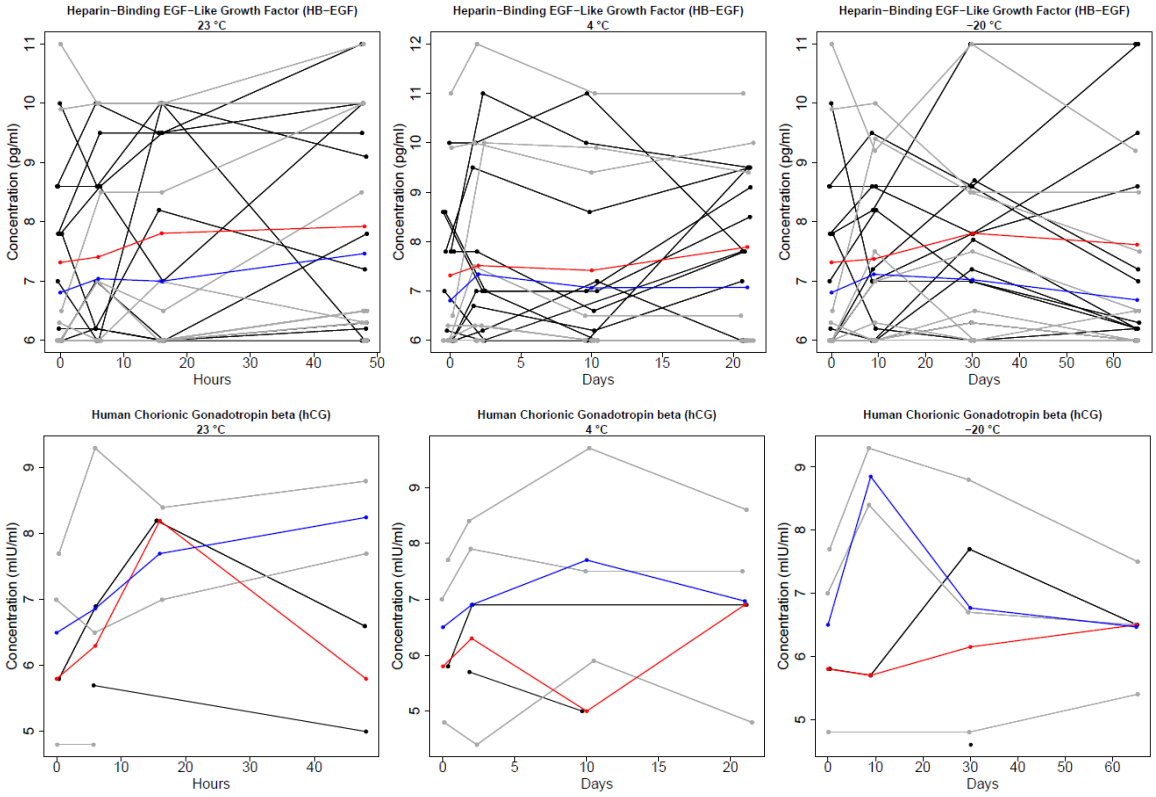

Figure 3.3: Time courses for clinical proteins in K_2EDTA plasma at all temperatures. Longitudinal results for individual patients/donors are shown. Blue points & lines represent the mean of the cancer-free control donors while grey points & lines represent the individuals; red points & lines represent the mean of the GI cancer patients while black points & lines represent the individuals.

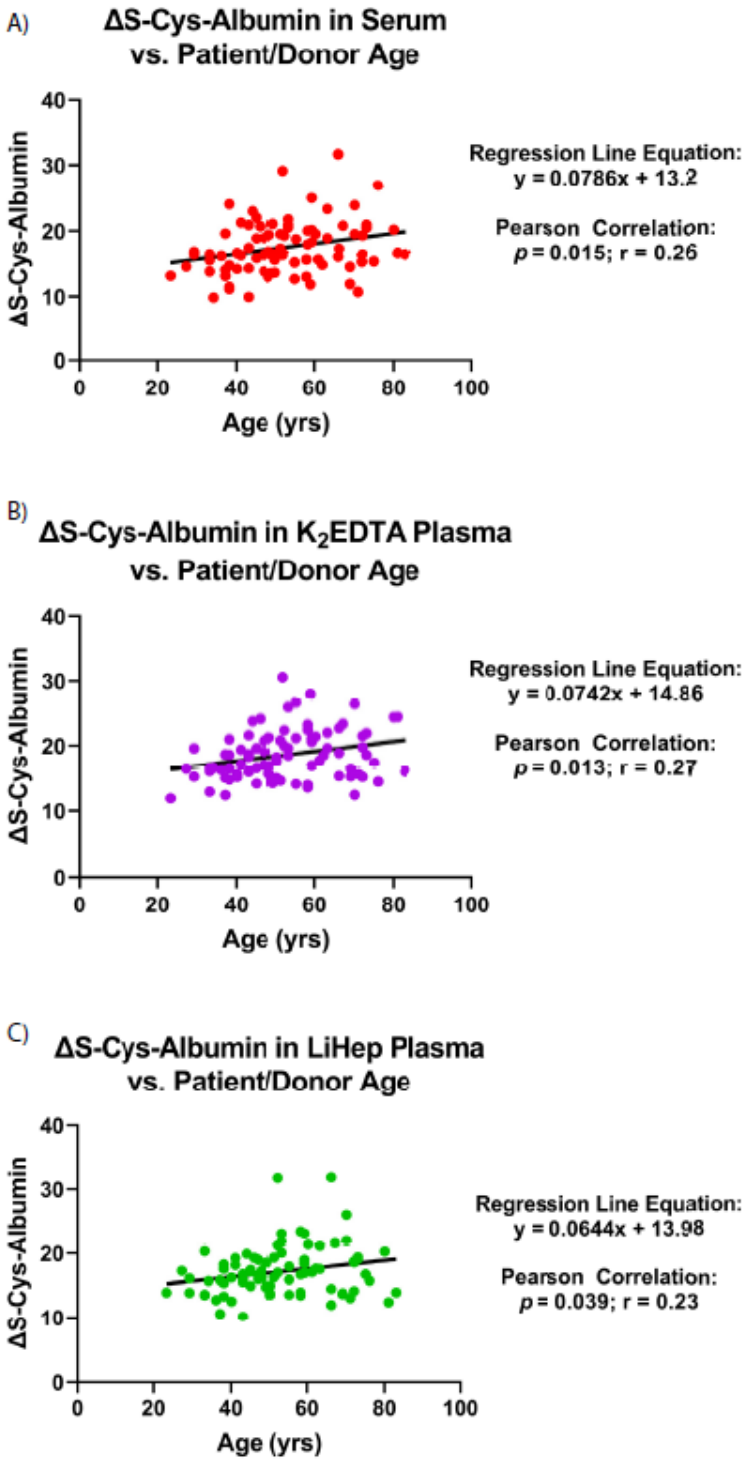

Figure 3.4: Linear correlations of baseline ΔS-Cys-Albumin with age. In A) Serum, B) K_2EDTA plasma, and C) LiHep plasma.

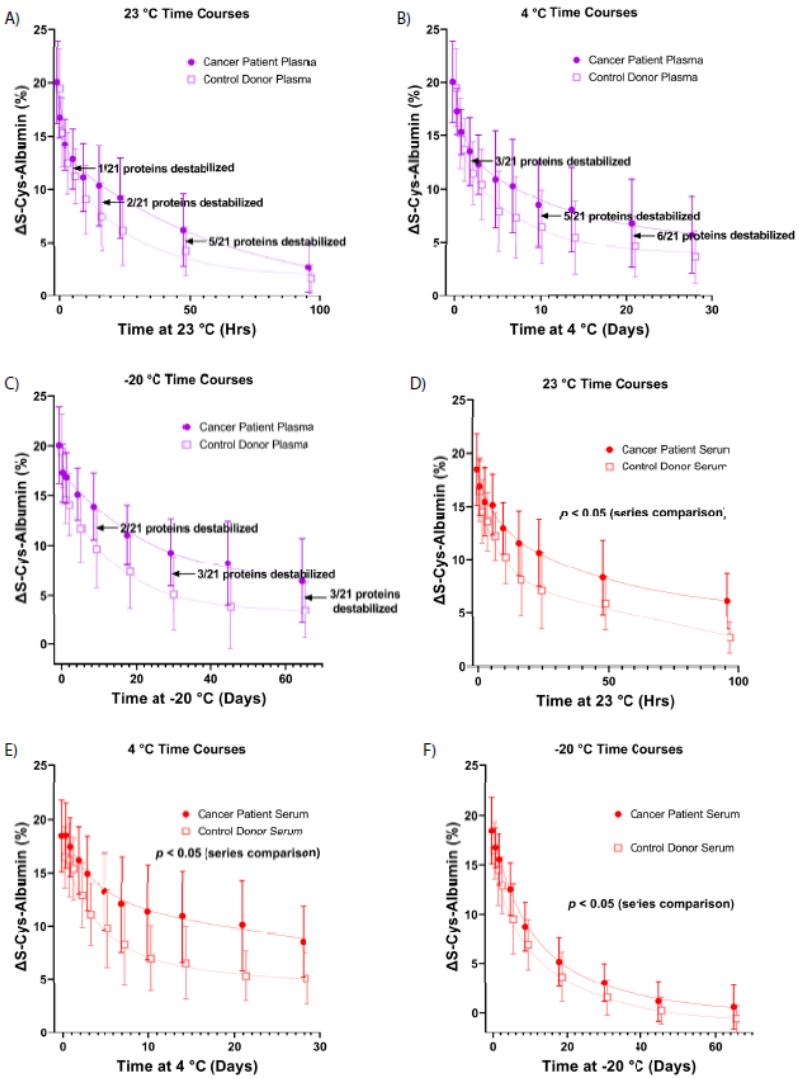

Figure 3.5: ΔS-Cys-Albumin time courses at 23 °C, 4 °C, and -20 °C. ΔS-Cys-Albumin profiles over time in K_2EDTA plasma at A) 23 °C, B) 4 °C, and C) -20 °C; and in serum at D) 23 °C, E) 4 °C, and F) -20 °C. Jitter was added to the x-axis to prevent data point/error bar overlap. Mixed effects models indicated that the differences between GI cancer patients and cancer-free control donors were not statistically significant in K_2EDTA plasma time courses, but were significant in serum time courses at all three temperatures (Bonferroni adjusted $p < 0.05$). Modeled interactions of patient health status x time and patient age x time were not statistically significant in any matrix or at any temperature (Bonferroni adjusted $p < 0.05$)— meaning that there was no statistical evidence that patient age or health status impacted the manner in which ΔS-Cys-Albumin decayed over time. n = 12 patient samples per data point. Error bars indicate standard deviation. Lines are fitted 2-phase exponential decay curves that are intended to serve only as visual guides.

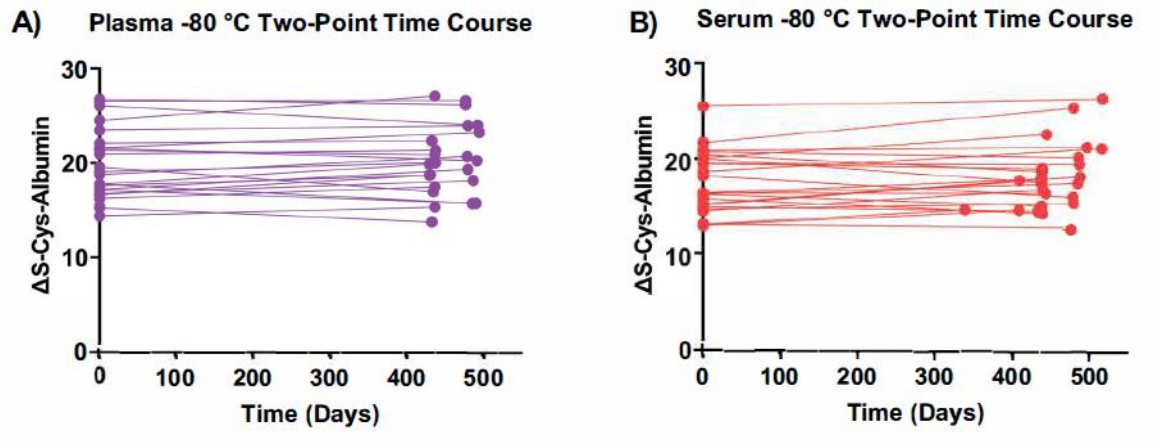

Figure 3.6: Control plasma and serum time courses at -80 °C. Two-point control time courses for A) K_2EDTA plasma and B) serum samples kept at -80 °C for approximately one year. Data were acquired from separate, never-thawed aliquots of the same patient samples from which the time course data in Figure 3.5 were acquired. Time 0 on these plots represents the first day on which each specimen was analyzed. (It was not possible to place the first time point at the actual age of the specimens because in the interest of protecting patient identities the agencies that conducted these prospective collections did not provide the exact dates of collection.) The second data point represents time elapsed since the time 0 data point was acquired. ΔS-Cys-Albumin was not significantly altered in either K_2EDTA plasma or serum ($p > 0.1$; paired t-tests; $n = 23$ for K_2EDTA plasma (due to loss of one sample) and $n = 24$ for serum). That stated, the non-significant average relative percent change for K_2EDTA plasma was +1.8% and for serum was

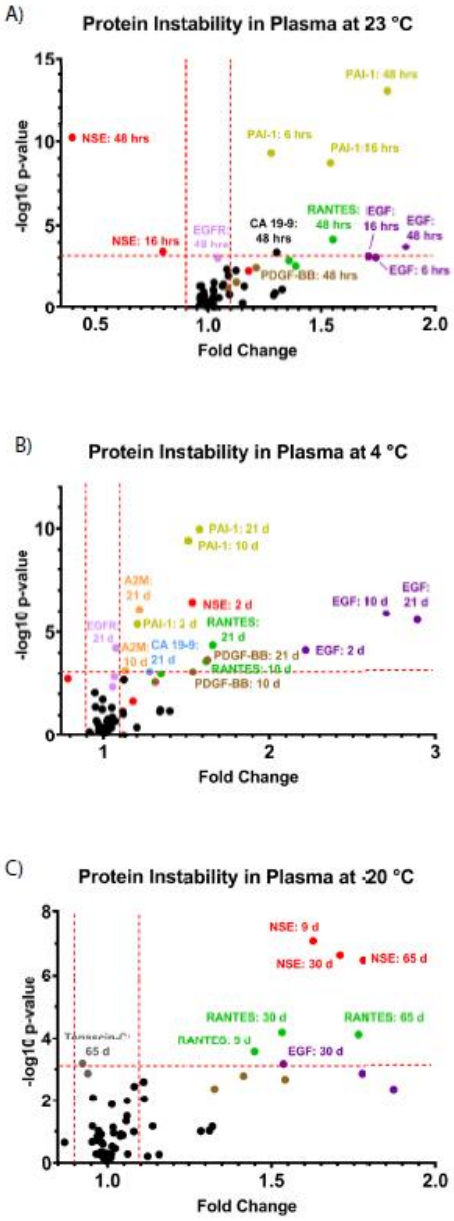

Figure 3.7: Clinically relevant protein instability in K2EDTA plasma exposed to thawed conditions. Volcano plots are shown for A) 23 °C, B) 4 °C, and C) -20 °C. Raw p-values were determined using repeated measures-based mixed effects models on natural log-transformed data. Each data point represents the -log10 p-value and mean of measurements made on 24 separate donor samples (including 12 from GI cancer patients and 12 from cancer-free control donors). Proteins in the upper left and upper right regions delineated by dashed red lines representing a -log10 p-value of -log10 (0.05/63) = 3.10 and fold change > 10% were considered significantly altered by the indicated exposure conditions.

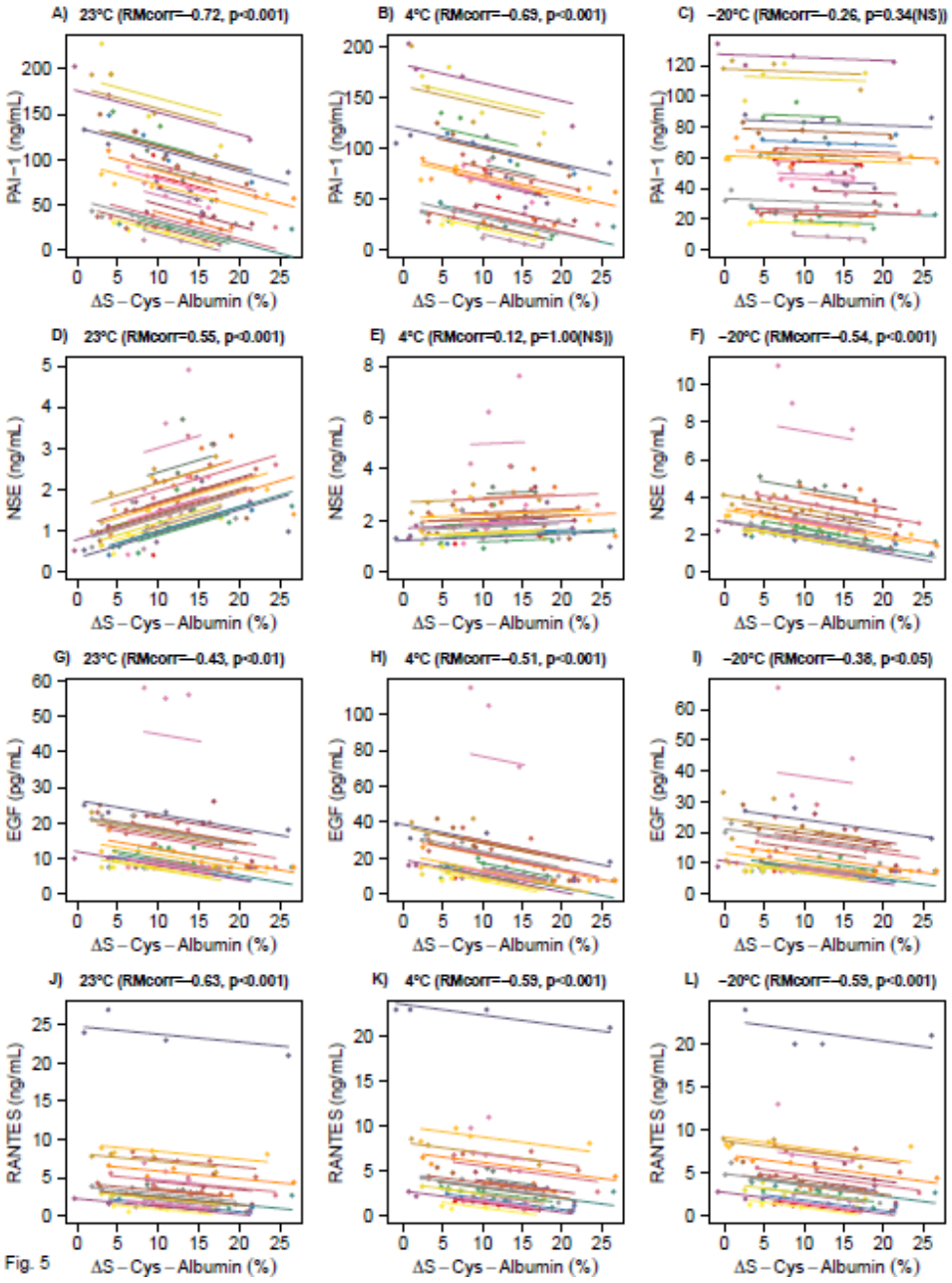

Figure 3.8: Relationships between ΔS-Cys-Albumin and specific destabilized proteins. Repeated measures (RM) correlation plots for plasminogen activator inhibitor-1 (PAI-1) (A-C), neuron specific enolase (NSE) (D-F), epidermal growth factor (EGF) (G-I), and RANTES (J-L). The threshold for statistical significance was placed at $p < 0.05/12$ or 0.0042 due to multiple comparisons.

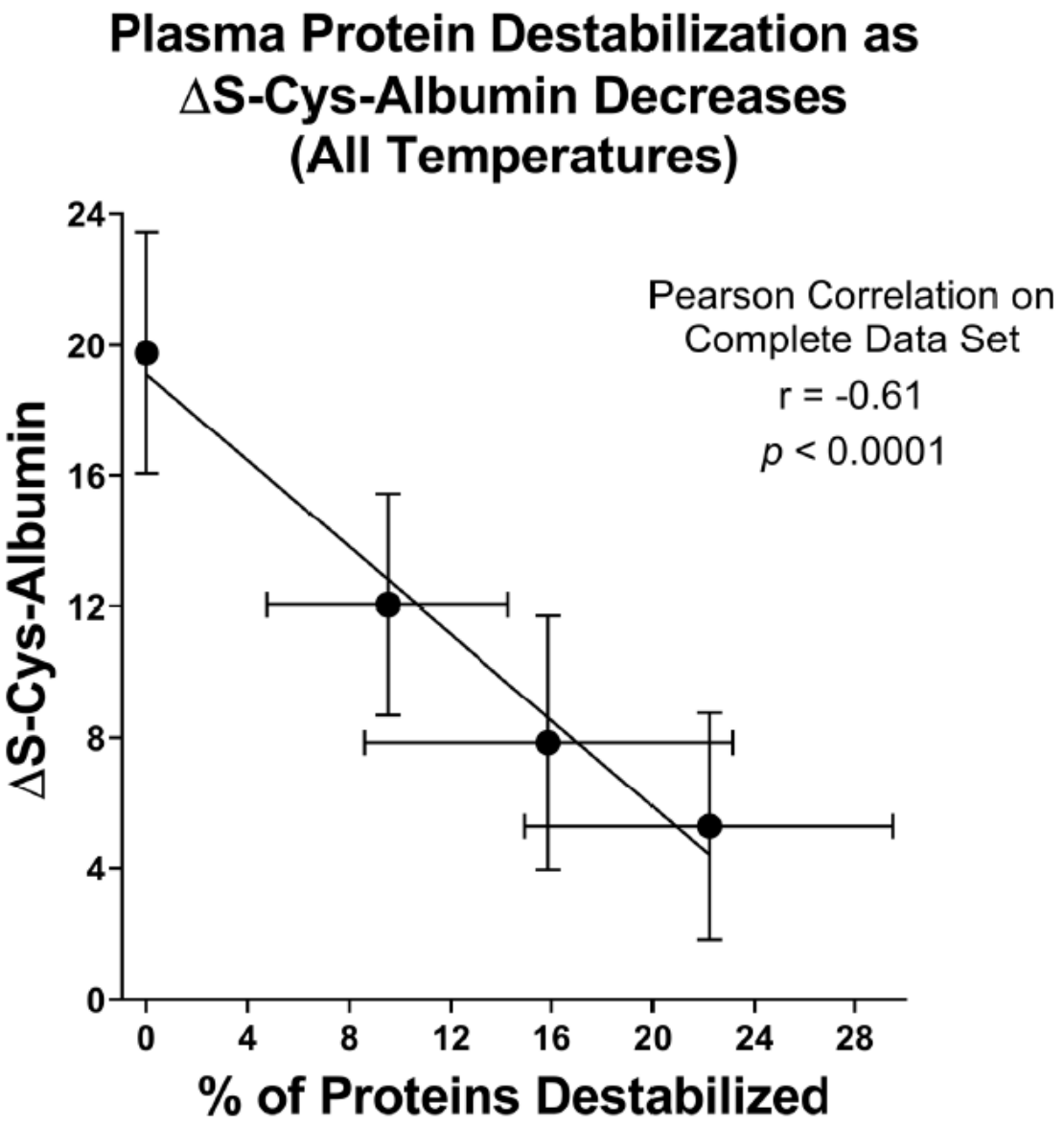

Figure 3.9: Relationship between ΔS-Cys-Albumin and the percentage of proteins destabilized in K_2EDTA plasma regardless of specific time-temperature exposure. Each point represents the mean ΔS-Cys-Albumin value at the 0^{th} (n = 24), 1^{st} (n = 72), 2^{nd} (n = 72) and 3^{rd} (n = 72) exposure time points from all three temperatures (23 °C, 4 °C, and -20 °C) combined. Error bars represent standard deviation. Pearson correlation results shown (r = -0.61, $p < 0.0001$) were based on all 240 individual data points, not just the four mean values shown.

Tables

Table 3.1: Patient characteristics for the baseline ΔS-Cys-Albumin and protein stability studies.

	Patient samples for determination of baseline ΔS-Cys-Albumin values	**Patient samples for stability study**
Patient demographics	**n (%)**	**n (%)**
Number of Patients	84	24
Sex		
Males	35 (41.7)	13 (54.2)
Females	49 (58.3)	11 (45.8)
Age (years)		
<40	16 (19.1)	3 (12.5)
40-60	44 (52.3)	11 (45.8)
>60	24 (28.6)	10 (41.7)
Ethnicity/Race		
White	75 (89.3)	20 (83.3)
Black	7 (8.3)	4 (16.7)
Other	2 (2.4)	0 (0)
Disease status		
Cancer-Free	47 (56.0)	12 (50.0)
Cancer	37 (44.0)	12 (50.0)
Stage I	1 (2.70)	1 (8.3)
Stage III	1 (2.70)	1 (8.3)
Stage III	4 (10.8)	1 (8.3)
Stage IV	10 (27.0)	3 (25.0)
Stage undetermined	21 (56.8)	6 (50.0)

Table 3.2: Clinically relevant proteins that were quantified in K2EDTA plasma samples using the Luminex bead based multiplex immunoassay, their numbers of free cysteine and methionine residues, and the clonality of capture and detection antibodies employed.

Protein	Clinical Utility	Number of Free Cysteine Residues	Number of Methionine Residues	Capture Antibody Clonality	Detection Antibody Clonality
Adiponectin	Biomarker for obesity-related diseases, i.e., metabolic syndromes and coronary artery disease	1-2	4	monoclonal	monoclonal
Alpha-2-Macroglobulin (A2M)	Biomarker for kidney and liver diseases	0	25	polyclonal	- [a]
Alpha-Fetoprotein (AFP)	Cancer Biomarker	2	8	monoclonal	monoclonal
Cancer Antigen 125 (CA-125)	Cancer Biomarker	0-29	434	monoclonal	monoclonal
Cancer Antigen 19-9 (CA-19-9)	Cancer Biomarker	N/A [b]	N/A [b]	monoclonal	monoclonal
Carcinoembryonic Antigen (CEA)	Cancer Biomarker	0-10	0	monoclonal	monoclonal
EN-RAGE	Marker for inflammation/Immune responses	0	0	polyclonal	polyclonal
Epidermal Growth Factor (EGF)	Cancer Biomarker	0	1	monoclonal	polyclonal
Epidermal Growth Factor Receptor (EGFR)	Cancer Biomarker	0	10	monoclonal	monoclonal
Ferritin (FRTN)	Cancer and inflammatory response marker	3 in heavy chain; 1 in light chain	4 per chain	monoclonal	polyclonal
Heparin-Binding EGF-Like Growth Factor (HB-EGF)	Cancer Biomarker	0	0	polyclonal	polyclonal
Myoglobin	Marker for cardiac and vascular diseases, cancer, and renal function/toxicity	1	3	monoclonal	monoclonal
Neuron Specific Enolase (NSE)	Cancer Biomarker	6	8	monoclonal	monoclonal
Plasminogen Activator Inhibitor 1 (PAI-1)	Marker for cardiac and vascular diseases, neurological diseases, and cancer	0	16	polyclonal	polyclonal
Platelet-Derived Growth Factor BB (PDGF-BB)	Cancer Biomarker	0	1	monoclonal	monoclonal
Pulmonary and Activation-Regulated Chemokine (PARC)	Marker for cardiac and vascular diseases and inflammatory/immune response	0	0	polyclonal	polyclonal
T-Cell-Specific Protein RANTES (RANTES)	Marker for neurological diseases and inflammatory/immune response	0	1	monoclonal	polyclonal
Tenascin-C	Cancer Biomarker	0-14	21	monoclonal	monoclonal
Tissue Inhibitor of Metalloproteinases 1 (TIMP-1)	Marker for cardiac and vascular diseases and inflammatory/immune response	0	3	monoclonal	polyclonal
Tumor necrosis factor receptor 2 (TNFR2)	Marker for cancer and inflammation/Immune responses	0-2	4	monoclonal	polyclonal
Vascular Cell Adhesion Molecule-1 (VCAM-1)	Marker for cardiac and vascular diseases, neurological diseases, cancer, autoimmune diseases, and inflammatory/ immune response	0-7	14	polyclonal	polyclonal

[a] A competitive assay was used for detection.
[b] Not applicable. CA 19-9 is the sialyl-Lewis[A] tetrasaccharide that exists on more than one unique protein.

Table 3.3: Linear regression analysis results for baseline concentrations of clinical proteins with patient age. Statistically insignificant associations are shown in grey font.

Protein	Slope	Slope Stnd. Error	p-value	Bonferroni-Adjusted p-value
Adiponectin (ug/ml)	0.00833	0.0079	7.9E-12	1.7E-10
Myoglobin (ng/ml)	0.02196	0.0118	3.9E-15	8.2E-14
Alpha-2-Macroglobulin (mg/ml)	0.01139	0.0031	1.2E-14	2.5E-13
Neuron specific enolase (ng/ml)	0.00822	0.0042	4.7E-09	9.9E-08
Alpha Fetoprotein (ng/ml)	9.11E-04	0.0076	3.3E-02	6.9E-01
Plasminogen Activator Inhibitor 1 (ng/ml)	-0.00899	0.0106	5.4E-18	1.1E-16
Cancer Antigen 125 (U/ml)	0.01051	0.0055	5.9E-18	1.2E-16
Platelet-Derived Growth Factor BB (pg/ml)	0.01006	0.0109	1.3E-20	2.8E-19
Cancer Antigen 19-9 (U/ml)	0.03497	0.0160	4.3E-10	9.0E-09
Pulmonary and Activation-Regulated Chemokine (ng/ml)	0.01149	0.0049	7.7E-28	1.6E-26
Carcinoembryonic antigen (ng/ml)	0.03175	0.0144	1.3E-01	1.0E+00
T-Cell-Specific Protein RANTES (ng/ml)	0.01205	0.0124	6.9E-04	1.4E-02
EN-RAGE (ng/ml)	-0.00861	0.0104	5.3E-19	1.1E-17
Tenascin-C (ng/ml)	-8.35E-05	0.0099	1.1E-22	2.2E-21
Epidermal growth factor (pg/ml)	-8.45E-04	0.0032	2.5E-24	5.1E-23
Tissue Inhibitor of Metalloproteinases 1 (ng/ml)	0.00739	0.0045	7.4E-28	1.6E-26
Epidermal growth factor receptor (ng/ml)	-0.00707	0.0026	3.7E-20	7.8E-19
Tumor necrosis factor receptor 2 (ng/ml)	0.01243	0.0049	7.2E-19	1.5E-17
Ferritin (ng/ml)	-0.01253	0.0139	4.7E-19	9.9E-18
Vascular Cell Adhesion Molecule-1 (ng/ml)	0.00954	0.0048	1.2E-30	2.6E-29
Heparin-Binding EGF-Like Growth Factor (HB-EGF) (pg/ml)	0.00578	0.0025	1.2E-24	2.6E-23

CHAPTER 4

OXIDIZED LDL IS STABLE IN HUMAN SERUM UNDER EXTENDED THAWED-STATE CONDITIONS RANGING FROM -20 °C TO ROOM TEMPERATURE

4.1. Introduction

Oxidized low-density lipoprotein (oxLDL) is a form of LDL in which 10s to 100s of the primary amine-bearing lysine residue side chains of apolipoprotein B molecules within LDL have covalently bonded with aldehyde byproducts of lipid peroxidation such as malondialdehyde (153–155). In vivo, oxidation of LDL is believed to occur in arterial walls—especially those that are atherosclerotic and contain increased concentrations of copper and iron (153), which are key mediators of lipid peroxidation. OxLDL is then recognized by scavenger receptors on macrophages (156, 157), which take it up. This results in the conversion of macrophages to foam cells which are key initiators of atherosclerosis (158, 159).

The first ELISA for oxLDL in blood plasma was developed in the 1990s (154). Since that time, the measurement of oxLDL in plasma/serum has been carried out in numerous clinical studies (160–167) and, over the past couple of decades, has become incorporated into clinical practice (168–170) where it is used as a marker for the presence of CAD (160–163, 165) and of the risk of developing metabolic syndrome (167) and CHD (166). (It's value as an *independent* predictor of CHD, however, has been questioned (171).)

Given that oxLDL is a downstream product of lipid peroxidation (153) and that some lipids are highly susceptible to ex vivo peroxidation in thawed plasma/serum (56, 172,

173) (i.e., plasma/serum warmer than -30 °C (50)), there is cause for concern about the ex vivo stability of oxLDL (154, 174, 175). It has been claimed (without direct evidence) that LDL oxidation does not occur in the presence of plasma/serum (153), but given the popularity of oxLDL as a biomarker, the lack of a systematic study of its ex vivo stability in plasma or serum is surprising. A couple of studies have evaluated the stability of oxLDL in blood specimens under specific conditions such as heparin-anticoagulated whole blood kept on cold packs for 24 or 36 hours (174) or plasma/serum kept for 2 hours at room temperature or 24 hours in a refrigerator (175)—and in most cases it was found to be stable.

To our knowledge, however, no systematic evaluation of oxLDL stability under a series of temperatures and time ranges has been conducted. The purpose of this study was to comprehensively evaluate the stability of oxLDL in human serum over time courses at 23 °C, 4 °C, and -20 °C while simultaneously measuring ΔS-Cys-Albumin—a well characterized marker of plasma/serum exposure to thawed conditions that is based on the ex vivo oxidation of albumin to S-cysteinylated albumin (34, 64).

4.2. Material and Methods

4.2.1. Materials

Serum was collected from cancer-free donors and gastrointestinal (GI) cancer patients under informed consent and local IRB approval by the Cooperative Human Tissue Network (CHTN; Nashville, TN). Basic donor demographics and disease status are provided in **Table 4.1**. Detailed inclusion and exclusion criteria are provided in Supplementary Data. Notably, patients with poor kidney function (eGFR < 60 mL/min

per 1.73m^2) were excluded because poor kidney function can, in theory, result in abnormally high ΔS-Cys-Albumin measurements (64). All samples were obtained in compliance with the Declaration of Helsinki principles. Specimen receipt and analysis were approved by the Arizona State University IRB. ELISA kits for measuring oxLDL in plasma or serum were purchased from Mercodia (Uppsala, Sweden). These kits employ the 4E6 mouse monoclonal antibody developed by Holvoet et al (154) in a capture or "sandwich" format. Water and acetonitrile (LC/MS grade) and formic acid (ACS certified grade) were purchased from Fisher Scientific.

4.2.2. Blood Collection and Related Pre-Analytical Information

Blood was collected and processed according to a strict protocol: A standard 10-mL tube of serum (without separator gel) was collected from each patient. Blood was drawn by forearm venipuncture using an 18 or 20-gauge needle. Tubes were properly filled then immediately inverted five times (never shaken). Tubes were allowed to clot for 45 minutes followed by centrifugation at 1,300 x g for 10 minutes at room temperature. Serum was then immediately aliquoted on ice. Aliquots were put into a -80 °C freezer within 2 hours of the initial draw time. In order to verify the processing timing steps, time stamps were recorded at 1) the time of initial draw, 2) the time centrifugation was completed, and 3) the time at which aliquots were placed at -80 °C. Serum samples with visually noted hemolysis > 250 mg/dL were excluded. Unless otherwise noted, all serum samples were kept at -80 °C prior to analysis.

Serum was shipped to Arizona State University (Tempe, AZ) overnight on dry ice. Once received, specimens were verified to be frozen then unpacked into a -80 °C freezer

equipped with continuous temperature monitoring. All specimens were kept in the -80 °C for at least 7 days prior to thawing to ensure that any residual CO_2 in the headspace was exchanged for air in order to avoid CO_2-induced sample acidification (140).

4.2.3. Study Design

Serum specimens were randomized before analysis using a random number generator to create the run order assignments. ΔS-Cys-Albumin and oxLDL in separate pristine, never-thawed aliquots was measured within a time range of 12-20 months after initial specimen collection (20-30 months for oxLDL), during which time specimens were kept continually at -80 °C. (These large ranges of time were primarily due to the fact that the specimens were collected over a period of multiple months.)

Following collection of baseline ΔS-Cys-Albumin data, serum from 12 cancer-free control donors and 12 GI cancer patients were selected for inclusion in thawed-state stability studies based on their initial ΔS-Cys-Albumin values being equally distributed across the entire range of initial ΔS-Cys-Albumin values measured in 84 total patients. Thawed-state stability studies involved incubation of separate serum aliquots for up to 96 hours at 23 °C, 28 days at 4 °C, or 65 days at -20 °C.

A separate aliquot for each individual non-baseline thawed-state ΔS-Cys-Albumin time point *and* oxLDL assay (either 20 µL for ΔS-Cys-Albumin or 50 µL for oxLDL measurements), was created from a parent aliquot that had never previously been thawed. To create these aliquots, the parent sample was thawed and kept on ice with strict time tracking for a period of 3.4 ± 1.1 (SD) min for the 23 °C-exposed samples, 8.5 ± 2.0 min for the 4 °C-exposed samples, and 14.2 ± 3.0 min for the -20 °C-exposed samples—by

which times all temperature exposure time courses were started. Aliquots for the time courses were immediately placed in a -80 °C freezer upon completion of their time/temperature exposure period. Once all time courses were completed, all time course aliquots were randomized and ΔS-Cys-Albumin or oxLDL were measured in them. Oxidized LDL at all stability time points (including baseline) was measured as a randomized set of 240 serum samples (each measured in duplicate) using Mercodia ELISA kits.

Given that the serum samples were collected from patients over a period of about one year, oxLDL was analyzed within 18-30 months after initial specimen collection. Except for intentional thawed-state incubation periods, all samples were continually kept at -80 °C prior to analysis. After all ΔS-Cys-Albumin and oxLDL time course aliquots were analyzed, ΔS-Cys-Albumin was again measured in a separate never-thawed aliquot of each sample in order to confirm the long term stability of ΔS-Cys-Albumin at -80 °C. This happened one year after the initial ΔS-Cys-Albumin measurements in never-thawed samples were made.

4.2.4. Laboratory procedures

4.2.4.1. Measurement of ΔS-Cys-Albumin

Randomized serum specimens were prepared and the percentage of albumin in the S-cysteinylated form (S-Cys-Albumin) was measured as we have described previously (34, 64). Briefly, one microliter of serum was diluted 1000-fold in 0.1% (v/v) trifluoroacetic acid (TFA) and injected onto an LC-MS instrument where albumin was concentrated and desalted on a capillary sized OPTI-TRAP^{TM} cartridge designed for protein analysis then

directly eluted into the mass spectrometer for measurement of the intact protein and relative quantification of its proteoforms. Nine microliters of the same serum sample was then put in a 0.6-mL polypropylene Eppendorf snap-cap tube and incubated in a dry oven at 37 °C for 24 hours. One microliter of the incubated sample was then diluted 500-fold in 0.1% TFA and injected onto the LC-MS for analysis. ΔS-Cys-Albumin is defined as the *difference* between the percentage of albumin in the S-cysteinylated form before and after the overnight incubation at 37 °C that drives the percentage of S-Cys-Albumin to its maximum value (64).

4.2.4.2. Measurement of oxLDL

OxLDL was measured using Mercodia ELISA kits according to the manufacturer's instructions but with one exception: We found that the recommended dilution factor of 1/6,561 was insufficient for many samples and therefore opted for a 1/13,225 dilution factor. This was accomplished by two serial dilution steps of 10 µL (of serum or 115-fold diluted serum sample) added into 1,140 µL of sample buffer to give a total volume of 1,150 µL. Each sample was measured in duplicate. Each batch contained 5 calibrator samples (each measured in duplicate and fit with a second order polynomial regression curve without averaging any values), a low-concentration QC sample and a high concentration QC sample that were both supplied with the ELISA kit, and two aliquots of a randomly selected human plasma sample that was not supplied in the ELISA kit. In total, six ELISA kits were required for this project; each one was run on a different day.

4.2.5. Statistical Analysis

To evaluate the stability of oxLDL in serum, the concentration at each time-temperature condition was compared with its respective control aliquot that was kept continuously at -80 °C. Data consisted of 24 subject specimens, each measured longitudinally over time at temperatures of 23 °C, 4 °C, and -20 °C. First, we performed descriptive statistics and analyzed ΔS-Cys-Albumin at baseline (time = 0), comparing the effect of health status (cancer-free vs. cancer), gender (female vs. male), and race (black vs. white) using a two-sample t-test. The age effect was assessed using basic linear regression. Next, we analyzed longitudinal ΔS-Cys-Albumin data using linear mixed effects models to account for the repeated measures within subjects. Specifically, we considered the full model as follows:

$$y_{ij} = \beta_0 + \beta_1 age_i + \beta_2 status_i + \sum_{j=1}^{q} \beta_{3j} t_{ij} + \sum_{j=1}^{q} \beta_{4j} age_i t_{ij} + \sum_{j=1}^{q} \beta_{5j} status_i t_{ij} + \epsilon_{ij}$$

where y_{ij} is the concentration of ΔS-Cys-Albumin for the i^{th} subject at j^{th} time point, age_i is the age for the i^{th} subject, $status_i$ is 1 if i^{th} subject's status is cancer and 0 otherwise, t_{ij}=1 if y_{ij} is observed at the j^{th} time point, and t_{ij}=0 otherwise, ϵ_{ij} is an error term, and q is the number of time points observed excluding the baseline. We employed a step-down approach that dropped the interaction term of status and time if they were not significant and used reduced models with only the main effects.

The same approach was used to analyze oxLDL, with natural logarithm transformed y values to improve normality. Bonferroni-adjusted *p*-values less than 0.05 were regarded as statistically significant. All the analyses were conducted at each temperature separately.

GraphPad Prism® software (version 9.3.1) was employed for descriptive statistics and t-tests, and MIXED procedure in SAS 9.4 (SAS Inst. Inc., Cary, NC) for linear mixed effects models.

4.3. Results

Basic demographics and clinical characteristics of the patients who provided specimens for this study are provided in **Table 4.1**. OxLDL was measured in randomized human serum samples that had either been kept continuously at -80 °C since collection (Time 0/baseline) or exposed to three different time points at 23 °C, 4 °C, or -20 °C (**Figure 4.1**). For all three exposure temperatures, no significant differences were observed between baseline concentrations of oxLDL and those at any of the exposure time points. OxLDL concentrations observed in baseline serum specimens were not different between donors of different gender, race, or health status (GI cancer patients or cancer-free individuals) as determined by a t-test ($p > 0.05$). Neither was there a correlation of baseline oxLDL with age (Pearson correlation coefficient = -0.035, $p > 0.05$). For reference, the standard curves for each of the six ELISA plates are provided (**Figure 4.2**). All but one standard curve had coefficient of determination (R^2) values greater than 0.99; all were greater than 0.98. The %CV for the inter-batch QC plasma sample that was run in duplicate in each batch was 18% (sans one outlier value; Grubb's test with $\alpha = 0.10$) and the %CV for both the high and low control samples included with the ELISA kits was 12-13%.

Measurement of ΔS-Cys-Albumin in the same samples as those in which oxLDL were measured confirmed that the thawed state exposures to which the serum samples were

subjected resulted in the ex vivo oxidative instability of a different protein/small molecule system (albumin and cysteine/cystine (64)) while oxLDL remained stable (**Figure 4.3**). Mixed effects models of the ΔS-Cys-Albumin data revealed no interactions between patient health status and time or between patient age and time. After removing these interactions from the model, data were re-analyzed to focus solely on main effects. As anticipated (64), exposure time at all three thawed-state temperatures induced major changes in ΔS-Cys-Albumin (**Figure 4.3**; Bonferroni adjusted $p < 1 \times 10^{-8}$). Simultaneous observation of these oxidative changes in the same samples in which oxLDL was measured confirmed the ex vivo stability of oxLDL under the thawed-state conditions examined. Notably, ΔS-Cys-Albumin in never-thawed serum aliquots kept continuously for an additional year at -80 °C following the time zero measurements shown in **Figure 4.3** did not differ from the original results shown (paired t-test; n = 24).

4.4. Discussion

Previous studies on the stability of oxLDL in serum, plasma or whole blood had pointed toward its relative stability but were rather limited with regard to the scope of ex vivo conditions examined. In 2002 Pai et al showed that oxLDL in sodium heparin plasma was stable when whole blood was kept on cold packs for up to 36 hours prior to processing (174). Two years later Perman et al (175) reported that oxLDL was stable in EDTA plasma and serum for 2 hours at room temperature or up to 3 years at -80 C. On the other hand, they reported a decrease in oxLDL when plasma or serum was kept for 24 hours in a refrigerator. Notably, however, the authors did not state whether samples were randomized within or between batches, meaning that a batch effect cannot be ruled out as

a possible explanation for the instability observed. Both of these reports employed the same ELISA from Mercodia as was employed in the present study.

Two limitations were relevant to this study. First, it was partially limited by the modest precision of the ELISA employed. Inter-batch CV values for the in-kit controls and an actual EDTA plasma sample were 12% and 18%, respectively. These were higher than the 8.3 %CV values reported for total assay variation by the manufacturer (though it is unclear whether this lower value reported by the manufacturer resulted from the repeated analysis of the in-kit controls or an actual plasma or serum sample). The large number of paired measurements (n = 24 per temperature) provided some compensation for partial loss of the ability to detect subtle changes caused by higher than expected analytical imprecision. Moreover, analyses were conducted by experienced personnel, so the precision observed here is likely to be similar that that which has occurred in the hands of others (but has not been reported). Thus on the whole, if the precision of the Mercodia ELISA kit is good enough to facilitate use of this assay as a biomarker (166, 167), then changes with disease must be substantial enough to overcome this analytical limitation—meaning that any minor instabilities masked by imprecision are essentially irrelevant on this larger scale on which oxLDL changes as a biomarker.

The second limitation is that this study assessed the stability of oxLDL in serum exposed to thawed conditions but not plasma. Perman et al, however, have reported that there are no significant differences between matched serum, EDTA plasma or heparin plasma analyzed using the Mercodia ELISA kit (175).

Measurement of ΔS-Cys-Albumin in parallel aliquots of serum provided a positive control for a second protein/small molecule redox system found in serum. Detailed analysis of ΔS-Cys-Albumin data that included matched K_2EDTA and lithium heparin plasma samples as well as higher n-values at time 0 has been recently published (75). This separate study also included an analysis of the subtle differences in ΔS-Cys-Albumin between GI cancer patients and cancer-free donors.

Considering that this article is part of a special issue on pre-analytics, we feel it is important to point out that the U.S. Food and Drug Administration's draft guidance on biomarker qualification (7) states that "Sample collection, preparation, and storage protocols (as applicable for the biomarker type) should be established and assessed in the analytical validation studies to determine acceptability." This statement implies that as part of their validation, candidate biomarkers should undergo stability testing within their natural biological matrix. The absence of such testing—particularly when it occurs in the absence of proper pre-analytical reporting—may not only leave undiscovered pitfalls for future researchers, but can also lead to scientific irreproducibility, irreconcilable controversies and/or the reporting of false negative or (more likely) false positive results. It is fortunate that oxLDL in serum remains stable under a wide range of thawed-state conditions.

Conclusions: As measured by the Mercodia ELISA kit, oxLDL is stable in human serum that has been exposed to temperatures of 23 °C for 48 hours, 4 °C for 21 days, or -20 °C for 65 days.

Figures

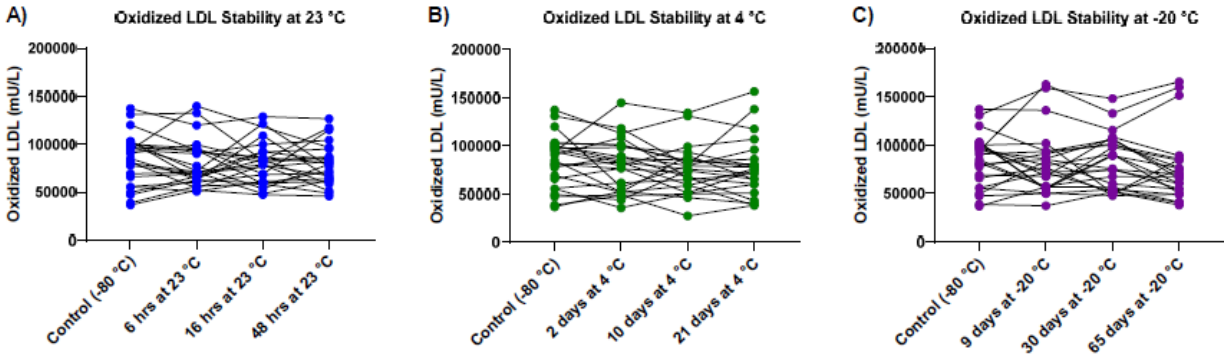

Figure 4.1: Stability of oxLDL in serum over time under thawed conditions at A) 23 °C, B) 4 °C, and C) -20 °C. Serum aliquots from 12 GI cancer patients and 12 cancer-free donors were monitored at each temperature. No significant differences were observed between any thawed state exposure time point and a single set of control aliquots kept continuously at -80 °C.

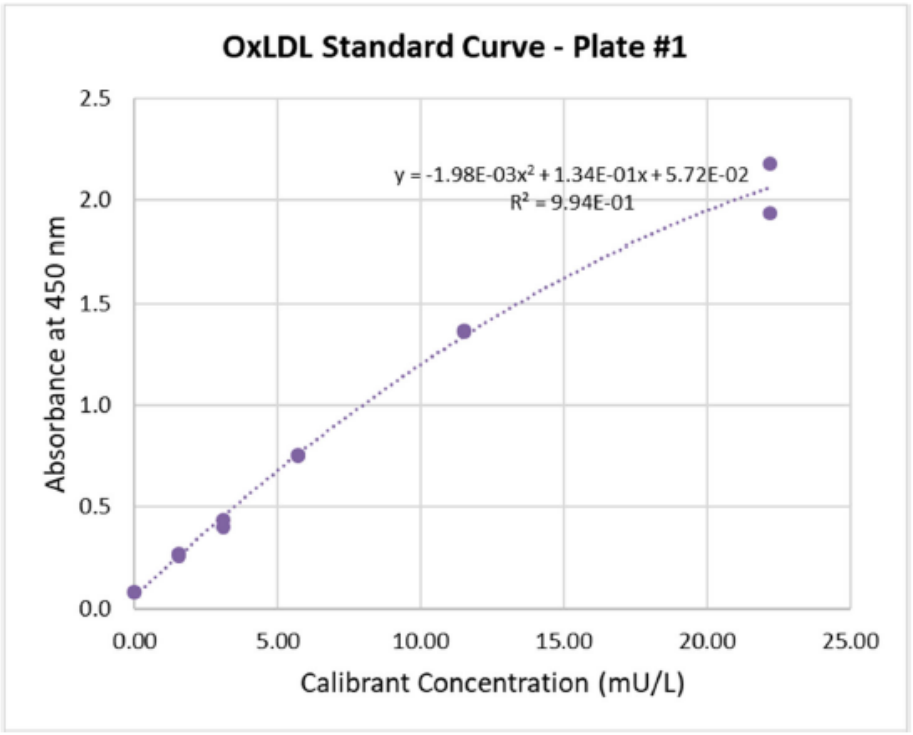

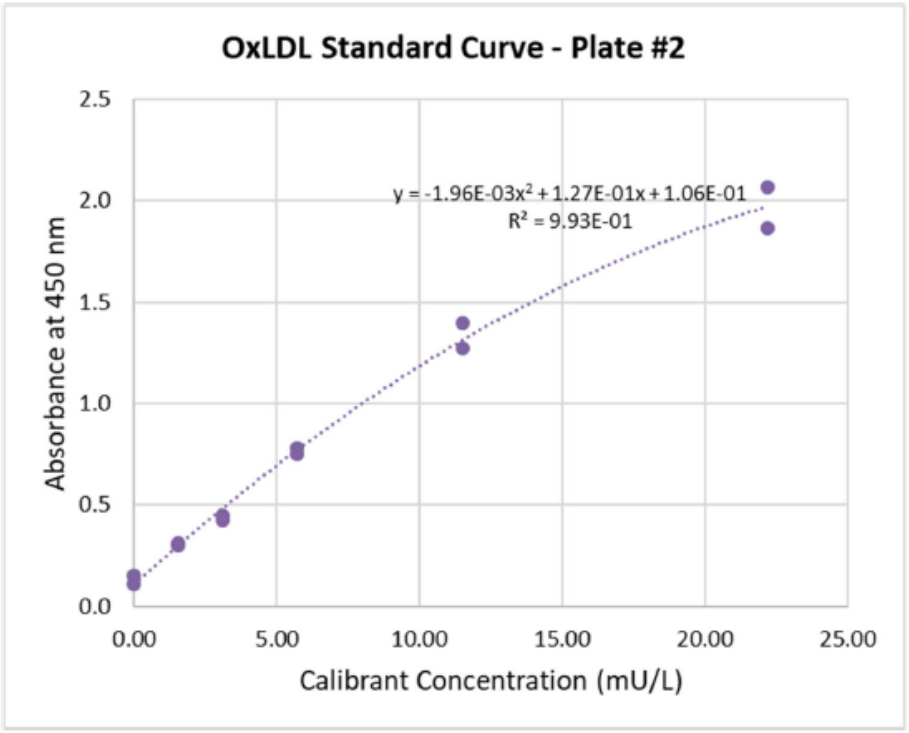

Figure 4.2: Continued on next page

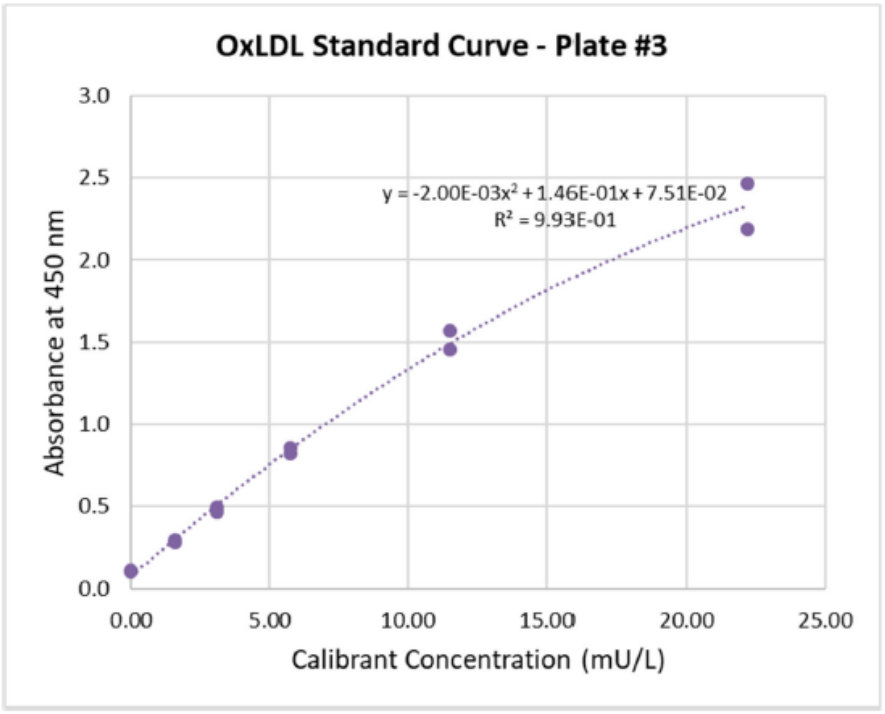

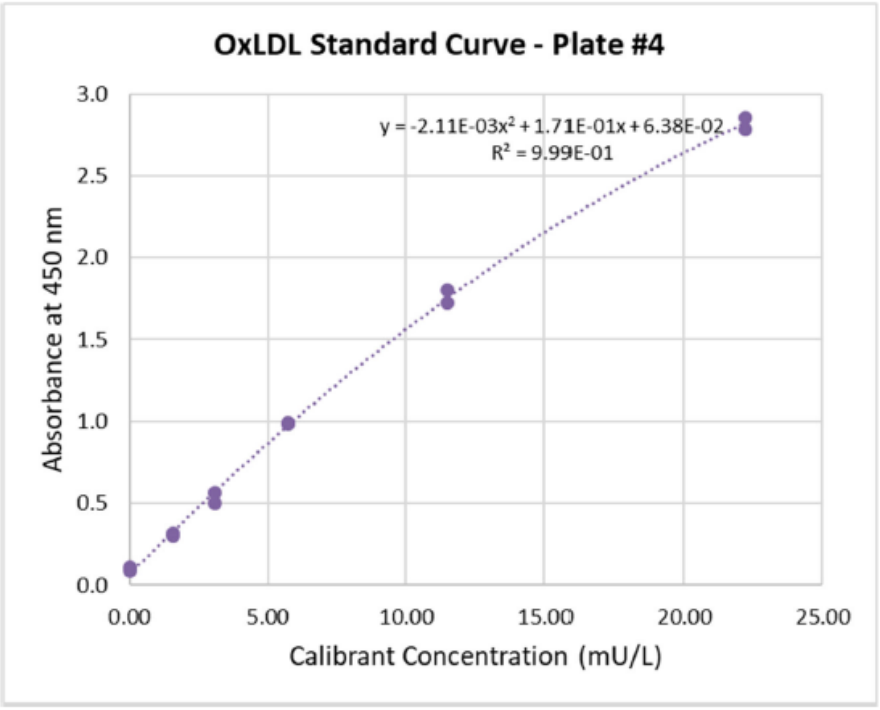

Figure 4.2: Continued on next page

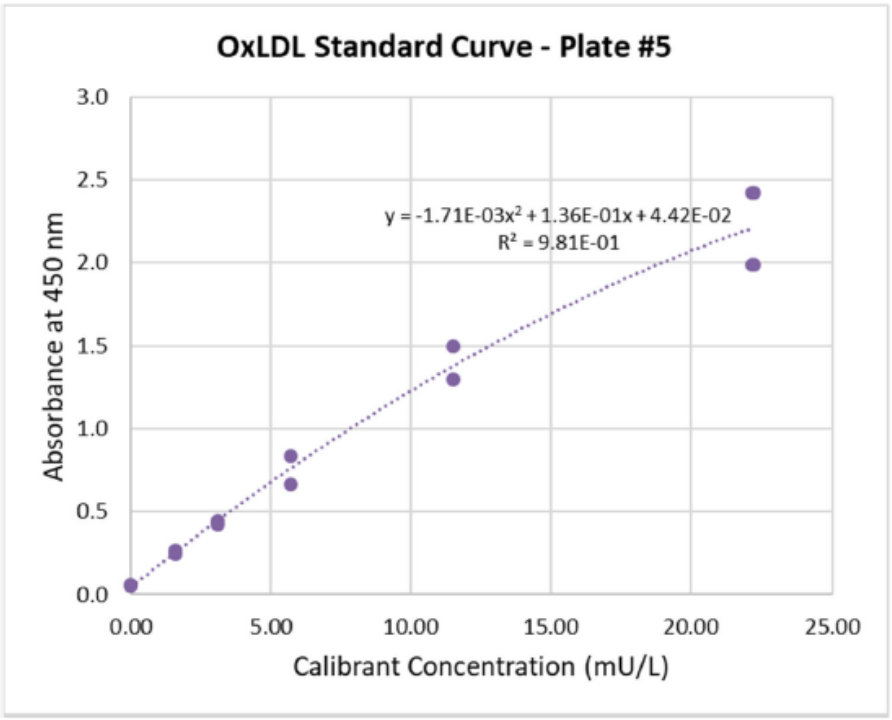

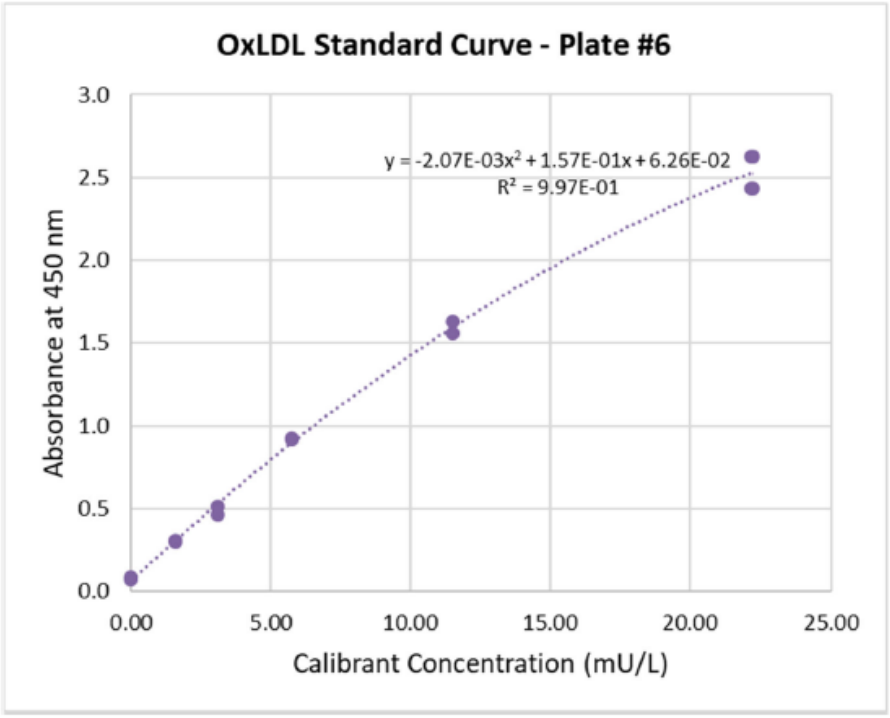

Figure 4.2: Standard curves for oxLDL ELISA plates

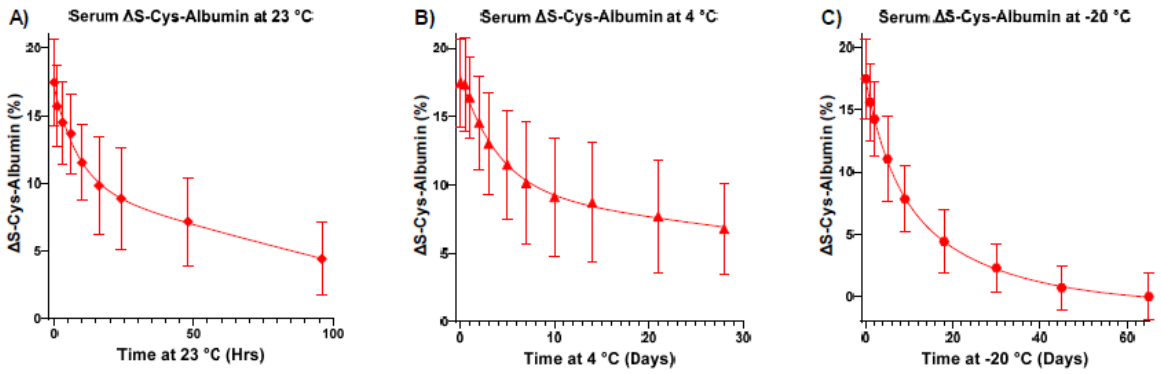

Figure 4.3: ΔS-Cys-Albumin inversely reflects the oxidation of albumin to S-cysteinylated albumin. Here it serves as a positive control for ex vivo changes that occur in a different protein/small molecule redox system present in serum when it is exposed to thawed conditions at A) 23 °C, B) 4 °C, and C) -20 °C. Serum aliquots from the same 12 GI cancer patients and 12 cancer-free donors shown in Figure 4.1 were monitored at each temperature. Data points represent the average of all 24 individuals and error bars represent inter-donor standard deviation.

Tables

Table 4.1: Patient/donor characteristics

Patient Demographics	n (%)
Number of Patients	24
Gender	
Males	13 (54.2)
Females	11 (45.8)
Age (yrs)	
<40	3 (12.5)
40-60	11 (45.8)
>60	10 (41.7)
Race	
White	20 (83.3)
Black	4 (16.7)
Other	0 (0)
Disease status	
Cancer-Free	12 (50.0)
Cancer	12 (50.0)
Stage I	1 (8.3)
Stage III	1 (8.3)
Stage III	1 (8.3)
Stage IV	3 (25.0)
Stage undetermined	6 (50.0)

CHAPTER 5

ABSORBANCE ASSAY AS AN ALTERNATIVE TO ΔS-CYS-ALBUMIN

5.1. Introduction

High quality specimens that have been optimally stored and handled are crucial to (pre)clinical cancer research because many clinically important biomolecules in plasma/serum (P/S) that serve as cancer and tumor immunology markers such as α-Fetoprotein (176), VEGF, TIMP-1 (150), CA-125, CA 15-3 (151), IL-1α, IL-1β, IL-10, IL-15, IL-17, IFN-γ (149, 177), and important miRNAs such as miR-21 (58, 178) are unstable under commonly encountered ex vivo thawed-state conditions. In fact, ex vivo storage and handling conditions can quantitatively impact numerous biomolecules as much or more than in vivo (clinical) conditions of interest which can lead directly to false conclusions (12, 26, 28–33, 67, 80, 81, 83, 124, 179–183). This has created an urgent, growing call to minimize ex vivo changes to P/S and to identify such changes when they occur (27–30, 32, 66–68, 83, 184) a need recognized by top-tier clinical chemistry journals, which have made earnest calls to require documentation of specimen handling conditions in manuscript submissions(36–43).

While numerous pre-analytical variables (PAVs) can compromise the integrity of P/S samples collected for biomedical research, the most difficult PAV to control and track over the life of most archived P/S samples, is exposure to thawed conditions (i.e., temperatures > -30 °C (50, 51)), especially at the individual aliquot level. Such exposures are all too common and occur, for example, as the result of temporary storage at -20 °C, a -80 °C freezer failure, delays in shipment and loss of dry ice, or the need to re-aliquot

samples. A common “solution” to this problem is to seek out biospecimens collected by reputable investigators using an acceptable standard operating procedure (SOP) and for which there is at least an oral history of storage conditions. While this usually passes as acceptable, it lacks rigor. It lacks rigor because it does not include empirical verification of biospecimen quality. Evidence-based verification of biospecimen quality is critical because, while seldom discussed, investigators in charge of procuring and archiving specimens for biomedical research have an inherent professional conflict of interest with disclosing incidents that may result in some or all of their collection being deemed less than pristine.

Our group experienced more than one occasion that critical information was missing from such documentation attached to nominally pristine samples provided to our lab by well-intentioned, highly reputable collaborators. We discovered integrity problems with the samples forensically using a novel assay that we have developed for P/S exposure to thawed conditions known as ΔS-Cys-Albumin which has been explained in Chapter 2 of this report, and with these discoveries we prompted/forced disclosure of the paper trail omissions which otherwise never would have been noticed (64, 65). On one occasion, sets of serum samples from stage I lung cancer patients as well as age/gender/smoking matched controls were provided to our group by highly reputable investigators whose work in collecting the samples was sponsored by the National Cancer Institute (NCI) / Early Detection Research Network (EDRN). In fact, the samples were slated for distribution by the NCI/EDRN to other investigators until we forensically discovered the integrity problem, which forced the investigators to disclose a major thaw incident that occurred to the control samples (but not the cases) during a natural disaster (64). On a

second occasion involving a multisite collection study of plasma samples from lung cancer patients and cancer-free donors in France, the investigators had completed processing, storage, and handling logs for every sample. Yet upon analysis of ΔS-Cys-Albumin in the control samples, we discovered that two batches of control samples must have been exposed to thawed conditions for a prolonged period of time. Our data prompted an investigation by our French collaborators who discovered that the contract lab who had collected plasma samples from cancer-free donors had moved its location while it held the two batches in question—revealing that a thaw event must have occurred during this change of lab locations (65).

These incidents illustrate how paper trails alone provide a false sense of security and are ultimately insufficient for tracking biospecimen integrity—and it points to the critical need to empirically verify the integrity of archived specimens. Indeed, our data argue for a new standard: namely, that molecular evidence-based verification (not just paper trails) should be the new normal when it comes to qualification of biospecimens for use in biomedical research.

The ΔS-Cys-Albumin assay, which was discussed in Chapter 2 has shown itself to be a success as proven by its near-perfect performance in blind challenges and its "real life" track record of having forced disclosure of sample mishandling events that were otherwise unreported in paper trails. At this point in time, no other marker of P/S integrity is as highly developed, mechanistically understood, and performance-proven as ΔS-Cys-Albumin. But it needs to be put in the hands of all investigators who employ pre-

existing P/S in their research. Its main limitation toward this end is that it requires LC/MS, which limits its availability. In turn, this dis-incentivizes its use.

During the development of the ΔS-Cys-Albumin assay, it was noticed that cysteine in P/S is not just oxidized to cystine or other small molecule mixed disulfides when exposed to thawed conditions, but that it is oxidatively consumed by proteins, primarily albumin (**Figure 5.1**) (64). Cystine, the most abundant source of cysteine equivalents in P/S, undergoes disulfide exchange with albumin, which ultimately consumes it as well. Since cysteine and cystine make up ≥ 90% of the sum total of all small molecule thiols and disulfides (SMT&D) in P/S (89, 90, 185, 186) but albumin exists at a few fold greater abundance than all of these together (91), this meant that, effectively, small molecule thiols and disulfides in plasma and serum become almost completely depleted from existence when P/S is exposed to thawed conditions. Thus quantification of SMT & Ds by an absorbance method will act as an alternative that provides similar information as the ΔS-Cys-Albumin assay.

This chapter explains the development and validation of an absorbance assay as an alternative to the ΔS-Cys-Albumin assay. To employ quantification by absorbance, first the disulfides (mainly cystine) should be reduced to thiols before they can be quantified using a thiol specific absorbance based detection method using Ellman's reagent. This reduction is obtained either by reacting with immobilized Tris(2-carboxyethyl)phosphine (TCEP) slurry which can then easily be removed by centrifugation in a filter or by treating with TCEP solution and subsequently quenching excess of it by 4-azidobenzoic acid (4-ABA) treatment. The first approach was later found to be cumbersome and

performed poorly which led to the adaptation of the latter approach which was successfully developed and validated as discussed in this chapter in detail. **Figure 5.2** gives a general overview of the experimental strategy used in this assay.

5.2. Materials and Methods

5.2.1. Materials and Reagents

Tris(2-carboxyethyl)phosphine Hydrochloride (TCEP, T1656), and 4-Azidobenzoic Acid (ABA, A0930) were purchased from TOKYO CHEMICAL INDUSTRY CO., LTD. (Tokyo, Japan). Pierce™ BCA Protein Assay Kit (23227), Sodium hydroxide monohydrate (041281-06), Greiner Bio-One Small Volume™ 384 Well Polystyrene Flat Bottom Microplates (07-000-32), Corning™ Costar™ Spin-X™ Centrifuge Tube Filters (07-200-386) and Pierce™ Immobilized TCEP Disulfide Reducing Gel (77712) were purchased from ThermoFisher Scientific (Waltham, MA). Albumin from human serum (A1653), Ammonium acetate (A7330), HEPES (H3375), hydrochloric acid (50-878-166), Acetic acid (320099), trifluoroacetic acid (TFA, 299537), Ellman's reagent (D218200), Ethylenediaminetetraacetic acid dipotassium salt dihydrate (03659), DL-Homocysteine (H4628), L-Cystine dihydrochloride (C6727), L-Cysteine (C7352), L-Glutathione reduced (G4251), L-Glutathione oxidized (G6654), γ-L-Glutamyl-L-cysteine (G0903), Cysteinylglycine (C0166), Maleimide (129585), Sodium chloride (S7653), Sodium phosphate monobasic (S8282), Sodium phosphate dibasic (S7907) Amicon Ultra-4 centrifugal filter, MWCO = 50 kDa (UFC805024), and Amicon Ultra-0.5 centrifugal filter, MWCO = 3kDa (UFC500396) were purchased from Sigma-Aldrich (Saint Louis, MO). Chelex 100 resin (1421253) was purchased from Bio-Rad Laboratories (Hercules, CA).

5.2.2. Plasma and serum

Plasma and serum samples collected from MIHS, CHTN and VWH for previous studies mentioned in Chapter 1, 2 and 3 were used herein this assay.

5.2.3. Preparation of artificial matrix

Completely reduced and alkylated HSA at 650 µM was used as the artificial matrix. To create this, 1 mM concentration of commercially available HSA was prepared in Hepes buffered saline (HBS; pH 7.4). The sample was aliquoted into 500 µL volumes and mixed with 300 µL of 10 mM Cys in HBS, followed by incubation for 1 hour at room temperature. After the incubation period, 1 µL of sample was diluted in 500 µL of 0.1% TFA and analyzed to verify complete reduction of albumin by LC-MS using previously established protocols (64) (**Figure 5.3A**). To alkylate the free thiol group in the Cys34 of HSA, the sample was mixed with 800 µL of 50 mM maleimide in ammonium acetate buffer (pH 5) and incubated at 50 °C for 15 minutes. In order to verify alkylation, 1 µL of sample was mixed with 500 µL of 0.1% TFA and analyzed by LC-MS by the same protocol (**Figure 5.3B**). The reaction mixture was then split into 400 µL aliquots in Amicon Ultra- 4 centrifugal spin filters (MWCO 50K). Each aliquot had 4 mL of HBS buffer added and then was centrifuged for 10 minutes at 4,000 g to a final volume of approximately 200 µL, this process was repeated 7 times, facilitating Cys and maleimide removal and protein concentration. All aliquots were then combined and albumin concentration was determined with a BCA protein assay, following the manufacturer's protocol. Then the protein sample was diluted with HBS to final concentration of 650 µM HSA and stored at -80 °C until further analysis.

5.2.4. Preparation of SMT & D stock solution

For analytical validation experiments that need fortification of SMT & D at different concentrations, a stock solution that contains cystine, cysteine, oxidized glutathione, reduced glutathione, reduced cysteinyl glycine, and γ-glutamyl cysteine in respective molar ratios of 60:10:0.1:2:4:1:1 was prepared. These concentrations ratios were chosen to represent the average physiological values in a human population (185). The stock solution was prepared at 960 µM cystine concentration and other components in the above ratio. Whenever a sample was fortified with the SMT & D solution and mentioned at a particular cystine concentration, this refers to the particular cystine concentration plus the other SMT & D in the above mentioned ratio.

5.2.5. Initial immobilized TCEP (iTCEP) protocol

The iTCEP assay was performed in the following manner. First, 25 µL aliquots of the samples to be analyzed were diluted to 500 µL with deionized water on ice and then completely transferred to prewashed (500 µL water was added to the filter and centrifuged at 14000 g for 10 mins and the filter was inverted upside down and spun for 1 min to remove any residual water) Amicon Ultra-0.5 centrifugal filter, MWCO = 3 kDa on ice and centrifuged at 14000 g in a centrifuge placed in a 4 °C refrigerator. After the centrifugation, exactly 400 µL of the flowthrough containing small molecule thiols and disulfides were transferred to 1.5 mL Eppendorf tubes and dried in a SAVANT SC250EXP SpeedVac Concentrator connected to a SAVANT RVT5105 refrigerated vapor trap (speedvac) at 35 °C and 3 Torr for 2.5 hours to complete dryness. To reduce the dislufides present in the dried samples to thiols, prewashed iTCEP slurry (20 µL of commercially available iTCEP slurry was transferred to a 1.5 mL Eppendorf tube

centrifuged at 1000 g for 1 min and supernatant was removed. This was then washed twice with 100 µL of 0.1 M phosphate buffered saline containing 1 mM K_2EDTA, pH 8.0 (0.1M PBS.EDTA) and finally mixed in 25 µL of 0.1M PBS.EDTA) was added and incubated at room temperature for 1 hour while mixing with flea-sized stir bars. These mixture was then then transferred to a Costar centrifuge tube filter and centrifuged at 1000 g for 1 min. Then 20 µL of the supernatant of the sample was recovered, combined with 5 µL of 0.32 mg/mL Ellman's reagent dissolved in 0.1M PBS.EDTA and incubated at room temperature for 15 minutes. Accurately 22 µL of each reaction mixture was transferred to a clear 384 well plate and the absorbance was read at 412 nm in a ThermoScientific MULTISKAN GO spectrophotometer.

5.2.6. Initial TCEP protocol

An alternative approach to the iTCEP method was employed named TCEP method. In this procedure, a 25 µL aliquot of plasma or serum is diluted to 500 µL with pre chilled water in a 1.5 mL Eppendorf tube on ice. The diluted sample is then spin filtered in a prewashed 0.5-mL 3 kDa cutoff spin filter at 14,000 g for 30 minutes at 4 °C, to remove proteins and large molecules present in the sample. Exactly 400 µL of the filtrate is transferred to a 1.5 mL Eppendorf tube and the sample is completely dried in a speed-vac for 2.5 hours at 35 °C & 3 Torr. The dried sample is then reconstituted in 23 µL of 0.1 M PBS.EDTA, briefly vortexed, and spun down. Then, 1 µL of freshly prepared 80 nmol/µL TCEP dissolved in 0.1 M PBS.EDTA pH 8.0 is added to the sample, briefly vortexed, spun down, and incubated at room temperature for 1 hour. During this step all the small molecule disulfides are reduced to small molecule thiols. Next, 1 µL of 800 nmol/µL 4-ABA dissolved in water; pH adjusted to 11.5 with NaOH is added into the

sample briefly vortexed, spun down, and incubated at room temperature for 1 hour, to completely quench remaining unreacted TCEP which would interfere during the detection step if present in the sample. After this step, 5 µL of freshly prepared 4 mM Ellman's reagent dissolved in 0.1 M PBS.EDTA is added to the sample, briefly vortexed, spun down, and incubated at room temperature for 15 minutes. Then, 22 uL of the reaction mixture is accurately transferred to a 384 well plate and the absorbance is measured at 412 nm.

5.3. Results

5.3.1. Method Development

5.3.1.1. Analysis using iTCEP

First, fresh and expired (incubated at 37 °C for 24 hours to ensure the samples have reached maximum level of S-Cys-Alb by consuming available cystine and cysteine) plasma and serum samples (n= 2 replicates per sample) were analyzed using the initial iTCEP method. In all the experiments, analogously analyzed duplicate buffer samples served as blanks and negative controls. Net absorbance was calculated by subtracting the average blank absorbance from the absorbance of each sample. The fresh plasma and serum samples showed higher net absorbance values than the expired samples. Differences between the fresh and expired plasma and serum were 0.0328 and 0.0221, respectively. Intra assay precision was checked by performing the above mentioned procedures on 6 replicates of fresh and expired (incubated at 37 °C for 18 hours) aliquots of plasma samples. Average intra assay precision was 5.7% and 5.0% CV for fresh and expired plasma. To analyze the behavior of the absorbance change in plasma samples after exposure to thawed conditions, separate aliquots of plasma samples incubated at 37

°C for 0, 1, 3, 6, 12, 18, 24, 48, 72 and 96 hours were analyzed using the above mentioned procedure. Time course incubation showed a similar decay pattern to the ΔS-Cys-Albumin in the plasma sample (**Figure 5.4**) (64). However, the data points were not completely consistent and the range between fresh and the completely oxidized samples were very low. Also handling the iTCEP with a small reaction volume was cumbersome especially in keeping assay volumes constant for all the samples that were simultaneously analyzed. Hence an easier alternative approach that can improve signal was required.

5.3.1.2. TCEP method

Absorbance measurement of 2-nitro-5-thiobenzoate at 412nm wavelength (TNB; ε = 14,150 $M^{-1}cm^{-1}$) generated by the classic thiol-specific Ellman's reagent (DTNB) is used in the detection step (**Figure 5.5C**) (187). This detection method is specific for thiols and thus create a need for reducing disulfides to thiols which can be obtained by reacting with TCEP (**Figure 5.5A**) (188). However, TCEP can also react with DTNB which would give falsely elevated absorbance values (189) and to prevent this, excess TCEP should be removed from the reaction mixture. First we thought using commercially available iTCEP slurry would be the easiest approach since the excess iTCEP can be removed by a simple spinfilter step. However, we were dealing with very small volumes and the use of iTCEP slurry caused precision issues due to difficulties in maintaining constant volumes across all the samples used in the assay. Therefore, we had to come up with a different approach where the disulfides (cystine) are first reduced by adding TCEP solution to the reaction mixture and then completely quenched by 4-ABA. Addition of 4-ABA to the reaction mixture oxidizes TCEP to TCEP oxide which is unreactive towards any molecules used in the assay (**Figure 5.5B**) (189).

To check the feasibility of this approach, 25 µL buffer containing 60 µM cystine along with appropriate positive and negative controls were simultaneously analyzed by this approach and the iTCEP approach. Comparison of iTCEP and TCEP methods resulted in expected observations (**Figure 5.6**). Average absorbance values for buffer samples processed by iTCEP and TCEP methods were 0.0408 and 0.0447, respectively suggesting that the excess TCEP was completely quenched by 4-ABA. Buffer samples processed by TCEP method without the addition of 4-ABA showed an average of 2.3386 absorbance indicating that the TCEP added into the reaction mixture was active. Absorbance for the 60 µM cystine in buffer samples analyzed by iTCEP and TCEP were 0.0395 and 0.2763, respectively which showed a significant increase in the yield when used TCEP method. However, the expected theoretical maximum absorbance for 25 µL of 60 µM cystine was 0.4675 and this was not reached by either of the methods (The theoretical maximum absorbance was calculated based on the concentration and volume of the cystine solution, the volume of the final reaction mixture, molar absorptivity of TNB from Ellman's reagent (14,150 $M^{-1}cm^{-1}$) and the pathlength of 22 µL solution in a 384 well plate (0.25 cm)). Plasma samples showed 0.1076 and 0.0932 absorbance respectively for iTCEP and TCEP methods. It was expected that the plasma sample would also show a higher absorbance for TCEP method than iTCEP method, but it was not observed.

5.3.1.3. Efforts to reduce yield inefficiencies in TCEP method

Although, the TCEP method showed improved signal, there were some yield inefficiencies observed. There are several factors that can contribute to this signal loss and several troubleshooting efforts were made to increase the net absorbance of 60 µM cystine sample to the theoretical maximum absorbance. First, during the resolubilization

step after speedvac drying, not all the dried cystine might go into the solution. To increase the solubility of the speedvac dried samples during the resolubilization step, the samples were heated at 90 °C for 10 mins before the addition of TCEP. Inclusion of this step increased the net absorbance to an average of 0.2797. Second, Cu^{2+} is a catalyst in cysteine to cystine oxidation reaction and there is a possibility that some of the reduced cysteine may be reoxidized to cystine during the quenching step (4-ABA treatment) resulting in signal loss. To check the effect of transition metal ion content (specifically Cu^{2+}) and oxygen concentration on absorbance, differently treated PBS buffers were used to reconstitute cystine after the speedvac drying step. Buffers used in this comparisons were, chelex treated N_2 sparged PBS, chelex treated non N_2 sparged PBS, non chelex treated N_2 sparged PBS, and non chelex treated non N_2 sparged PBS. Absorbance of 60 µM cystine processed with the TCEP method and reconstituted using these buffers were compared (n = 2 replicates in each buffer). Sparging buffers with nitrogen did not show any impact on the absorbance. On the other hand, chelex treated buffer showed the highest net absorbance value of 0.3475 suggesting the reduction in Cu^{2+} increases the signal by reducing Cu^{2+} catalyzed oxidation of cysteine to cystine. This suggested reducing reaction times, specially the 4-ABA incubation times would reduce the degree of reoxidation and thus would increase the signal. So to check this, optimization of TCEP concentration, TCEP incubation time, and 4-ABA incubation time were carried out. Tested incubation time combinations were TCEP 20 min & 4-ABA 20 min, TCEP 20 min & 4-ABA 60 min, TCEP 60 min & 4-ABA 20 min, and TCEP 60 min & 4-ABA 60 min (n=3 replicates at each condition) at 3.2 mM TCEP concentration. This whole set was repeated with 9.6 mM TCEP concentration to check the effect of increased TCEP

concentration. The results showed that lower (20 mins) incubations time for both TCEP treatment and 4-ABA worked the best and resulted in the highest absorbance values as expected (**Figure 5.7**). Increasing the concentration of TCEP did not show any effect on absorbance.

To ensure that no signal loss occurs during the reduction or quenching step, 23 µL aliquots of 60 µM cystine in buffer (n= 3 replicates) were dried in a speedvac, reconstituted in 23 µL of buffer and were analyzed using optimized reaction times. For this experiment, all glassware used to make reagents were pre-rinsed overnight with high purity 2% nitric acid and all the buffers and reagents were prepared with high resistivity deionized water (18.2 $M\Omega cm^{-1}$) to ensure removal of transition metals. This resulted in average net absorbance of 0.5262 (98 % signal recovery) where the expected theoretical maximum absorbance was 0.5376 (This value is higher since spin filter step was omitted here). This suggested removal of Cu^{2+} from the reaction mixture and reducing the reaction times improves nearly completely eliminates signal loss due to reoxidation. Along with this, fresh and expired plasma samples (n= 3 replicates per sample) were also analyzed. Signal for fresh and expired plasma significantly increased when used the latest optimized protocols. Average net absorbance for fresh and expired plasma samples were 0.2128 and 0.0262, respectively (**Figure 5.8**). It was hypothesized that the signal loss in plasma might be due to non-covalent interaction of SMT & Ds to proteins in plasma samples which leads to the loss of SMT & D with proteins during the spin filter step. To release any non-covalently attached SMT & D to proteins, that is lost during the spin filter step, denaturation of plasma proteins prior to dilution was tried. For this purpose,

acid denaturation with HCl and TFA and methanol precipitation were carried out. But none of these methods improved assay signal.

To compare the absorbance assay with the ΔS-Cys-Albumin assay over a time course at room temperature, a plasma sample for which the ΔS-Cys-Albumin time course data were available, was selected. A never-thawed aliquot of the fresh plasma sample was thawed on ice and made into several 25 µL aliquots. These aliquots were incubated at room temperature 0, 1, 3, 6, 12, 24, 48, 72, 96, and 120 hours (n = 6 for first and last time points; n = 1 for all others). After each time point incubation was over, the respective aliquots were immediately transferred to -80 °C until all the time point incubations are completed. After all the incubations were completed, absorbance assay was performed on all the aliquots and net absorbance readings were recorded. Absorbance assay exhibited a similar decay pattern as the ΔS-Cys-Albumin assay (**Figure 5.9**). And the precision was very good as indicated by tight error bars for SD.

5.3.1.4. Matrix effect

With the aim of moving forward to the analytical validation, first, we checked the possibility of absolute quantification with the external standard (ES) approach since it is the most convenient approach. To employ the ES approach, the first step is to check for a matrix effect—in which the plasma or serum matrix itself might interfere with SMT & D quantification as assessed using a synthetic matrix ES approach. We hoped to use artificial matrix to create standard curves to do quantification in plasma and serum samples, because artificial matrix can be created without any presence of SMT & D in it and this cannot be achieved when using a plasma or serum sample as matrix since they

possess SMT & T and this would make quantification difficult. During the artificial matrix preparation the HSA was completely reduced and alkylated to prevent any consumption of SMT & Ds by HSA present in the artificial matrix. To check the feasibility of using the ES approach, presence of matrix effect between plasma, serum and artificial matrix should be checked. To check matrix effects, standard curves with different matrices (expired plasma, expired serum and the artificial matrix) were created. Each matrix (22 µL) was fortified with 3 µL of SMT & D solution to result in additional 0, 3.75, 7.5, 15, 30, 60, 90, and 120 µM cystine concentration (n= 2 replicates per concentration). Two standard curves were made on different days for each matrix and slopes of all the standard curves were compared. Serum and artificial matrices showed similar slopes indicating those matrices were compatible (**Figure 5.10**). However, plasma exhibited a lower slope than the other two matrices. The observed lower slope in plasma raised the question, "What if different serum samples exhibit different slopes?" To check this, standard curves were created with different serum samples as matrices. For this, serum samples from 10 different patients were expired at 37 °C for 24 hours and 22 µL aliquots of these serum samples were fortified with 3 µL of SMT & D solution to result in additional 0, 5, 15, 45, and 90 µM cystine concentration and standard curves were created based on net absorbance of these samples. Standard curves with all serum samples resulted in similar slopes suggesting there are no matrix effects between serum samples from different people (**Figure 5.11**). The average slope of the serum samples was 0.006827 and the %CV was 8%. However, an unexpected issue arose during this observation. It was expected that completely oxidized serum samples should result in net

absorbance closer to zero. However, net baseline absorbance in analyzed serum samples ranged from 0.0158 to 0.3385.

5.3.1.5. Explaining the slope difference in plasma

In serum approximately 95% of copper is bound to ceruloplasmin (102). But in EDTA plasma, most of it is chelated by EDTA and much more catalytically available compared to serum which would catalyze the oxidative consumption of cystine in plasma faster than in serum. It was hypothesized that acidification of plasma would increase the slope by preventing this oxidation. To check the effect of acidification, 22 µL aliquots of expired plasma samples from 4 different patients were diluted with 0.015M HCl on ice and spiked with 3 µL of SMT & D solution on ice to result in additional 0, 5, 15, 45, and 90 µM cystine concentration. These samples were then transferred to prewashed 0.5-mL 3 kDa cutoff spin filters centrifuged at 14,000 g for 30 minutes at 4 °C. Exactly 400 µL of the filtrate of each sample were transferred to a 1.5 mL Eppendorf tubes and were completely dried in a speed-vac for 2.5 hours at 35 °C & 3 Torr. The dried samples were then reconstituted in 23 µL of 0.4 M PBS.EDTA and processed similarly to get the absorbance readings. When standard curves were created with this method using expired plasma samples from 9 different people as matrices, similar slopes to the serum and artificial matrix were observed (**Figure 5.12**)—though they varied a bit amongst themselves which was a hint that the Method of Standard Addition (MosA) approach might be required for absolute quantification. The average slope of all the standard curves with plasma was 0.007320 with a %CV of 13%. Similar to serum samples, different expired plasma samples exhibited different baseline absorbance ranging from 0.0206 to 0.1349.

5.3.1.6. Delta absorbance approach

Much like the ΔS-Cys-Albumin assay, the observed range of absorbance in completely oxidized plasma and serum samples made it impossible to use a single point absorbance measurement as an indicator for samples exposure to thawed condition. Hence, an alternative approach was created that was named and involved delta absorbance measurements. The delta absorbance values are calculated by subtracting the baseline absorbance (net absorbance of a 25 µL aliquot of the same sample after forced oxidation by incubation for 24 hours at 37 °C) from the net absorbance of the fresh sample. To check the feasibility of this approach, the absorbance assay was performed using the optimized protocols on fresh and expired aliquots of plasma samples from 5 different people (2 replicates of each aliquot on 3 different days) and the delta absorbance values were determined (**Figure 5.13**). The delta absorbance values in plasma ranged from 0.1327 to 0.3073. The same experiment was carried out with 5 different serum samples to calculate the delta absorbance values in serum and the those samples resulted in delta absorbance ranging from 0.3137 to 0.4694 (**Figure 5.14**). These results suggested that the delta absorbance value has an acceptable range that can be used as an indicator for plasma or serum exposure to thawed conditions.

5.3.2. Final optimized protocols

Below are the final optimized protocols used in analytical validation, population range and time course analysis experiments.

5.3.2.1. Serum samples

- A 25 µL aliquot of fresh serum is diluted to 500 µL with pre chilled water in a 1.5 mL Eppendorf tube on ice.
- The diluted sample is then spin filtered in a prewashed 0.5-mL 3 kDa cutoff spin filter at 14,000 g for 30 minutes at 4 °C, to remove proteins and large molecules present in the sample.
- Exactly 400 µL of the filtrate is transferred to a 1.5 mL Eppendorf tube and the sample is completely dried in a speed-vac for 2.5 hours at 35 °C & 3 Torr.
- The dried sample is then reconstituted in 23 µL of 0.1 M phosphate buffered saline containing 1 mM K_2EDTA (0.1 M PBS.EDTA) pH 8.0, briefly vortexed, spun down, and incubated in a 90 °C water bath for 5 minutes.
- Again, the sample is briefly vortexed, spun down, and incubated in a 90 °C water bath for 5 minutes. This incubation at 90 °C helps to ensure complete solubilization of SMT&Ds.
- Then, 1 µL of freshly prepared 80 nmol/µL TCEP dissolved in 0.1 M PBS.EDTA pH 8.0 is added to the sample, briefly vortexed, spun down, and incubated at room temperature for 20 minutes. During this step all the SM disulfides are reduced to SMTs.
- Next, 1 µL of 800 nmol/µL 4-ABA dissolved in water; pH adjusted to 11.5 with NaOH is added into the sample briefly vortexed, spun down, and incubated at room

temperature for 20 minutes, to completely quench remaining unreacted TCEP which would interfere during the detection step if present in the sample.

- After this step, 5 µL of freshly prepared 4 mM Ellman's reagent dissolved in 0.1 M PBS.EDTA is added to the sample, briefly vortexed, spun down, and incubated at room temperature for 15 minutes.
- Then, 22 uL of the reaction mixture is accurately transferred to a 384 well plate and the absorbance is measured at 412 nm.

A 25 µL aliquot of the same serum sample is incubated for 24 hours at 37 °C. After this step, SMT&D in P/S would be oxidatively consumed by proteins and only a basal level of SMT&D will be left unreacted in the sample. This sample is processed similarly to that of the fresh sample and the delta absorbance is calculated by subtracting the net absorbance of the oxidized sample from the fresh sample.

5.3.2.2. Plasma samples

- A 25 µL of fresh plasma aliquot is diluted to 500 µL with pre chilled 0.015 M HCl in a 1.5 mL Eppendorf tube on ice.
- The diluted sample is then spin filtered in a prewashed 0.5-mL 3 kDa cutoff spin filter at 14,000 g for 30 minutes at 4 °C.
- Exactly 400 uL of the filtrate is transferred to a 1.5 mL Eppendorf tube and the sample is completely dried in a speed-vac for 2.5 hours at 35 °C & 3 Torr.

- The dried sample is reconstituted in 23 µL of 0.4M PBS.EDTA pH 8.0, briefly vortexed, spun down, and incubated in a 90 °C water bath for 5 minutes.
- Again, the sample is briefly vortexed, spun down, and incubated in a 90 °C water bath for 5 minutes.
- Then, 1 µL of freshly prepared 80 nmol/µL TCEP dissolved in 0.4 M PBS.EDTA pH 8.0 is added to the sample, briefly vortexed, spun down, and incubated at room temperature for 20 minutes.
- Then, 1 µL of 800 nmol/µL 4-ABA (dissolved in water; pH adjusted to 11.5 with NaOH), is added into the sample, briefly vortexed, spun down, and incubated at room temperature for 20 minutes.
- After the incubation, 5 µL of freshly prepared 4 mM Ellman's reagent dissolved in 0.4 M PBS.EDTA pH 8.0 is added, briefly vortexed, spun down, and incubated at room temperature for 15 minutes.
- Then, 22 uL of the reaction mixture is accurately transferred to a 384 well plate and the absorbance is measured at 412 nm.

A 25 µL aliquot of the same plasma sample is incubated for 24 hours at 37 °C. After this step, sample is processed similarly to that of the fresh sample. The delta absorbance is calculated by subtracting the net absorbance of the oxidized sample from the fresh sample.

5.3.3. Analytical validation

After the development of the assay, analytical validation was conducted to ensure the analytical integrity of the newly optimized assay. For some validation criteria, validation approaches for both an ES approach and an approach that would be used if the Method of Standard Addition (MoSA) were required for absolute quantification. Validation designs employing synthetic matrix were used for the former and designs involving actual plasma and serum were used for the latter. Ultimately, it was determined that the MoSA must be used for absolute quantification. This method was validated for each of the criteria seen below.

5.3.3.1. Limits of Detection & Quantification (LOD and LOQ)

Both absolute and functional LODs & LOQs were determined. The absolute LODs of the assay was determined according to standard analytical procedures (190) by measuring the absorbance of synthetic matrix blank samples using n = 6 experimental replicates on 4 different days, pooling all data. Functional limits of detection (i.e., MoSA-based LODs) were determined analogously using pre-expired plasma and serum samples with low and high baselines (n = 5 experimental replicates on 3 different days). In brief, for both the absolute and functional LOD/LOQ experiments, the minimum distinguishable analytical signal (S_m) was determined by summing the mean of the blank signal ($\bar{S}_{bl}$) plus a multiple k of the standard deviation of the blank signal (ks_{bl}) for the LOD and LOQ. That is, $S_m = \bar{S}_{b_l} + ks_{bl}$. Using S_m and the slope of the standard curve with each matrix (low and high baseline plasma and serum), the LOD and LOQ were calculated as $LOD\ or\ LOQ = (S_m - \bar{S}_{bl})\ /\ m$. Where k = 3 for LOD and k = 10 for LOQ. Minimum

distinguishable analytical signal (k= 3 SD) in low and high baseline serum were 0.0763 and 0.2497, respectively and in low and high baseline plasma those were 0.0403 and 0.1879, respectively. This was 0.0126 in artificial matrix. To enable absolute quantification, absolute and functional LOD and LOQ were calculated. Absolute LOD and LOQ using a blank signal was 4.94 and 14.97 µM, respectively. Then, functional LOD and LOQs at low and high baselines plasma and serum samples were calculated. For serum, LODs in low and high baseline samples were 5.14 and 4.44 µM and LOQs were 17.12 and 14.80 µM, respectively. For plasma, LODs in low and high baseline samples were 2.50 and 6.85 µM and LOQs were 8.32 and 22.84 µM, respectively.

5.3.3.2. Linear dynamic range and sensitivity

Linear dynamic range and sensitivity were evaluated in synthetic matrix, pre-expired plasma and serum samples with high and low baseline absorbance values. Several 25 µL of aliquots of each matrix were diluted with 472 µL of water (artificial matrix and serum) or 0.015 M HCl (plasma) and fortified with 3 µL of SMT & D solution to reach additional 0-120 µM additional cystine concentration (2 replicates at each concentration) and absorbance assay was performed on these samples. For each matrix, standard curves were created on 4 different days using the same approach. Curve parameters including R^2, standard deviation about regression, were calculated on the pooled set of standard curves **(Figure 5.15**). All standard curves were linear from 0 to 120 µM cystine concentration in all matrices as indicated by R^2 values greater than 0.99 for standard curves created with each matrix. Standard deviation about regression for low baseline serum, high baseline serum, low baseline plasma, and high baseline plasma were 0.0308, 0.0312, 0.0264, and 0.0251 respectively. Sensitivity was calculated for each matrix by

dividing the slope of the standard curve for each matrix by standard deviation about the regression. Sensitivity values for artificial matrix, low baseline serum, high baseline serum, low baseline plasma and high baseline plasma were, 0.2589, 0.2386, 0.2682, and 0.3468 μM^{-1}, respectively.

5.3.3.3. Precision

Initially, intra and inter day precision of the delta absorbance measurements were checked on 5 plasma and 5 serum samples. Absorbance assay protocol was performed on duplicate aliquots of fresh and expired plasma and serum samples. The delta absorbance values were determined by subtracting the absorbance of expired samples from the respective fresh samples and the intraday precision of absorbance and delta absorbance values were calculated. This experiment was repeated on three nonconsecutive days to calculate inter day precision which resulted in 10 and 8 %CV values for delta absorbance values for plasma and serum samples respectively (**Figures 5.13 & 5.14**). Then this experiment was expanded to calculate intra and inter day precision at low, medium and high concentration of SMT &D in plasma and serum samples that showed low and high baseline absorbance. For this, matched plasma and serum from 10 patients were selected and duplicate (25 µL) aliquots of each sample were incubated at 37 °C for 24 hours to drive the absorbance to baselines. After the incubation, the standard absorbance assay was performed on these aliquots to calculate average baseline absorbances of each sample (**Figure 5.16**). From this, a patient which showed low baseline absorbanceM values for both plasma and serum was selected as low baseline (MIHS04) sample and one showed high baseline absorbance was selected as high baseline sample (MIHS114). For the precision assay on the low baseline serum sample, several pre-expired (incubated at

37 °C for 24 hours) aliquots (25 µL) were diluted with 472 µL of water on ice and spiked with 3 µL of SMT & D solutions to result in additional 0, 10, 30 and 80 µM cystine concentration (5 replicates per concentration). These samples were analyzed by the standard absorbance protocol for intra assay precision, and this experiment was repeated on 3 nonconsecutive days to calculate inter assay precision. The intra assay and inter assay precision on high baseline serum was conducted in a similar manner. For plasma, similar approach was carried out with the exception of diluting the pre-expired samples with 0.015M HCl instead of water. Intra and inter assay precision values for plasma and serum samples with high and low baselines at different concentration of SMT & Ds fortification are listed in **Table 5.1**. Above the LODs, average % CVs were less than 10% indicating acceptable intra and inter day precision.

5.3.3.4. Accuracy

Accuracy was checked in plasma and serum samples with low and high baseline absorbance fortified with SMT & D mixture at 0, 10, 30 and 80 µM cystine concentration (5 replicates per concentration) following the standard absorbance protocols. The delta absorbance values were calculated by subtracting the baseline absorbance from all other absorbance values. To check the accuracy using the external standard (ES) approach, standard curves with artificial matrix were prepared. For this several 25 µL aliquots of artificial matrix were diluted with 472 µL of water and fortified with 3 µL SMT & D solution to result in additional 0, 3.75, 7.5, 15, 30, 60, 90 and 120 µM cystine concentrations (2 replicates per concentration). These samples were analyzed by standard absorbance protocol and the standard curve was created based on delta absorbance values. This process was repeated on 5 different days to create 5 standard curves and the

average slope was calculated by plotting all points together (**Figure 5.17**). Concentration of the fortified cystine in each aliquot was back calculated using delta absorbance values and the average equation of slope of the standard curves with artificial matrix and the percentage errors were calculated (**Table 5.2**). When ES approach was used for concentration calculations, most of the values resulted in less than 10% error except for the high baseline serum sample which exhibited higher than 15% error at all concentrations. However the MoSA approach was found to be accurate in all the matrices above the LOQs calculated. To check the accuracy with MoSA, separate standard curves were prepared for each matrix to quantify the amount of thiols in fresh samples (n=15 for each samples at each concentration; 5 replicates on each day for 3 days). Then using the calculated cystine concertation in the unfortified pre-expired sample (calculated based on all fortification points) and the difference in absorbance between spiked samples, concentrations of fortified cystine were back calculated using the single point addition method (**Table 5.3**). Results showed that above the LOQs MoSA resulted in high accuracy. When the fortified concentration of cystine at a 30 µM concentration was back calculated using single point addition method using the absorbance difference between 30 µM fortified sample and 80 µM fortified samples, calculated concentrations resulted with an average of 2% error showing very high accuracy (**Table 5.3**)

5.3.4. Population survey of fresh and expired plasma and serum samples

To determine the range of the delta absorbance measurements that can be expected in plasma and serum samples from different patient cohorts the delta absorbance assay was performed on matched plasma and serum samples from 20 GI cancer patients and 20 nominally healthy donors. Plasma and serum were analyzed separately. Serum samples

were analyzed in a randomized order in 4 sets. For each set, never thawed aliquots of 5 serum samples stored in -80 °C freezer were transferred to ice and thawed. Each sample was aliquoted into three different 1.5 ml Eppendorf tubes. First aliquot was diluted with 475 µL of water and the second aliquot was diluted with 472 µL of water and fortified with 3 µL of SMT & D solution to result in additional 30 µM cystine concentration. These two aliquots were immediately analyzed by the standard absorbance assay. The third aliquot of each sample were incubated at 37 °C for 24 hours. Once all the third aliquots from all the serum samples were ready, they were analyzed in a random order in two sets. Until the analysis the expired aliquots were stored in a -80 °C freezer. The delta absorbance values were calculated by subtracting the absorbance of the third aliquot from the respective first and second aliquots. Similar approach was followed for plasma samples except that the plasma samples were diluted with 0.015M HCl instead of water. The observed range for delta absorbance values of unfortified samples were 0.1132 – 0.6259 in plasma and 0.2333 - 0.6441 in serum. Mean (± 95% CI) delta absorbance values in plasma and serum were 0.2766 (± 0.1855) and 0.4149 (± 0.1805), respectively and these two groups were significantly different (paired t test, $p < 0.05$) (**Figure 5.18**). Difference between cancer and healthy populations were not significant suggesting that the delta absorbance assay is not affected by the disease status (**Figure 5.19**). As explained in Chapter 2, the "non-pristine sample" cutoffs for plasma and serum samples were set as 0.1773 for serum and 0.0324 for plasma (mean – 2.58 SDs) based on normal distribution, 99% of the plasma or serum samples would show delta absorbance values in the range of mean ± 2.58 SDs. Hence, this assay will be useful in serum samples but not in plasma samples since the cutoff value is very close to zero.

By applying the ES approach, concentration of SMT & D in each group were calculated using the delta absorbance values and the average equation of the standard curve with artificial matrix (**Figure 5.20**). Mean (± 95% CI) cystine concentration in plasma and serum were 37 µM (± 12 µM) and 54 µM (± 12 µM), respectively. To check the accuracy of ES approach in absolute quantification, one more aliquot of each sample which was fortified with SMT & T solution to result in additional 30 µM cystine concentration was also employed. The calculated difference between the fortified aliquot and the fresh aliquot of each sample should result in a 30 µM difference if the ES approach was accurate in quantification. However, calculated concentrations ranged from 17 to 47 µM in plasma and 15 to 57 µM in serum (**Figure 5.21**). This suggest that the ES approach is not accurate enough for absolute quantification purposes. MoSA would be the optimal approach to use when absolute quantification is required given that average percentage error for MoSA in all the matrices at 30 µM fortification was 2% during accuracy experiments as explained in the accuracy section.

5.3.5. Time course incubations

Matched P/S samples from 10 GI cancer patients and 10 healthy donors displayed high, medium and low delta absorbance values were selected for this study. Separate aliquots from each plasma and serum samples were made on ice. These aliquots were incubated for 0, 1, 3, 6, 10, 16, 24, 48, 96 and 120 hours at 23 °C; 0, 0.5, 1, 3, 5, 7, 10, 14, 21, 28 and 56 days at 4 °C; and 0, 1, 2, 5, 9, 18, 30, 40, 50, 70 and 150 days at -20 °C. One aliquot from each temperature from each patient was incubated at 37 °C for 24 hours and used to calculate the delta absorbance value. After the incubation was over at each temperature, the absorbance assay was performed on these aliquots following the

optimized protocols. Results showed that at all the temperatures checked the delta absorbance values decreased in a similar manner to the ΔS-Cys-Albumin values. There was inter individual variability among different samples. However, there was no difference in the decay pattern was observed between the different group of samples. All the samples reached closer to zero delta absorbance values after 120 hours incubation at room temperature or 56 days at 4 °C (**Figure 5.22**). After 150 days incubation at -20 °C samples reached a delta absorbance of zero. However some samples exhibited negative delta absorbance values especially the serum samples. This observation was similar to what was observed in the ΔS-Cys-Albumin assay. To prevent this, each aliquot should be expired after the incubation period is over rather than using only one aliquot as an expired sample to calculate the delta absorbance value.

5.4. Discussion

Development and analytical validation of a delta absorbance assay that acts as a marker to assess the sample exposure to thawed conditions is discussed here. We have already developed and validated an assay named ΔS-Cys-Albumin assay as discussed in chapter 2. This assay was proved successful in identifying expired samples during blind challenges and caused forced disclosure of sample mishandling in two different incidents (64, 65). However, this assay requires an LC-MS instrument and the analysis time per sample is longer which limits the implementation of this assay to all clinical laboratories. Therefore we have developed delta absorbance assay, a plate reader based assay as an alternative to the ΔS-Cys-Albumin assay.

Thus we developed an absorbance method to measure the SMT & D in plasma serum samples. For this, first small molecules from plasma and serum should be separated from large molecules like proteins. We used a spin filter with 3kDa cutoff for this purpose. This assay uses 25µL of plasma or serum samples for the analysis and the viscosity of undiluted plasma and serum, which, when spun, provides very low (and quantitatively inconsistent) quantities of filtrate. Therefore the sample is diluted to 500 µL with pre-chilled water on ice before transferring it to the spin filter for centrifugation. Keeping the temperature lower until the centrifugation step is critical to keep oxidative consumption of cystine by albumin minimal. For this reason, the centrifuge that is used to spin the samples is prechilled and kept at 4 °C throughout the centrifugation period. After the centrifugation, 400 µL of the filtrate is transferred to a 1.5 mL Eppendorf tube, dried in speedvac to complete dryness and reconstituted in buffer. These steps can be carried out at room temperature because, at this point albumin is not present in the sample to consume cystine.

With the aim of moving forward to the analytical validation, first, we checked the possibility of absolute quantification with ES approach. To employ ES, the first step is to check for matrix effect. We hoped to use artificial matrix to create standard curves to do quantification in plasma and serum samples. When plasma, serum and artificial matrix were checked for slopes the plasma produced a lower slope indicating a matrix effect. In theory we assumed that plasma and serum should behave similarly as the principle behind this assay is closely related to that of ΔS-Cys-Alb assay. However, this was not the case. So it was crucial to check for matrix effects even when working with closely related samples.

When we checked different serum and plasma samples for matrix effect we identified that different samples exhibited different baseline absorbance values. And our results showed that they behave differently not in slopes but in baseline absorbance values. This indicates the importance of testing several different plasma or serum samples rather than using a pooled plasma or serum during assay development and this could be applied for any assays that involve biological samples.

This assay exhibited acceptable intra and inter day precision and accuracy. When absorbance assay was performed on plasma and serum samples from healthy and GI donors the disease state did not affect the range in the population. This was true for both plasma and serum. However the range observed in plasma samples was significantly lower than serum samples (**Figure 5.18**). This was unexpected because this assay is analogous to the ΔS-Cys-Albumin assay and plasma samples exhibit a higher range of ΔS-Albumin-values than serum sample. However, a study that compared the abundance of metabolites between plasma and serum from 15 different people using GC-MS have shown that serum contains 33% higher abundance of cystine than plasma (191) . Numerous coagulation proteins possess free cysteine residues. Thus there might be a protein-based disulfide exchange network of proteins in plasma (for which albumin has the lowest reduction potential) that involves coagulation cascade proteins that are removed in serum. This might explain higher delta-S-Cys-Albumin in plasma than serum despite the fact that serum, on average, may have more cystine in it. However at this point we do not have any conclusive explanation for the discrepancy between the ΔS-Cys-Albumin assay and the delta absorbance assay in plasma samples. Regardless, the range that we see in the serum samples allows us to set an acceptable cutoff value for

fresh samples where it is not possible in plasma. It might be possible to improve this range by using a larger volume of plasma for the analysis or by employing a detection method that can increase the range such as a fluorescence assay. Even though the current approach will not be useful in identifying exposure of *individual* plasma samples to thawed conditions, it is possible to use this assay to check for *groups* of plasma samples. For an example, if there are two groups of plasma samples where one group has been kept pristine and the other was exposed to thawed conditions, the average of delta absorbance in the pristine group would be higher and the exposed group would show a lower average delta absorbance, and the two groups could be distinguished using simple statistical analysis.

Finally, absolute quantification is not necessary to use this assay since the delta absorbance value alone should be sufficient to differentiate between fresh and exposed samples. But when absolute quantification is required, it should be done by MoSA and not by ES approach because ES approach did not accurately quantify spiked concentrations above LOQs in all samples examined (**Table 5.2 and Figure 5.21**).

Figures

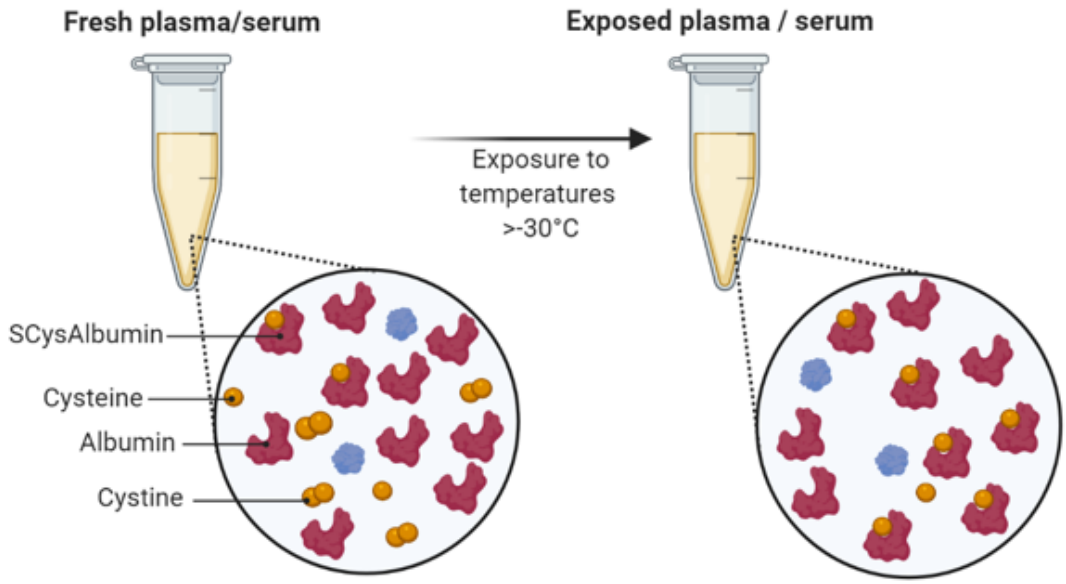

$$AlbSH + Cys\text{-}Cys \underset{k_2}{\overset{k_1}{\rightleftharpoons}} SCysAlb + Cys \quad (1)$$

$$2Cys + O_2 \xrightarrow[k_3]{Cu(II)} Cys\text{-}Cys + H_2O_2 \quad (2)$$

Figure 5.1: Schematic explanation and reactions of cystine and cysteine consumption by albumin during oxidation

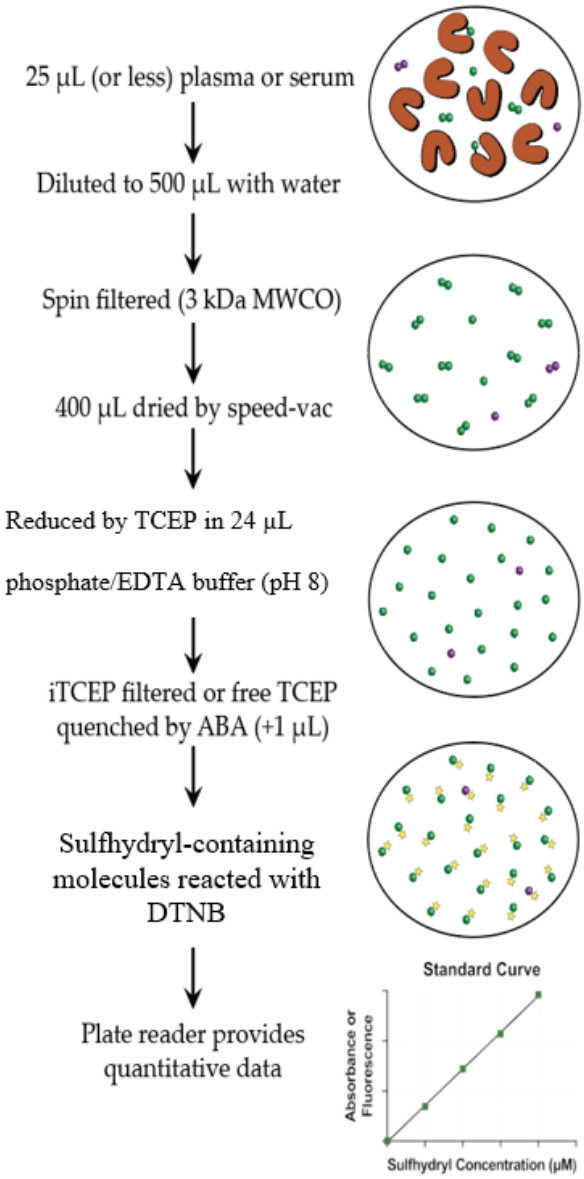

Figure 5.2: General overview of the methodological strategy

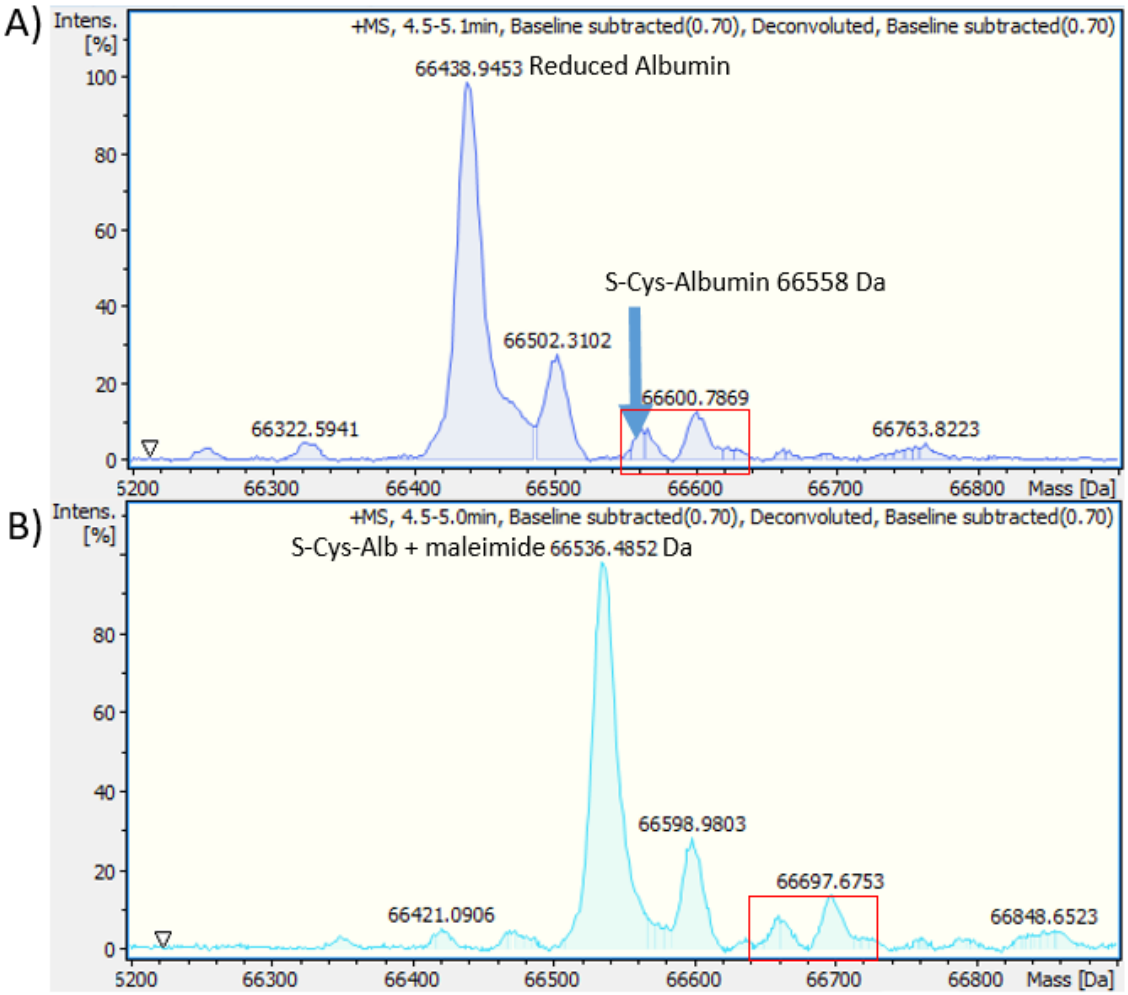

Figure 5.3: Charge deconvoluted ESI-mass spectra of the A) completely reduced commercially available HSA and B) completely reduced and alkylated with maleimide. The mass shift of exactly +97 Da, with no peaks at +2*97 Da (66,633 Da, corresponding to two alkylation events) or +3*97 Da etc. indicate that the reduced albumin possessed only a single free Cys residue as expected. In A) a peak closer to the S-Cys-Albumin mass was observed. But the peak shifts by +97 Da (indicated by the red box) after maleimide treatment conforming that the peak did not correspond to S-Cys-Albumin.

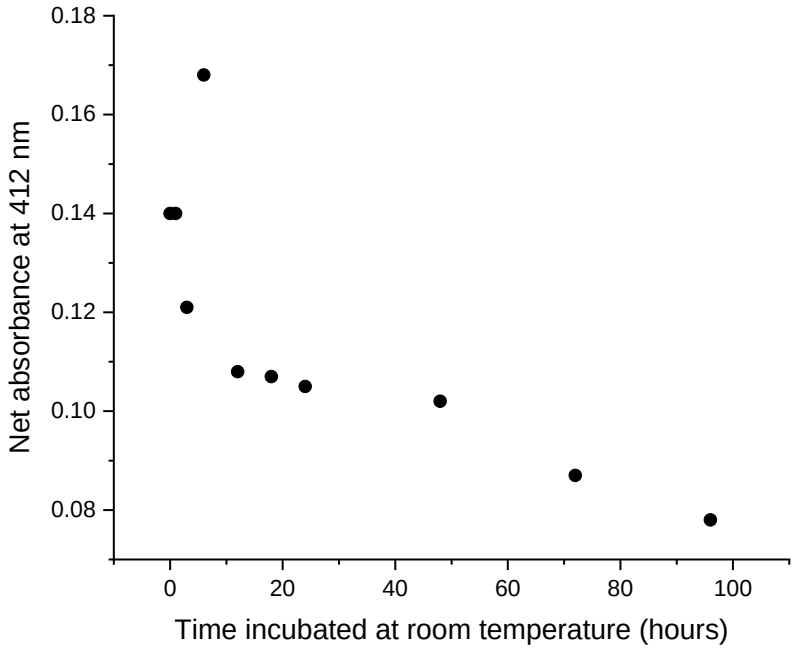

Figure 5.4: Blank subtracted absorbance (at 412 nm) of plasma aliquots incubated for different times at room temperature. All the aliquots were analyzed together and the net absorbance was calculated by subtracting the average blank absorbance from the absorbance of each aliquots.

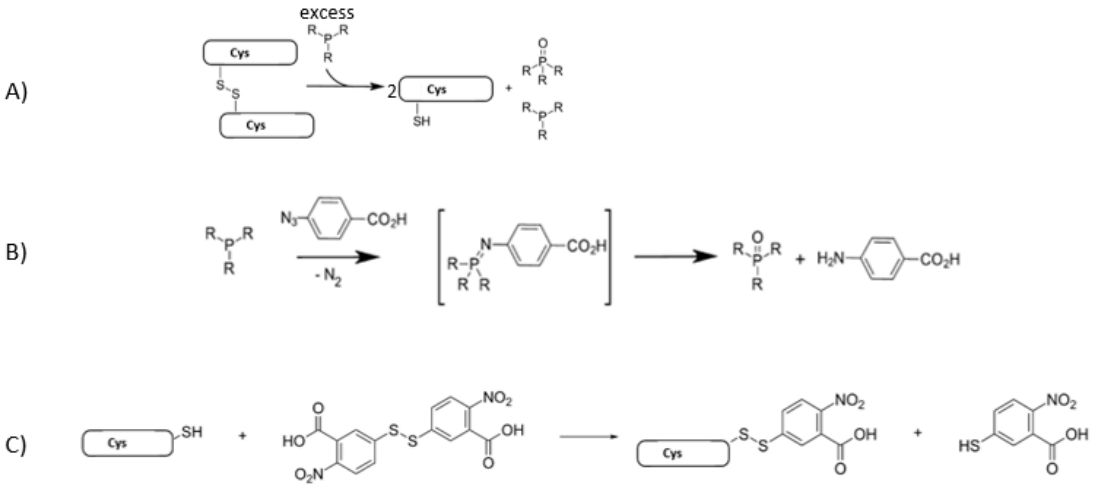

Figure 5.5: Illustration of the roles of chemicals involved in absorbance assay. A) Reduction of disulfides using TCEP B) Quenching excess TCEP by 4-ABA C) Detection of thiols with Ellman's reagent.

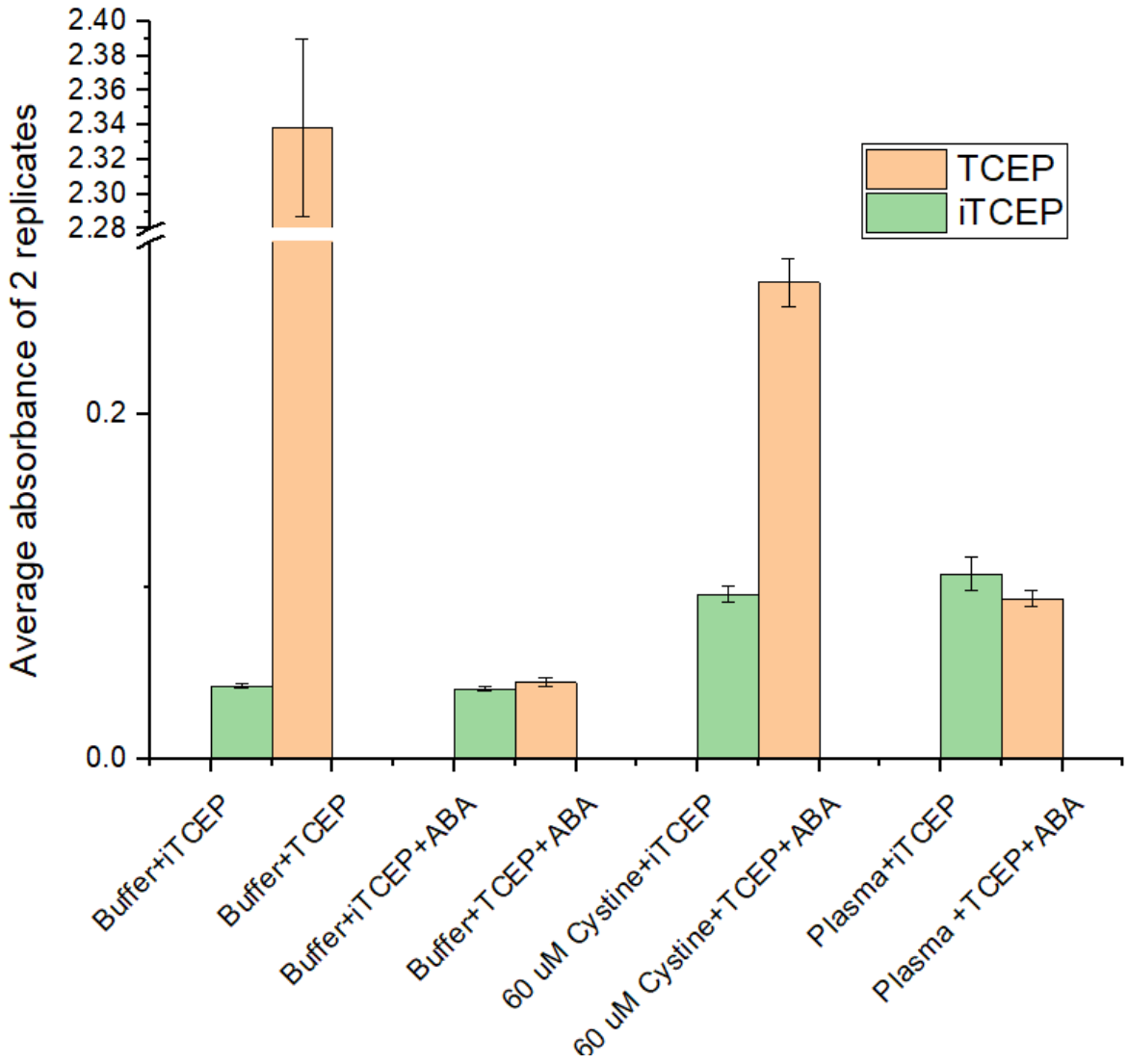

Figure 5.6: Comparison of iTCEP and TCEP methods. Error bars indicate standard deviation.

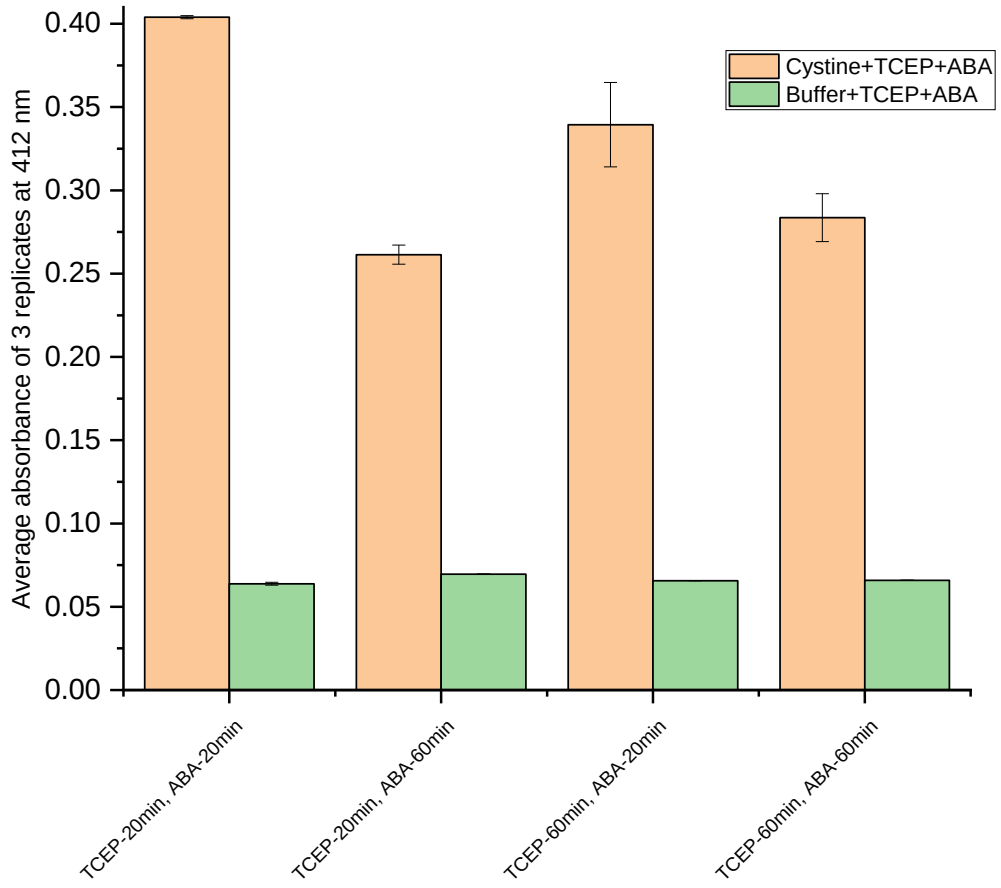

Figure 5.7: Effect of reaction times on absorbance checked with 60 µM cystine fortified buffer and unfortified blank buffer. Error bars indicate standard deviation

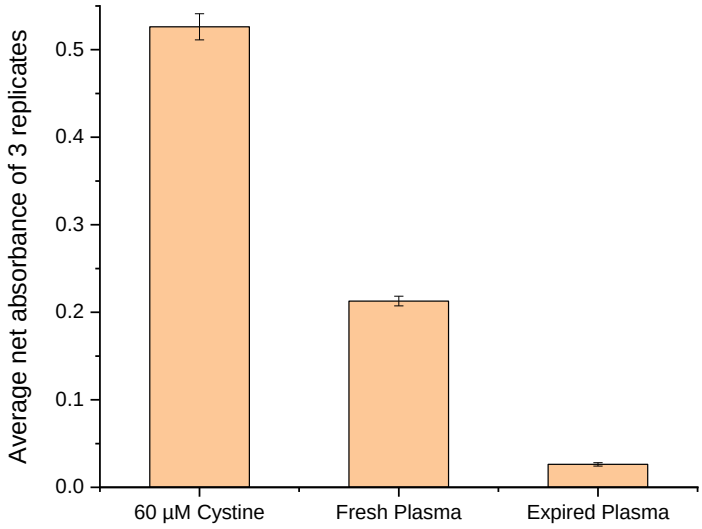

Figure 5.8: Comparison of average net absorbance (at 412 nm) of 23 µL buffer contains 60 µM cystine processed using the newly optimized protocol without the spin filter step and fresh plasma and expired plasma samples analyzed using the newly optimized protocol with buffers made with 18.2 MΩcm^{-1}resistivity deionized water in acid washed glass bottles. Error bars indicate standard deviation.

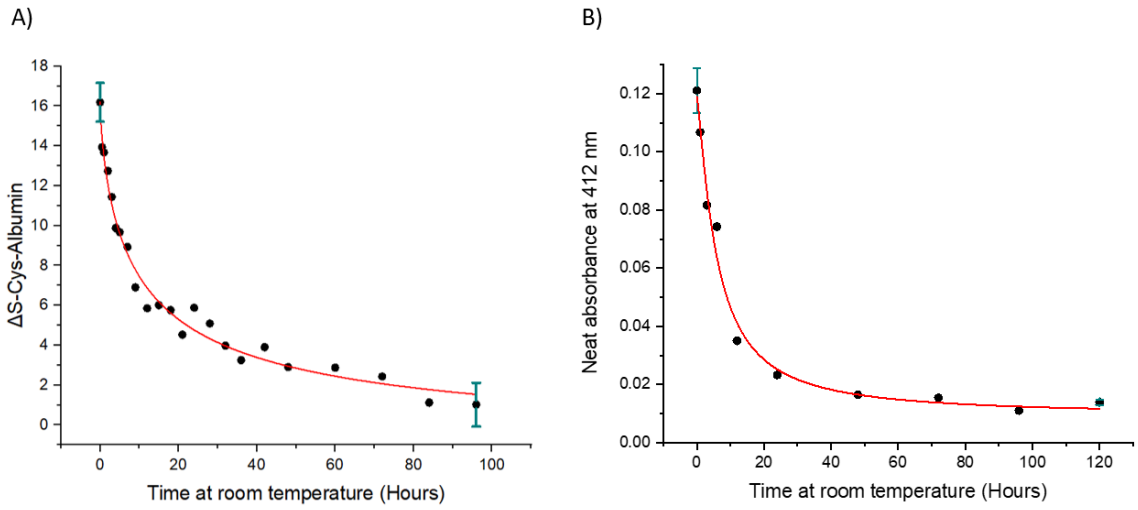

Figure 5.9: Analysis of plasma aliquots incubated for different times at room temperature by A) ΔS-Cys-Albumin assay and B) final optimized absorbance assay. Net absorbance was calculated by subtracting the absorbance of buffer blank from the absorbance of plasma samples. N=6 for first and last time points and n=1 for all other time points. Error bars indicate standard deviation.

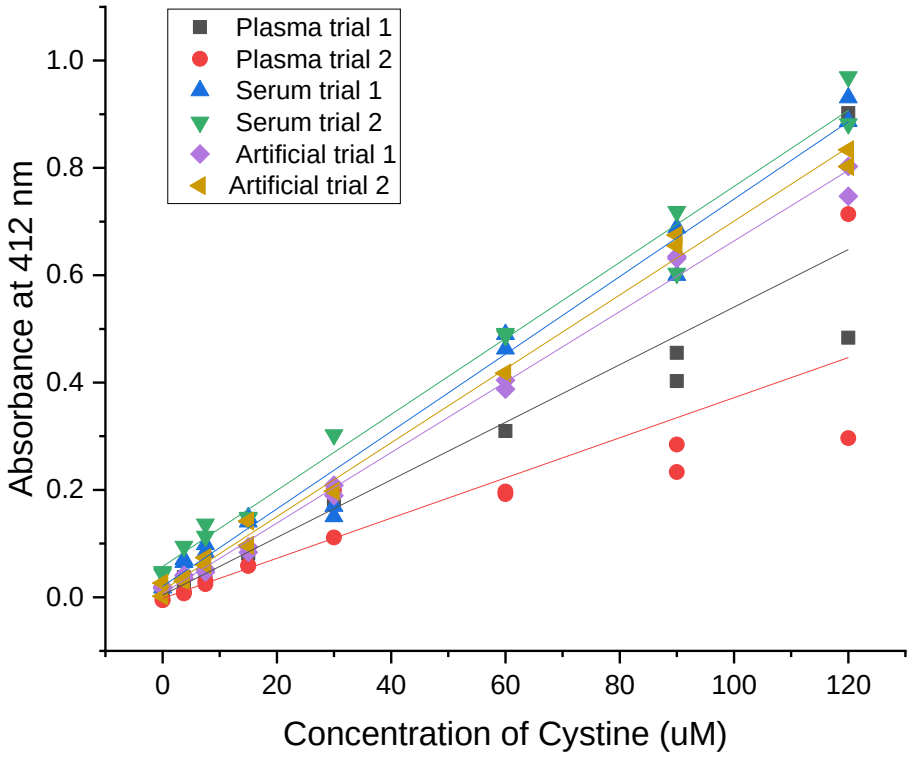

Figure 5.10: Standard curves created with different matrices for comparison of slopes to examine matrix effect. X-axis indicates the concentration of additional cystine concentration that was fortified into each sample (other SMT & D are also present in the ratio mentioned in section 5.2.4.). Net absorbance was calculated by subtracting the absorbance of buffer blank from each sample.

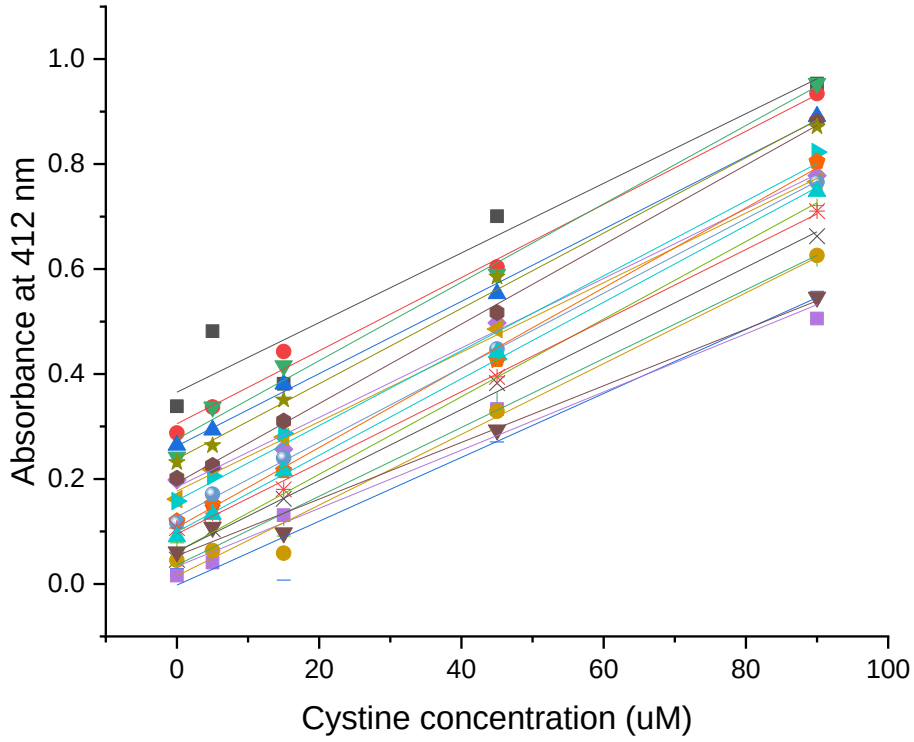

Figure 5.11: Standard curves created with different expired serum samples as matrices for comparison of slopes to examine matrix effect. X-axis indicates the concentration of additional cystine concentration that was fortified into each sample (other SMT & D are also present in the ratio mentioned in section 5.2.4.). Net absorbance was calculated by subtracting the absorbance of buffer blank from each sample.

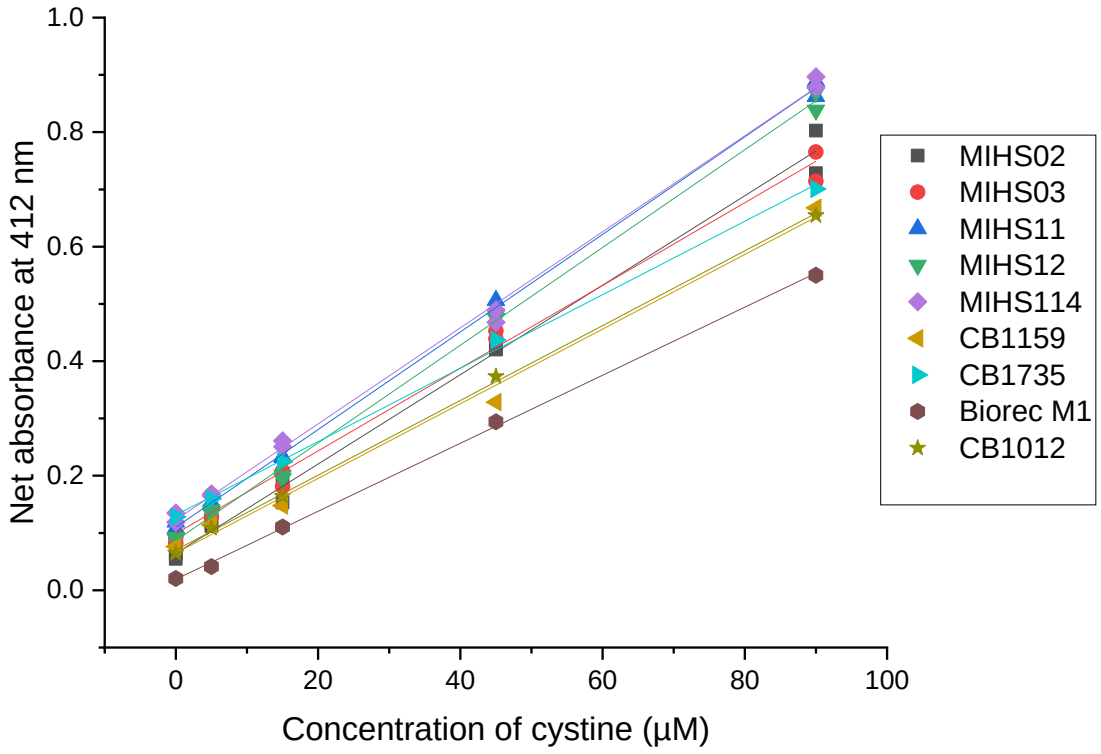

Figure 5.12: Standard curves created with different expired plasma samples as matrices for comparison of slopes to examine matrix effect. These samples werde diluted with 0.015 M HCl instead of water and resuspended in 0.4M PBS.EDTA. X-axis indicates the concentration of additional cystine concentration that was fortified into each sample (other SMT & D are also present in the ratio mentioned in section 5.2.4.). Net absorbance was calculated by subtracting the absorbance of buffer blank from each sample.

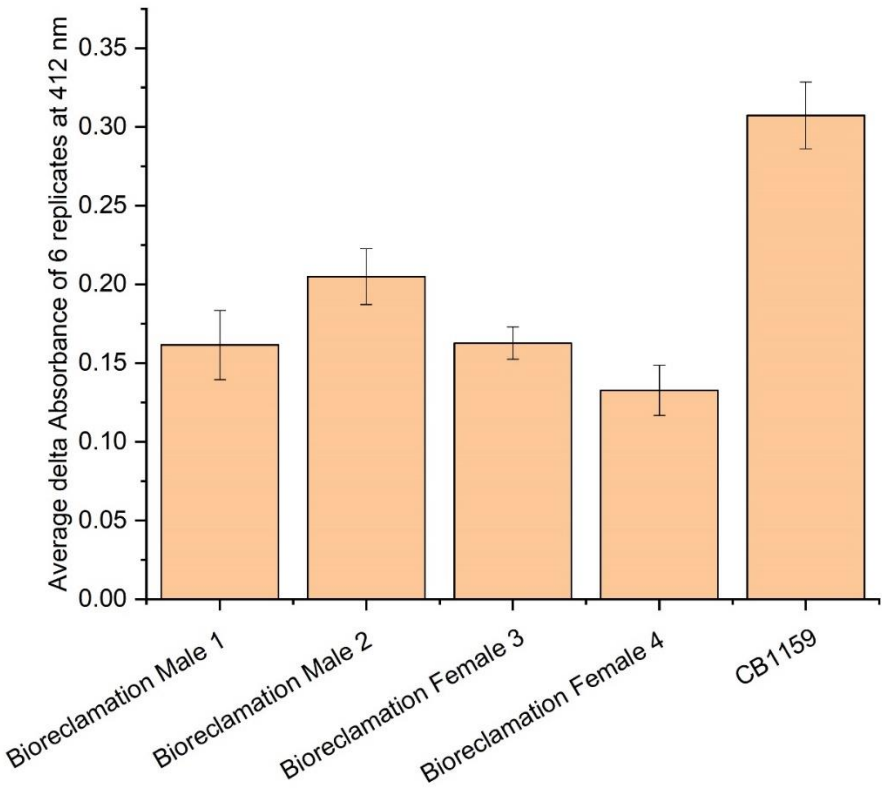

Figure 5.13: Delta absorbance measurements in different plasma samples. Error bars indicate standard deviation.

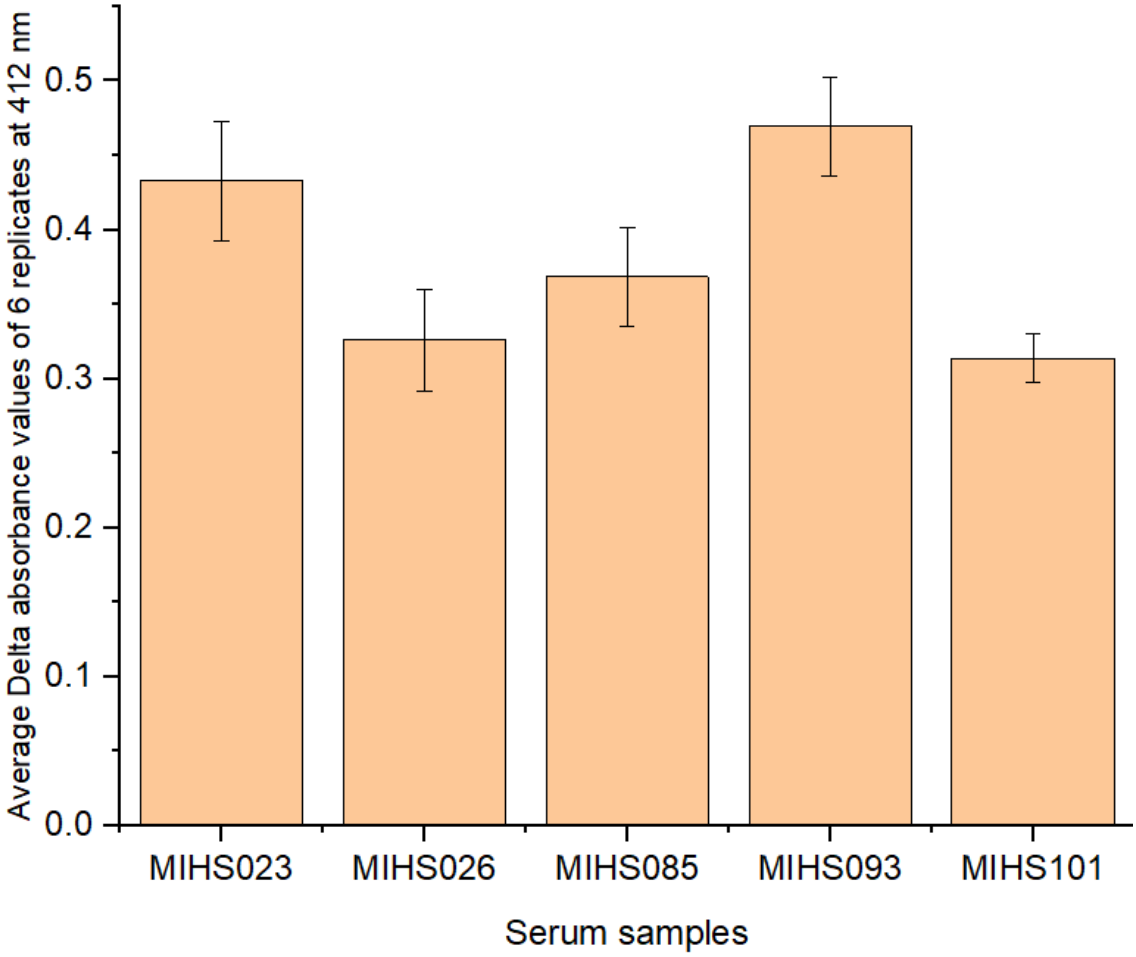

Figure 5.14: Delta absorbance measurements in different plasma samples. Error bars indicate standard deviation.

A)

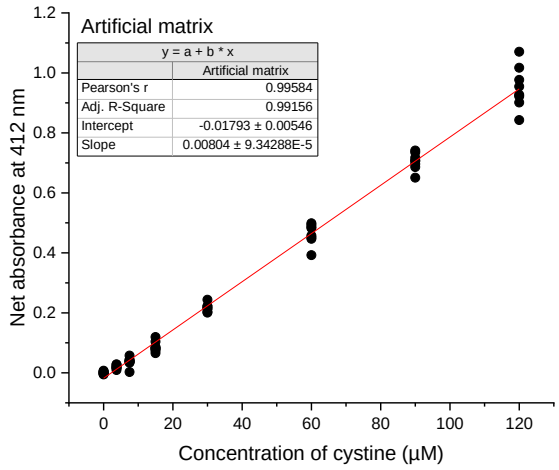

B)

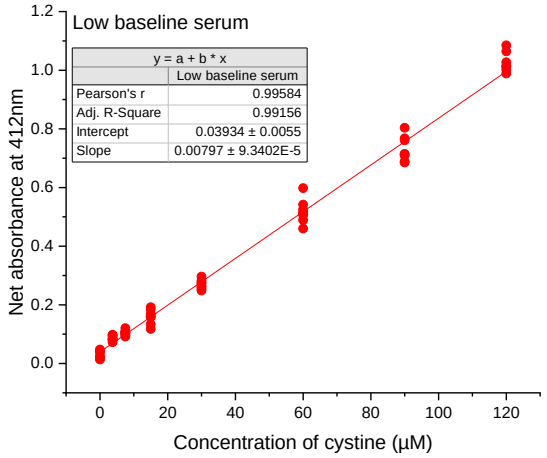

C)

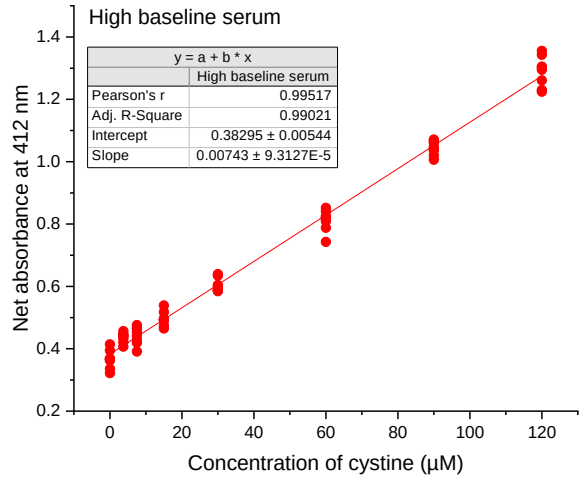

Figure 5.15: continued on next page

D)

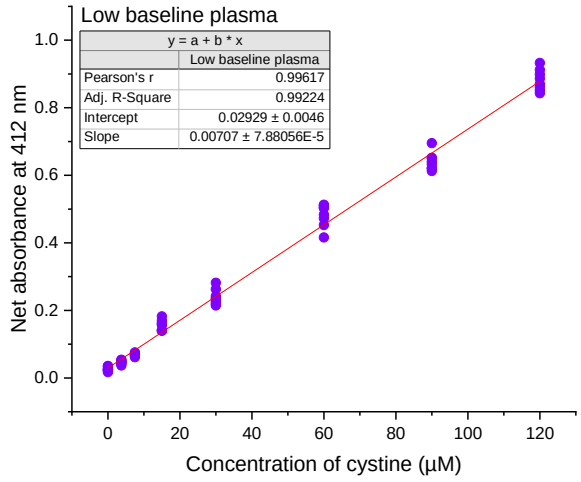

E)

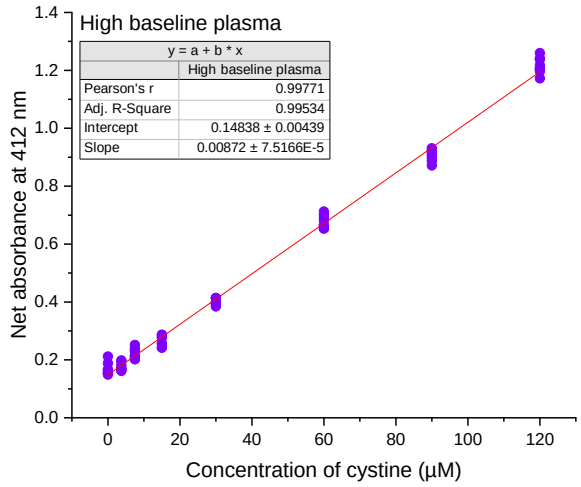

Figure 5.15: Standard curves created with different matrices. A) Artificial matrix B) Low baseline serum C) high baseline serum D) low baseline plasma E) high baseline plasma. All plasma and serum samples were incubated at 37 °C for 24 hours to drive the absorbance to baseline. Several 25 µL aliquots of each matrix were diluted with water (artificial matrix and serum) or 0.015M HCl (plasma) and spiked with different concentration of SMT & D solution. For each matrix standard curves were created on 4 different days (n=2 replicates at each concentration) and all the points are combined to create an average standard curve for each matrix. X-axis indicates the concentration of additional cystine concentration that was fortified into each sample (other SMT & D are also present in the ratio mentioned in section 5.2.4.). Net absorbance was calculated by subtracting the absorbance of buffer blank from each sample.

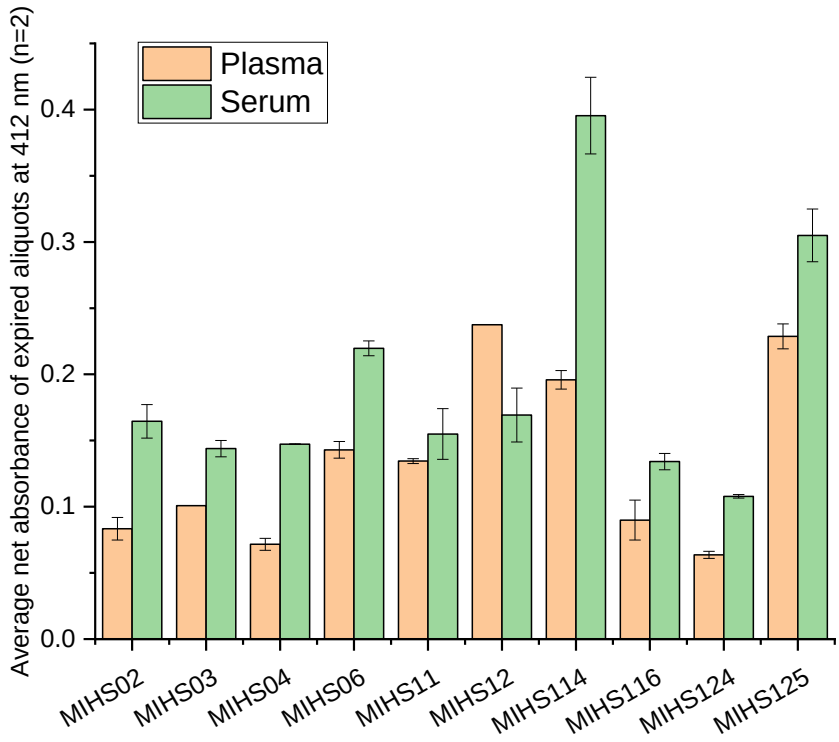

Figure 5.16: Net absorbance of expired aliquots of matched plasma and serum samples from 10 people which was used to select samples with high and low baseline absorbance to be employed in precision experiments. Each sample was measured in duplicates. Error bars indicate standard deviation

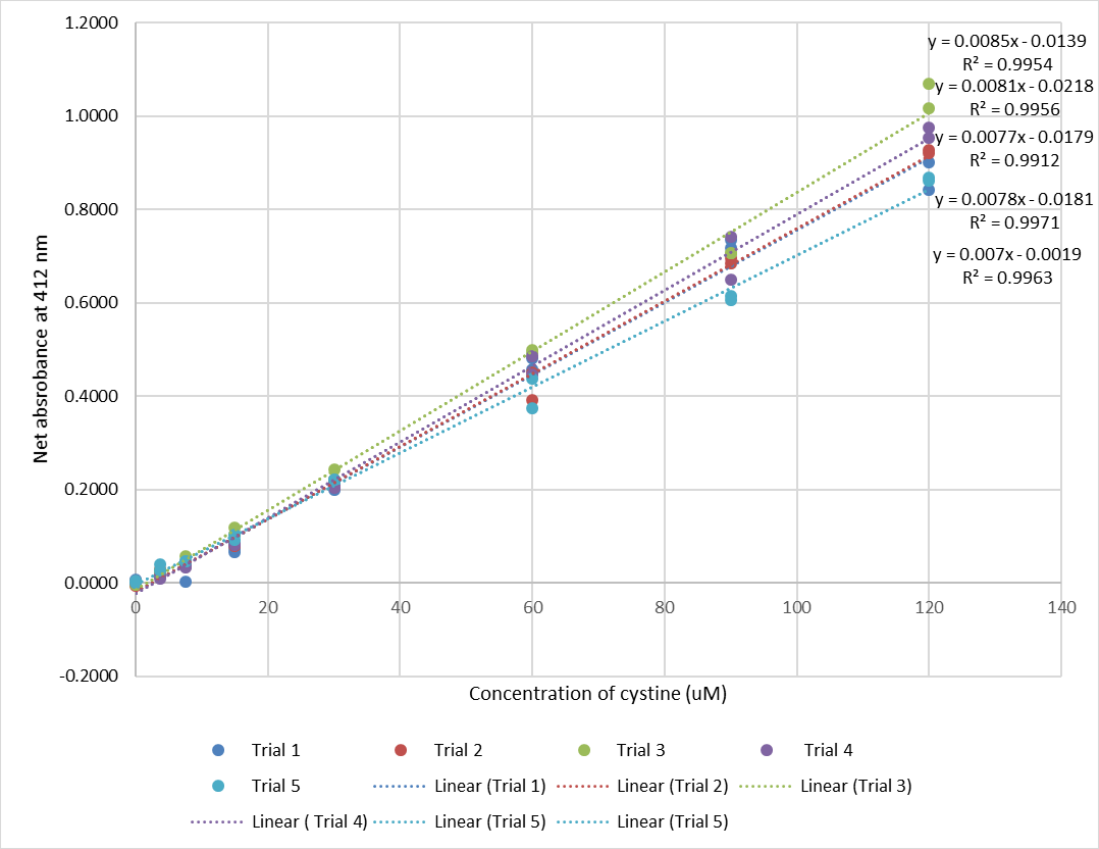

Figure 5.17: Standard curves created with artificial matrix. X-axis indicates the concentration of additional cystine concentration that was fortified into each sample (other SMT & D are also present in the ratio mentioned in section 5.2.4.). Net absorbance was calculated by subtracting the absorbance of buffer blank from each sample. 5 different curves were created on 5 different days by measuring each concentration in duplicates for each graph.

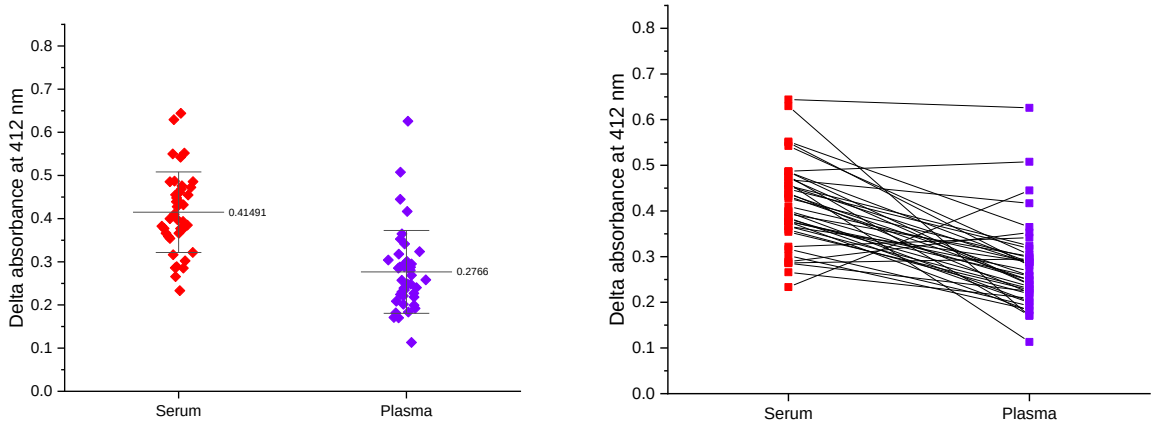

Figure 5.18: Delta absorbance values in matched plasma and serum samples during population range experiments. Error bars indicate standard deviation.

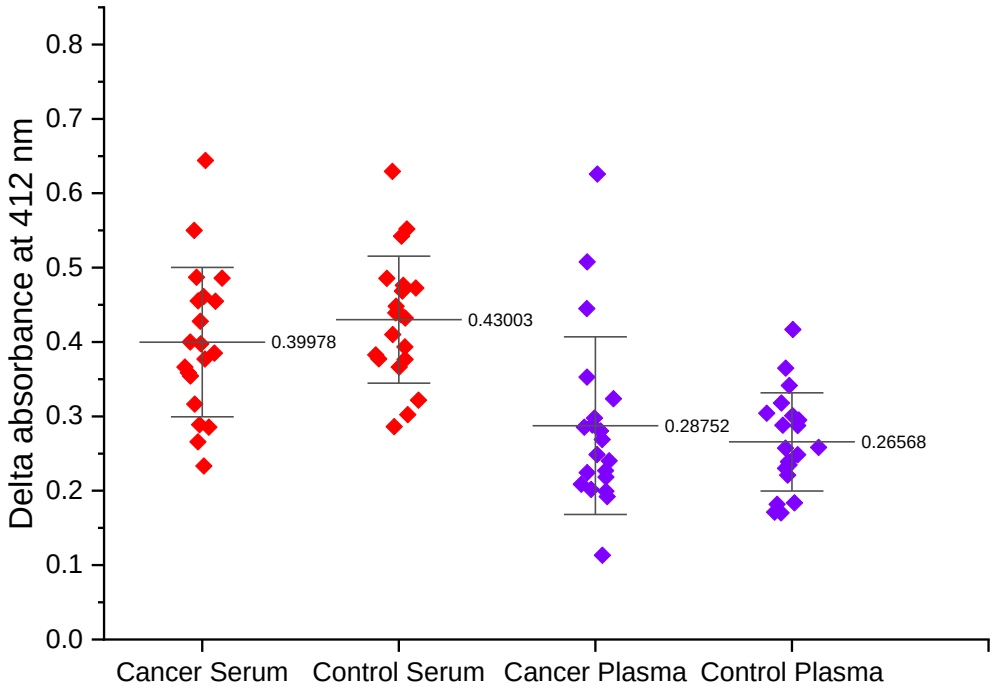

Figure 5.19: Delta absorbance values in healthy and cancer plasma and serum samples during population range experiments. Error bars indicate standard deviation.

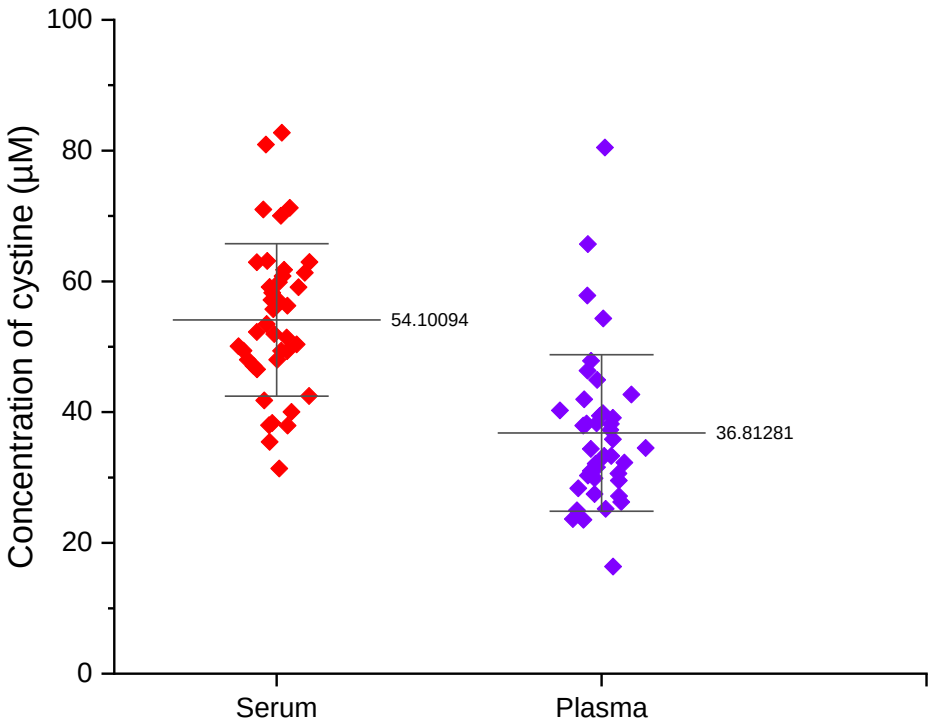

Figure 5.20: Calculation of the concentration of cystine by ES approach in plasma and serum samples. Error bars indicate standard deviation.

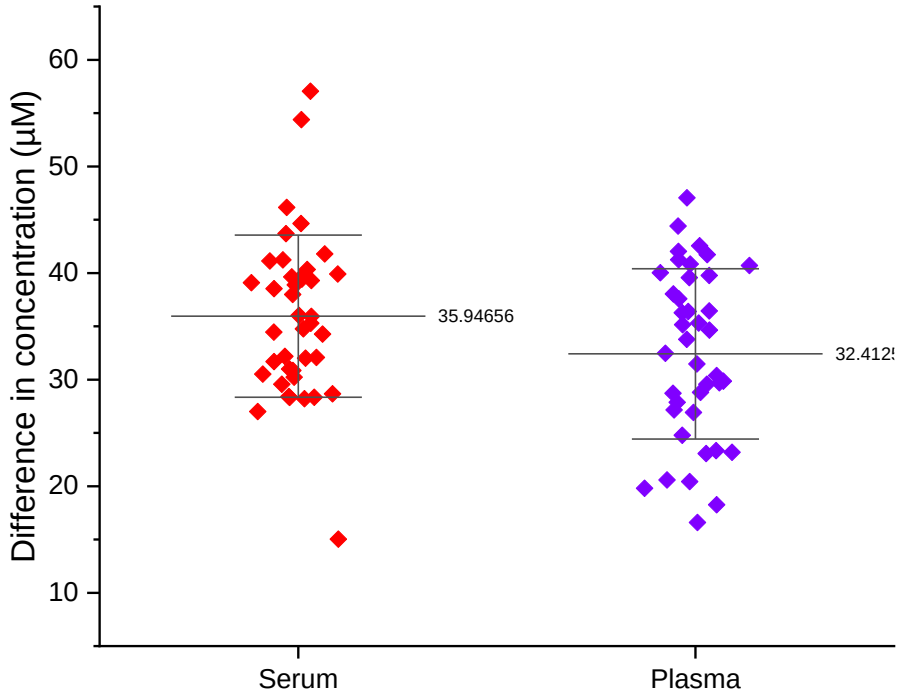

Figure 5.21: Calculation of the difference in concentration between 30 µM cystine (along with other SMT & Ds in the ratio mentioned in section 5.2.4) fortified aliquot and the fresh unfortified aliquot by ES approach. Error bars indicate standard deviation.

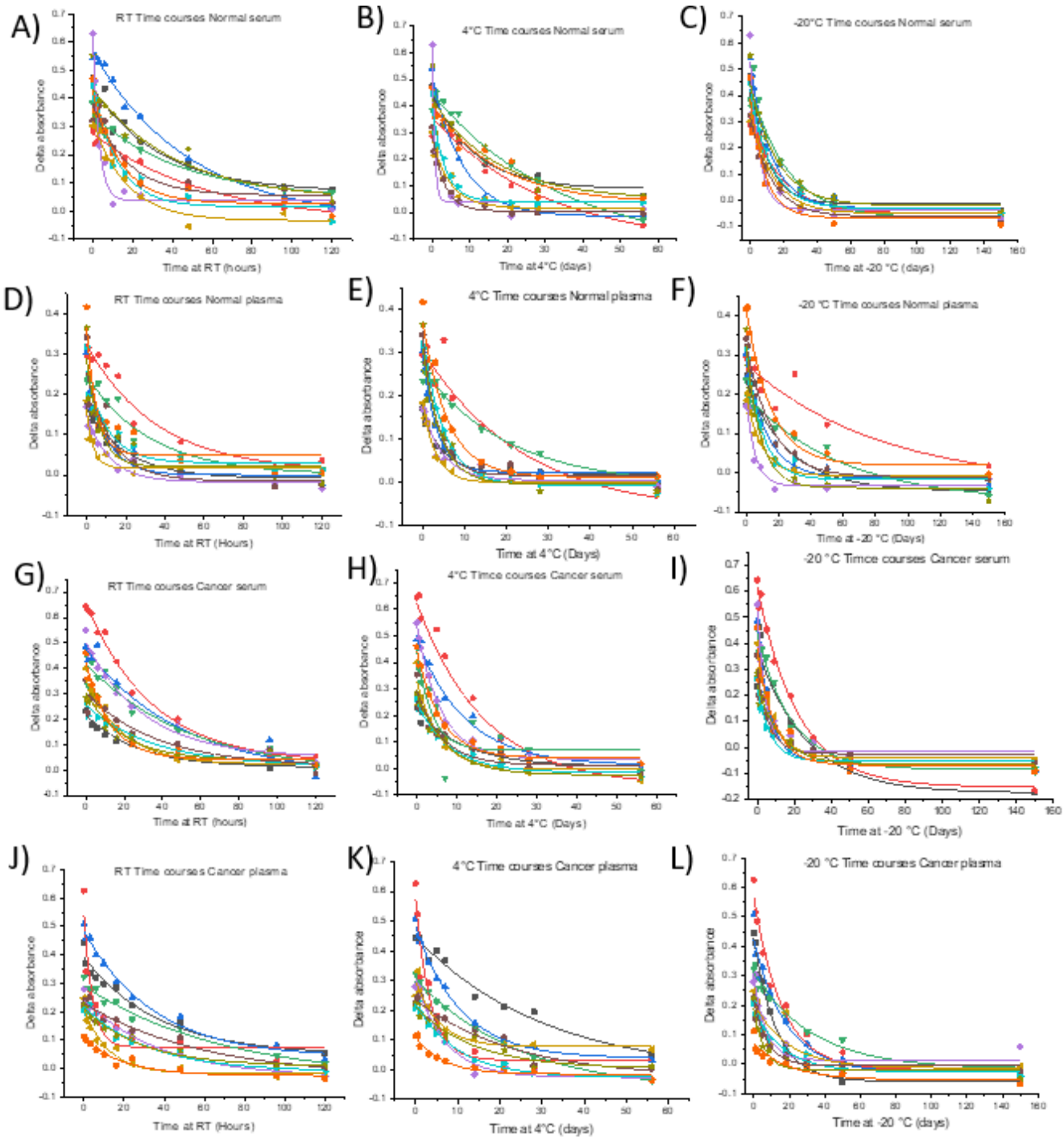

Figure 5.22: Change in delta absorbance values over a time course in normal serum (A) cancer serum (G), normal plasma (D), cancer plasma (J) at room temperature; normal serum (B) cancer serum (H), normal plasma (E), cancer plasma (K) at 4 °C and normal serum (C) cancer serum (I), normal plasma (F), cancer plasma (L) at -20 °C

Tables

Table 5.1: Intra and inter assay precision values for plasma and serum samples with high and low baselines at different concentration of fortified SMT & Ds.

Low baseline Serum				
	Intraday precision (%CV)			Interday precision (%CV)
Fortification (µM)	Day 1	Day 2	Day 3	
80	6	5	3	4
30	6	4	5	9
10	16	9	24	19
0	46	33	35	38
Low baseline Plasma				
	Intraday precision (%CV)			Interday precision (%CV)
Fortification (µM)	Day 1	Day 2	Day 3	
80	4	5	2	5
30	12	4	2	8
10	4	10	4	9
0	20	37	6	26
High baseline Serum				
	Intraday precision (%CV)			Interday precision (%CV)
Fortification (µM)	Day 1	Day 2	Day 3	
80	5	12	7	7
30	4	2	2	3
10	17	6	6	12
0	3	6	6	5
High baseline Plasma				
	Intraday precision (%CV)			Interday precision (%CV)
Fortification (µM)	Day 1	Day 2	Day 3	
80	5	2	2	11
30	3	2	5	6
10	6	5	6	8
0	9	12	8	11

Table 5.2: Analysis of accuracy by ES approach at different fortified concentrations of SMT & Ds into low and high baseline plasma and serum samples.

Low baseline Serum			
Fortification (µM)	Calculated concentration	Absolute error	% error
80	87.1	7.1	9
30	32.1	2.1	7
10	9.1	0.9	9
0	1.9	1.9	
Low baseline Plasma			
Fortification (µM)	Calculated concentration	Absolute error	% error
80	71.6	8.4	11
30	28.5	1.5	5
10	10.6	0.6	6
0	1.9	1.9	
High baseline Serum			
Fortification (µM)	Calculated concentration	Absolute error	% error
80	91.8	11.8	15
30	37.1	7.1	24
10	15.1	5.1	51
0	1.9	1.9	
High baseline Plasma			
Fortification (µM)	Calculated concentration	Absolute error	% error
80	73.8	6.2	8
30	30.3	0.4	1
10	15.6	5.6	56
0	1.9	1.9	

Table 5.3: Analysis of accuracy by MoSA approach at different fortified concentrations of SMT&Ds into low and high baseline plasma and serum samples. All values are average of 15 replicates of each sample at each concentration (n=5 replicates at each concentration repeated for 3 days). % errors were calculated based on the absolute concentrations determined using the standard curves of each matrix including all 3 fortification points.

A)

	Calculated concentration of cystine in pre-expired unfortified samples with standard curves of respective matrix using all three points (µM)
Sample	Fresh
Low baseline serum	5.1
Low baseline plasma	6.2
High baseline serum	21.8
High baseline plasma	28.0

B)

	Calculated concentration of cystine in pre-expired unfortified samples using single point addition method						
Sample	Absolute concentration	Using 10 µM	%error	Using 30 µM	%error	Using 80 µM	%error
Low baseline serum	5.1	10.1	97	7.2	42	6.8	34
Low baseline plasma	6.2	6.0	3	5.9	5	6.0	3
High baseline serum	21.8	17.6	19	19.7	9	20.6	5
High baseline plasma	28.0	16.1	42	23.3	17	24.6	12

C)

	Calculated concentration of cystine in 10 µM additional cystine fortified pre-expired samples using single point addition method				
Sample	Absolute concentration	using 30 µM	%error	using 80 µM	%error
Low baseline serum	15.1	12.7	16	13.0	14
Low baseline plasma	16.2	15.6	4	16.0	1
High baseline serum	31.8	33.1	4	33.2	4
High baseline plasma	38.0	48.5	28	43.0	13

D)

	Calculated concentration of cystine in 30 µM additional cystine fortified pre-expired samples using single point addition method		
Sample	Absolute concentration	80 µM	%error
Low baseline serum	35.1	34.0	3
Low baseline plasma	36.2	37.0	2
Highbaseline serum	51.8	53.4	3
High baseline plasma	58.0	58.1	0

CHAPTER 6

CONCLUSIONS AND FUTURE DIRECTIONS

In this report we have developed and validated two different assays to assess plasma and serum integrity. As demonstrated in Chapter 2 paper trails are always not enough to ensure the quality of the biospecimen especially when handling archived samples for research purposes. We have proved that the ΔS-Cys-Albumin assay we developed is effective in identifying different types of exposures to thawed conditions. Using a Luminex assay we have shown that several clinically relevant biomolecules lose their integrity upon exposure to room temperature, 4 °C and -20 °C for a prolonged period of time. An inverse linear relationship between the ΔS-Cys-Albumin value and the percentage of proteins that became unstable was observed supporting the possibility of using ΔS-Cys-Albumin as a surrogate marker to check plasma or serum integrity. We have also evaluated the stability of oxidized LDL in serum samples at room temperature, 4 °C and -20 °C using ΔS-Cys-Albumin as a positive control and the results showed that the oxidized LDL is stable at all the tested temperatures for the time frames evaluated.

Although the ΔS-Cys-Albumin assay is a useful marker to check plasma or serum integrity, it requires the use of an LC-MS instrument which limits the availability of this assay to most clinical research labs. Hence we have developed a plate reader-based absorbance assay which can be performed in a 384 well plate format in a common plate reader which is available in almost all clinical research labs. We have developed this assay and analytically validated it. We have determined the population range of delta absorbance values in control and cancer patient samples and documented the change in

delta absorbance over time at room temperature, 4 °C and -20 °C. This assay will be useful in assessing the integrity of individual and group serum samples, but the low range in plasma limits this assay from correctly identifying individual plasma samples. However, individual and group-based blind challenge experiments should be conducted to test its efficiency in correctly identifying exposed samples. Also, a different detection method with better sensitivity such as a fluorescence method should be employed to make sure that this assay would be useful in identifying individual plasma aliquots exposed to thawed conditions.

REFERENCES

1. Atkinson, A. J., Colburn, W. A., DeGruttola, V. G., DeMets, D. L., Downing, G. J., Hoth, D. F., Oates, J. A., Peck, C. C., Schooley, R. T., Spilker, B. A., Woodcock, J., and Zeger, S. L. (2001) Biomarkers and surrogate endpoints: Preferred definitions and conceptual framework. *Clin. Pharmacol. Ther.* 69, 89–95

2. Aronson, J. K., and Ferner, R. E. (2017) Biomarkers—A General Review. *Curr. Protoc. Pharmacol.* 76, 9.23.1-9.23.17

3. Genin, E., Hannequin, D., Wallon, D., Sleegers, K., Hiltunen, M., Combarros, O., Bullido, M. J., Engelborghs, S., De Deyn, P., Berr, C., Pasquier, F., Dubois, B., Tognoni, G., Fiévet, N., Brouwers, N., Bettens, K., Arosio, B., Coto, E., Del Zompo, M., Mateo, I., Epelbaum, J., Frank-Garcia, A., Helisalmi, S., Porcellini, E., Pilotto, A., Forti, P., Ferri, R., Scarpini, E., Siciliano, G., Solfrizzi, V., Sorbi, S., Spalletta, G., Valdivieso, F., Vepsäläinen, S., Alvarez, V., Bosco, P., Mancuso, M., Panza, F., Nacmias, B., Boss, P., Hanon, O., Piccardi, P., Annoni, G., Seripa, D., Galimberti, D., Licastro, F., Soininen, H., Dartigues, J. F., Kamboh, M. I., Van Broeckhoven, C., Lambert, J. C., Amouyel, P., and Campion, D. (2011) APOE and Alzheimer disease: A major gene with semi-dominant inheritance. *Mol. Psychiatry* 16, 903–907

4. Basu, N. N., Ingham, S., Hodson, J., Lalloo, F., Bulman, M., Howell, A., and Evans, D. G. (2015) Risk of contralateral breast cancer in BRCA1 and BRCA2 mutation carriers: a 30-year semi-prospective analysis. *Fam. Cancer* 14, 531–538

5. Wehling, M. (2021) in *Principles of Translational Science in Medicine* (Elsevier), pp 135–165.

6. Chung, W. H., Hung, S. I., Hong, H. S., Hsih, M. S., Yang, L. C., Ho, H. C., Wu, J. Y., and Chen, Y. T. (2004) A marker for Stevens-Johnson syndrome. *Nature* 428, 486

7. Biomarker Qualification: Evidentiary Framework Guidance for Industry and FDA Staff (Draft Guidance) (2018) (Rockville, MD)

8. Saah, A. J. (1997) “Sensitivity” and “Specificity” Reconsidered: The Meaning of These Terms in Analytical and Diagnostic Settings. *Ann. Intern. Med.* 126, 91

9. Micheel, C. M., and Ball, J. R. (2010) *Evaluation of Biomarkers and Surrogate Endpoints in Chronic Disease*

10. Shreffler, J., and Huecker, M. R. (2022) Diagnostic Testing Accuracy: Sensitivity, Specificity, Predictive Values and Likelihood Ratios. *StatPearls*,

11. Zhu, W., Zeng, N., and Wang, N. (2010) in *NESUG proceedings: health care and*

life sciences (Baltimore, Maryland), p 67.

12. Lim, M. D., Dickherber, A., and Compton, C. C. (2011) Before You Analyze a Human Specimen, Think Quality, Variability, and Bias. *Anal. Chem.* 83, 8–13

13. Xu, X., and Veenstra, T. D. (2008) Analysis of biofluids for biomarker research. *PROTEOMICS - Clin. Appl.* 2, 1403–1412

14. Tuck, M. K., Chan, D. W., Chia, D., Godwin, A. K., Grizzle, W. E., Krueger, K. E., Rom, W., Sanda, M., Sorbara, L., Stass, S., Wang, W., and Brenner, D. E. (2009) Standard Operating Procedures for Serum and Plasma Collection: Early Detection Research Network Consensus Statement Standard Operating Procedure Integration Working Group. *J. Proteome Res.* 8, 113–117

15. Ruiz-Godoy, L., Enríquez-Cárcamo, V., Suárez-Roa, L., Lopez-Castro, M. L., Santamaría, A., Orozco-Morales, M., and Colín-González, A. L. (2019) Identification of specific pre-analytical quality control markers in plasma and serum samples. *Anal. Methods* 11, 2259–2271

16. Luque-Garcia, J. L., and Neubert, T. A. (2007) Sample preparation for serum/plasma profiling and biomarker identification by mass spectrometry. *J. Chromatogr. A* 1153, 259–276

17. Mattsson-Carlgren, N., Palmqvist, S., Blennow, K., and Hansson, O. (2020) Increasing the reproducibility of fluid biomarker studies in neurodegenerative studies. *Nat. Commun. 2020 111* 11, 1–11

18. Voyle, N., Baker, D., Burnham, S. C., Covin, A., Zhang, Z., Sangurdekar, D. P., Tan Hehir, C. A., Bazenet, C., Lovestone, S., Kiddle, S., and Dobson, R. J. B. (2015) Blood Protein Markers of Neocortical Amyloid-β Burden: A Candidate Study Using SOMAscan Technology. *J. Alzheimer's Dis.* 46, 947–961

19. Begley, C. G., and Ellis, L. M. (2012) Raise standards for preclinical cancer research. *Nature* 483, 531–533

20. Prinz, F., Schlange, T., and Asadullah, K. (2011) Believe it or not: how much can we rely on published data on potential drug targets? *Nat. Rev. Drug Discov.* 10, 712–712

21. Garrison, L. P., Babigumira, J. B., Masaquel, A., Wang, B. C. M., Lalla, D., and Brammer, M. (2015) The Lifetime Economic Burden of Inaccurate HER2 Testing: Estimating the Costs of False-Positive and False-Negative HER2 Test Results in US Patients with Early-Stage Breast Cancer. *Value Health* 18, 541–546

22. Kong, F. M. S., Zhao, L., Wang, L., Chen, Y., Hu, J., Fu, X., Bai, C., Wang, L., Lawrence, T. S., Anscher, M. S., Dicker, A., and Okunieff, P. (2017) Ensuring sample quality for blood biomarker studies in clinical trials: a multicenter

international study for plasma and serum sample preparation. *Transl. Lung Cancer Res.* 6, 625

23. Moyer, V. A. (2012) Screening for prostate cancer: U.S. preventive services task force recommendation statement. *Ann. Intern. Med.* 157, 120–134

24. Hemingway, H., Philipson, P., Chen, R., Fitzpatrick, N. K., Damant, J., Shipley, M., Abrams, K. R., Moreno, S., McAllister, K. S. L., Palmer, S., Kaski, J. C., Timmis, A. D., and Hingorani, A. D. (2010) Evaluating the Quality of Research into a Single Prognostic Biomarker: A Systematic Review and Meta-analysis of 83 Studies of C-Reactive Protein in Stable Coronary Artery Disease. *PLOS Med.* 7, e1000286

25. Janssens, A. C. J. W., Gwinn, M., Bradley, L. A., Oostra, B. A., van Duijn, C. M., and Khoury, M. J. (2008) A Critical Appraisal of the Scientific Basis of Commercial Genomic Profiles Used to Assess Health Risks and Personalize Health Interventions. *Am. J. Hum. Genet.* 82, 593–599

26. Poste, G., Compton, C. C., and Barker, A. D. (2015) The national biomarker development alliance: confronting the poor productivity of biomarker research and development. *Expert Rev. Mol. Diagn.* 15, 211–218

27. Ikeda, K., Ichihara, K., Hashiguchi, T., Hidaka, Y., Kang, D., Maekawa, M., Matsumoto, H., Matsushita, K., Okubo, S., Tsuchiya, T., and Furuta, K. (2015) Evaluation of the Short-Term Stability of Specimens for Clinical Laboratory Testing. *Biopreserv. Biobank.* 13, 135–143

28. Lippi, G., Chance, J. J., Church, S., Dazzi, P., Fontana, R., Giavarina, D., Grankvist, K., Huisman, W., Kouri, T., Palicka, V., Plebani, M., Puro, V., Salvagno, G. L., Sandberg, S., Sikaris, K., Watson, I., Stankovic, A. K., and Simundic, A. M. (2011) Preanalytical quality improvement: From dream to reality. *Clin. Chem. Lab. Med.* 49, 1113–1126

29. Moore, H. M., Kelly, A., Jewell, S. D., McShane, L. M., Clark, D. P., Greenspan, R., Hainaut, P., Hayes, D. F., Kim, P., Mansfield, E., Potapova, O., Riegman, P., Rubinstein, Y., Seijo, E., Somiari, S., Watson, P., Weier, H. U., Zhu, C., and Vaught, J. (2011) Biospecimen Reporting for Improved Study Quality. *Biopreserv. Biobank.* 9, 57

30. Moore, H. M., Compton, C. C., Alper, J., and Vaught, J. B. (2011) International approaches to advancing biospecimen science. *Cancer Epidemiol. Biomarkers Prev.* 20, 729–732

31. Betsou, F., Barnes, R., Burke, T., Coppola, D., DeSouza, Y., Eliason, J., Glazer, B., Horsfall, D., Kleeberger, C., Lehmann, S., Prasad, A., Skubitz, A., Somiari, S., and Gunter, E. (2009) Human Biospecimen Research: Experimental Protocol and Quality Control Tools. *Cancer Epidemiol. Biomarkers Prev.* 18, 1017–1025

32. Robb, J. A., Moore, H. M., and Compton, C. C. (2008) Documenting Biospecimen Conditions in Reports of Studies. *JAMA* 300, 650–651

33. Compton, C. (2007) Getting to personalized cancer medicine: taking out the garbage. *Cancer* 110, 1641–1643

34. Borges, C. R., Rehder, D. S., Jensen, S., Schaab, M. R., Sherma, N. D., Yassine, H., Nikolova, B., and Breburda, C. (2014) Elevated Plasma Albumin and Apolipoprotein A-I Oxidation under Suboptimal Specimen Storage Conditions. *Mol. Cell. Proteomics* 13, 1890–1899

35. Engel, K. B., Vaught, J., and Moore, H. M. (2014) National Cancer Institute Biospecimen Evidence-Based Practices: A Novel Approach to Pre-analytical Standardization. *Biopreserv. Biobank.* 12, 148–150

36. Rifai, N., Annesley, T. M., Berg, J. P., Brugnara, C., Delvin, E., Lamb, E. J., Ness, P. M., Plebani, M., Wick, M. R., Wu, A., and Delanghe, J. (2012) An appeal to medical journal editors: The need for a full description of laboratory methods and specimen handling in clinical study reports. *Clin. Chem. Lab. Med.* 50, 411–413

37. Rifai, N., Annesley, T. M., Berg, J. P., Brugnara, C., Delvin, E., Lamb, E. J., Ness, P. M., Plebani, M., Wick, M. R., and Wu, A. (2012) An appeal to medical journal editors: the need for a full description of laboratory methods and specimen handling in clinical study reports. *Transfusion* 52, e17–e19

38. Rifai, N., Annesley, T. M., Berg, J. P., Brugnara, C., Delvin, E., Lamb, E. J., Ness, P. M., Plebani, M., Wick, M. R., Wu, A., and Delanghe, J. (2012) An Appeal to Medical Journal Editors: The Need for a Full Description of Laboratory Methods and Specimen Handling in Clinical Study Reports. *Clin. Chem.* 58, 483–485

39. Rifai, N., Annesley, T. M., Berg, J. P., Brugnara, C., Delvin, E., Lamb, E. J., Ness, P. M., Plebani, M., Wick, M. R., Wu, A., and Delanghe, J. (2012) An appeal to medical journal editors: the need for a full description of laboratory methods and specimen handling in clinical study reports. *Am. J. Hematol.* 87, 347–348

40. Rifai, N., Annesley, T. M., Berg, J. P., Brugnara, C., Delvin, E., Lamb, E. J., Ness, P. M., Plebani, M., Wick, M. R., Wu, A., and Delanghe, J. (2012) An Appeal to Medical Journal Editors: The Need for a Full Description of Laboratory Methods and Specimen Handling in Clinical Study Reports. *Scand. J. Clin. Lab. Invest.* 72, 89–91

41. Rifai, N., Annesley, T. M., Berg, J. P., Brugnara, C., Delvin, E., Lamb, E. J., Ness, P. M., Plebani, M., Wick, M. R., Wu, A., and Delanghe, J. (2012) An appeal to medical journal editors: the need for a full description of laboratory methods and specimen handling in clinical study reports. Statement by the Consortium of Laboratory Medicine Journal Editors. *Ann. Clin. Biochem. Int. J. Lab. Med.* 49, 105–107

42. Rifai, N., Annesley, T. M., Berg, J. P., Brugnara, C., Delvin, E., Lamb, E. J., Ness, P. M., Plebani, M., Wick, M. R., Wu, A., and Delanghe, J. (2012) An appeal to medical journal editors: The need for a full description of laboratory methods and specimen handling in clinical study reports. *Clin. Chim. Acta* 413, 653–655

43. Rifai, N., Annesley, T. M., Berg, J. P., Brugnara, C., Delvin, E., Lamb, E. J., Ness, P. M., Plebani, M., Wick, M. R., Wu, A., and Delanghe, J. (2012) An appeal to medical journal editors: The need for a full description of laboratory methods and specimen handling in clinical study reports. *Clin. Biochem.* 45, 185–186

44. Compton, C. C., Robb, J. A., Anderson, M. W., Berry, A. B., Birdsong, G. G., Bloom, K. J., Branton, P. A., Crothers, J. W., Cushman-Vokoun, A. M., Hicks, D. G., Khoury, J. D., Laser, J., Marshall, C. B., Misialek, M. J., Natale, K. E., Nowak, J. A., Olson, D., Pfeifer, J. D., Schade, A., Vance, G. H., Walk, E. E., and Yohe, S. L. (2019) Preanalytics and precision pathology: Pathology practices to ensure molecular integrity of cancer patient biospecimens for precision medicine. *Arch. Pathol. Lab. Med.* 143, 1346–1363

45. Lippi, G., von Meyer, A., Cadamuro, J., and Simundic, A.-M. (2019) Blood sample quality. *Diagnosis* 6, 25–31

46. Bais, R., and Edwards, J. B. (1980) Increased creatine kinase activities associated with haemolysis. *Pathology* 12, 203–207

47. Timms, J. F., Arslan-Low, E., Gentry-Maharaj, A., Luo, Z., T'Jampens, D., Podust, V. N., Ford, J., Fung, E. T., Gammerman, A., Jacobs, I., and Menon, U. (2007) Preanalytic Influence of Sample Handling on SELDI-TOF Serum Protein Profiles. *Clin. Chem.* 53, 645–656

48. de Gramont, A., Watson, S., Ellis, L. M., Rodón, J., Tabernero, J., de Gramont, A., and Hamilton, S. R. (2015) Pragmatic issues in biomarker evaluation for targeted therapies in cancer. *Nat. Rev. Clin. Oncol.* 12, 197–212

49. Kang, H. J., Jeon, S. Y., Park, J. S., Yun, J. Y., Kil, H. N., Hong, W. K., Lee, M. H., Kim, J. W., Jeon, J. P., and Han, B. G. (2013) Identification of clinical biomarkers for pre-analytical quality control of blood samples. *Biopreserv. Biobank.* 11, 94–100

50. Bravo, M. I., Grancha, S., and Jorquera, J. I. (2006) Effect of temperature on plasma freezing under industrial conditions. *Pharmeur. Sci. Notes* 2006, 31–5

51. McIntosh, R. V., Dickson, A. J., Smith, D., and Foster, P. R. (1990) in *Cryopreservation and low temperature biology in blood transfusion* (Springer US, Boston, MA), pp 11–24.

52. Irani, D. N., Anderson, C., Gundry, R., Cotter, R., Moore, S., Kerr, D. A., McArthur, J. C., Sacktor, N., Pardo, C. A., Jones, M., Calabresi, P. A., and Nath,

A. (2006) Cleavage of cystatin C in the cerebrospinal fluid of patients with multiple sclerosis. *Ann. Neurol.* 59, 237–247

53. Carrette, O., Burkhard, P. R., Hughes, S., Hochstrasser, D. F., and Sanchez, J.-C. (2005) Truncated cystatin C in cerebrospiral fluid: Technical artefact or biological process? *Proteomics* 5, 3060–3065

54. Ocké, M. C., Schrijver, J., Obermann-De Boer, G. L., Bloemberg, B. P. M., Haenen, G. R. M. M., and Kromhout, D. (1995) Stability of blood (pro)vitamins during four years of storage at −20 °C: Consequences for epidemiologic research. *J. Clin. Epidemiol.* 48, 1077–1085

55. Gunter, E. W., Driskell, W. J., and Yeager, P. R. (1988) Stability of vitamin E in long-term stored serum. *Clin. Chim. Acta* 175, 329–335

56. Barden, A. E. E., Mas, E., Croft, K. D. D., Phillips, M., and Mori, T. A. A. (2014) Minimizing artifactual elevation of lipid peroxidation products (F2-isoprostanes) in plasma during collection and storage. *Anal. Biochem.* 449, 129–131

57. Boomsma, F., Alberts, G., van Eijk, L., Man in 't Veld, A. J., and Schalekamp, M. A. (1993) Optimal collection and storage conditions for catecholamine measurements in human plasma and urine. *Clin. Chem.* 39, 2503–8

58. Sourvinou, I. S., Markou, A., and Lianidou, E. S. (2013) Quantification of circulating miRNAs in plasma: Effect of preanalytical and analytical parameters on their isolation and stability. *J. Mol. Diagnostics* 15, 827–834

59. Chalmers, D., Nicol, D., Kaye, J., Bell, J., Campbell, A. V., Ho, C. W. L., Kato, K., Minari, J., Ho, C.-H., Mitchell, C., Molnár-Gábor, F., Otlowski, M., Thiel, D., Fullerton, S. M., and Whitton, T. (2016) Has the biobank bubble burst? Withstanding the challenges for sustainable biobanking in the digital era. *BMC Med. Ethics* 17, 39

60. Henderson, G. E., Cadigan, R. J., Edwards, T. P., Conlon, I., Nelson, A. G., Evans, J. P., Davis, A. M., Zimmer, C., and Weiner, B. J. (2013) Characterizing biobank organizations in the U.S.: Results from a national survey. *Genome Med.* 5, 1–12

61. Simeon-Dubach, D., Zeisberger, S. M., and Hoerstrup, S. P. (2016) Quality Assurance in Biobanking for Pre-Clinical Research. *Transfus. Med. Hemotherapy* 43, 353

62. Vaught, J., Rogers, J., Myers, K., Lim, M. D., Lockhart, N., Moore, H., Sawyer, S., Furman, J. L., and Compton, C. (2011) An NCI perspective on creating sustainable biospecimen resources. *J. Natl. Cancer Inst. Monogr.* 2011, 1–7

63. Hughes, S. E., Barnes, R. O., and Watson, P. H. (2010) Biospecimen use in cancer research over two decades. *Biopreserv. Biobank.* 8, 89–97

64. Jeffs, J. W., Jehanathan, N., Thibert, S. M. F., Ferdosi, S., Pham, L., Wilson, Z. T., Breburda, C., and Borges, C. R. (2019) Delta-S-Cys-Albumin: A Lab Test that Quantifies Cumulative Exposure of Archived Human Blood Plasma and Serum Samples to Thawed Conditions*[S]. *Mol. Cell. Proteomics* 18, 2121–2137

65. Hu, Y., Mulot, C., Bourreau, C., Martin, D., Laurent-Puig, P., Radoï, L., Guénel, P., and Borges, C. R. (2020) Biochemically Tracked Variability of Blood Plasma Thawed-State Exposure Times in a Multisite Collection Study. *Biopreserv. Biobank.* 18, 376–388

66. Labaer, J. (2012) Improving international research with clinical specimens: 5 achievable objectives. *J. Proteome Res.* 11, 5592–5601

67. Chaigneau, C., Cabioch, T., Beaumont, K., and Betsou, F. (2007) Serum biobank certification and the establishment of quality controls for biological fluids: examples of serum biomarker stability after temperature variation. *Clin. Chem. Lab. Med.* 45, 1390–1395

68. Betsou, F., Gunter, E., Clements, J., DeSouza, Y., Goddard, K. A. B., Guadagni, F., Yan, W., Skubitz, A., Somiari, S., Yeadon, T., and Chuaqui, R. (2013) Identification of Evidence-Based Biospecimen Quality-Control Tools: A Report of the International Society for Biological and Environmental Repositories (ISBER) Biospecimen Science Working Group. *J. Mol. Diagnostics* 15, 3–16

69. Lengellé, J., Panopoulos, E., and Betsou, F. (2008) Soluble CD40 ligand as a biomarker for storage-related preanalytic variations of human serum. *Cytokine* 44, 275–282

70. Otagiri, M., and Giam Chuang, V. T. (2016) *Albumin in Medicine* eds Otagiri M, Chuang VTG (Springer Singapore, Singapore)

71. Fanali, G., di Masi, A., Trezza, V., Marino, M., Fasano, M., and Ascenzi, P. (2012) Human serum albumin: From bench to bedside. *Mol. Aspects Med.* 33, 209–290

72. Daniels, J. R., Cao, Z., Maisha, M., Schnackenberg, L. K., Sun, J., Pence, L., Schmitt, T. C., Kamlage, B., Rogstad, S., Beger, R. D., and Yu, L. R. (2019) Stability of the Human Plasma Proteome to Pre-analytical Variability as Assessed by an Aptamer-Based Approach. *J. Proteome Res.* 18, 3661–3670

73. Cao, Z., Kamlage, B., Wagner-Golbs, A., Maisha, M., Sun, J., Schnackenberg, L. K., Pence, L., Schmitt, T. C., Daniels, J. R., Rogstad, S., Beger, R. D., and Yu, L. R. (2019) An Integrated Analysis of Metabolites, Peptides, and Inflammation Biomarkers for Assessment of Preanalytical Variability of Human Plasma. *J. Proteome Res.* 18, 2411–2421

74. Foster, M. W., Forrester, M. T., and Stamler, J. S. (2009) A protein microarray-

based analysis of S-nitrosylation. *Proc. Natl. Acad. Sci. U. S. A.* 106, 18948–18953

75. Kapuruge, E. P., Jehanathan, N., Rogers, S. P., Williams, S., Chung, Y., and Borges, C. R. (2022) Tracking the Stability of Clinically Relevant Blood Plasma Proteins with Delta-S-Cys-Albumin—a Dilute-and-Shoot LC/MS Based Marker of Specimen Exposure to Thawed Conditions. *Mol. Cell. Proteomics*, 100420

76. Oddoze, C., Lombard, E., and Portugal, H. (2012) Stability study of 81 analytes in human whole blood, in serum and in plasma. *Clin. Biochem.* 45, 464–469

77. Kamlage, B., Maldonado, S. G., Bethan, B., Peter, E., Schmitz, O., Liebenberg, V., and Schatz, P. (2014) Quality Markers Addressing Preanalytical Variations of Blood and Plasma Processing Identified by Broad and Targeted Metabolite Profiling. *Clin. Chem.* 60, 399–412

78. Anton, G., Wilson, R., Yu, Z. H., Prehn, C., Zukunft, S., Adamski, J., Heier, M., Meisinger, C., Römisch-Margl, W., Wang-Sattler, R., Hveem, K., Wolfenbuttel, B., Peters, A., Kastenmüller, G., and Waldenberger, M. (2015) Pre-analytical sample quality: metabolite ratios as an intrinsic marker for prolonged room temperature exposure of serum samples. *PLoS One* 10, e0121495–e0121495

79. Kamlage, B., Neuber, S., Bethan, B., Maldonado, S. G., Wagner-Golbs, A., Peter, E., Schmitz, O., and Schatz, P. (2018) Impact of Prolonged Blood Incubation and Extended Serum Storage at Room Temperature on the Human Serum Metabolome. *Metabolites* 8,

80. McLerran, D., Grizzle, W. E., Feng, Z., Bigbee, W. L., Banez, L. L., Cazares, L. H., Chan, D. W., Diaz, J., Izbicka, E., Kagan, J., Malehorn, D. E., Malik, G., Oelschlager, D., Partin, A., Randolph, T., Rosenzweig, N., Srivastava, S., Srivastava, S., Thompson, I. M., Thornquist, M., Troyer, D., Yasui, Y., Zhang, Z., Zhu, L., and Semmes, O. J. (2008) Analytical validation of serum proteomic profiling for diagnosis of prostate cancer: sources of sample bias. *Clin. Chem.* 54, 44–52

81. Ransohoff, D. F., and Gourlay, M. L. (2010) Sources of bias in specimens for research about molecular markers for cancer. *J. Clin. Oncol.* 28, 698–704

82. Tsuchida, S., Satoh, M., Umemura, H., Sogawa, K., Takiwaki, M., Ishige, T., Miyabayashi, Y., Iwasawa, Y., Kobayashi, S., Beppu, M., Nishimura, M., Kodera, Y., Matsushita, K., and Nomura, F. (2018) Assessment by Matrix-Assisted Laser Desorption/Ionization Time-of-Flight Mass Spectrometry of the Effects of Preanalytical Variables on Serum Peptidome Profiles Following Long-Term Sample Storage. *PROTEOMICS - Clin. Appl.* 12, 1700047

83. Ellervik, C., and Vaught, J. (2015) Preanalytical Variables Affecting the Integrity of Human Biospecimens in Biobanking. *Clin. Chem.* 61, 914–934

84. Salvagno, G. L., Danese, E., and Lippi, G. (2017) Preanalytical variables for liquid chromatography-mass spectrometry (LC-MS) analysis of human blood specimens. *Clin. Biochem.* 50, 582–586

85. Carrick, D. M., Mette, E., Hoyle, B., Rogers, S. D., Gillanders, E. M., Schully, S. D., and Mechanic, L. E. (2014) The Use of Biospecimens in Population-Based Research: A Review of the National Cancer Institute's Division of Cancer Control and Population Sciences Grant Portfolio. *Biopreserv. Biobank.* 12, 240–245

86. Buettner, G. R. (1988) In the absence of catalytic metals ascorbate does not autoxidize at pH 7: ascorbate as a test for catalytic metals. *J. Biochem. Biophys. Methods* 16, 27–40

87. Gevantman, L. H. (2015) Solubility of selected gases in water. *CRC Handb. Chem. Phys.*, 5–8

88. United States Center for Disease Control and Prevention, National Health and Nutrition Examination Survey (NHANES) (2015)

89. Jones, D. P., Mody, V. C., Carlson, J. L., Lynn, M. J., and Sternberg, P. (2002) Redox analysis of human plasma allows separation of pro-oxidant events of aging from decline in antioxidant defenses. *Free Radic. Biol. Med.* 33, 1290–1300

90. Blanco, R. A., Ziegler, T. R., Carlson, B. A., Cheng, P.-Y., Park, Y., Cotsonis, G. A., Accardi, C. J., and Jones, D. P. (2007) Diurnal variation in glutathione and cysteine redox states in human plasma. *Am. J. Clin. Nutr.* 86, 1016–23

91. Weaving, G., Batstone, G. F., and Jones, R. G. (2016) Age and sex variation in serum albumin concentration: an observational study. *Ann. Clin. Biochem. Int. J. Lab. Med.* 53, 106–111

92. Skoog, D. A., West, D. M., Holler, J., and Crouch, S. R. (2014) *Fundamentals of analytical chemistry* (Belmont, CA: Brooks/Cole, Cengage Learning). 9th Ed.

93. Kachur, A. V., Koch, C. J., and Biaglow, J. E. (1999) Mechanism of copper-catalyzed autoxidation of cysteine. *Free Radic. Res.* 31, 23–34

94. Atkins, P., and Paula, J. De (2010) *Physical Chemistry* (Oxford University Press)9th editio.

95. Orsak, T., Smith, T. L., Eckert, D., Lindsley, J. E., Borges, C. R., and Rutter, J. (2012) Revealing the allosterome: Systematic identification of metabolite-protein interactions. *Biochemistry* 51, 225–232

96. Johnson, J. M., Strobel, F. H., Reed, M., Pohl, J., and Jones, D. P. (2008) A rapid LC-FTMS method for the analysis of cysteine, cystine and cysteine/cystine steady-state redox potential in human plasma. *Clin. Chim. Acta* 396, 43–48

97. Ohie, T., Fu, X. W., Iga, M., Kimura, M., and Yamaguchi, S. (2000) Gas chromatography–mass spectrometry with tert.-butyldimethylsilyl derivatization: use of the simplified sample preparations and the automated data system to screen for organic acidemias. *J. Chromatogr. B Biomed. Sci. Appl.* 746, 63–73

98. Liebisch, G., Lieser, B., Rathenberg, J., Drobnik, W., and Schmitz, G. (2004) High-throughput quantification of phosphatidylcholine and sphingomyelin by electrospray ionization tandem mass spectrometry coupled with isotope correction algorithm. *Biochim. Biophys. Acta - Mol. Cell Biol. Lipids* 1686, 108–117

99. Liebisch, G., Lieser, B., Rahtenberg, J., Drobnik, W., and Schmitz, G. (2005) Erratum to "High-throughput quantification of phosphatidylcholine and sphingomyelin by electrospray ionization tandem mass spectrometry coupled with isotope corrections algorithm" [Biochimica et Biophysics Acta, 1686 (2004) 108–117]. *Biochim. Biophys. Acta - Mol. Cell Biol. Lipids* 1734, 86–89

100. Bocedi, A., Cattani, G., Stella, L., Massoud, R., and Ricci, G. (2018) Thiol disulfide exchange reactions in human serum albumin: the apparent paradox of the redox transitions of Cys 34. *FEBS J.* 285, 3225–3237

101. Berthon, G. (1995) The stability constants of metal complexes of amino acids with polar side chains. *Pure Appl. Chem.* 67, 1117–1240

102. Hellman, N. E., and Gitlin, J. D. (2002) Ceruloplasmin metabolism and function. *Annu. Rev. Nutr.* 22, 439–58

103. Kasper, C. B., Deutsch, H. F., and Beinert, H. (1963) Studies on the State of Copper in Native and Modified Human Ceruloplasmin. *J. Biol. Chem.* 238, 2338–2342

104. Nakanishi, T., Hasuike, Y., Otaki, Y., Hama, Y., Nanami, M., Miyagawa, K., Moriguchi, R., Nishikage, H., Izumi, M., and Takamitsu, Y. (2003) Free cysteine is increased in plasma from hemodialysis patients. *Kidney Int.* 63, 1137–1140

105. Borges, C. R., Rehder, D. S., and Boffetta, P. (2013) Multiplexed surrogate analysis of glycotransferase activity in whole biospecimens. *Anal. Chem.* 85, 2927–2936

106. Zaare, S., Aguilar, J. S., Hu, Y., Ferdosi, S., and Borges, C. R. (2016) Glycan Node Analysis: A Bottom-up Approach to Glycomics. *J. Vis. Exp.* 2016, 1–11

107. Hu, Y., and Borges, C. R. (2017) A spin column-free approach to sodium hydroxide-based glycan permethylation. *Analyst* 142, 2748–2759

108. Ferdosi, S., Rehder, D. S., Maranian, P., Castle, E. P., Ho, T. H., Pass, H. I., Cramer, D. W., Anderson, K. S., Fu, L., Cole, D. E. C., Le, T., Wu, X., and Borges, C. R. (2018) Stage Dependence, Cell-Origin Independence, and

Prognostic Capacity of Serum Glycan Fucosylation, β1–4 Branching, β1–6 Branching, and α2–6 Sialylation in Cancer. *J. Proteome Res.* 17, 543–558

109. Ferdosi, S., Ho, T. H., Castle, E. P., Stanton, M. L., and Borges, C. R. (2018) Behavior of blood plasma glycan features in bladder cancer. *PLoS One* 13, e0201208

110. Jeffs, J. W., Ferdosi, S., Yassine, H. N., and Borges, C. R. (2017) Ex vivo instability of glycated albumin: A role for autoxidative glycation. *Arch. Biochem. Biophys.* 629, 36–42

111. Hubel, A., Spindler, R., and Skubitz, A. P. N. (2014) Storage of Human Biospecimens: Selection of the Optimal Storage Temperature. *Biopreserv. Biobank.* 12, 165–175

112. Boerema, D. J., An, B., Gandhi, R. P., Papineau, R., Regnier, E., Wilder, A., Molitor, A., Tang, A. P., and Kee, S. M. (2017) Biochemical comparison of four commercially available human α 1 -proteinase inhibitors for treatment of α 1 -antitrypsin deficiency. *Biologicals* 50, 63–72

113. Farrugia, A., Hill, R., Douglas, S., Karabagias, K., and Kleinig, A. (1992) Factor VIII/von willebrand factor levels in plasma frozen to - 30 ° C in air or halogenated hydrocarbons. *Thromb. Res.* 68, 97–102

114. Kolb, A. M., Smit, N. P. M., Lentz-Ljuboje, R., Osanto, S., and van Pelt, J. (2009) Non-transferrin bound iron measurement is influenced by chelator concentration. *Anal. Biochem.* 385, 13–19

115. Rehder, D. S., and Borges, C. R. (2010) Cysteine sulfenic Acid as an Intermediate in Disulfide Bond Formation and Nonenzymatic Protein Folding. *Biochemistry* 49, 7748–7755

116. Kadota, K., Yui, Y., Hattori, R., Murohara, Y., and Kawai, C. (1991) Decreased sulfhydryl groups of serum albumin in coronary artery disease. *Jpn. Circ. J.* 55, 937–41

117. Bar-Or, D., Heyborne, K. D., Bar-Or, R., Rael, L. T., Winkler, J. V., and Navot, D. (2005) Cysteinylation of maternal plasma albumin and its association with intrauterine growth restriction. *Prenat. Diagn.* 25, 245–249

118. Terawaki, H., Yoshimura, K., Hasegawa, T., Matsuyama, Y., Negawa, T., Yamada, K., Matsushima, M., Nakayama, M., Hosoya, T., and Era, S. (2004) Oxidative stress is enhanced in correlation with renal dysfunction: Examination with the redox state of albumin. *Kidney Int.* 66, 1988–1993

119. Soejima, A., Matsuzawa, N., Hayashi, T., Kimura, R., Ootsuka, T., Fukuoka, K., Yamada, A., Nagasawa, T., and Era, S. (2004) Alteration of Redox State of

Human Serum Albumin before and after Hemodialysis. *Blood Purif.* 22, 525–529

120. Terawaki, H., Nakayama, K., Matsuyama, Y., Nakayama, M., Sato, T., Hosoya, T., Era, S., and Ito, S. (2007) Dialyzable Uremic Solutes Contribute to Enhanced Oxidation of Serum Albumin in Regular Hemodialysis Patients. *Blood Purif.* 25, 274–279

121. Regazzoni, L., Del Vecchio, L., Altomare, A., Yeum, K. J., Cusi, D., Locatelli, F., Carini, M., and Aldini, G. (2013) Human serum albumin cysteinylation is increased in end stage renal disease patients and reduced by hemodialysis: mass spectrometry studies. *Free Radic. Res.* 47, 172–180

122. Galliano, M., Minchiotti, L., Porta, F., Rossi, A., Ferri, G., Madison, J., Watkins, S., and Putnam, F. W. (1990) Mutations in genetic variants of human serum albumin found in Italy. *Proc. Natl. Acad. Sci.* 87, 8721–8725

123. Seibig, S., and Van Eldik, R. (1997) Kinetics of [FeII(edta)] Oxidation by Molecular Oxygen Revisited. New Evidence for a Multistep Mechanism. *Inorg. Chem.* 36, 4115–4120

124. Lippi, G., Guidi, G. C., Mattiuzzi, C., and Plebani, M. (2006) Preanalytical variability: the dark side of the moon in laboratory testing. *Clin. Chem. Lab. Med.* 44, 358–365

125. Hewitt, S. M., Badve, S. S., and True, L. D. (2012) Impact of Preanalytic Factors on the Design and Application of Integral Biomarkers for Directing Patient Therapy. *Clin. Cancer Res.* 18, 1524–1530

126. Khan, J., Lieberman, J. A., and Lockwood, C. M. (2017) Variability in, variability out: Best practice recommendations to standardize pre-analytical variables in the detection of circulating and tissue microRNAs. *Clin. Chem. Lab. Med.* 55, 608–621

127. Agrawal, L., Engel, K. B., Greytak, S. R., and Moore, H. M. (2018) Understanding preanalytical variables and their effects on clinical biomarkers of oncology and immunotherapy. *Semin. Cancer Biol.* 52, 26–38

128. Hunt, J. V., Dean, R. T., and Wolff, S. P. (1988) Hydroxyl radical production and autoxidative glycosylation. Glucose autoxidation as the cause of protein damage in the experimental glycation model of diabetes mellitus and ageing. *Biochem. J.* 256, 205

129. Wolff, S. P., and Dean, R. T. (1987) Glucose autoxidation and protein modification. The potential role of "autoxidative glycosylation" in diabetes. *Biochem. J.* 245, 243

130. Niederkofler, E. E., Kiernan, U. A., O'Rear, J., Menon, S., Saghir, S., Protter, A.

A., Nelson, R. W., and Schellenberger, U. (2008) Detection of endogenous B-type natriuretic peptide at very low concentrations in patients with heart failure. *Circ. Heart Fail.* 1, 258–264

131. Craft, D., Yi, J., and Gelfand, C. A. (2009) Time-Dependent and Sample-to-Sample Variations in Human Plasma Peptidome are Both Minimized Through Use of Protease Inhibitors. *Anal. Lett.* 42, 1398–1406

132. Yi, J., Kim, C., and Gelfand, C. A. (2007) Inhibition of intrinsic proteolytic activities moderates preanalytical variability and instability of human plasma. *J. Proteome Res.* 6, 1768–1781

133. Yi, J., Liu, Z., Craft, D., O'Mullan, P., Ju, G., and Gelfand, C. A. (2008) Intrinsic peptidase activity causes a Sequential Multi-Step Reaction (SMSR) in digestion of human plasma peptides. *J. Proteome Res.* 7, 5112–5118

134. Karlsen, A., Blomhoff, R., and Gundersen, T. E. (2007) Stability of whole blood and plasma ascorbic acid. *Eur. J. Clin. Nutr.* 61, 1233–1236

135. Lawrence, J. M., Umekubo, M. A., Chiu, V., and Petitti, D. B. (2000) Split sample analysis of serum folate levels after 18 days in frozen storage. *Clin. Lab.* 46, 483–486

136. Devanapalli, B., Bermingham, M. A., and Mahajan, D. (2002) Effect of long-term storage at −80 °C on the various lipid parameters in stored plasma samples. *Clin. Chim. Acta* 322, 179–181

137. Dědova, T., Grunow, D., Kappert, K., Flach, D., Tauber, R., and Blanchard, V. (2018) The effect of blood sampling and preanalytical processing on human N-glycome. *PLoS One* 13, e0200507

138. Hu, Y., Ferdosi, S., Kapuruge, E. P., Diaz De Leon, J. A., Stücker, I., Radoï, L., Guénel, P., and Borges, C. R. (2019) Diagnostic and Prognostic Performance of Blood Plasma Glycan Features in the Women Epidemiology Lung Cancer (WELCA) Study. *J. Proteome Res.* 18, 3985–3998

139. Amez Martín, M., Wuhrer, M., and Falck, D. (2021) Serum and Plasma Immunoglobulin G Fc N-Glycosylation Is Stable during Storage. *J. Proteome Res.* 20, 2935–2941

140. Murphy, B. M., Swarts, S., Mueller, B. M., Van Der Geer, P., Manning, M. C., and Fitchmun, M. I. (2013) Protein instability following transport or storage on dry ice. *Nat. Methods 2013 104* 10, 278–279

141. Bakdash, J. Z., and Marusich, L. R. (2017) Repeated measures correlation. *Front. Psychol.* 8, 456

142. Nazha, B. (2015) Hypoalbuminemia in colorectal cancer prognosis: Nutritional marker or inflammatory surrogate? *World J. Gastrointest. Surg.* 7, 370

143. Abudayyeh, A., Abdelrahim, M., and Salahudeen, A. (2014) Fluid and Electrolyte Abnormalities in Patients with Cancer. *Ren. Dis. Cancer Patients*, 167–182

144. Gupta, D., and Lis, C. G. (2010) Pretreatment serum albumin as a predictor of cancer survival: A systematic review of the epidemiological literature. *Nutr. J.* 9, 1–16

145. Brogren, H., Wallmark, K., Deinum, J., Karlsson, L., and Jern, S. (2011) Platelets Retain High Levels of Active Plasminogen Activator Inhibitor 1. *PLoS One* 6, e26762

146. Huebner, B. R., Moore, E. E., Moore, H. B., Stettler, G. R., Nunns, G. R., Lawson, P., Sauaia, A., Kelher, M., Banerjee, A., and Silliman, C. C. (2018) Thrombin provokes degranulation of platelet A-granules leading to the release of active plasminogen activator inhibitor-1 (PAI-1). *Shock* 50, 671–676

147. Nabuchi, Y., Fujiwara, E., Ueno, K., Kuboniwa, H., Asoh, Y., and Ushio, H. (1995) Oxidation of recombinant human parathyroid hormone: effect of oxidized position on the biological activity. *Pharm. Res.* 12, 2049–52

148. Gao, J., Yao, Y., and Squier, T. C. (2001) Oxidatively Modified Calmodulin Binds to the Plasma Membrane Ca-ATPase in a Nonproductive and Conformationally Disordered Complex. *Biophys. J.* 80, 1791–1801

149. De Jager, W., Bourcier, K., Rijkers, G. T., Prakken, B. J., and Seyfert-Margolis, V. (2009) Prerequisites for cytokine measurements in clinical trials with multiplex immunoassays. *BMC Immunol.* 10, 52

150. Kisand, K., Kerna, I., Kumm, J., Jonsson, H., and Tamm, A. (2011) Impact of cryopreservation on serum concentration of matrix metalloproteinases (MMP)-7, TIMP-1, vascular growth factors (VEGF) and VEGF-R2 in Biobank samples. *Clin. Chem. Lab. Med.* 49, 229–235

151. Kugler, K. G., Hackl, W. O., Mueller, L. A. J., Fiegl, H., Graber, A., and Pfeiffer, R. M. (2011) The Impact of Sample Storage Time on Estimates of Association in Biomarker Discovery Studies. *J. Clin. Bioinforma.* 1,

152. Jung, K., Lein, M., Brux, B., Sinha, P., Schnorr, D., and Loening, S. A. (2000) Different Stability of Free and Complexed Prostate-Specific Antigen in Serum in Relation to Specimen Handling and Storage Conditions. *Clin. Chem. Lab. Med.* 38, 1271–1275

153. Holvoet, P., and Collen, D. (1994) Oxidized lipoproteins in atherosclerosis and thrombosis. *FASEB J.* 8, 1279–1284

154. Holvoet, P., Donck, J., Landeloos, M., Brouwers, E., Luijtens, K., Arnout, J., Lesaffre, E., Vanrenterghem, Y., and Collen, D. (1996) Correlation between Oxidized Low Density Lipoproteins and von Willebrand Factor in Chronic Renal Failure. *Thromb. Haemost.* 76, 663–669

155. Holvoet, P., Macy, E., Landeloos, M., Jones, D., Nancy, J. S., Van de Werf, F., and Tracy, R. P. (2006) Analytical Performance and Diagnostic Accuracy of Immunometric Assays for the Measurement of Circulating Oxidized LDL. *Clin. Chem.* 52, 760–764

156. Ylä-Herttuala, S., Rosenfeld, M. E., Parthasarathy, S., Sigal, E., Särkioja, T., Witztum, J. L., and Steinberg, D. (1991) Gene expression in macrophage-rich human atherosclerotic lesions. 15-lipoxygenase and acetyl low density lipoprotein receptor messenger RNA colocalize with oxidation specific lipid-protein adducts. *J. Clin. Invest.* 87, 1146–1152

157. Holvoet, P., Perez, G., Zhao, Z., Brouwers, E., Bernar, H., and Collen, D. (1995) Malondialdehyde-modified low density lipoproteins in patients with atherosclerotic disease. *J. Clin. Invest.* 95, 2611–2619

158. Steinberg, D. (1990) Lipoproteins and Atherogenesis. *JAMA* 264, 3047

159. Berliner, J. A., Navab, M., Fogelman, A. M., Frank, J. S., Demer, L. L., Edwards, P. A., Watson, A. D., and Lusis, A. J. (1995) Atherosclerosis: Basic Mechanisms. *Circulation* 91, 2488–2496

160. Holvoet, P., Stassen, J.-M., Van Cleemput, J., Collen, D., and Vanhaecke, J. (1998) Oxidized Low Density Lipoproteins in Patients With Transplant-Associated Coronary Artery Disease. *Arterioscler. Thromb. Vasc. Biol.* 18, 100–107

161. Holvoet, P., Mertens, A., Verhamme, P., Bogaerts, K., Beyens, G., Verhaeghe, R., Collen, D., Muls, E., and Van de Werf, F. (2001) Circulating Oxidized LDL Is a Useful Marker for Identifying Patients With Coronary Artery Disease. *Arterioscler. Thromb. Vasc. Biol.* 21, 844–848

162. Holvoet, P., Vanhaecke, J., Janssens, S., Van de Werf, F., and Collen, D. (1998) Oxidized LDL and Malondialdehyde-Modified LDL in Patients With Acute Coronary Syndromes and Stable Coronary Artery Disease. *Circulation* 98, 1487–1494

163. Nishi, K., Itabe, H., Uno, M., Kitazato, K. T., Horiguchi, H., Shinno, K., and Nagahiro, S. (2002) Oxidized LDL in Carotid Plaques and Plasma Associates With Plaque Instability. *Arterioscler. Thromb. Vasc. Biol.* 22, 1649–1654

164. Holvoet, P., Kritchevsky, S. B., Tracy, R. P., Mertens, A., Rubin, S. M., Butler, J., Goodpaster, B., and Harris, T. B. (2004) The Metabolic Syndrome, Circulating Oxidized LDL, and Risk of Myocardial Infarction in Well-Functioning Elderly

People in the Health, Aging, and Body Composition Cohort. *Diabetes* 53, 1068–1073

165. Tsimikas, S., Brilakis, E. S., Miller, E. R., McConnell, J. P., Lennon, R. J., Kornman, K. S., Witztum, J. L., and Berger, P. B. (2005) Oxidized Phospholipids, Lp(a) Lipoprotein, and Coronary Artery Disease. *N. Engl. J. Med.* 353, 46–57

166. Meisinger, C., Baumert, J., Khuseyinova, N., Loewel, H., and Koenig, W. (2005) Plasma Oxidized Low-Density Lipoprotein, a Strong Predictor for Acute Coronary Heart Disease Events in Apparently Healthy, Middle-Aged Men From the General Population. *Circulation* 112, 651–657

167. Holvoet, P., Lee, D. H., Steffes, M., Gross, M., and Jacobs, D. R. (2008) Association Between Circulating Oxidized Low-Density Lipoprotein and Incidence of the Metabolic Syndrome. *JAMA* 299, 2287–2293

168. OxLDL - Cleveland HeartLab, Inc.

169. 123023: Oxidized Low-density Lipoprotein (OxLDL) | Labcorp

170. OxLDL | Test Detail | Quest Diagnostics

171. Wu, T., Willett, W. C., Rifai, N., Shai, I., Manson, J. A. E., and Rimm, E. B. (2006) Is Plasma Oxidized Low-Density Lipoprotein, Measured With the Widely Used Antibody 4E6, an Independent Predictor of Coronary Heart Disease Among U.S. Men and Women? *J. Am. Coll. Cardiol.* 48, 973–979

172. Morrow, J. D., Harris, T. M., and Jackson Roberts, L. (1990) Noncyclooxygenase oxidative formation of a series of novel prostaglandins: Analytical ramifications for measurement of eicosanoids. *Anal. Biochem.* 184, 1–10

173. Ito, F., Sono, Y., and Ito, T. (2019) Measurement and Clinical Significance of Lipid Peroxidation as a Biomarker of Oxidative Stress: Oxidative Stress in Diabetes, Atherosclerosis, and Chronic Inflammation. *Antioxidants 2019, Vol. 8, Page 72* 8, 72

174. Pai, J. K., Curhan, G. C., Cannuscio, C. C., Rifai, N., Ridker, P. M., and Rimm, E. B. (2002) Stability of Novel Plasma Markers Associated with Cardiovascular Disease: Processing within 36 Hours of Specimen Collection. *Clin. Chem.* 48, 1781–1784

175. Perman, J., Fagerlund, C., and Hulthe, J. (2004) Methodological aspects of measuring oxidized low density lipoproteins in human serum and plasma. *Scand. J. Clin. Lab. Invest.* 64, 753–756

176. Wu, J. T., and Knight, J. A. (1985) In-vitro stability of human alpha-fetoprotein. *Clin. Chem.* 31, 1692–1697

177. Ayache, S., Panelli, M., Marincola, F. M., and Stroncek, D. F. (2006) Effects of Storage Time and Exogenous Protease Inhibitors on Plasma Protein Levels. *Am. J. Clin. Pathol.* 126, 174–184

178. Yamada, A., Cox, M. A., Gaffney, K. A., Moreland, A., Boland, C. R., and Goel, A. (2014) Technical Factors Involved in the Measurement of Circulating MicroRNA Biomarkers for the Detection of Colorectal Neoplasia. *PLoS One* 9, e112481

179. Schully, S. D., Carrick, D. M., Mechanic, L. E., Srivastava, S., Anderson, G. L., Baron, J. A., Berg, C. D., Cullen, J., Diamandis, E. P., Doria-Rose, V. P., Goddard, K. A. B., Hankinson, S. E., Kushi, L. H., Larson, E. B., McShane, L. M., Schilsky, R. L., Shak, S., Skates, S. J., Urban, N., Kramer, B. S., Khoury, M. J., and Ransohoff, D. F. (2015) Leveraging Biospecimen Resources for Discovery or Validation of Markers for Early Cancer Detection. *JNCI J. Natl. Cancer Inst.* 107, 12

180. Vaught, J. B., Henderson, M. K., and Compton, C. C. (2012) Biospecimens and Biorepositories: From Afterthought to ScienceBiospecimens and Biorepositories: From Afterthought to Science. *Cancer Epidemiol. Biomarkers Prev.* 21, 253–255

181. Andre, F., McShane, L. M., Michiels, S., Ransohoff, D. F., Altman, D. G., Reis-Filho, J. S., Hayes, D. F., and Pusztai, L. (2011) Biomarker studies: a call for a comprehensive biomarker study registry. *Nat. Rev. Clin. Oncol. 2011 83* 8, 171–176

182. Vaught, J., Baust, J. G., Heacox, A. E., Riegman, P., Betsou, F., Mazur, P., Baust, J. M., Stacey, G., and Barnes, M. (2010) What Are Three Actionable Strategies to Improve Quality in Biomedical Research. *Biopreserv. Biobank.* 8, 121–125

183. McLerran, D., Grizzle, W. E., Feng, Z., Thompson, I. M., Bigbee, W. L., Cazares, L. H., Chan, D. W., Dahlgren, J., Diaz, J., Kagan, J., Lin, D. W., Malik, G., Oelschlager, D., Partin, A., Randolph, T. W., Sokoll, L., Srivastava, S., Srivastava, S., Thornquist, M., Troyer, D., Wright, G. L., Zhang, Z., Zhu, L., and Semmes, O. J. (2008) SELDI-TOF MS whole serum proteomic profiling with IMAC surface does not reliably detect prostate cancer. *Clin. Chem.* 54, 53–60

184. Betsou, F., Roussel, B., Guillaume, N., and Lefrère, J. J. (2009) Long-term stability of coagulation variables: Protein S as a biomarker for preanalytical storage-related variations in human plasma. *Thromb. Haemost.* 101, 1172–1175

185. Fu, X., Cate, S. A., Dominguez, M., Osborn, W., Özpolat, T., Konkle, B. A., Chen, J., and López, J. A. (2019) Cysteine Disulfides (Cys-ss-X) as Sensitive Plasma Biomarkers of Oxidative Stress. *Sci. Reports 2019 91* 9, 1–9

186. Jones, D. P., Carlson, J. L., Mody, V. C., Cai, J., Lynn, M. J., and Sternberg, P. (2000) Redox state of glutathione in human plasma. *Free Radic. Biol. Med.* 28,

625–635

187. Ellman, G. L. (1959) Tissue sulfhydryl groups. *Arch. Biochem. Biophys.* 82, 70–77

188. Winther, J. R., and Thorpe, C. (2014) Quantification of thiols and disulfides. *Biochim. Biophys. Acta - Gen. Subj.* 1840, 838–846

189. Henkel, M., Röckendorf, N., and Frey, A. (2016) Selective and Efficient Cysteine Conjugation by Maleimides in the Presence of Phosphine Reductants. *Bioconjug. Chem.* 27, 2260–2265

190. Crouch, S., Skoog, D., and Holler, F. J. (2016) *Principles of Instrumental Analysis Seventh Edition*

191. Liu, L., Aa, J., Wang, G., Yan, B., Zhang, Y., Wang, X., Zhao, C., Cao, B., Shi, J., Li, M., Zheng, T., Zheng, Y., Hao, G., Zhou, F., Sun, J., and Wu, Z. (2010) Differences in metabolite profile between blood plasma and serum. *Anal. Biochem.* 406, 105–112

APPENDIX A

COPYRIGHT PERMISSIONS

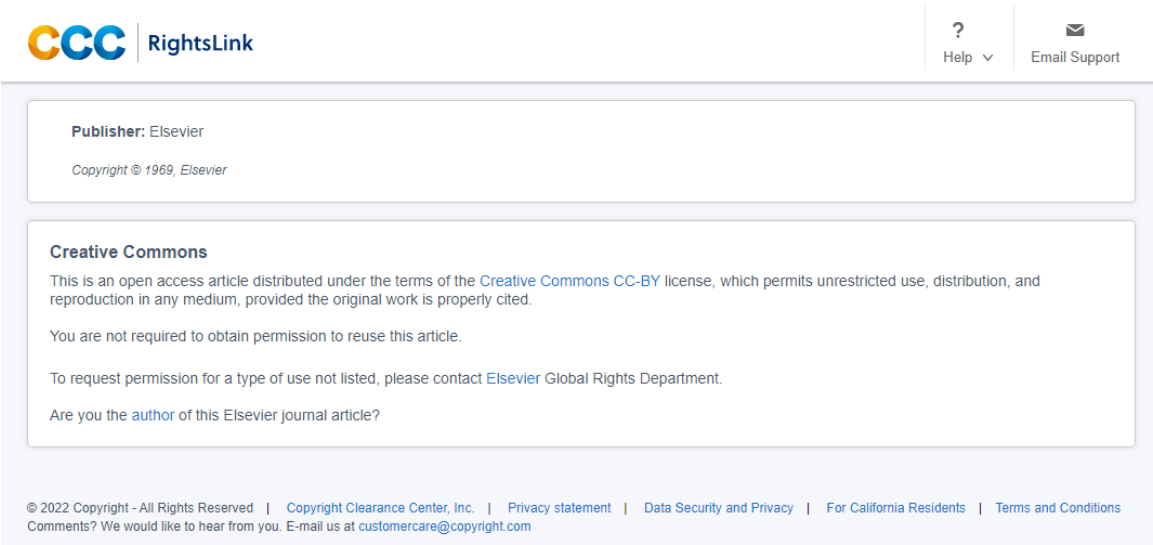

More details are provided in: https://www.elsevier.com/journals/molecular-and-cellular-proteomics/1535-9476/open-access-journal